THE INFLUENCE OF OVERWEIGHT- AND OBESITY-ASSOCIATED MAMMARY ADIPOSE INFLAMMATION ON PROGRESSION OF TRIPLE-NEGATIVE BREAST CANCER

Alyssa Joy Cozzo

A dissertation submitted to the faculty at the University of North Carolina at Chapel Hill in partial fulfillment of the requirements for the degree of Doctor of Philosophy in the Department of Nutrition (Nutritional Biochemistry) in the Gillings School of Global Public Health.

Chapel Hill
2018

Approved by:

Liza Makowski Hayes

Melinda Beck

Stephen Hursting

Carey K. Anders

H. Shelton Earp, III

ABSTRACT

Alyssa Joy Cozzo: The Influence of Overweight- and Obesity-associated Mammary Adipose Inflammation on Progression of Triple-Negative Breast Cancer
(Under the direction of Liza Makowski Hayes)

Triple-negative breast cancers (TNBCs) are a collection of highly proliferative and invasive breast cancers primarily comprised of the basal-like (BBC) and claudin-low (CLBCs) molecular subtypes. We previously reported that weight gain and weight loss regulated pre-neoplastic lesion formation, tumor latency, and tumor progression in C3(1)-TAg mice, a transgenic model of spontaneous BBC. These findings coincided with elevated concentration of hepatocyte growth factor (HGF), ligand for the proto-oncogene cMET, in the mammary microenvironment of high-fat diet (HFD)-fed mice. Thus, herein we conducted a two-phase study investigating whether crizotinib, an inhibitor of cMET, would delay onset of BBC in low-fat (LFD) and HFD-fed C3(1)-TAg mice. When administered prophylactically – before tumor onset – crizotinib did not significantly affect tumor progression or tumor burden. However, with therapeutic treatment following tumor development, crizotinib significantly reduced tumor multiplicity and vascularity in LFD- and HFD-fed C3(1)-TAg mice. These findings emphasize the importance of clarifying “windows of susceptibility” during which HGF/cMET signaling may play disproportionately greater roles in BBC onset and progression.

We next hypothesized that adult weight gain and an inflammatory overweight mammary microenvironment would augment CLBC progression, while weight loss before tumor development would normalize overweight-associated tumor promotion. Therefore, a C3(1)-TAg-derived CLBC cell line was orthotopically transplanted into lean, overweight, and formerly overweight female FVB/NJ mice. Indeed, overweight accelerated tumor progression and

induced pro-inflammatory changes in the mammary gland, including increased growth factor expression and crown-like structure formation. Weight loss abrogated overweight-induced tumor growth and reduced expression of mitogenic and metastasis-associated signaling pathways in tumors, significantly attenuating inflammation-induced CLBC progression. Interestingly, overweight also resulted in enhanced expression of a mast cell transcriptional signature in whole mammary tissue. Increased mast cell scores were also observed in cancer-adjacent breast tissue of overweight and obese relative to normal weight breast cancer patients. Conversely, lower intratumoral mast cell score was significantly associated with both triple-negative subtype and elevated risk-of-recurrence score in human breast cancers. Taken together, our results support that excess adiposity facilitates TNBC aggression. Further elucidation of adiposity-driven mechanisms of tumor progression and the efficacy of preventive measures such as weight loss could have tremendous potential for public health.

ACKNOWLEDGEMENTS

This dissertation represents the culmination of a four-year period of intensive training and development as a scientist as well as self-reflection and personal growth. I owe a tremendous debt to my advisor, Liza Makowski, Ph.D., my husband, Brad Martin, and my family, whose patience and steadfast belief in me during this time have made completion of the studies presented herein possible. I am also grateful for my undergraduate research assistant, Ottavia Zattra and my colleague Ashley Fuller, for their help with everything from brainstorming to data acquisition to formatting and editing during manuscript preparation. A particularly special thanks to our lab manager, Alex Freemerman Ph.D., who on a daily basis provided extensive expertise for troubleshooting experiments, a great sense of humor, and unwavering faith in me.

I owe many thanks to Melissa Troester, Ph.D. for providing human breast histology and gene expression data obtained through the UNC Normal Breast Study and to Laura Bowers, Ph.D., and Stephen Hursting, Ph.D., for sharing mouse mammary histology. I would also like to acknowledge the tremendous amount of support I received from the Animal Studies Core Facility within the Lineberger Comprehensive Cancer Center (LCCC), and particularly facility director Charlene Santos. Moreover, the training and guidance provided by the UNC Flow Cytometry Core Facility over the last three years has been pivotal in completion of the studies contained within this dissertation and in other collaborations not included. Finally, this dissertation would not have been possible without funding provided through the Royster Society of Fellows (Chancellor's Fellowship), the Integrative Vascular Biology Fellowship (T32), the National Institutes of Health, the Mary Kay Foundation, the UNC University Cancer Research Fund (UCRF), and a LCCC Innovation Developmental Funding Grant.

TABLE OF CONTENTS

LIST OF TABLES ix

LIST OF FIGURES x

LIST OF ABBREVIATIONS AND SYMBOLS xiii

CHAPTER 1: CONTRIBUTION OF ADIPOSE TISSUE TO DEVELOPMENT OF CANCER 1

Didactic Synopsis 1

Introduction 2

The Adipose Organ 4

Obesity and Cancer 6

Current status of the obesity epidemic, globally and in the United States 6

The obesity-cancer link 8

Anatomy of the Breast and Prostate 11

Mammary gland anatomy and adipose-cancer interaction in humans vs. mice 11

Prostate gland anatomy and adipose-cancer interaction in humans vs. mice 14

Microenvironmental Links between Adipose Tissue and Cancer 16

Context matters: extracellular matrix in adipose tissue and cancer 16

Adipocytes and adipocyte-cancer interactions 25

Adipose-derived Stem Cells 36

Adipose and Endothelial/Lymphendothelial cells 39

Adipose Tissue Immune Populations in Cancer Development and Progression 47

T cells in Adipose and Cancer 50

Macrophages and myeloid-derived suppressor cells 56

Myeloid-derived suppressor cells 66

Neutrophils 68

Mast cells 73

Eosinophils 78

Conclusion 80

CHAPTER 2: CMET INHIBITOR CRIZOTINIB IMPAIRS ANGIOGENESIS AND REDUCES TUMOR BURDEN IN THE C3(1)-TAG MODEL OF BASAL-LIKE BREAST CANCER 82

Background 82

Methods 84

Results 89

Diet-induced adiposity accelerated tumor latency in C3(1)-TAg mice 89

Crizotinib treatment inhibited secondary tumor development, reduced overall tumor burden 90

Crizotinib treatment disrupted tumor vascularization 91

Prophylactic crizotinib administration did not affect body weight or adiposity 93

Prophylactic crizotinib administration increased primary tumor progression without significantly altering tumor burden or precursor lesion development 94

Discussion 96

CHAPTER 3: WEIGHT LOSS NORMALIZES OVERWEIGHT-ASSOCIATED CLAUDIN-LOW BREAST CANCER PROGRESSION: ROLE OF MAMMARY FAT PAD INFLAMMATION AND MYELOID CELL INFILTRATES 99

Background 99

Methods 102

Results 113

High-fat feeding and diet switch-induced weight loss modulated mammary adiposity and CLBC tumor growth 113

Accelerated tumor growth rate in Overweight mice was associated with macrophage and neutrophil influx into mammary adipose 116

Weight loss reversed overweight-associated increases in growth factor and inflammatory cytokine production 119

Weight loss reduced expression of mitogenic and metastasis-associated gene pathways 122

Adiposity status regulated mast cell density and activation in mouse mammary fat pad 124

Mast cell score is increased in breast tissue of overweight and obese women 126

Lower intratumoral mast cell score is associated with triple-negative breast cancer and elevated risk of recurrence 128

Discussion 129

CHAPTER 4: SYNTHESIS, SIGNIFICANCE, AND FUTURE DIRECTIONS 135

Triple-negative breast cancers: a heterogeneous disease 135

Diet, overweight, obesity, and weight loss in breast cancer outcomes 137

Directions for future research 140

APPENDIX: SUPPLEMENTAL FIGURES 144

REFERENCES 146

LIST OF TABLES

Table 1. Antibodies and dilutions used in analysis. 108

Table 2. Demographic and clinicopathologic features of Normal Breast Study participants. ... 126

LIST OF FIGURES

Figure 1. Tumors as communities. 2

Figure 2. The adipose organ is comprised of several distinct adipose depots..... 5

Figure 3. Approximate composition of human white adipose tissue stromal-vascular fraction (percent cellularity)..... 6

Figure 4. Rising global and US obesity rates. 8

Figure 5. Comparison of mouse and human mammary gland anatomical structure 12

Figure 6. Comparison of mouse and human mammary gland histology 13

Figure 7. Adipose-breast cancer interactions in mice and humans..... 14

Figure 8. Anatomical comparison of mouse (left) and human (right) prostate glands 15

Figure 9. Desmoplasia and cancer-associated adipocytes 18

Figure 10. Obesity-associated modifications in the adipose tissue microenvironment. 23

Figure 11. HGF/cMET: an oncogenic signaling cascade..... 24

Figure 12. Adipocyte subtypes and secreted factors 26

Figure 13. Adipocytes promote tumor progression and metastasis. 34

Figure 14. Obesity, cancer increase circulating ASCs..... 39

Figure 15. Hypoxia & the Angiogenic Switch. 41

Figure 16. Mammary HGF/cMET signaling in the in C3(1)-TAg mouse model of basal-like breast cancer..... 45

Figure 17. Summary of changes in immune cell profile during progression to obesity..... 49

Figure 18. Macrophage activation as a spectrum. 57

Figure 19. Adipose tissue macrophage ontogeny..... 59

Figure 20. Tumor-associated neutrophils have N1 and N2-like phenotypes 70

Figure 21. Mast cells: Unappreciated players in adipose and tumor biology. 74

Figure 22. Model of Treatment Study design. 89

Figure 23. High-fat diet exposure accelerated basal-like tumor latency in C3(1)-TAg mice..... 90

Figure 24. Crizotinib treatment inhibited subsequent tumor development 91

Figure 25. Crizotinib impaired tumor vascularization 92

Figure 26. High fat diet exposure increased active cMET in tumors 92

Figure 27. Model of Prevention Study design 93

Figure 28. Crizotinib prophylactic treatment did not affect body weight or adiposity 94

Figure 29. Preventive administration of crizotinib prior to tumor onset did not alter tumor latency or overall tumor burden 95

Figure 30. Phenotyping of C3-Tag-luc cell line 105

Figure 31. Study design with orthotopic transplant model and tissue collection diagram 114

Figure 32. High fat diet induced adiposity in female FVB/NJ mice was normalized by weight loss 115

Figure 33. Increased mammary fat pad mass in Overweight mice was associated with increased tumor growth rate 116

Figure 34. Overweight and weight loss regulated mammary adipocyte diameter 117

Figure 35. Accelerated tumor growth in Overweight mice occurred in association with increased mammary adipose myeloid cell content 118

Figure 36. Overweight increased mammary adipose CLS density and expression of macrophage markers. 119

Figure 37. Weight loss restored mammary fat pad expression of mixed inflammatory cytokines, growth factors, and markers of neutrophil infiltration to lean levels 120

Figure 38. Accelerated early tumor growth in Overweight was not explained by differences in vascular density or leukocyte infiltration. 121

Figure 39. Weight loss altered intratumoral expression of pathways associated with growth, ECM remodeling, immune response, and metastasis 123

Figure 40. Overweight and weight loss regulated mast cell density and activation in normal and tumor-adjacent mammary adipose 125

Figure 41. Overweight and obesity increased expression of mast-cell associated genes within human breast tissue samples. 127

Figure 42. Intratumoral mast cell score was subtype-specific and associated with risk-of-recurrence score 129

Supplemental Figure 43. Complete gating scheme for analysis of total leukocyte and CD11b+ myeloid cell content of Lean and Overweight mammary fat pads 144

Supplemental Figure 44. Complete gating scheme for analysis of leukocyte infiltration into claudin-low tumors of Lean, Overweight, and WeLo mice . 145

LIST OF ABBREVIATIONS AND SYMBOLS

ADH/AH	Atypical ductal hyperplasia/atypical hyperplasia
AMPK	AMP-activated protein kinase
APC	Antigen-presenting cell
ASC	Adipose stromal cell, Adipose-derived stem cell
ASCO	American Society of Clinical Oncology
α-SMA	Alpha smooth muscle actin
ATGL	Adipocyte triglyceride lipase
ATM	Adipose tissue macrophages
ATP	Adenosine triphosphate
BAI	Body Adiposity Index
BBC	Basal-like breast cancer
BI-RADS	Breast Imaging Reporting and Data System
BMI	Body mass index
CAA	Cancer-associated adipocytes
CAFs	Cancer-associated fibroblasts
CAR	Chimeric antigen receptors
CCK	Cholecystokinin
CIDEA	Cell death activator
CLBC	Claudin-low breast cancer
CLS	Crown like structure
COX-2	Cyclooxygenase-2
CPT1	Carnitine palmitoyltransferase 1
DAMPs	Damage-associated molecular patterns
DCIS	Ductal carcinoma in situ
ECM	Extracellular matrix

EMT	Epithelial-to-mesenchymal transition
ER	Estrogen receptor
FACS	Fluorescence activated cell sorting
FGF	Fibroblast growth factor
FOXP3	Forkhead box P3 transcription factor
GEMM	Genetically engineered mouse model
HER2	Human epidermal growth factor receptor 2
HFD	High-fat diet
HGF	Hepatocyte growth factor
HIF-1, HIF-1α	Hypoxia-inducible factor, 1α subunit
IDC	Invasive ductal carcinoma
IGF-1	Insulin-like growth factor-1
IHC	Immunohistochemistry
IL-6	Interleukin-6
ILCs	Innate lymphoid cells
ILC2s	Innate lymphoid type 2 cells
iNOS	Inducible nitric oxide synthase
LFD	Low-fat diet
M1, M2	Macrophage phenotypes
MCP-1/CCL2	Monocyte-chemoattractant protein, or CC chemokine ligand 2
MDSCs	Myeloid-derived suppressor cells
MMP	Matrix metalloprotease
MMTV-PyMT	Mouse mammary tumor virus, Polyoma middle T antigen
MVD	Microvessel density
N1, N2	Subtypes of tumor-associated neutrophils (see TAN)
NF-κB	Nuclear factor kappa-light-chain-enhancer of activated B cells

NHANES	(United States) National Health and Nutrition Examination Survey
NK cells	Natural killer cells
PAI-1	Plasminogen activator inhibitor-1
PD-1	Programmed Death-1
PDGF	Platelet-derived growth factor
PD-L1	Programmed death-1 ligand
PGE_2	Prostaglandin E2
PIN	Prostatic intraepithelial neoplasia
PPARγ	Peroxisome proliferator-activated receptor gamma
PR	Progesterone receptor
PTHrP	Parathyroid hormone-related protein
TAM	Tumor-associated macrophage
TAN	Tumor-associated neutrophil
Tc	Cytotoxic T cell
TCR	T cell receptor
TDLU	Terminal ductal lobular unit
TEB	Terminal end bud
TGF-β	Transforming growth factor beta
Th1, Th2, Th17	T helper cell subtypes
TNBC	Triple-negative breast cancer
TNF-α	Tumor necrosis factor alpha
Tregs	Regulatory T cells
UCP-1	Uncoupling protein 1
VEGF	Vascular endothelial growth factor
WHO	World Health Organization

CHAPTER 1: CONTRIBUTION OF ADIPOSE TISSUE TO DEVELOPMENT OF CANCER[1]

Didactic Synopsis

Major teaching points:

1. Solid tumor growth requires the interaction of tumor cells with the surrounding tissue, leading to a view of tumors as communities rather than exclusively tumor cells.
2. Adipose tissue, or fat, plays important roles in cancer risk and outcome because many tumors grow close to or in direct contact with adipose.
3. The adipose community – or microenvironment - includes adipocytes and adipose-associated stromal and vascular components, such as fibroblasts and other connective tissue cells, stem cells, endothelial cells, innate and adaptive immune cells, and extracellular signaling and matrix components.
4. Herein, we review the cellular and non-cellular parts of the adipose “organ” and the mechanisms by which varied microenvironmental components contribute to tumor development, with emphasis on obesity.
5. Obesity dramatically modifies the adipose tissue microenvironment in numerous ways, which intriguingly resemble shifts observed within the tumor microenvironment.
6. Understanding neighboring adipose is critical in tumorigenesis.

[1]This chapter was published as an Overview Article within the journal Comprehensive Physiology. The original citation is as follows: Cozzo, A.J., Fuller, A.M. and Makowski, L., Contribution of Adipose Tissue to Development of Cancer. Comprehensive Physiology. Published Online: 12 DEC 2017. DOI: 10.1002/cphy.c170008

Introduction

Cancer is characterized by fundamental aberrations in cellular behavior, including the ability to multiply indefinitely in the absence of growth-promoting factors and a resistance to signals that normally result in programmed cell death (apoptosis) [1]. In the case of solid tumors, carcinogenic transformation and cell proliferation are followed by establishment of a vascular supply, called tumor angiogenesis, which facilitates the delivery of oxygen and nutrients to the growing tumor [1]. Subsequent invasion into and migration through surrounding tissues allows for the establishment of nearby satellite tumors or entry into the lymphatic or vascular systems for dissemination and secondary tumor formation (metastases) [1]. Solid tumor growth and tissue invasion require the interaction of tumor cells with the surrounding tissue, and it is well established that communication between cancer cells and the tissue-level context in which they reside, collectively referred to as the tumor "microenvironment", is pivotal in determining whether a given tumor will exist in dormancy or progress to malignancy [2]. The tumor microenvironment includes, but is not limited to, the tumor cells themselves, blood vessels (endothelial cells and pericytes), lymphatic vessels (lymphendothelial cells), adipocytes, fibroblasts, and various stem and progenitor cells [3] (**Figure 1**). Also present is a wide variety of innate and adaptive immune cells, which can act as critical anti-tumor defenses or,

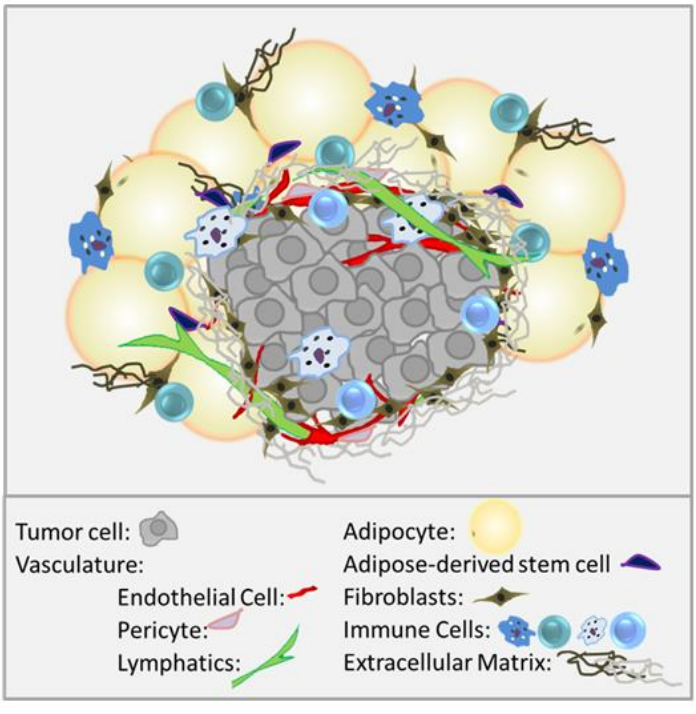

Figure 1. Tumors as communities. Tumor cells co-exist with a variety of stromal and immune cells and reside in a complex mixture of signaling molecules and extracellular matrix components. Adjacent adipose tissue may provide a hospitable environment to developing tumors.

alternatively, play central roles in tumor promotion. The tumor “stroma” is the connective, functionally supportive framework of the tumor, and by definition refers to a complex mixture of signaling molecules and extracellular matrix (ECM) components, as well as the stromal cells (e.g., fibroblasts and pericytes) that produce and are embedded within them [4]. However, the term “stroma” may also be used to collectively refer to all of the aforementioned cell types and secreted factors, as all are present within the cancer cell-adjacent tissue. Thus, considerable heterogeneity, both within the cancer cells themselves and among the interacting stromal cells, leads to a view of tumors as communities, and the process of tumorigenesis as a tissue-level phenomenon occurring in conjunction with intrinsic genetic deviations within individual cancer cells [5].

Due to the ubiquitous nature of adipose tissue, many types of solid tumors grow in proximate or direct contact with adipocytes and other adipose-associated cell populations. Although the specific nature of the reciprocal communication occurring between a developing tumor and adjacent adipose tissue is an area of active study, a growing body of literature indicates that these interactions with the local adipose milieu are important drivers of malignancy. Many of these studies have focused on dysregulated adipose and associated systemic metabolic dysfunction in the context of obesity, as there is now adequate evidence establishing a link between obesity/adiposity and elevated risk for, or accelerated progression of, several cancers. Following an overview of the adipose organ, we will briefly address epidemiologic links between obesity and cancer. Subsequently, we have chosen to emphasize the local physical and paracrine roles of adipose tissue in solid tumor development and malignancy by focusing on individual components of the adipose tissue microenvironment. Although adipose dysfunction in obesity will be addressed frequently throughout this review, we aim to provide the reader with an understanding of the recently described mechanistic links between cancer development or progression and adipose tissue *per se*, as opposed to obesity-associated systemic alterations such as metabolic dysfunction.

The Adipose Organ

Adipose tissue is a type of loose connective tissue that was long considered to be largely physiologically inert, primarily storing energy in the form of lipids while cushioning and insulating the body. However, adipose tissue is also a substantial contributor to whole body endocrine signaling, modulating feeding behavior and total body energy expenditure, as well as hematopoiesis and lymphopoiesis, overall immune function, and reproduction [6, 7]. Additionally, adipose tissue is now understood to contribute to the pathogenesis of a variety of regional and systemic diseases. The adipose tissue "organ" is in fact comprised of several distinct adipose depots (**Figure 2**), each of which differentially exerts systemic and regional control on overall energy metabolism and signaling based on location and adipose tissue subtype. Broadly, adipose depots can be divided according to anatomic location into subcutaneous and visceral subtypes. Whole adipose depots, or specific regions within depots, may be further subclassified as white, brown, or beige depending on, among other factors, adipocyte mitochondrial content, with a higher relative number of mitochondria corresponding to a darker adipocyte hue. In humans, subcutaneous adipose tissue comprises ~80% of total body fat, and is contained primarily in the abdominal, gluteal, and femoral depots [8] (**Figure 2A**). The breast fat pad is also a nontrivial contributor to total subcutaneous fat content in women. On the other hand, visceral depots represent approximately 5-20% of total body fat in normal weight (i.e., not overweight or obese) individuals [8]. Visceral adipose tissue surrounds vital organs, and includes omental, mesenteric, and epiploic adipose, as well as the gonadal, epicardial, and retroperitoneal fat pads. Finally, numerous smaller depots, such as intramuscular, intraorbital, and bone marrow adipose, nourish and protect tissues throughout the body. While the majority of these depots are comprised of white adipose tissue – discussed further in the *Adipocytes* section below – smaller brown and beige adipose tissue caches are also found in adults [9, 10]. Importantly, due to similarities in the location and composition of adipose depots and endocrine

function relative to humans, the laboratory mouse (*Mus musculus*) is a commonly used model for investigation of adipose tissue anatomy and physiology (**Figure 2B)**.

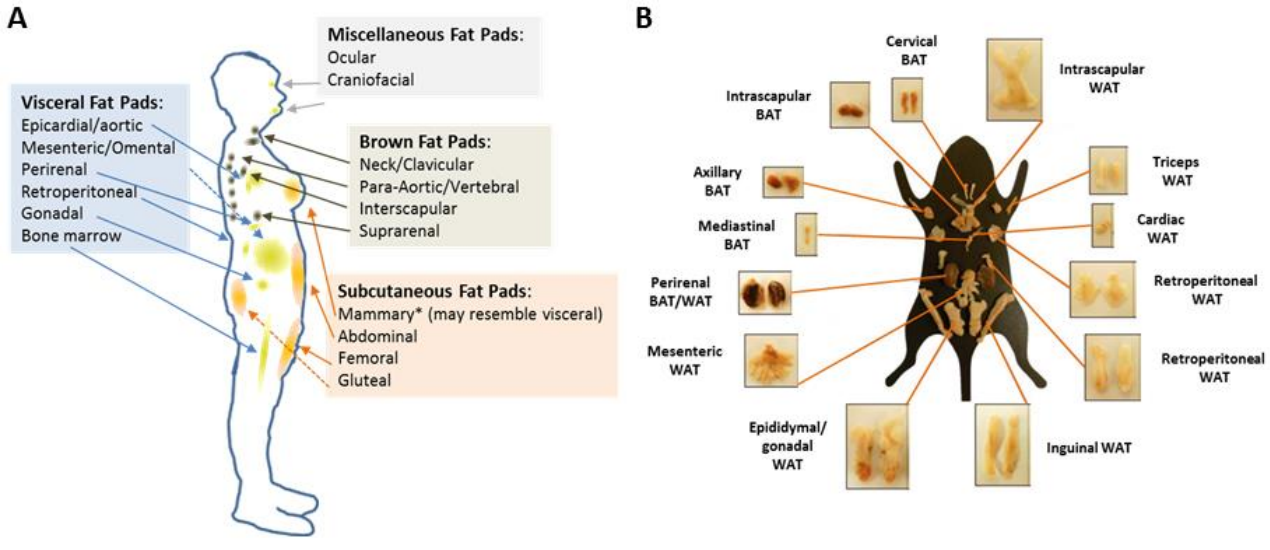

Figure 2. The adipose organ is comprised of several distinct adipose depots. Adipose depot locations and subtypes in A) humans and B) mice (panel B adapted from [11] with permission).

Although adipocytes constitute approximately 90% of adipose tissue *volume*, the adipose tissue microenvironment is a rich ecosystem of additional stromal and vascular components (often referred to collectively as stromal-vascular cells). The stromal-vascular compartment of human white adipose tissue includes endothelial cells (10-20% of cells), pericytes (3-5%), fibroblasts and other connective tissue cells (15-30%), and stem and progenitor cells (0.1%), which reside within a complex milieu of signaling molecules and ECM components [12] (**Figure 3**). Adipose tissue also contains a rich and varied collection of innate and adaptive immune cells (macrophages, dendritic cells, mast cells, eosinophils, neutrophils, and lymphocytes; 25-45%) [12]. However, the exact cellular proportions, degree of vascularity, ECM composition, metabolic characteristics, and secretory products of adipose tissue vary according to numerous factors, including depot location, sex, age, health status, and extent of adipose accumulation [8].

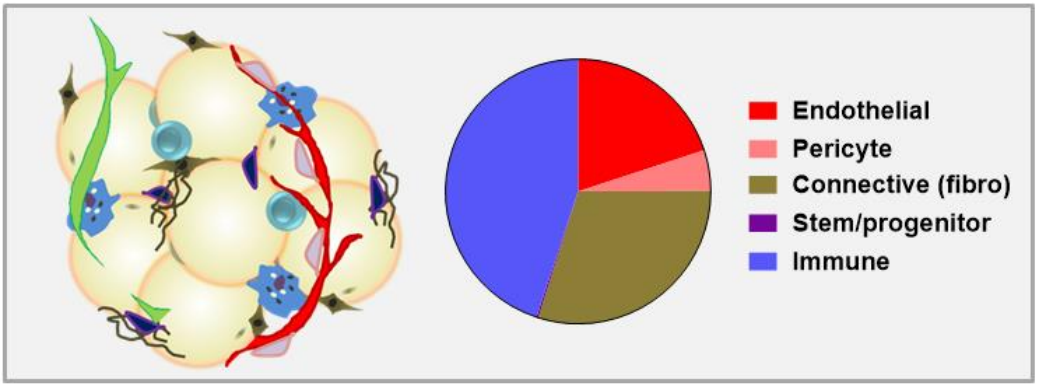

Figure 3. Approximate composition of human white adipose tissue stromal-vascular fraction (percent cellularity).

Obesity and Cancer

Adipose tissue exhibits an almost unlimited capacity to expand, a unique property that has received increased attention in recent years as obesity has moved to the forefront of global public health concerns. Overweight and obesity, defined by the World Health Organization (WHO) as abnormal or excessive adiposity that presents a risk to health, are frequently measured at the population level using the body mass index (BMI), an individual's weight in kilograms divided by the square of his or her height in meters. However, it must be acknowledged that, at an individual level, the BMI formula can vary considerably by sex and race and says little about body composition, often underestimating adiposity [13, 14]. For this reason, additional measures specifically of adiposity, such as waist circumference or the Body Adiposity Index (BAI; [hip circumference (cm)/height (m)$^{1.5}$-18]) developed by Bergman et al. [15], are sometimes used to correlate adiposity with disease risk.

Current status of the obesity epidemic, globally and in the United States

Since the recognition of obesity as a global epidemic in 1997 [16], increasing resources have been allocated to more completely understanding the prevalence, risk factors, and long-term consequences of this health hazard. For example, a recent quantitative meta-analysis

published in *The Lancet* analyzed 1,698 population-based data sources, encompassing 186 countries and more than 19.2 million adult participants (9.9 million men and 9.3 million women), to evaluate trends in mean BMI over the last four decades [17]. The authors reported a global increase in overall age-adjusted prevalence of obesity in men from 3.2% to 10.8%, and in women from 6.4% to 14.9%, between 1975 and 2014 [17] (**Figure 4A**). An additional cross-sectional analysis of the United States National Health and Nutrition Examination Survey (NHANES) for the years 2013-2014 reports that the overall age-adjusted prevalence of obesity (again by BMI) among men and women in the US has now reached a staggering 35% and 40.4%, respectively [18]. Furthermore, extreme obesity (or class 3 obesity, defined as BMI >40) in the US is currently 9.9% for women and 5.5% for men [18], considerably higher than the global prevalence of 1.6% and 0.64%, respectively [17] (**Figure 4B**). Importantly, a disproportionate burden of obesity and overweight is observed among women who self-identify as Hispanic or non-Hispanic black minorities; NHANES data indicate that the overall age-adjusted prevalence of obesity in non-Hispanic black and Hispanic women measures 57.2% and 46.9% respectively, compared to 38.2% in non-Hispanic white women [18] (**Figure 4C**). Finally, it should be noted that rising obesity rates are not restricted to adults. The prevalence of obesity in US children and adolescents ages 2 to 19 years old rose from approximately 10% during the 1988-1994 NHANES period to 17.0% in the 2011-2014 period, with extreme obesity more than doubling from approximately 2.5% to 5.8% [19].

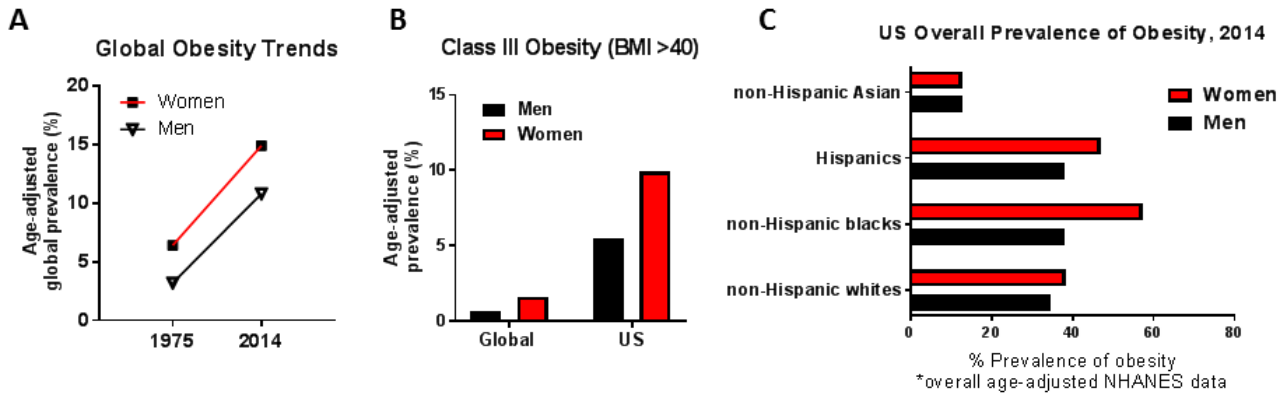

Figure 4. Rising global and US obesity rates. A) Global age-adjusted prevalence of obesity in men and women, 1975 and 2014; B) Class III obesity (BMI >40), globally and US; C) US obesity prevalence by race, ethnicity [17].

The obesity-cancer link

Cancer is currently the second leading cause of death in the United States and is expected to surpass heart disease as the leading cause of death within the next few years [20]. Approximately 40-60% of cancer patients are classified as overweight or obese [21, 22], and in 2004 it was estimated that overweight and obesity accounted for one in seven cancer deaths in men and one in five in women [23]. Importantly, obesity is differentially associated with increased risk of cancer *development* and increased risk of poorer cancer *prognosis*. Indeed, there is adequate evidence to support an association between obesity and increased risk of developing colorectal, post-menopausal breast, endometrial, kidney, esophageal, liver, gallbladder, pancreatic, and thyroid cancers, as well as non-Hodgkin's lymphoma and myeloma [24-28]. There is also strong support for an influence on outcome for several cancer types for which an association between obesity and increased risk of onset remains ambiguous. The American Society of Clinical Oncology (ASCO) has acknowledged that obesity contributes to poorer cancer prognosis following diagnosis in a number of ways, including by impairing the delivery of systemic cancer therapies and by elevating risk of both tumor recurrence and development of additional primary malignancies [29].

Interestingly, there is also a body of literature that supports a protective effect of obesity in overall survival for some cancer types, a finding known as the “obesity paradox”. Potential explanations for the obesity paradox emphasize methodological issues, such as unmeasured confounders and/or a reliance on BMI as a metric for obesity [30, 31]. As mentioned previously, BMI is a rather crude mathematical estimate that does not capture important considerations such as percent adiposity, regional distribution of adiposity (e.g., android vs gynoid obesity), or differences in lean mass. Gonzalez et al. reported that the use of body composition indices resulted in a disappearance of the obesity paradox in 175 cancer patients in which BMI was previously associated with a protective effect, emphasizing the importance of considering body composition in epidemiologic analyses of cancer outcomes [32]. In fact, when body composition was included, loss of lean mass (sarcopenia) was a more important prognostic indicator than BMI for patients exhibiting cancer-associated cachexia, a systemic wasting syndrome frequently observed in end-stage cancer patients that is characterized by a rapid loss of both skeletal muscle and adipose tissue [32, 33]. Thus, additional evidence is needed to determine whether isolated reports of the obesity paradox are simply artefactual or in fact clinically relevant.

Nevertheless, leading hypotheses seeking to explain observed connections between obesity and increased cancer morbidity and mortality emphasize factors such as metabolic disruption-induced growth factor dysregulation; higher levels of circulating adipokines and cytokines secreted by inflamed obese adipose tissue; and elevated production of estrogens by adipose tissue [34, 35]. These hypotheses emphasize the role of adipose as an endocrine organ and obesity as a potential state of adipose endocrine dysfunction. However, the mechanisms whereby adipose accumulation increases risk of tumor onset and/or mediates tumor progression in adipose-adjacent cancers are multifactorial, complex, and likely tissue/organ-specific, in part due to unique paracrine and physical interactions occurring between cancer cells and adjacent adipose tissue. Moreover, growth and invasion of some solid tumors into adjacent adipose may promote tumor aggression even in the absence of obesity. For example, irrespective of BMI, adipose tissue invasion at the tumor margin is associated with

an increase in lymph node metastasis in patients with invasive breast carcinoma [36]. Thus, whether select adipose-mediated mechanisms of tumor promotion are merely exacerbated by obesity or are unique to a dysregulated obese adipose microenvironment in many cases remains to be determined. In this review, we have especially highlighted the role of adipose tissue in the development and progression of breast and prostate cancers due to the prevalence of these cancer types in the US population and their significant contributions to cancer-related mortality (see below).

Breast and prostate cancers are the most frequently diagnosed cancers and the second leading causes of cancer-related death among US men and women, respectively [20]. Due to their now recognized genetic and molecular heterogeneity, these cancer types have been shown to exhibit complex associations with obesity. For example, although the association between obesity and risk of postmenopausal breast cancer is now well established, the relationship between obesity and premenopausal breast cancer risk remains controversial and appears to be dependent upon breast cancer subtype. Specifically, recent work has clarified an association between obesity and premenopausal onset of triple-negative breast cancers (TNBCs), with differential risk according to race [37-41]. Studies from our lab and others have also demonstrated that diet-induced obesity is associated with accelerated TNBC latency (time to development of a palpable tumor) in ovary-intact preclinical mouse models [42-45]. In patients with confirmed breast cancers, obesity is associated with increased risk of breast cancer invasion [46, 47], development of distant metastases [48-50], tumor recurrence [51, 52], and mortality [24, 53-59] irrespective of molecular subtype. On the other hand, the role of obesity in risk of prostate cancer development remains equivocal [60-63], in part because, similar to breast cancer, prostate cancer risk in obese individuals also appears to vary by race [60, 64]. However, in confirmed prostate cancers, obesity is consistently associated with an elevated risk of cancer aggression (clinically advanced cases or high Gleason scoring, a grading system is used to inform the prognosis of men with prostate cancer) and prostate

cancer-associated mortality [65, 66]. Thus, rising obesity rates present an oncological crisis, both globally and within the US.

Following a brief consideration of the anatomy of breast and prostate in humans and laboratory mice - a frequently used model in basic science and translational/pre-clinical cancer studies - potential mechanistic links between adipose tissue and breast and prostate cancer development or progression will be discussed in detail below through a comprehensive examination of the available literature regarding adipose-cancer interactions in each organ.

Anatomy of the Breast and Prostate

The laboratory mouse remains the most widely used animal model for the study of cancer pathophysiology. Consequently, integration of experimental findings with studies of human disease requires an understanding of human and veterinary pathology and anatomy, as well as developmental, molecular, and cellular biology. While this level of detail is beyond the scope of this review, this section will provide a brief comparative biology overview of the breast and prostate in humans and mice as a backdrop for the studies reviewed in subsequent sections.

Mammary gland anatomy and adipose-cancer interaction in humans vs. mice

In both mice and humans, the mammary gland is a unique, dynamic organ that continuously undergoes anatomic and functional changes over the life course [67]. In mice, the nascent mammary gland (“mammary tree”) consists of a network of epithelial ducts, each of which terminates in a stem cell-enriched structure called a terminal end bud (TEB; **Figure 5A**). During sexual maturation, inductive hormonal and growth factor-derived signals stimulate the proliferation of ectodermal cells within these TEBs, driving ductal elongation and branching [68-70]. The mature mammary epithelium continues to undergo further differentiation during later life

stages such as pregnancy, lactation, and post-partum involution, or epithelial regression [70, 71]. Development of the mammary tree and pregnancy/lactation-associated expansion and involution require remodeling of the surrounding stroma. In mice, mammary ductal-adjacent stroma is primarily comprised of adipose tissue, without a significant collagenous matrix layer (**Figure 6**).

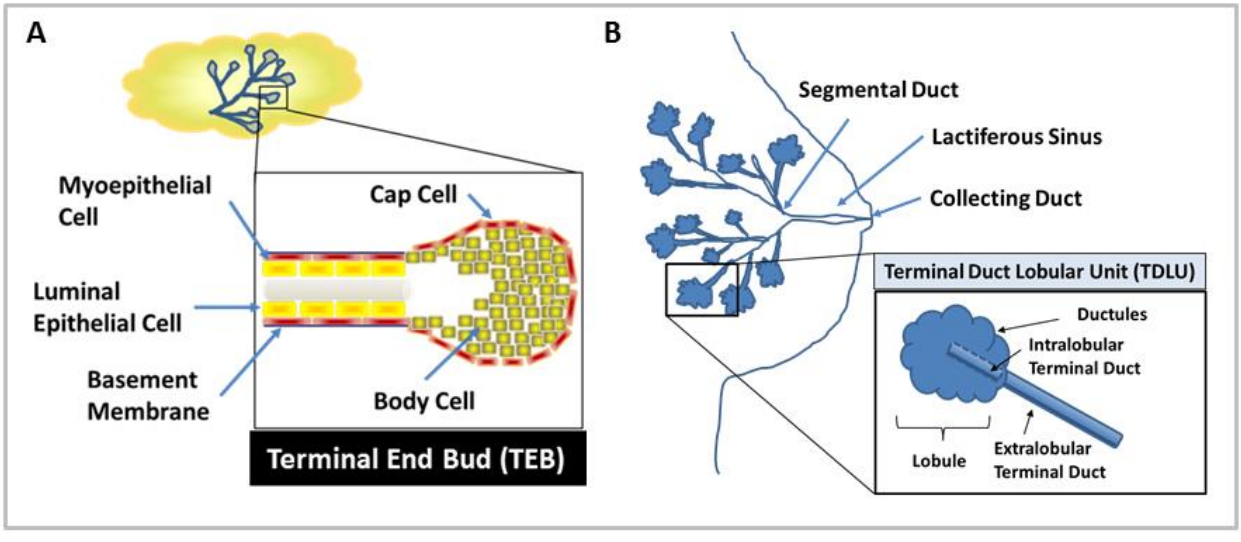

Figure 5. Comparison of mouse and human mammary gland anatomical structure. A) Murine ductal elongation and branching occur at the Terminal End Buds (TEBs). B) The human mammary gland is extensively branched, culminating in the functional terminal ductal lobular unit (TDLU).

In comparison to mouse, the human mammary gland is a more extensively branching structure. Beginning at the nipple, the lactiferous sinus branches into segmental, or interlobular, ducts (**Figure 5B**). Segmental ducts branch further into terminal ducts and lobules, which together comprise the functional unit of the human mammary gland, the terminal ductal lobular unit (TDLU). Immediately surrounding the TDLU is a loose intra-lobular stroma, referred to as "specialized stroma", which contains abundant fibroblasts (**Figure 6**) [71]. Dense, collagenous inter-lobular stroma surrounds the entire human TDLU structure, forming a thick layer between the TDLU and adjacent adipose tissue. Fibroblasts within the intra-lobular stroma exhibit phenotypic and functional differences from those found within inter-lobular stroma, including expression of select collagen isoforms [72] and ectoenzymes [73]. Surrounding the inter-lobular

stroma is a large depot of subcutaneous adipose, comprising 7 to 56% of the volume of the adult breast [74].

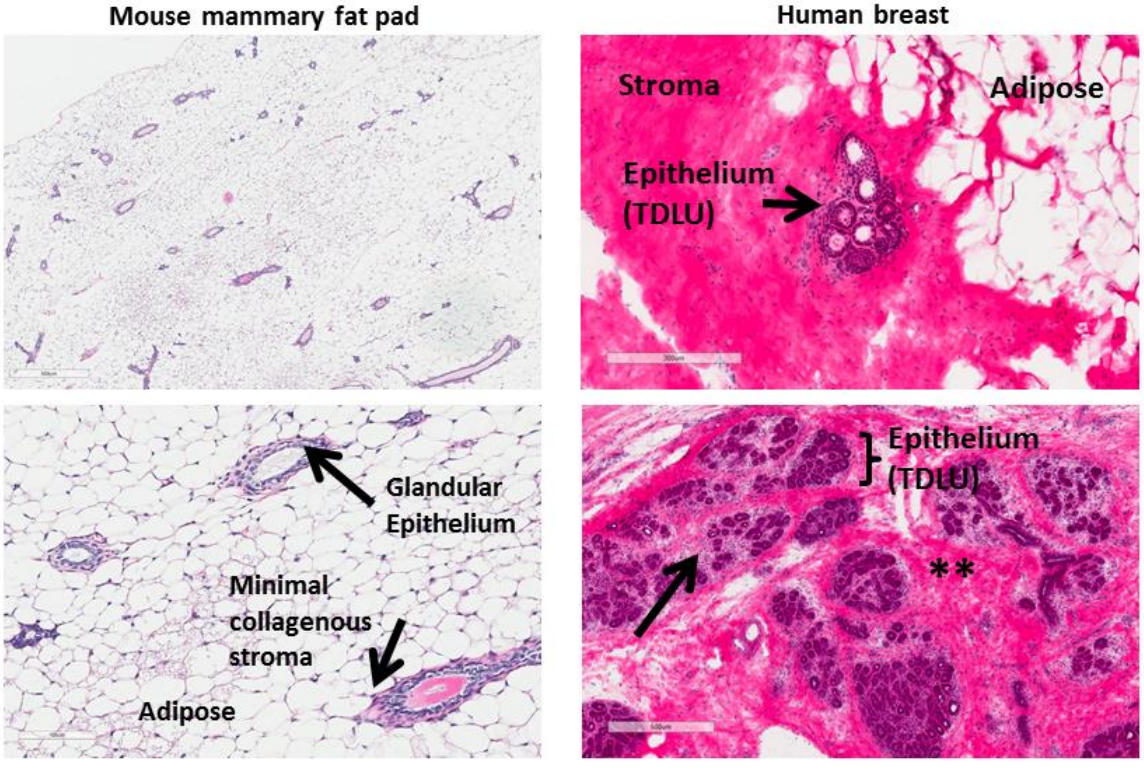

Figure 6. Comparison of mouse and human mammary gland histology. Left: Adult mouse mammary fat pad from nulliparous C57BL/6 mouse (4x and 10x, H&E staining). Right: H&E-stained normal human breast tissue. Arrowhead and asterisks in right panel refer to loose intra- and dense inter-lobular stroma, respectively. Human histology images courtesy of Melissa Troester and the UNC Normal Breast Study (unpublished).

The most extreme example of tumor infiltration into adipose tissue is seen in breast cancer. Breast cancer most frequently begins in ductal epithelial cells, which proliferate to fill the ductal lumen and generate a pre-cancerous lesion called *ductal carcinoma in situ* (DCIS). Subsequently, *invasive ductal carcinoma* (IDC) cells invade the mammary stromal compartment. On the other hand, approximately 1 in 10 invasive breast cancers originate in the lobules, beginning as *lobular carcinoma in situ* and progressing to *invasive lobular carcinoma.* The lack of intra-lobular stroma in mice [71] and relatively thinner collagenous matrix means that tumor cell invasion in mouse models of breast cancer results in immediate encounter of

adipocytes and other adipose cell populations (**Figure 7A**), whereas human invasive breast carcinoma must invade through both intra- and interlobular stroma before direct interaction with an area rich in adipose tissue (**Figure 7B**).

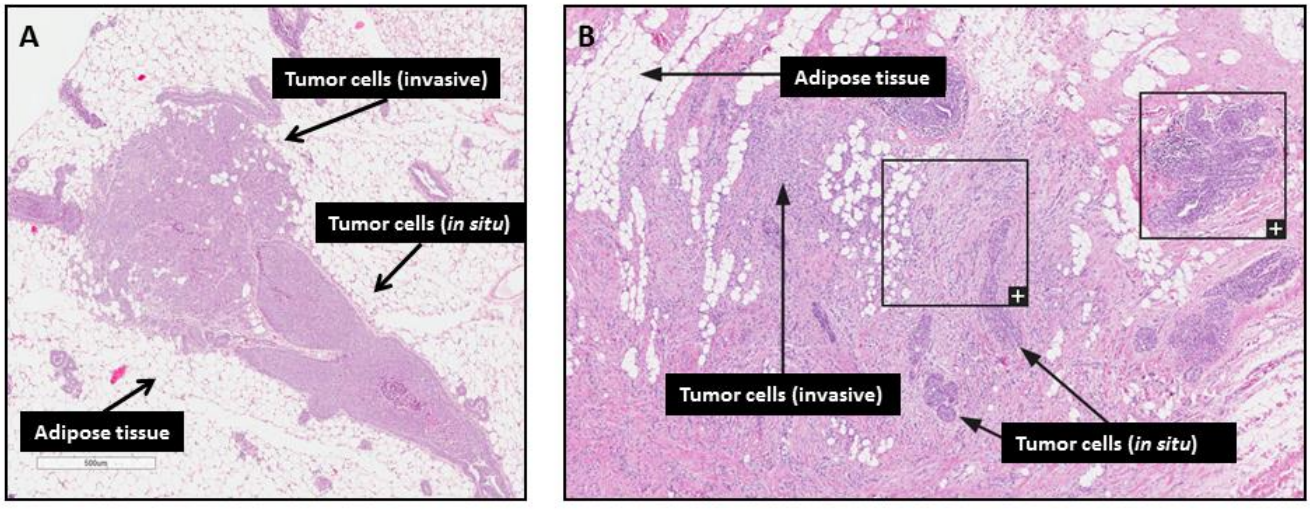

Figure 7. Adipose-breast cancer interactions in mice and humans. A) Early invasive lesions in H&E-stained mammary gland tissue from the C3(1)-TAg genetically-engineered mouse model of spontaneous basal-like breast cancer (unpublished images). B) Human breast cancer - Female, 50 years, lobular carcinoma, grade 1, Elston-Ellis score 5. Image credit: The Human Protein Atlas [75, 76].

Prostate gland anatomy and adipose-cancer interaction in humans vs. mice

Like the mammary gland, the prostate exhibits important inter-species differences between mice and humans. However, before progressing to a comparison of mouse and human prostate anatomy, it should be acknowledged that rat and canine models have generated important mechanistic knowledge in prostate cancer research, particularly in the context of the spontaneous development of prostate lesions [77]. With that said, genetically engineered or xenografted mice remain the most commonly used model in prostate cancer research. For an overview and critique of currently available mouse models of human prostate cancer, the reader is directed to [77, 78].

In mice, the prostate is comprised of four lobes lying anterior and lateral to the urethra. These lobes are named after their spatial orientation (anterior, dorsal, ventral, and lateral lobes,

see diagram in **Figure 8**) and exhibit distinctive histology [77, 79]. The glandular acini of the prostatic lobes are surrounded by a thin fibromuscular tunica, and are embedded in a loose connective tissue stroma with minimal smooth muscle cells and sparse collagen fibers [79]. Individual mouse prostate lobes are surrounded by a delicate mesothelium-lined capsule, and are separated from each other by fibrous and adipose connective tissue [79].

In contrast to mice, the human male prostate does not have exterior lobation, but instead contains distinct glandular regions (a peripheral zone, a central zone, and a transition zone; see diagram in **Figure 8**) [79], again with characteristic histology. Like the breast, a conspicuous histological difference between mouse and human prostate lies in the stromal component. In humans, the prostate gland bears an anterior, well-developed, non-glandular fibromuscular stromal region. Abundant adipose tissue is present surrounding most of the posterolateral aspects of the prostate [80], and is used as a marker of extraprostatic tissue in biopsy samples [81]. This region of adipose is referred to in subsequent sections as *periprostatic adipose*. Intraprostatic adipose, when present, consists of a small focus of a few adipocytes, and is rarely observed histologically [81].

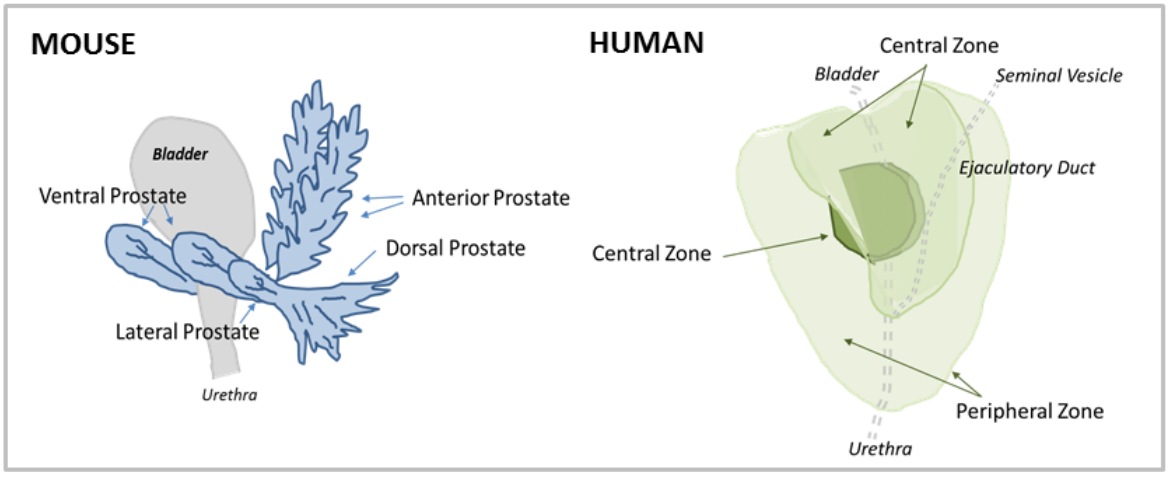

Figure 8. Anatomical comparison of mouse (left) and human (right) prostate glands.

The most common type of prostate cancer is acinar adenocarcinoma, which originates from the glandular epithelium. Pre-neoplastic *prostatic intraepithelial neoplasia* (PIN) progresses to *invasive adenocarcinoma*, in which extension of prostatic carcinoma through the prostatic capsule (extraprostatic extension) and resulting interaction with the surrounding adipose is an indicator of malignant progression and advanced histopathological stage [82]. The periprostatic adipose depot unambiguously contributes to prostate cancer malignancy [83-85]. In fact, interaction with periprostatic adipose tissue has been suggested to be a more important determinant of cancer recurrence than an invasive phenotype [86]. Analogous to breast cancer, recent advances in molecular phenotyping by The Cancer Genome Atlas Research Network have identified several genomically distinct molecular subtypes of prostate cancers [87]. Whether these subtypes interact differentially with adjacent adipose remains to be determined.

Microenvironmental Links between Adipose Tissue and Cancer

Context matters: extracellular matrix in adipose tissue and cancer

Adipocytes and stromal cells are embedded in a loose, three-dimensional ECM, the non-cellular tissue component that provides both structural and biochemical support to surrounding cells, such as cell adhesion, paracrine communication, and differentiation signals. Maintenance of the adipose tissue ECM – primarily comprised of fibronectin and collagens [88] – involves a variety of cell types, including fibroblasts, macrophages, adipocytes, and preadipocytes. Importantly, adipocyte function and survival is tightly regulated by both the molecular composition and mechanical properties of the surrounding ECM [89].

The structural flexibility of adipose tissue ECM facilitates transient volume changes in response to normal fluctuations in lipid stores throughout the feed-fast cycle. However, rapid adipocyte hypertrophy (increased adipocyte volume) during the development of obesity can result in intracellular or regional hypoxia. Reduced tissue oxygenation induces transcriptional

programs in adipocytes and other stromal cells that ultimately lead to excess deposition of fibrillar ECM components such as collagens I, III, and VI and development of tissue fibrosis [88, 90]. Indeed, adipose depots of obese subjects often exhibit greater total fibrosis, and particularly pericellular fibrosis around adipocytes, than lean individuals [91, 92]. Importantly, hypoxia-induced adipose tissue fibrosis is associated with onset of metabolic perturbations in adipocytes [88, 93], while dysregulation in visceral adipose function is linked to the pathogenesis of insulin resistance and type II diabetes mellitus [92-94]. Furthermore, as adipocytes become encapsulated in a shell of rigid ECM, impaired cellular function also results in apoptosis and necrosis [95]. Release of damage-associated molecular patterns (DAMPs) from dead and dying adipocytes and adjacent live adipocytes promotes recruitment of macrophages and other inflammatory cells; histologically, these macrophages can be observed within crown-like structures (CLS), foci of macrophages and other inflammatory cells surrounding dead and dying adipocytes [96]. Macrophages are fully integrated into all stages of the fibrotic process through secretion of soluble mediators and cytokines such as transforming growth factor β1 (TGF-β1), platelet-derived growth factor (PDGF), and chemokines that attract and activate fibroblasts and collagen-producing myofibroblasts [88, 97].

Interestingly, while adipose tissue fibrosis in the context of obesity is well described, increased adipose ECM deposition, fibrosis, and immune cell infiltration are also observed in cancer-associated cachexia [98]. Abdominal subcutaneous adipose depots of lean cachectic subjects bearing gastrointestinal cancers displayed extensive adipose ECM remodeling, including a dramatic increase in deposition of collagens I, III, and VI as well as elastin and fibronectin [99]. These changes were associated with increased myofibroblast content and elevated activation of TGF-β/SMAD signaling pathways [99]. As described later in the *Adipocytes and adipocyte-cancer interactions section*, cancer-associated cachexia is also associated with metabolic dysfunction in adipocytes, which may be mediated in part by ECM modifications.

In addition to adipocytes, epithelial tissue homeostasis and tissue organization is also heavily dependent upon a dynamic dialogue with the surrounding ECM. Disruption of ECM structure or misinterpretation of ECM-derived signals due to alterations in signaling receptor profiles is associated with development of a malignant phenotype in transformed epithelial cells [100-102]. Enhanced ECM stiffness also triggers the process known as epithelial-to-mesenchymal transition (EMT) in cancer cells, which is characterized by the loss of epithelial polarity, de-differentiation, and local migration and invasion [103-106]. Hence, modifications in the adipose tissue ECM that provide a hospitable environment to developing tumors, such as enhanced stiffness in obese breast tissue, may provide a link between adipose tissue and tumorigenesis.

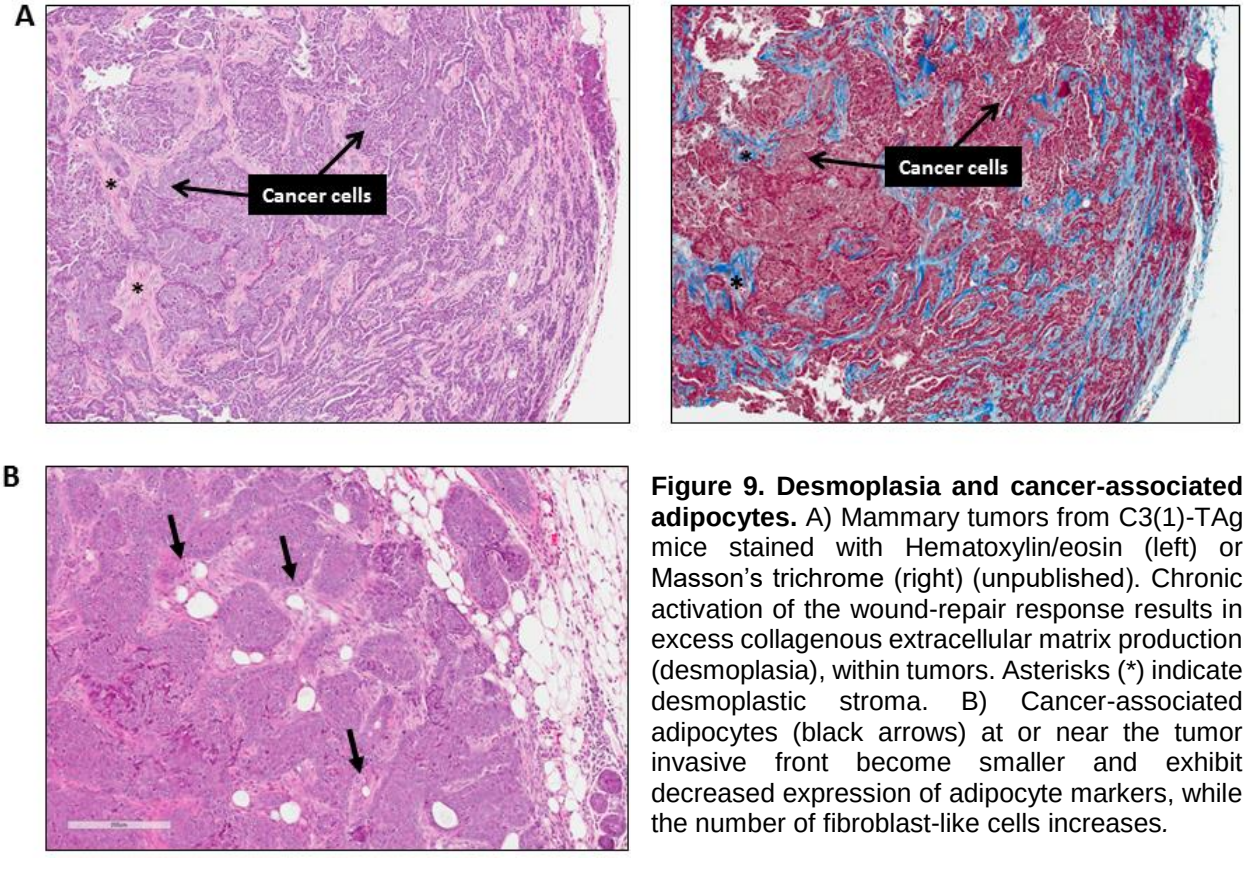

Figure 9. Desmoplasia and cancer-associated adipocytes. A) Mammary tumors from C3(1)-TAg mice stained with Hematoxylin/eosin (left) or Masson's trichrome (right) (unpublished). Chronic activation of the wound-repair response results in excess collagenous extracellular matrix production (desmoplasia), within tumors. Asterisks (*) indicate desmoplastic stroma. B) Cancer-associated adipocytes (black arrows) at or near the tumor invasive front become smaller and exhibit decreased expression of adipocyte markers, while the number of fibroblast-like cells increases.

As discussed in later sections, chronic low-grade inflammation, macrophage infiltration, hypoxia, and aberrant wound healing responses, including an increase in myofibroblast and

activated fibroblast content, are features of both the tumor and adipose tissue microenvironments [4, 102, 107]. Chronic activation of the wound repair response leads to excess deposition of ECM components and accumulation of scar-like fibrotic tissue in a process known as *desmoplasia*, or the *desmoplastic reaction* (**Figure 9A**). In both breast and prostate cancers desmoplasia is associated with poor outcomes [108, 109], and can facilitate cancer progression by interfering with drug delivery. Thus, ECM remodeling and the resultant disturbances in cytoskeletal tension and mechanotransduction have emerged as important factors that promote neoplastic transformation, cancer malignancy, and cancer metastasis [4, 102, 110], and may provide another connection between adipose dysregulation and cancer.

Adipose extracellular matrix composition and viscoelasticity: influence on the normal breast and breast cancer

Mammographic density denotes the radiologic appearance of the breast, and is a metric of the fibroglandular (epithelial and non-fatty stromal) content in that tissue [111]. A number of qualitative and quantitative methods have been developed to estimate mammographic density, including Breast Imaging Reporting and Data System (BI-RADS) categories, Wolfe's parenchymal patterns, Tabar's classification scheme, and numerous two- and three-dimensional image analysis techniques [112]. Within heterogeneous breast tissue, tumors most frequently arise within the most mammographically dense regions of the breast, suggesting that denser fibroglandular tissue directly influences carcinogenesis [113]. Indeed, regardless of the reporting method [111], high mammographic density is consistently and strongly associated with both elevated risk of breast cancer [114] and more aggressive tumor characteristics [115], even after adjustment for other risk factors such as age and BMI [116].

At the molecular level, high mammographic density reflects the development of a dense, collagenous stroma rich in type I and/or type III collagen [117, 118]. Similar stromal changes are also observed in breast cancers [119], wherein they are orchestrated by a heterogeneous,

reactive population of so-called “cancer-associated fibroblasts” (CAFs). CAFs display remarkable plasticity, and frequently differentiate into myofibroblasts, a cell type exhibiting properties of both fibroblasts and smooth muscle cells [120-122]. In non-malignant tissue, myofibroblasts play an important role in wound healing responses, secreting a fibronectin- and collagen type I-rich ECM characterized by fibrillary architecture and increased cross-linking and density [123]. They are also the predominant source of fibrogenic and/or inflammatory cytokines in fibrotic lesions [124]. Despite the utility of this cell type to normal wound healing programs, however, the presence of myofibroblasts in tumors contributes to pathological desmoplasia [122], and may thus promote cancer progression [125].

In addition to fibroblasts, local (adipose-derived) mesenchymal stem cells, bone marrow-derived mesenchymal stem cells, myeloid precursors, and cells derived from EMT may also present alternative sources of myofibroblasts in tumor stroma [126-128]. Furthermore, in tumors growing in an adipose tissue-rich microenvironment, cancer cell-induced reprogramming of local adipocyte gene expression and function has been observed to promote adipocyte delipidation and atrophy/regression [129]. This process occurs concurrently with the accumulation of fibroblast-like cells and a desmoplastic stroma; this synchronicity raises the possibility that some CAFs might be derived from dedifferentiated adipocytes [129] (**Figure 9B**). However, the extent to which their specific lineages determine the contribution of CAFs to tumor progression remains inconclusive.

Although obesity is associated with reduced mammographic density – in part because fat is radiolucent – several studies have unveiled close links between chronic inflammation and the development of fibrosis and associated ECM rigidity in obese mammary adipose tissue [123, 130, 131]. Myofibroblasts are typically absent from normal, uninflamed breast tissue [132]. However, Seo et al. showed that obesity elevated matrix rigidity in non-cancerous breast tissue by enhancing myofibroblast content in mammary adipose [123]. Adipose stromal cells (ASCs, also called adipose-derived stem cells) isolated from obese mice exhibited increased expression of α-smooth muscle actin (α-SMA, a myofibroblast marker), as well as increased

fibronectin and a more fibrillar, partially unfolded, and stiffer ECM [123], implicating ASCs as a source of myofibroblasts in obesity. Furthermore, obese ASCs also exhibited enhanced proliferative capacity and secreted increased quantities of matrix components [123], thereby mimicking characteristics of tumor-associated stromal cells [122, 133]. Consistent with findings in mice, histologically normal breast tissue from obese patient mastectomies exhibited increased α-SMA staining and collagen fiber length and thickness relative to tissue from lean individuals [123]. Obesity-associated increases in α-SMA levels also correlated with formation of CLS, further implicating macrophages in the development of mammary adipose tissue fibrosis [123]. However, distinct from tumors [133], obesity-associated increases in myofibroblast content and matrix rigidity occurred in a TGFβ-independent manner [123], suggesting that ECM composition and stiffness may be differentially regulated in benign obese and malignant breast tissue.

Increased matrix rigidity in breast adipose tissue may be an important mediator of cancer initiation and progression in obese individuals. To test the effects of obesity and ECM on tumor cell behavior, Seo et al. cultured pre-invasive human MCF10AT cells upon decellularized matrices produced by ASCs isolated from lean or obese mice. The authors reported that, relative to ECMs deposited by lean ASCs, obesity-associated ECMs increased MCF10AT cell motility and promoted the formation of disorganized three-dimensional acini, indicative of greater tumorigenic potential [123]. Additionally, ECM generated by obese mammary ASCs significantly enhanced the proliferation of the highly invasive MDA-MB-231 cancer cell line by altering mechanotransduction through enhanced RhoA/ROCK-mediated cell contractility and YAP/TAZ transcription factor activity [123]. Collectively, these results are suggestive of a relationship between obesity-associated mammary adipose tissue fibrosis and accelerated tumor initiation and/or proliferative capacity.

In addition to fibroblasts/myofibroblasts, adipocytes play a vital role in defining the ECM environment through secretion and processing of factors such as collagen VI, an ECM component with both structural and signaling roles that is highly enriched in adipose tissue [93,

134, 135]. Excess adipocyte collagen VI expression in obesity is associated with adipose tissue fibrosis and metabolic dysregulation, while the absence of collagen VI in mouse models of obesity allowed for uninhibited adipocyte expansion and an improved metabolic phenotype [93]. Increased adipocyte collagen VI expression is also associated with elevated local concentrations of endotrophin, the collagen VI α3 chain cleavage product, which has been identified as a driving factor in adipose tissue fibrosis, macrophage chemotaxis, and inflammation, and appears to mediate adipose metabolic dysregulation in obesity (**Figure 10**) [131, 135]. Unsurprisingly, increased collagen VI production also coincides with increased adipose tissue macrophage content [130, 135].

To further illustrate parallels in the obese adipose and tumor microenvironments, collagen VI and its cleavage product have also been implicated in the initiation and progression of breast cancers. Collagen VI is abundantly expressed by breast cancer-associated adipocytes (discussed at greater length in the *Adipocytes* section below), and its increased deposition in the ECM promotes tumorigenesis and malignant progression both *in vitro* and *in vivo* by inducing alterations in cancer cell signaling programs, gene expression patterns, and post-translational modifications [136, 137]. For example, treatment of MCF-7 human invasive breast cancer cells with collagen VI significantly elevated activity of the oncogenic Akt-GSK3β–β-catenin–Tcf/Lef pathway, ultimately resulting in cyclin D1 protein stabilization and enhanced cell proliferation [136, 137]. Accordingly, expression of the proto-oncogenes GSK3β and cyclin D1 in mammary tumors exhibited a steep immunohistochemical gradient, with increased staining intensities observed proximate to adipocytes. A similar gradient in collagen VI expression was also observed, further implicating adipocyte-derived collagen VI in the induction of mitogenic signaling pathways [136]. In addition, collagen VI-derived endotrophin induces markers of EMT in cancer cells and acts as a potent adipokine that exerts growth-stimulatory and pro-survival effects on developing tumors [135]. In the breast tumor microenvironment, endotrophin overexpression is associated with increased rate of metastasis [135] and resistance to the platinum-based chemotherapeutic cisplatin [138]. Thus, increased collagen VI deposition and

endotrophin concentration in obese adipose may influence both early tumor development and treatment outcomes.

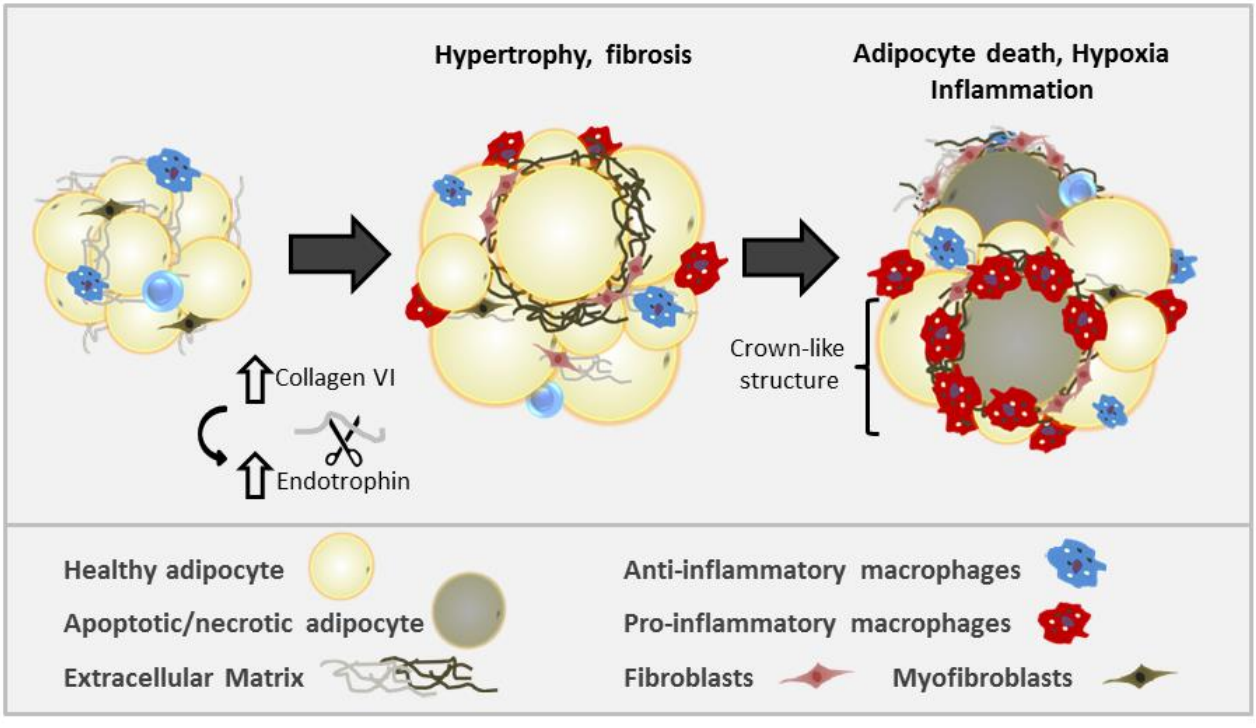

Figure 10. Obesity-associated modifications in the adipose tissue microenvironment. Adipose tissue expansion in obesity occurs in association with extracellular matrix changes such as fibrosis. Adipocyte hypertrophy and hypoxia trigger macrophage infiltration and crown-like structure formation, which further exacerbates development of fibrosis and inflammation.

Adipose extracellular matrix-derived factors: direct effects on epithelial cells

In addition to modulating composition and viscoelasticity of the breast ECM, stromal cells within the obese breast microenvironment secrete numerous soluble signaling mediators that have direct effects on epithelial cells. In particular, HGF is an excellent candidate for stromal-mediated breast cancer promotion in the context of obesity. Although HGF is classified as an adipokine [139], it is produced by a number of breast cell types including stromal fibroblasts and has been detected in both normal and malignant breast tissue [140]. In advanced tumors, HGF signaling through its receptor cMET initiates an invasive growth program that promotes cell migration, invasion, proliferation, and angiogenesis (**Figure 11**)

[141]. HGF is also elevated in the serum of breast cancer patients and correlates with advanced disease [142-145]. However, HGF signaling impacts the phenotypes of both early- and late-stage breast cancers. With respect to early-stage lesions, we have reported that treatment of pre-malignant basal-like breast cells with HGF-blocking antibodies inhibited 3D morphogenesis, reflecting a reduction in epithelial malignant potential [142]. An HGF gene expression signature generated via treatment of pre-malignant breast cells with recombinant HGF was also found to correlate with both basal-like subtype and poor survival in >700 breast cancer samples from three publicly available datasets [142].

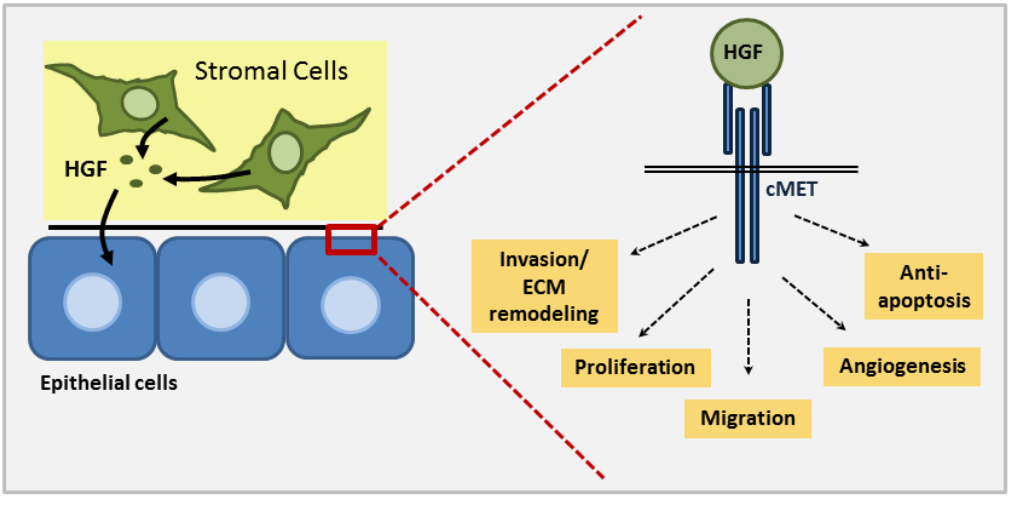

Figure 11. HGF/cMET: an oncogenic signaling cascade. HGF secretion by stromal cells such as fibroblasts, adipocytes, and macrophages initiates an invasive growth program in epithelial cells.

Importantly, basal-like breast cancer is a clinically intractable TNBC subtype that is more prevalent in obese individuals [37-41], while serum HGF is also elevated in obese individuals and is reduced with weight loss [146-148]. Our laboratory previously demonstrated that high fat diet-induced obesity increased HGF concentration and enhanced expression and activation of cMET in the mammary fat pad of C3(1)-T-antigen (TAg) mice, a unique genetically engineered mouse model (GEMM) of spontaneous basal-like breast cancer [43, 149, 150]. We also reported that obesity increased HGF production by primary murine fibroblasts isolated from both normal mammary glands and tumors, and that CAFs isolated from obese animals induced epithelial cell

migration in an HGF-dependent manner [43]. Obesity-mediated regulation of HGF secretion from other stromal cell types such as adipocytes is currently under investigation.

Adipose extracellular matrix in prostate cancer

Despite being a common feature of mouse models of prostate cancer, histologically conspicuous reactive stroma is much less prevalent in human prostate tumors compared to breast cancers [77]. However, like the breast, induction of a myofibroblastic phenotype and degree of reactive stroma carry important prognostic value for prostate cancer malignancy [109, 151, 152]. Notably, as the literature regarding the contribution of adipose tissue to breast cancer onset and progression has greatly outpaced that of prostate cancer, obesity-associated ECM modifications are currently better characterized in the mammary, relative to the periprostatic, fat pad. Additionally, conflicting data exist regarding the association between periprostatic fat density (measured by magnetic resonance imaging or computed tomography) and tumor aggressiveness in prostate cancer patients [153-155]. Our literature search also revealed no publications reporting that periprostatic adipose tissue fibrosis occurs in obesity, but whether this is due to a lack of occurrence or a lack of examination is unknown. Furthermore, no studies investigating links between adipocyte-derived endotrophin and prostate cancer were available at the time of writing this review. Therefore, future obesity-prostate cancer studies may be informed by the sundry findings linking breast cancer and adipocyte-associated fibrosis, modifications in ECM dynamics, and endotrophin release.

Adipocytes and adipocyte-cancer interactions

Adipocytes are specialized connective tissue cells that constitute a major cell type in both the normal-weight and obese breast. The majority of adipocytes in adult humans are white adipocytes, which contain a large, unilocular lipid droplet and are specialized for storage of

neutral lipids. However, brown and/or beige adipocytes (also called “brite” or “inducible” adipocytes [9]) have also been reported in adults, and likely play important roles in thermogenesis [156]. More recently, “pink” adipocytes have been described in murine mammary gland, arising exclusively during pregnancy and lactation due to a process wherein white adipocytes progressively transdifferentiate to acquire secretory, epithelial-like features [9]. Adipocytes secrete a broad range of signaling molecules that exert local and/or systemic effects with the potential to influence tumor growth. Among the better studied adipocyte-derived factors are metabolic factors such as leptin, adiponectin, resistin, visfatin, and plasminogen activator inhibitor-1 (PAI-1); hematopoietic factors such as GM-CSF; growth factors such as angiopoietins, HGF, vascular endothelial growth factor (VEGF), insulin-like growth factor-1 (IGF-1), and TGF-β; and a variety of cytokines, including interleukin-6 (IL-6) and TNF-α and the chemokine monocyte chemoattractant protein (MCP-1) [also referred to as chemokine (C-C motif) ligand 2 (CCL2)] (**Figure 12**) [157, 158].

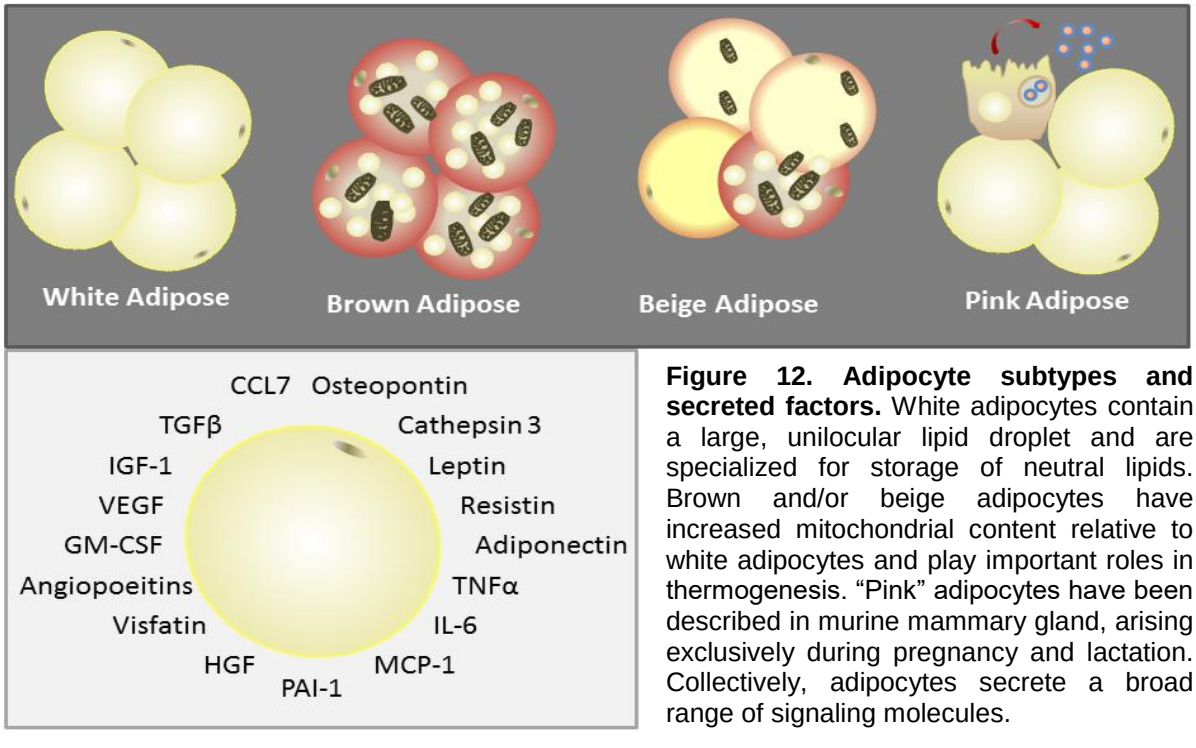

Figure 12. Adipocyte subtypes and secreted factors. White adipocytes contain a large, unilocular lipid droplet and are specialized for storage of neutral lipids. Brown and/or beige adipocytes have increased mitochondrial content relative to white adipocytes and play important roles in thermogenesis. “Pink” adipocytes have been described in murine mammary gland, arising exclusively during pregnancy and lactation. Collectively, adipocytes secrete a broad range of signaling molecules.

Several of the aforementioned adipocyte-derived growth factors influence development of a tumor vascular supply (*tumor angiogenesis*), as discussed in the *Endothelial Cells/Lymphendothelial Cells* section below. Whereas leptin and adiponectin are considered true adipokines, many of the other signaling molecules, including resistin, visfatin, TNF-α, IL-6, MCP-1 and PAI-1, are not, as they are expressed by both adipocytes and immune cell populations such as macrophages, and play a variety of well-known roles in immunity [157]. Thus, select functions for several of these signaling molecules will be discussed within the section titled *Adipose Tissue Immune Populations in Cancer Development and Progression*. Finally, although there are clear and important roles for leptin and adiponectin in tumorigenesis and malignancy, these roles have been reviewed extensively by others [139, 159-162] and will be addressed only briefly within this review.

Adipocytes exhibit both short- and long-range interactions with cancer cells, and may be found in close proximity to tumors, along tumor margins, and within the tumor body. These *cancer-associated adipocytes* (CAAs; also referred to as peritumoral, intratumoral, or tumor-infiltrating adipocytes) influence tumor biology in a number of ways, including by promoting angiogenesis and inflammation [reviewed in 163, 164, 165]. Although it is reasonable to hypothesize that proliferation and invasion of tumor cells into cancer-adjacent adipose may account for the presence of CAAs within the tumor body, the origin of CAAs in fact remains unclear. As explained in further detail in the section on *Adipose-derived Stromal Cells* below, several cell types may give rise to intratumoral CAAs.

In addition to indirect mechanisms of tumor growth promotion (e.g., stimulation of angiogenesis, production of proinflammatory cytokines), the proximity of CAA to growing tumors may also provide direct metabolic benefits to cancer cells. In the phenomenon known as *metabolic symbiosis*, cancer cells within hypoxic regions of a tumor undergo metabolic shifts that facilitate increased utilization of fuel sources such as lactate, glutamine, and fatty acids released by surrounding cells, including other cancer cells [166, 167] and adipocytes [168, 169]. As mentioned previously, CAAs have been frequently observed to undergo delipidation. Lipid

droplet size within mature white adipocytes is the net result of several processes, including fatty acid uptake or *de novo* fatty acid synthesis, esterification, and lipolysis. Interestingly, Nieman et al. showed that co-culture of primary omental adipocytes with ovarian cancer cells, which frequently metastasize to the omentum, induced lipolysis in adipocytes, upregulation of β-oxidation in cancer cells, and direct transfer of lipids between the two cell types [170]. Notably, the transfer of lipids from adipocytes to cancer cells has also been observed in prostate cancer [171] and breast cancer [172]. These findings indicate that active heterotypic cellular interactions between cancer cells and adipocytes induce metabolic symbiosis.

CAAs may also influence cancer cell phenotypes through the shedding of exosomes, small vesicular bodies released from cells as a form of short- or long-range communication. Lazar et al. [173] reported that exosome shedding by mature human adipocytes induced increased migratory and invasive behavior in melanoma cells, which grow in proximity to the hypodermal adipose layer. Proteomic analysis of adipocyte-derived exosome composition revealed enrichment for proteins involved in mitochondrial lipid metabolism, particularly fatty acid oxidation. Remarkably, their results suggested that these enzymes were incorporated and utilized by melanoma cells. Melanoma cells pre-treated with exosomes exhibited an increased ability to form lung metastases in mice and an increase in fatty acid oxidation without a concomitant change in glycolysis, indicating that augmentation of lipid oxidation pathways occurred in the absence of complete metabolic reprogramming. In further support of these findings, administration of the mitochondrial fatty acid oxidation inhibitors etomoxir or trimetazidine reversed exosome-induced enhancement of migration without affecting basal migration levels. Importantly, increasing adiposity in obese individuals enhanced both the number of exosomes released from adipocytes as well as the potency of their effect on melanoma cell migration. Collectively, these studies reveal important roles for adipocytes in regulating cancer cell metabolism, migration, and metastatic potential.

Adipocytes in the normal breast and breast cancer

Mouse models have revealed that adipocytes act as local regulators of normal mammary epithelial cell growth and function. In fact, mammary epithelial cells require adjacent adipocytes during embryonic and postnatal development, as well as throughout later life stages such as pregnancy, lactation, and involution [174]. Indeed, using the novel FAT-ATTAC mouse, a model of inducible and reversible adipocyte loss developed by Scherer and colleagues, Landskroner-Eiger et al. showed that adipocytes play crucial roles in normal growth and development of mammary ductal epithelium [175, 176], contributing both to ductal branching morphogenesis during puberty and to maintenance of normal alveolar structures in adulthood [176].

Due to the proximity of the adipose pad to the mammary glandular organ, ductal tumor invasion results in interaction of breast cancer cells with adipocytes (**Figures 6 & 7**), with dramatic implications for tumor cell biology. Carter and Church reported that mature breast adipocytes, but not preadipocytes, increased motility of both normal and malignant breast epithelial cell lines through secretion of PAI-1 [177]. Similarly, higher levels of CAA-specific IL-6 expression in human breast tumors were associated with larger tumor size and more extensive lymph node involvement [178]. Co-culture with adipocytes also induced mesenchymal features in human breast cancer cells, including repolarization of vimentin and downregulation of E-cadherin, thereby promoting tumor cell invasion and metastasis [178]. Furthermore, adipocytes co-cultured with malignant breast epithelial cells exhibited the profound phenotypic changes associated with CAA, including delipidation and decreased expression of adipocyte markers [178]. Hence, bidirectional communication between adipocytes and breast tumor cells also alters adipocyte biology.

For example, reminiscent of findings in melanoma [173], prostate [171], and ovarian cancers [170] (discussed in the *Adipocytes and adipocyte-cancer interactions* intro section above), following co-culture of breast cancer cells with adipocytes Wang et al. reported increased lipolysis by adipocytes and concomitantly increased fatty acid oxidation by breast cancer cells [172]. Importantly, the signal released by tumor cells to induce adipocyte

delipidation was not identified, although IL-6 and β-adrenergic stimulation – factors previously implicated in lipolytic induction in cancer-associated cachexia [179] – were eliminated as potential candidates [172]. Similar to Lazar et al. [173], Wang et al. reported that co-culture with adipocytes increased both *in vitro* invasion toward a stimulus and formation of breast cancer lung metastases *in vivo*, each of which were restored to basal levels by administration of the fatty acid oxidation inhibitor etomoxir [172]. *In vitro* etomoxir administration also reduced the morphological hallmarks of EMT. Remarkably, the increase in fatty acid oxidation by breast cancer cells appeared to be dependent on an upregulation of both adipocyte triglyceride lipase (ATGL) and the carnitine palmitoyltransferase 1 (CPT1) isoform CPT1A, enzymes not expressed at appreciable levels in noncancerous human breast epithelial cells. Short-hairpin (sh)RNA-mediated knockdown of CPT1A and ATGL reduced hallmarks of EMT and invasive potential, respectively.

In addition to oxidizing transferred fatty acids, breast cancer cells also esterified free fatty acid from adipocyte lipolysis [172], incorporating the newly synthesized triglyceride into lipid droplets within the cancer cells themselves. Breast cancer cell lipid droplet accumulation was supported by both *in vitro* co-culture experiments employing radiolabeled palmitate and the observation of lipid droplet accumulation in breast cancer cells along the tumor margin in histological sections (i.e., in close proximity to adipocytes). Interestingly, despite increased fatty acid oxidation, breast cancer cells also showed reduced ATP content and activation of AMP-activated protein kinase (AMPK). AMPK activation following co-culture with adipocytes was associated with increased mitochondrial biogenesis and function, indicated by increased levels of PGC-1α and its associated transcription factor PPARα as well as an increase in the ratio of mitochondrial to genomic DNA. AMPK also inhibited acetyl-CoA carboxylase, the rate limiting enzyme in fatty acid oxidation, ensuring uninterrupted flux of fatty acids into mitochondria. Furthermore, breast cancer cell fatty acid oxidation was determined to be uncoupled from ATP production and, unlike in melanoma [173], occurred with a concurrent increase in anaerobic glycolysis, consistent with activation of AMPK [172]. Collectively, these findings provide new

insight into mechanisms of metabolic symbiosis between adipocytes and cancer cells in breast tumors.

Interactions between cancer cells and adjacent adipose may also increase breast cancer stem cell abundance and facilitate metastatic progression. Picon-Ruiz et al. isolated human adipocyte stem cells and used adipogenic differentiation media to generate “immature” adipocytes. Co-culture of these “immature” adipocytes with both primary breast cancer cells and established cancer lines conferred stem-like features to the epithelial cells, including elevated expression of the pluripotency markers Sox2, c-Myc, and Nanog [180]. Co-culture with adipocytes also increased mammosphere-forming capacity, indicating a more stem-like phenotype due to a greater ability to grow under non-adherent conditions. Furthermore, when co-cultured breast cancer lines were orthotopically injected into mouse models, the resulting tumors exhibited reduced latency, increased abundance of tumor-initiating cells, and an enhanced capacity to form distant metastases. Taken together, this study demonstrates that interactions between immature adipocytes and breast cancer cells drive initiation of highly metastatic cancers by enhancing epithelial cell tumor-initiating potential.

Due to the practice of autologous fat grafting as a method of breast reconstruction (oncoplastic surgery) following breast-conserving tumor excision, the impact of adipocytes on tumor malignancy may be a consideration for recurrence following treatment. Indeed, using a model of autologous fat grafting, Massa et al. reported increased proliferation of several breast cancer lines co-cultured with either induced adipocytes (i.e., differentiated from fibroblasts) or intact adipose tissue samples obtained from liposuction patients [181]. However, a recently published prospective matched case-control analysis found no significant differences in locoregional recurrence in patients who received autologous fat grafting *vs.* those who did not [182]. Although cases and controls were matched for hormone receptor status in this study, no analysis was conducted to evaluate potential differences in recurrence by tumor molecular subtype, potentially due to the limited sample size and low locoregional event rate. However, based on the aforementioned complex relationships between obesity status and risk of specific

breast cancer subtypes, as well as the reported roles for adipocytes in regulating breast epithelial tumorigenicity and metastatic potential, additional studies are needed to address concerns regarding the potential risks associated with fat grafting in breast reconstructive surgery. Stratification by BMI and/or molecular tumor subtype may be necessary to fully assess the influence of fat grafting on breast cancer recurrence rates.

Adipocytes and prostate cancer

Bidirectional communication between adipocytes and prostate epithelial cells also influences prostate tumor biology, particularly with regard to chemokine activity. Chemokines, or chemotactic cytokines, are small secreted signaling proteins that induce directed, gradient-driven migration (chemotaxis) in nearby cells that express the appropriate chemokine receptor. The functions of chemokines in malignancy depend on both tumor characteristics and the specific chemokine in question, but are frequently associated with leukocyte infiltration as well as metastatic potential and site-specific spread of tumor cells [183]. Adipose tissue-specific expression of many CC subfamily chemokines and their receptors is upregulated in human obesity [184]. For example, Laurent et al. [185] identified a CCR3/CCL7 axis regulated by obesity, through which secretion of CCL7 by mature periprostatic adipocytes supported the directed migration of prostate cancer cells, thereby promoting cell migration toward the periprostatic fat pad and the spread of cancer cells outside of the prostate gland. This process appeared to be augmented in obesity by both enhanced secretion of CCL7 by hypertrophic adipocytes and increased expression of the CCL7 receptor, CCR3, by prostate cancer cells [185].

Adipocyte-derived CCL2 is also implicated in prostate cancer progression. Ito et al. reported that adipocyte-derived CCL2 directly stimulated prostate cancer cell proliferation, promoting invasion and migration through induction of matrix metalloprotease (MMP)-2 activity and ultimately leading to enhanced tumorigenesis and metastasis [186]. Importantly, increased

production of CCL2 by bone marrow adipocytes and other stromal cells is also strongly implicated in the propensity of prostate cancer cells to metastasize preferentially to bone [187, 188]. An increase in bone marrow adipocyte content with age, obesity, and obesity-associated metabolic pathologies [189, 190], suggests a potential link between obesity and elevated rates of prostate cancer metastasis [187, 188].

Interestingly, prostate cancer-adipocyte crosstalk also appears to induce tumor-promoting changes in periprostatic adipocytes. Treatment of periprostatic adipose tissue organotypic explants with PC3 prostate carcinoma cell-conditioned medium activated a cancer-promoting secretory profile, including increased secretion of osteopontin, TNF-α, and IL-6, and reduced production of adiponectin [191]. These changes were not observed upon treatment of cells comprising the periprostatic adipose stromal vascular fraction (i.e., all stromal populations except adipocytes) with PC3 cell-conditioned medium, suggesting that the observed increase in pro-tumorigenic factor production by explanted tissue was due specifically to tumor-mediated education of adipocytes [191]. Indeed, adipocytes appear to be a major source of microenvironmental IL-6 in prostate cancer. Periprostatic adipose tissue harvested from patients undergoing radical prostatectomy secreted IL-6 at concentrations 375 times greater than that in patient-matched serum and correlated with histological grade [192]. Additionally, Tang et al. [83] recently showed that co-culture of prostate cancer cells increased production of the cysteine protease cathepsin B by adipocytes. Further probing revealed that adipocyte co-culture induced secretion of the peptide hormone cholecystokinin (CCK) by prostate cancer cells, resulting in establishment of an autocrine/paracrine amplification loop in which CCK, acting through the CCK receptor CCKBR, induced expression of cancer stem cell markers such as CD49f and Sca-1 in prostate cancer cells and further production of cathepsin B by adipocytes. Importantly, cathepsin B has been shown to facilitate prostate cancer invasion and metastasis via degradation of ECM and basement membrane components [193, 194]. Collectively, these studies demonstrate that prostate cancer cell-induced alterations in adipocyte function are

important mediators of tumor progression. **Figure 13** briefly summarizes adipocyte-cancer cell crosstalk findings described above.

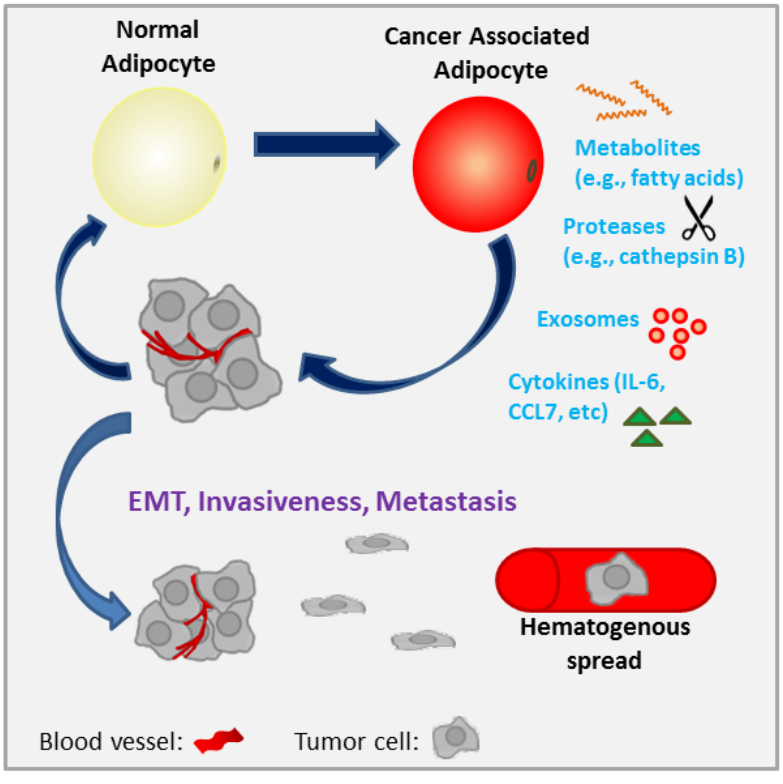

Figure 13. Adipocytes promote tumor progression and metastasis. Adipocytes may provide metabolic substrates directly to cancer cells, or may indirectly influence cancer metabolism through exosome secretion. Adipocytes also secrete a variety of factors that promote tumor growth, EMT (epithelial-mesenchymal transition), acquisition of stem-like features, invasive behavior, and metastasis.

Adipocytes and adipose wasting in cancer-associated cachexia

An example of long-range adipocyte-tumor interactions can be observed in cancer-associated cachexia (referred to hereafter as *cancer cachexia* or simply *cachexia*). Cancer cachexia is a fatal energy-wasting syndrome that is estimated to be the immediate cause of death in approximately 20-40% of end-stage cancer patients [195]. A key feature of cancer cachexia is white adipocyte “browning”, characterized by greatly increased levels of brown fat-mediated thermogenesis in white adipose depots [196, 197]. Accordingly, cachectic patients exhibit irreversible, pathologically elevated basal energy expenditure levels, adipocyte lipolysis and adipose tissue wasting, rapid weight loss, and eventually, death [196-199]. Although prolonged systemic inflammation plays a well-established role in cachexia-associated adipose tissue wasting [198, 199], tumor-derived factors have also been shown to contribute to the

pathophysiology of this syndrome. For example, in a murine model of Lewis lung carcinoma, Kir et al. [196] demonstrated that tumor-derived parathyroid hormone-related protein (PTHrP) induced the expression of thermogenesis-associated genes in adipose tissue, implying a crucial role for this hormone in energy expenditure and tissue wasting. Accordingly, administration of a PTHrP neutralizing antibody prevented cachexia-associated weight loss and ablated thermogenic gene expression in white and brown adipose tissue. Furthermore, compared to cancer patients lacking detectable levels of blood PTHrP, patients with detectable blood PTHrP levels exhibited significantly higher resting energy expenditure levels per kilogram of lean body mass, implying a clinically relevant association between this hormone and wasting.

On the other hand, Rohm et al. [200] reported that browning and associated thermogenesis in major white adipose depots was not the primary mechanism of adipose tissue wasting in mouse models of colon cancer-induced cachexia. Although the brown adipose-associated protein cell death activator (CIDEA) was upregulated in both brown and white adipose depots of cachectic mice relative to healthy controls, this upregulation occurred in the absence of changes in other proteins implicated in adipocyte browning and thermogenesis, such as uncoupling protein 1 (UCP-1). Furthermore, while increased free fatty acid release was observed in primary mouse adipocytes exposed to serum from cachectic mice, this increase in lipolysis was not associated with well-characterized lipolytic inducers such as increased expression of lipases (e.g., hormone-sensitive lipase and ATGL), or increased β-adrenergic receptor activation. Instead, CIDEA-mediated degradation of AMPK, evidenced by a reduction in AMPK protein and enzymatic activity, contributed to adipocyte metabolic dysfunction. For example, although increased lipolysis was observed, decreased AMPK activity also resulted in reduced inhibitory phosphorylation of acetyl-CoA carboxylase, suggesting the establishment of a futile cycle in adipocytes characterized by simultaneous increases in both lipolysis and lipogenesis. Microinjection of white adipose depots with a peptide designed to interfere with the AMPK-CIDEA interaction (termed AMPK–CIDEA-interfering peptide, or ACIP), followed by implantation of the cachexia-inducing colon cancer cell line C26, resulted in approximately 30%

greater retention of adipose depot mass and greater adipocyte lipid droplet size compared to the contralateral control-injected depot. No significant effect was observed from ACIP injection into adipose depots of control, non-cachectic mice, suggesting that the augmented AMPK-CIDEA interaction and downstream influences on lipid metabolism in adipocytes may be a cachexia-specific phenomenon.

These findings by Rohm et al. are particularly interesting in light of the reportedly opposite regulation of AMPK in breast cancer cells co-cultured with adipocytes that was highlighted in the previous section [172]. Also interesting to note is the lack of a role for β-adrenergic signaling in either of these two studies [172, 200], as catecholamines are well-established regulators of lipolysis, while lipid mobilizing factor – a tumor-derived factor frequently implicated in cachexia [179, 201] – also signals through beta receptors. Thus, although the causes of cachexia are multifactorial and systemic, it is clear that adipocyte-cancer cell interactions are key players in the pathophysiology of this syndrome. Future work should seek to identify additional tumor-derived paracrine and hormonal signals that contribute to cachexia pathogenesis and progression.

Adipose-derived Stem Cells

Human adipose tissue stroma is a rich source of multipotent mesenchymal stem cells, termed adipose stromal cells or adipose-derived stem cells (ASCs), that can differentiate toward the osteogenic, adipogenic, myogenic, and chondrogenic lineages [202]. Interestingly, several recent studies reviewed below suggest that ASC recruitment substantially contributes to stromal populations in both breast and prostate cancers. Due to the abundance of adipose tissue, as well as the minimally invasive procedures required to collect it, ASCs are a celebrated approach for tissue engineering and regenerative medicine. For example, lipoaspirate preparations may be “enriched” by the addition of ASCs to improve graft volume retention [203, 204]. However, the findings described below suggest that caution may be advised in use of ASCs in patients

with a history of cancer. Notably, factors such as age and menopausal status have been found to influence the proliferation and differentiation capacities of ASCs [205]. Future studies on the impact of age on ASC recruitment to tumors will yield interesting findings.

Adipose-derived stem cells in breast cancer

The varied stromal components of the tumor microenvironment must be recruited from either adjacent tissue or from distant precursor sources such as bone marrow. Kidd et al. [206] investigated the relative contribution of ASCs *versus* bone marrow-derived stem cells to stromal populations in mouse models of ovarian and breast cancers, and found that the majority (greater than 70%) of intratumoral myofibroblasts, pericytes, and endothelial cells were recruited from neighboring adipose tissue. However, CAF subpopulations were recruited from multiple distinct sources, with fibroblasts positive for fibroblast specific protein and fibroblast activation protein originating from bone marrow-derived mesenchymal stem cells, while α-smooth muscle actin$^+$/chondroitin sulfate proteoglycan 4$^+$ (α-SMA$^+$/NG2$^+$) CAFs were recruited from adjacent adipose. While the factors contributing to ASC recruitment to tumors are still ambiguous, Gehmert et al. have demonstrated that the PDGF-BB/PDGFR-β signaling pathway may be involved in ASC recruitment to breast cancers [207]. Together these results imply that the diversity of the tumor microenvironment can be attributed, at least in part, to the heterogeneous origin of stromal constituents.

Although ASCs are primarily localized to fat depots, circulating ASCs have also been detected in obese individuals and cancer patients, with greater levels observed in obese patients bearing colon, prostate, or breast cancers (relative to lean) [208-211]. Additionally, relative to ASCs from lean adipose, ASCs isolated from obese adipose show enhanced potential to traffic to breast tumors in both humans and mice [212, 213]. Similarly, Zhang et al. [213] recently reported hematogenous seeding of breast and ovarian tumors by ASCs in obese mice, resulting in infiltration and subsequent differentiation to pericytes and intratumoral

adipocytes/CAA. This process occurred in an obesity-dependent manner, with a 6-fold increase in “shedding” of precursors from adipose depots in obesity contributing to tumor cell survival and angiogenesis. It will be interesting to note in future studies whether specific adipose depots shed ASCs to the circulation at different rates. Ultimately, these findings reinforce the need to more comprehensively evaluate the risk of breast cancer recurrence after autologous fat grafting (see above), particularly in obese individuals.

Adipose-derived stem cells in prostate cancer

Similar to breast cancer, local and circulating ASCs have been reported in prostate cancer patients. Ribiero et al. observed higher levels of circulating ASCs in the blood of overweight or obese compared to lean prostate cancer patients [208]. The authors also reported that periprostatic adipose tissue of prostate cancer patients bore significantly higher numbers of ASCs than nearby visceral adipose tissue, independent of BMI. However, increased recruitment of ASCs into prostate tumors in obesity has been reported, and was recently attributed to secretion of the chemokines CXCL1 and CXCL8 by cancer cells (**Figure 14**) [210, 213]. CXCL8 expression was restricted to malignant cells and was obesity-independent; on the other hand, secretion of CXCL1 by non-malignant epithelium was exclusively observed in histological sections from obese individuals, while CXCL1 expression in tumor cells was found in a significantly higher percentage of tumor sections from obese as compared to lean patients [210]. The extent to which periprostatic ASCs, as opposed to circulating ASCs released from other adipose depots, contribute to the cellular composition of prostate tumor stroma was not quantified in the highlighted studies and requires further investigation.

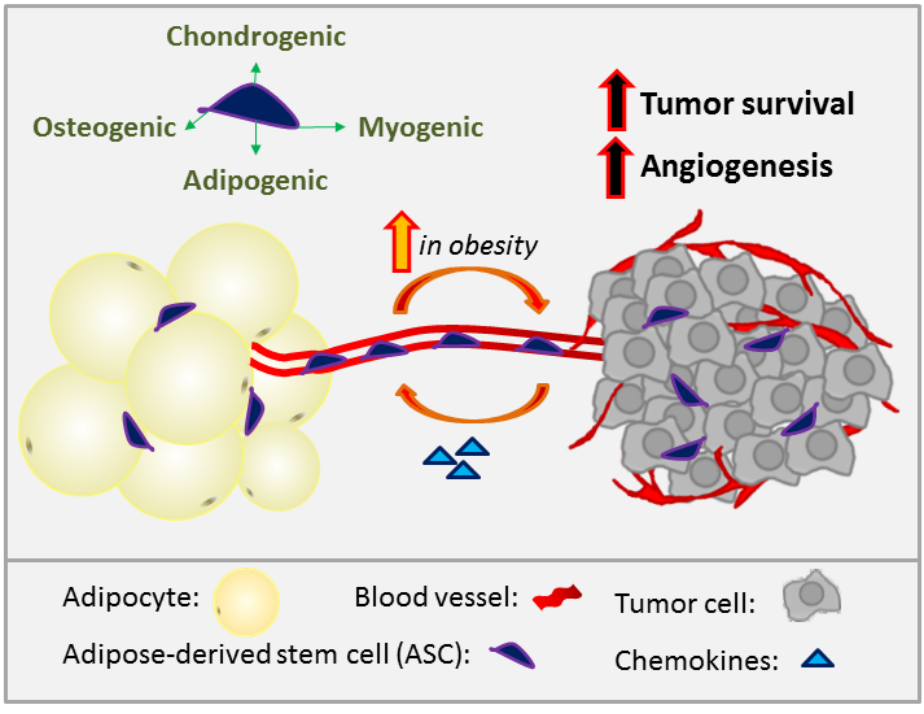

Figure 14. Obesity, cancer increase circulating ASCs. Human adipose tissue stroma is a rich source of multipotent ASCs, which enter the circulation and traffic to other tissues. This "shedding" process is increased in obese and/or tumor-bearing individuals. Tumor chemokine secretion (e.g., CXCL1, CXCL8) is influenced by obesity and is implicated in ASC recruitment to developing tumors and differentiation into stromal populations such as fibroblasts, pericytes, and adipocytes.

Adipose and Endothelial/Lymphendothelial cells

Vascularization mechanisms in adipose tissue and tumors

Expansion of adipose tissue during progression to obesity requires concomitant expansion of the adipose vascular bed through the process known as angiogenesis, the formation of new blood vessels from pre-existing vessels. In fact, administration of anti-angiogenic agents in models of both genetic and diet-induced obesity either prevented weight gain [214] or induced dose-dependent, reversible weight reduction and adipose tissue loss [215, 216]. When expansion of the vasculature does not occur in proportion to the expansion of adipocyte volume (hypertrophy), cellular and/or regional hypoxia develops, resulting in activation of the transcriptional complex hypoxia-inducible factor 1 (HIF-1) through stabilization of the HIF-1α subunit. HIF-1-mediated upregulation of inflammatory and pro-angiogenic signaling pathways in adipocytes, endothelial cells, and immune cells induces vascular growth, facilitating further tissue expansion [8, 217, 218]. In this way, the microenvironment during

accumulation of adipose tissue resembles the tumor microenvironment during tumor vascularization, described in detail below (**Figure 15**). The extensive list of signaling factors contributing to angiogenesis in both adipose tissue and tumors includes VEGF isoforms, angiopoietins 1 and 2, leptin, adiponectin, TNF-α, fibroblast growth factor (FGF) isoforms, TGFβ, HGF, and cytokines such as IL-6 and IL-8 [158, 219, 220]. Among these, the VEGF/VEGFR system - one of the best characterized and most potent of the known pro-angiogenic signaling pathways - is the main mediator of angiogenic activity in adipose tissue [219, 221, 222]. The VEGF-A ligand in particular is abundantly expressed by adipocytes and other adipose stromal populations [219, 221]. An additional shared factor of particular importance is angiopoietin-2, which signals through the receptor tyrosine kinase TIE2 to induce ECM degradation and disruption of endothelial-pericyte interactions during sprouting angiogenesis [223, 224]. Importantly, several of the pro-angiogenic factors listed above, including multiple VEGF isoforms, leptin, HGF, and angiopoietin-2, are also elevated in the serum of obese subjects and are implicated in systemic effects of obesity on cancer progression [147, 225, 226].

Similar to adipose tissue, growth of solid tumors is also heavily dependent upon synchronous expansion of their vascular beds. In early stage solid tumors, rapid proliferation leads to *diffusion limited hypoxia*, wherein cells within the tumor mass end up at a distance from the surrounding vasculature that is beyond the diffusion limit of oxygen. Resulting hypoxia-induced apoptosis and necrosis limit further tumor growth unless an intratumoral vascular system is established. The shift in developing primary or metastatic tumors from avascular to vascularized is termed the “angiogenic switch”, and is a discrete and requisite step for exponential tumor growth and progression to malignancy (**Figure 15**) [227-229]. Accordingly, tumor microvessel density is a powerful and independent prognostic indicator for several human cancers, including breast, prostate, melanoma, ovarian, gastric, and colon cancers [229]. However, in light of the myriad options for tumor vascularization described below, it is

interesting to note that the microvessel density in solid tumors is often lower than in their normal tissue counterparts [230].

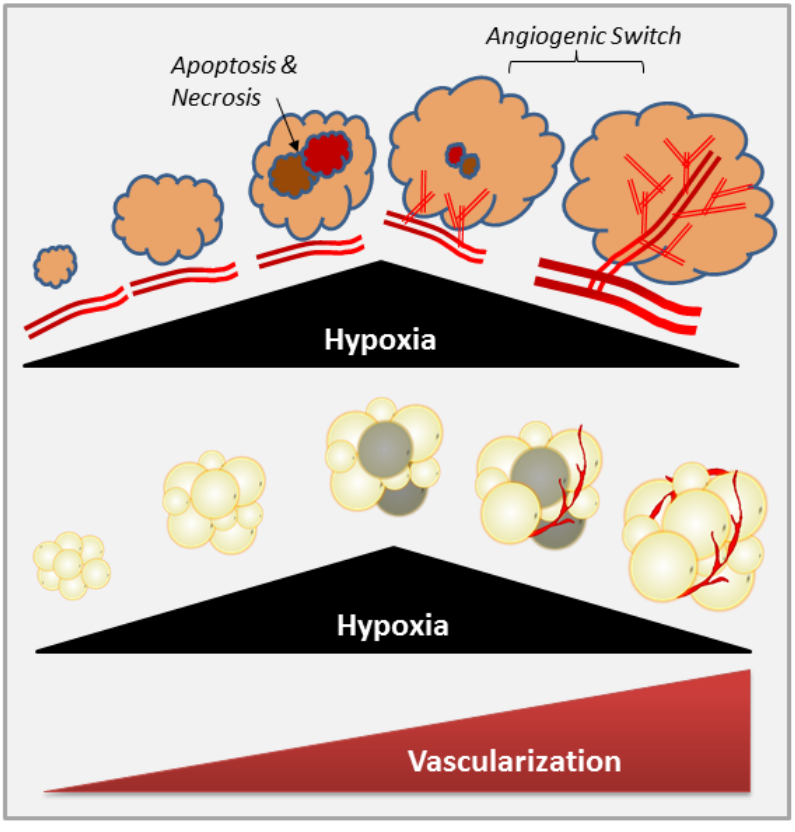

Figure 15. Hypoxia & the Angiogenic Switch. An extensive list of pro-angiogenic factors is involved in both induction of the angiogenic switch in developing solid tumors and expansion of adipose tissue during progression to obesity. As tumor cells proliferate or adipocytes hypertrophy, hypoxia develops and triggers stabilization of the HIF-1 complex, a transcription factor which promotes increased production of growth factors such as VEGF-A, FGF1, TGF-β, HGF, and angiopoietins 1 and 2. Additional proangiogenic factors include the adipokines leptin and adiponectin; cytokines such as TNF-α, IL-6, and IL-8; and matrix metalloproteases, which degrade the extracellular matrix. Ultimately, increased vascularization alleviates regional hypoxia and facilitates further tissue expansion.

New tumor vessel formation can occur through a number of non-mutually exclusive mechanisms, including sprouting and migration of endothelial cells ("classical" sprouting angiogenesis) or intussusceptive (non-sprouting) microvascular growth, a process in which tumor cells induce splitting and rapid remodeling of existing endothelial vessels [229]. Remarkably, along with endothelial cells, tumor cells themselves may integrate into newly forming blood vessels, resulting in mosaicism [229]. Tumor cells may also engage in a process known as *vasculogenic mimicry*, the arrangement of tumor cells into vascular channels which anastomose with adjacent blood vessels [229, 231, 232]. An additional mechanism for perfusion of tumors is vessel co-option, wherein tumor cells simply track alongside existing vessels for their own oxygen and nutrient gain, thereby exploiting nearby mature vessels in the host organ

[229]. Given that adipose tissue is one of the most vascularized tissues in the body [164, 219], it is unsurprising that co-option of adipose tissue vascular beds was recently shown to promote accelerated tumor growth and intratumoral vascularization [233].

Among other abnormal features, tumor vasculature is characterized by enhanced permeability, including transcellular holes and fenestrae, which drives further angiogenesis and increases nutrient and oxygen delivery, immune cell infiltration, and tumor cell extravasation during metastasis [234, 235]. Similar to adipose tissue, the VEGF/VEGFR system – and particularly VEGF-A – is highly expressed in tumors and is a potent inducer of tumor vascular permeability [236]. Given the extensive similarities of the pro-angiogenic signaling networks in adipose and tumors, it is unsurprising that the vasculature in these two tissue types is structurally similar. For example, adipose tissue capillaries also contain fenestrations, the presence of which depends upon a poorly understood synergistic relationship between VEGF, leptin, and FGF-2 signaling [237]. It is tempting to speculate that the fenestrations within adipose vasculature may provide a convenient means of escape for tumor cells invading into adipose tissue.

In addition to hematogenous metastasis, a tumor cell can also escape from its primary location through lymphatic dissemination. In a number of cancer types, including breast cancer, melanoma, and prostate cancer, metastasis to the tumor draining lymph node(s), also referred to as the “sentinel” lymph node(s), is a common initial route for the metastatic dissemination from solid tumors [238]. For this reason, sentinel lymph node biopsy in newly detected and early-stage cancers is a frequent and evidence-based clinical practice required for staging of disease, determination of prognosis, and development of the treatment approach. In a process similar in principle to classical sprouting angiogenesis, secreted factors in some solid tumor types and other inflamed tissues can also initiate lymphangiogenesis, the formation of new lymphatic vessels from preexisting vessels. These newly formed lymphatic vessels exhibit morphological differences from those in their healthy tissue counterparts, including structural disorganization [238]. Interestingly, tumor-associated lymphangiogenesis appears to involve

both incorporation of bone marrow-derived endothelial progenitors and endothelial mimicry by CD11b+ tumor-associated macrophages, although there are conflicting reports regarding the extent to which the latter occurs [239-242].

Although *peritumoral* lymphatic vessel density can act as a prognostic indicator in several cancer types, including cervical, colorectal, breast, and prostate cancers [243-247], several studies have suggested that *intratumoral* lymphatic vessels in solid tumors may be either collapsed due to intratumoral pressure, occluded by infiltrating tumor cells and therefore nonfunctional, or simply absent altogether [248-251]. Thus, the high frequency of cancer cell detection in regional lymph nodes implicates peripheral, peritumoral lymphatic vessels in mediating tumor metastasis in these tumor types [250, 252]. However, results showing non-functional intratumoral lymphatic vessels have not been uniformly supported [253]. Consequently, the role of tumor lymphangiogenesis and the relative contribution of intratumoral *versus* peritumoral lymphatics to lymph node metastasis remains controversial.

Adipose and breast cancer angiogenesis

In vivo tumor models have demonstrated the ability of breast tumors to obtain a blood supply through all of the aforementioned processes: vessel co-option, intussusceptive growth, vasculogenic mimicry, and classical sprouting angiogenesis [254, 255]. Additional mechanisms have also been described for breast cancers, such as vasculogenesis and glomeruloid angiogenesis, albeit to a lesser extent [255]. Nevertheless, remodeling of existing vessels appears to be the dominant mechanism for establishing new vasculature in human breast cancers [256, 257]. In support of this assertion, Lim et al. [233] demonstrated that implantation of the E0771 murine mammary tumor line into either brown or white adipose tissue resulted in accelerated tumor growth rates and increased intratumoral vessel densities as compared to tumors grown subcutaneously. These results were attributed to co-option of pre-existing adipose vascular beds, as tumor growth and vascularity reflected the differential degree of

vascularity within the respective adipose types. Furthermore, adjacent adipose tissue fostered both reduced pericyte coverage and enhanced permeability in tumor vessels, features associated with worse prognosis.

In obesity, both the increased abundance of white adipose and the resulting chronic inflammatory conditions of the microenvironment may promote tumor vascularization. Indeed, enhanced tumor angiogenesis in the context of obesity is observed in both mice and humans [45, 213, 258-260]. In one compelling study, Arendt et al. [45] developed a novel humanized mouse model wherein human adipose stromal populations overexpressing CCL2 were injected into cleared mammary fat pads (cleared of endogenous mammary epithelium) to generate an obese-like microenvironment. *Prior* to tumor formation, the authors reported enhanced angiogenesis in CCL2-overexpressing mammary fat pads, which was shown to be mediated by elevated levels of macrophage recruitment and activation. Upon transplantation of transformed human breast epithelial cells, the obese-like microenvironment augmented macrophage-associated angiogenesis in early premalignant lesions as well as tumor-adjacent adipose following tumor formation, which induced the formation of larger and higher-grade tumors. Whether the observed tumor-promoting effects were due to specific macrophage phenotypes in “obese” vs. lean mammary adipose or simply to an increase in macrophage numbers was not explored. Moreover, this study did not differentiate whether increased tumor-associated macrophage content in obesity was due to accelerated recruitment of bone marrow-derived macrophages or to co-option of nearby mammary adipose tissue macrophages. Nevertheless, similar results were reported by Cowen et al., who demonstrated that high-fat diet-induced obesity in the MMTV-PyMT model of spontaneous breast cancer resulted in mammary adipose tissue inflammation, enhanced macrophage recruitment, and increased mammary tumor vascular density [44].

As described in the previous section, obesity is also associated with elevated levels of circulating and infiltrating ASCs [213] which produce a range of proangiogenic factors, including VEGF and HGF [261]. Our lab has demonstrated that inhibition of the HGF receptor, cMET, *via*

the small molecule kinase inhibitor crizotinib significantly reduced tumor burden and tumor vascularity in both lean and obese C3(1)-TAg mice [262]. Reversal of high fat diet-induced elevation of HGF/cMET expression in both normal mammary gland and tumors was also observed with weight loss, which significantly blunted the effects of obesity on both pre-neoplastic lesion formation [263] and tumor progression [264] (**Figure 16**). Importantly, endothelial cell upregulation of cMET is one mechanism attributed to inherent or acquired resistance to anti-angiogenic therapies targeting VEGF [265, 266]. In fact, the HGF/cMET pathway has been reported to act synergistically with VEGF [265, 267], and clinical trials investigating crizotinib alone (ClinicalTrials.gov: NCT 02101385 [268]) or in combination with anti-VEGF therapy (ClinicalTrials.gov: NCT 02074878 [269]) for the treatment of advanced TNBC are currently underway at the time of preparation of this review.

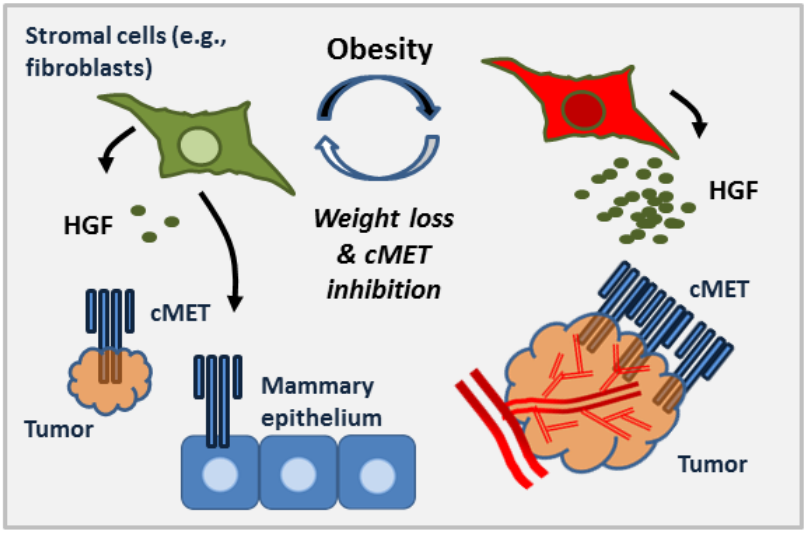

Figure 16. Mammary HGF/cMET signaling in the in C3(1)-TAg mouse model of basal-like breast cancer. Obesity increased HGF production by stromal cells, promoting tumor growth and angiogenesis. HGF/cMET-mediated tumor promotion was reversible by weight loss or cMET inhibition.

However, one response to anti-angiogenic therapies is vessel pruning and regression, leading to intratumoral hypoxia. Such hypoxic conditions induce an influx of tumor-associated macrophages and other myeloid cells, triggering tumor revascularization and tumor relapse [270-273]. In addition, peritumoral adipose tissue is characterized by a dense macrophage infiltrate and a high degree of vascularization. Indeed, Wagner et al. demonstrated that inflamed, tumor-associated adipose tissue acts as a source of both vascular endothelium and

activated pro-angiogenic macrophages, thereby fueling the growth of malignant cells [259, 274]. Importantly, the presence of macrophages within adipose tissue increases considerably in obesity [275]. Thus, obesity-associated mammary adipose inflammation and resulting macrophage infiltration and angiogenesis may contribute to tumor relapse following anti-angiogenic therapies.

Adipose tissue and lymphangiogenesis in breast and prostate cancers

Lymphatic vessels in the normal breast are dispersed throughout the interlobular stroma and adipose tissue [249], the latter of which acts a source of molecules that directly affect the lymphatic endothelium. For example, the lymphangiogenic factors VEGF-C and VEGF-D are chemotactic for macrophages in mice, and their blockade in a diet-induced obesity model attenuated macrophage infiltration, adipose tissue inflammation, and onset of insulin resistance [276]. An increase in circulating levels of pro-lymphangiogenic factors such as HGF and VEGF-C in obesity may also alter lymphatic vessel density or function by enhancing capillary permeability and inducing lymphendothelial hyperplasia [226, 277]. Indeed, obesity is associated with dysfunction of the adipose lymphatic system, including decreased lymph node size and number [278], reduced drainage of macromolecules [279], increased perilymphatic inflammation [280], and altered lymph node immune cell composition [278]. These changes were recently attributed to the condition of obesity *per* se – specifically injury to lymphatic endothelial cells caused by inflamed adipose tissue – rather than the high fat diet used to generate the obese phenotype [281]. Interestingly, using a model of *Prox1* haploinsufficiency, Harvey et al. demonstrated that lymphatic vascular defects and resulting abnormal lymph leakage into surrounding tissues induced adult-onset obesity [282]. A follow-up study by Escobedo, et al. further reported that the obese mutant phenotype of *Prox1*$^{+/-}$ mice could be rescued with tissue-specific restoration of *Prox1* in lymphatic endothelial cells [283]. Whether lymphatic vessel density is altered in peritumoral adipose, either normal or obese, has not been

reported. However, Yamaguchi et al. observed a >3-fold increase in lymph node metastasis with adipose tissue invasion at the tumor margin in patients with invasive breast carcinoma [36].

The role of adipose tissue in prostate carcinoma angiogenesis and lymphangiogenesis is not well understood. However, as mentioned previously, ASCs are abundant in periprostatic adipose tissue [208] and are a source of lymphangiogenic factors [284]. Indeed, implantation of ASCs has been used successfully in mice to induce lymphangiogenesis in a model of lymphedema [285, 286]. Importantly, obesity may influence the degree of pro-angiogenic/lymphangiogenic factors released from the periprostatic adipose depot. Venkatasubramanian et al. reported that conditioned media generated *via* explant culture of human obese periprostatic adipose stimulated prostate cancer cell proliferation and angiogenesis to a significantly greater degree than explants from lean patients, providing a potential link between obesity and worse prostate cancer prognosis [287]. Paradoxically, elevated leptin concentration in obese mouse models is associated with attenuated tumor cell proliferation and reduced angiogenesis and lymphangiogenesis in prostate cancers *in vivo* [288, 289]. Furthermore, rate of lymph node metastasis in patients with clinically localized prostate cancer does not appear to be altered by obesity [290]. Thus, there are lingering questions surrounding the role of periprostatic adipose tissue in prostate tumor progression in both lean and obese individuals, particularly with regard to its influence on tumor angiogenesis.

Adipose Tissue Immune Populations in Cancer Development and Progression

Acute inflammatory responses, such as those that occur in the context of pathogen infections, are usually self-limiting and are characterized by an “acute inflammatory infiltrate” consisting primarily of neutrophils and sometimes eosinophils [291]. However, when triggering factors persist or inflammatory resolution mechanisms fail, a shift occurs in the immune profile to a “chronic inflammatory infiltrate”, predominantly comprised of lymphocytes and mononuclear cells such as macrophages and dendritic cells. Chronic inflammation is consistently associated

with increased risk of carcinogenesis and is a well-known hallmark of cancer [291, 292], leading Dvorak to describe tumors as “wounds that do not heal” [107]. Solid tumors frequently contain a dense infiltrate of immune cells, including lymphocytes, neutrophils, macrophages and mast cells, each of which directly or indirectly influence the course of tumor progression. In fact, many of the changes that occur in the tumor microenvironment are orchestrated by immune cells [293-295]. Chronic inflammation is also highly prevalent in obesity, and as discussed in previous sections, plays pivotal roles in adipose tissue (lymph)angiogenesis and development of fibrosis. Thus, the final section of this review will focus on adipose tissue immune populations. We will emphasize the changing immune profile during adipose accumulation and progression to obesity and the potential impact of these alterations on adipose-adjacent tumor progression. However, it should be noted that the immune profile of adipose tissue depends upon both the degree and the duration of adiposity, as well as a variety of other factors that are beyond the scope of this review, including physical activity, dietary intake, the microbiome, and certain therapeutics such as thiazolidinediones [296].

Healthy adipose tissue contains a wide variety of innate and adaptive immune cells, including macrophages, dendritic cells, mast cells, eosinophils, neutrophils, and lymphocytes, which collectively constitute ~25-45% of stromal cells in humans [12]. In lean adipose, these “resident” immune cells maintain tissue homeostasis by clearing apoptotic cells, suppressing inflammation, and mediating basal ECM remodeling and angiogenesis in response to routine fluxes in caloric availability [114]. However, during progression to obesity, rapid expansion of adipose tissue and associated adipocyte dysfunction trigger a dynamic infiltration of innate and adaptive immune populations (**Figure 17**). These immune cells act as potent sources of inflammatory cytokines, chemokines, growth factors, and matrix-degrading enzymes such as MMPs, which rapidly remodel the tissue microenvironment and result in chronic low-grade, or “smoldering”, inflammation [88]. A decrease in relative influence of select adipose resident populations known for their anti-inflammatory action (e.g., immunosuppressive macrophages, eosinophils, regulatory T cells, and innate lymphoid cells [ILC2s]) may further exacerbate

adipose inflammation in obesity and associated sequelae, thereby indirectly mediating differential immune responses during tumor-adipose interactions in lean vs. obese individuals.

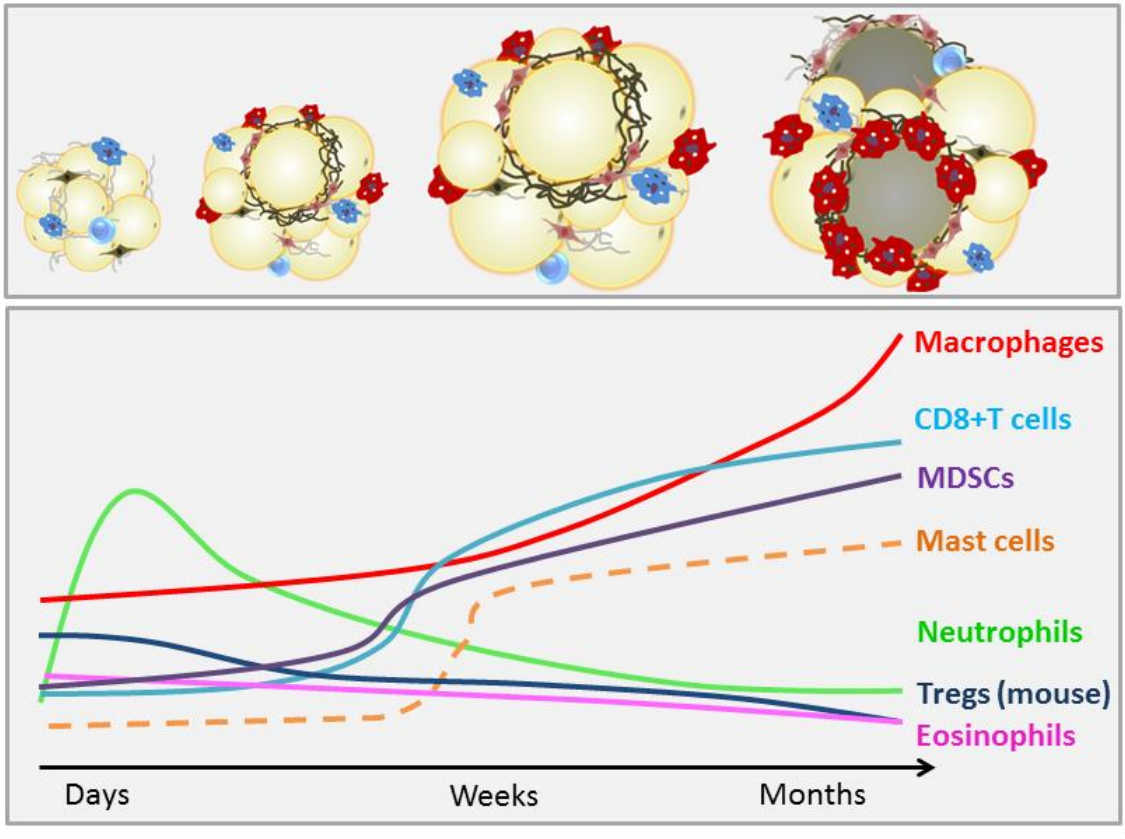

Figure 17. Summary of changes in immune cell profile during progression to obesity. In the lean state, adipose tissue contains a variety of immunoregulatory cells such as M2-like tissue-resident macrophages, regulatory T cells, and eosinophils. Neutrophils infiltrate adipose within days of exposure to an obesogenic diet. Over weeks to months, an increase in CD8+ T cells, macrophages, and myeloid-derived suppressor cells (MDSCs) results in a mix of pro- and anti-inflammatory cells. In prolonged obesity, adipose mast cell content may also increase.

Despite a surge in research over the past 15 years on the roles of immune cells in adipose tissue biology, many fundamental lines of investigation remain incompletely understood. For example, a growing understanding of the complexity of innate lymphocyte subsets and their remarkable parallels with adaptive lymphocyte subsets [297] complicates interpretation of innate *vs.* adaptive influence. In addition, data regarding roles for select immune cell types, such as basophils, in adipose tissue remain in short supply. Notably, while comparing the immune response to tumor growth in lean and obese individuals many studies

have failed to take into account co-morbidities associated with obesity which may alter the immunometabolic milieu. For example, type II diabetes is a metabolic condition in which insulin resistance, often due to prolonged obesity and associated inflammation, results in hyperinsulinemia, hyperglycemia, and dyslipidemia. In addition to elevating risk of both cancer development and cancer mortality in several solid tumor types [298, 299], metabolic dysregulation in type II diabetics shifts availability of metabolic substrates such as glucose and fatty acids, which can alter immune cell number and behavior [300-302]. Furthermore, medications prescribed for glucose control in type II diabetics, such as metformin, may have profound and confounding effects on anti-tumor immunity through suppression of inflammation in macrophages [303] or augmentation of the cytotoxic T cell response [304].

With these caveats acknowledged, the increased presence of adipose inflammatory cells in obesity may provide a link between adipose tissue and the pathophysiology of adipose-associated cancers. Thus, when considering the effects of adipose tissue on cancer development, the potential for cross-talk between adipose immune populations and the developing tumor is paramount. Due to a current dearth of literature addressing immune populations in periprostatic adipose, the structure for this final section of our review will diverge from the format above, which emphasized breast and prostate adipose pads individually, and instead focus more generally on literature regarding immune populations in a variety of adipose depots.

T cells in Adipose and Cancer

T cell diversity in the tumor microenvironment

T lymphocytes, or T cells, are central to cell-mediated immune responses and mediate exquisitely specific adaptive immune defenses within a given disease context, including cancer. Broadly speaking, T cells can be classified into CD4+ helper T (Th) and CD8+ cytotoxic T (Tc) cell subsets. CD4+ Th cells can be further subdivided into pro-inflammatory effector Th1 cells or immunoregulatory Th2 cells, which influence both generation and activity of CD8+ Tc cells and

antigen-presenting cells (APCs), such as macrophages and dendritic cells, within the tumor microenvironment. Other T cell subsets include Th17 cells, γδT cells, and certain types of natural killer (NK) cells, the latter of which exhibit cytotoxic activity and play a role in antitumor immune defense. While each of these T cell subsets, along with other, less well-characterized populations, influence both tumor progression and adipose immunity [305, 306], a comprehensive review of T cell function in these contexts is beyond the scope of this review. However, several of the most well characterized subsets will be addressed below, with particular emphasis on how adiposity-associated alterations in CD8+ T cells and a subset of CD4+ T cells termed “classical T regulatory cells”, or Tregs, may contribute to cancer development in obese individuals.

CD8+ Tc cells and CD4+ Tregs generally exhibit opposing immunologic functions in both the tumor microenvironment and normal tissues. CD8+ Tc cells are a critical component of antitumor immune defense, *directly* killing tumor cells through release of cytotoxic granules containing perforin and granzyme B, and *indirectly* promoting tumor rejection by stimulating APC activity. On the other hand, Tregs are a subset of CD4+ T cells identified by expression of the cell surface markers CD4 and CD25 and the transcription factor forkhead box P3 (FOXP3), which acts as the master regulator of the Treg phenotype [307, 308]. Tregs directly regulate the activity of other T cells through suppression of CD8+ Tc cell proliferation following T cell receptor (TCR) stimulation and activation of immune checkpoint pathways, which provide a critical defense against T cell-mediated responses to self-antigens (autoimmunity). Specifically, in T cells, the amplitude and duration of TCR-mediated immune responses are determined by immune checkpoint proteins, which exert co-stimulatory and/or inhibitory signals to effectively “tune” the immune response and curtail collateral tissue damage. For example, FOXP3-mediated constitutive expression of the immune checkpoint protein CTLA4 by Tregs inhibits development of self-reactive CD8+ Tc cells in secondary lymphoid organs such as lymph nodes [309]. In peripheral tissue, including tumors, expression of the inhibitory checkpoint protein

Programmed Death-1 (PD-1) by “exhausted” or chronically activated T cells impairs cell-mediated responses. Binding of ligands to the PD-1 receptor triggers T cell senescence, apoptosis, or conversion to a Treg phenotype [310, 311], thereby attenuating cell-mediated immune responses [312]. Additionally, Tregs potently suppress the function of other immune cells such as APCs, NK cells, and CD8+ Tc cells through production of cytokines including IL-10 and TGF-β [305, 306, 312]. While these immune-regulatory functions provide a critical defense against rampant immune responses, by suppressing immunosurveillance and promoting immune tolerance in the tumor microenvironment Tregs actively prevent robust elimination of developing cancers. Accordingly, the density of Tregs in solid tumors is correlated with adverse clinical outcomes in melanoma, as well as ovarian, gastric, pancreatic, hepatic, breast, and prostate cancers [313-315].

Differential T cell content and activation in lean and obese adipose tissue: links to cancer

In addition to their well-established roles in the tumor microenvironment, Tregs have also recently been shown to contribute to the maintenance of adipose tissue metabolic homeostasis. Feuerer et al. [316] demonstrated that nearly half of the CD4+ T cells in lean visceral adipose of male mice expressed FOXP3. In fact, visceral adipose in 30-week old mice contained a greater abundance of Tregs than lymphoid tissues such as spleen and lymph nodes. Interestingly, these adipose-resident Tregs were frequently detected in CLS, which are typically associated with inflammatory cells. Expression profiling of isolated adipose Tregs revealed a gene signature distinct from that of “conventional” T cells from spleen and lymph nodes. Divergent transcription patterns in adipose Tregs included a relative increase in chemokines involved in leukocyte migration and extravasation and greatly elevated IL-10 expression (>100-fold) as compared to lymph node Tregs. Adipose-resident Tregs also exhibited limited TCR diversity relative to spleen or lymph node Tregs [316]. Similarly, Yang et al. reported that adipose T cells

displayed a TCR profile distinct from that of splenic T cells, further demonstrating that depot-specific microenvironments modulate lymphocyte phenotypes [317].

Feuerer et al. [316] also noted that the presence of Tregs in visceral adipose declined with increasing adiposity in three mouse models of obesity, although the abundance of lymphoid tissue Tregs was unaffected. Subsequent mechanistic studies employing Treg stimulation and depletion suggested that IL-10 secretion by Tregs dampens inflammation in adipose tissue, thereby safeguarding insulin sensitivity. A second study published the same year by Nishimura et al. [318] also reported a decrease in Treg content in obese murine visceral adipose, with a simultaneous and substantial increase in the presence of CD8+ Tc cells displaying markers of activated effector T cells. Of note, in obese mice the accumulation of CD8+ Tc cells preceded macrophage infiltration by 3-4 weeks, indicating that T cells may affect microenvironmental changes enabling macrophage recruitment (**Figure 17**). An increase in CD8+ Tc cells, particularly within CLS, was also observed in subcutaneous adipose. Genetic or antibody-mediated depletion of CD8+ Tc cells during the course of high-fat feeding attenuated the onset of insulin resistance, prevented macrophage infiltration, and blunted obesity-associated increases in TNF-α and IL-6 expression in whole adipose tissue; these phenotypes were "rescued" upon reintroduction of CD8+ Tc cells *via* adoptive transfer. Similarly, CD8+ T cell depletion in *established* obesity reduced the presence of pro-inflammatory macrophages and CLS density in adipose tissue. These findings were confirmed *in vitro*, as co-culture of CD8+ T cells from obese adipose with macrophages induced significantly greater macrophage-specific TNF-α expression than did CD8+ T cells from lean adipose. In sum, these studies illustrate that reduced Treg content and increased CD8+ T cell presence promote macrophage-specific expression of pro-inflammatory mediators, thereby contributing to adipose inflammation and metabolic dysfunction in obesity, both of which are drivers of tumor malignancy.

However, the nature of these reported shifts in T lymphocyte profiles of obese murine adipose has not been consistent in human studies. In fact, the opposite has been observed. In obese adults, the expression of Treg activation markers and Treg cytokines increased with

increasing adiposity, particularly in subcutaneous as compared to visceral adipose [319, 320]. One potential explanation for these observed increases in Treg activation relates to increased local estrogen concentration in adipose tissue of obese subjects. Indeed, Subbaramaiah et al. provided evidence that elevated cyclooxygenase-2 (COX-2)-induced prostaglandin E2 (PGE_2) production by CLS-associated inflammatory cells mediates increased risk of breast cancer in obesity by inducing activity of aromatase in mammary adipose tissue [321, 322]. Increased aromatase activity in adipose tissue increases the conversion of circulating androgens to estrogens, and thus is of particular concern for development of estrogen receptor-positive breast cancers in postmenopausal women, a population in which obesity is strongly linked to elevated risk of cancer [323, 324]. Estrogen also exerts a positive effect on both expansion of Tregs and augmentation of their immunosuppressive activities [325, 326]. Elevated PGE_2 also induces FOXP3 expression and Treg function [327-329]. Paradoxically, however, elevated aromatase and PGE_2 levels are also present in adipose of obese mice. Thus, the significance of interspecies differences in obesity-associated Treg abundance and/or activation is unclear.

Interspecies differences in T cell content are not exclusive to Tregs. For example, although increases in Tc and Th1 cell content are frequently reported in murine models of obesity, the prevalence of these cell types in obese human adipose is controversial. Indeed, while Yang et al. reported that the stromal-vascular fraction of abdominal subcutaneous adipose from obese human subjects displayed an increased percentage of both CD4+ and CD8+ T cells compared to lean individuals [317], two additional studies profiling T cells in obese human adipose did not reach the same conclusions [319, 320]. Accordingly, although CD8+ T cells appear to contribute to adipose inflammation in mice, their role in human obese adipose remains ambiguous. Furthermore, in addition to identifying potentially critical cross-species differences in adipose T cell function, these results also suggest that, in humans, an increase in pro-inflammatory cell abundance in adipose occurs with a parallel protective response driven by Tregs. Should this be the case, an elevated presence of Tregs in human obese adipose may contribute to immunosuppression of anti-tumor responses in adipose-adjacent cancers.

In addition to influencing Treg-mediated immunosuppression, obesity may also impair T cell-mediated antitumor responses through systemic mechanisms. For example, obesity reportedly accelerates age-associated declines in immune function, including thymic atrophy. The thymus is a specialized primary lymphoid organ located in the mediastinum that houses maturing T lymphocytes. Beginning at puberty, the thymus undergoes involution, or atrophy, exhibiting fibrotic and fatty changes that culminate in its replacement by adipose tissue [330]. Following thymic involution, the peripheral T cell pool is primarily maintained independently of thymic lymphopoiesis, such as by expansion of existing T cell populations; however, it should be noted that some studies in humans have reported that the aged thymus retains a limited capacity to produce naïve T cells [331]. Eventually, the age-related decline in naïve T cell production, in combination with steady exposure to antigenic challenge and resulting expansion of effector-memory T cells, depletes the naïve T cell pool and reduces diversity of the TCR repertoire [332]. Thus, these processes reduce the capability of the adaptive immune system to respond to new antigenic challenges, increasing susceptibility to infection, autoimmune responses, and cancer. Importantly, Yang et al. [333] reported that prolonged obesity in mice increased perithymic adipose tissue content, reduced thymocyte counts, and enhanced thymocyte apoptosis relative to lean animals, each of which are associated with thymic aging. Similarly, increased frequencies of CD4+ and CD8+ effector-memory cells in subcutaneous adipose of obese mice, concomitant with a notable decrease in TCR diversity and depletion of the CD4+ and CD8+ naïve T cell pools, further supported an acceleration of the immune aging process. Moreover, splenic T cells isolated from obese mice exhibited reduced expression of pro-inflammatory mediators important for antitumor immune defenses, including interferon-γ and TNF-α. Finally, in humans, analysis of mature thymus-derived T cells demonstrated that increasing adiposity significantly correlated with a reduction in thymic output in overweight and obese middle-aged subjects. These obesity-related restrictions in TCR diversity and T cell function may account for reports of impaired adaptive immunity in obese patients [334, 335] and suggests a reduced capacity to mount an effective antitumor immune response.

Finally, recent clinical successes with tumor immunotherapies targeting the PD-1 immune checkpoint pathway have increased interest in the regulation of this pathway in the context of obesity. As described above, PD-1 expression by T cells is an important driver of immunosuppression and reduced cytotoxic T cell response in the tumor microenvironment [336], prompting development of PD-1-targeting monoclonal antibodies (e.g., pembrolizumab and nivolumab) for clinical use. Recently, Shirakawa et al. reported B cell-dependent accumulation of CD4+ T cells constitutively expressing PD-1 within visceral adipose of obese mice and human omental adipose from obese patients [337], further suggesting that tumor-adjacent adipose in obese individuals may present an immunosuppressive environment. In light of the accelerated thymic aging and naïve T cell depletion reported in obese patients, it will be interesting to see whether adipose contributes to increased PD-1+ T-cell content in the solid tumor microenvironment.

Macrophages and myeloid-derived suppressor cells

Macrophage ontogeny and activation

Macrophages, or “big eaters”, are myeloid-lineage immune cells typically classified within the innate immune system, yet they bridge innate and adaptive immunity through extensive interactions with adaptive immune cells such as T cells. Conventionally, macrophages have been classified according to the “M1/M2” dichotomy, wherein “M1” polarized, or “classically-activated”, macrophages are pro-inflammatory, and “M2” polarized, or “alternatively-activated”, macrophages are anti-inflammatory. M1 macrophages are generated *in vitro* upon exposure to Th1 cytokines (e.g., IFN-γ) or stimuli such as bacteria and lipids [338-340]. In contrast, M2 macrophages are most commonly generated by culture in the presence of Th2 cytokines such as IL-4 and/or IL-13 [341]. However, a variety of other compounds may also be used for M2 macrophage polarization, including TGF-β, IL-10, glucocorticoid hormones, M-CSF, and PGE_2 [342].

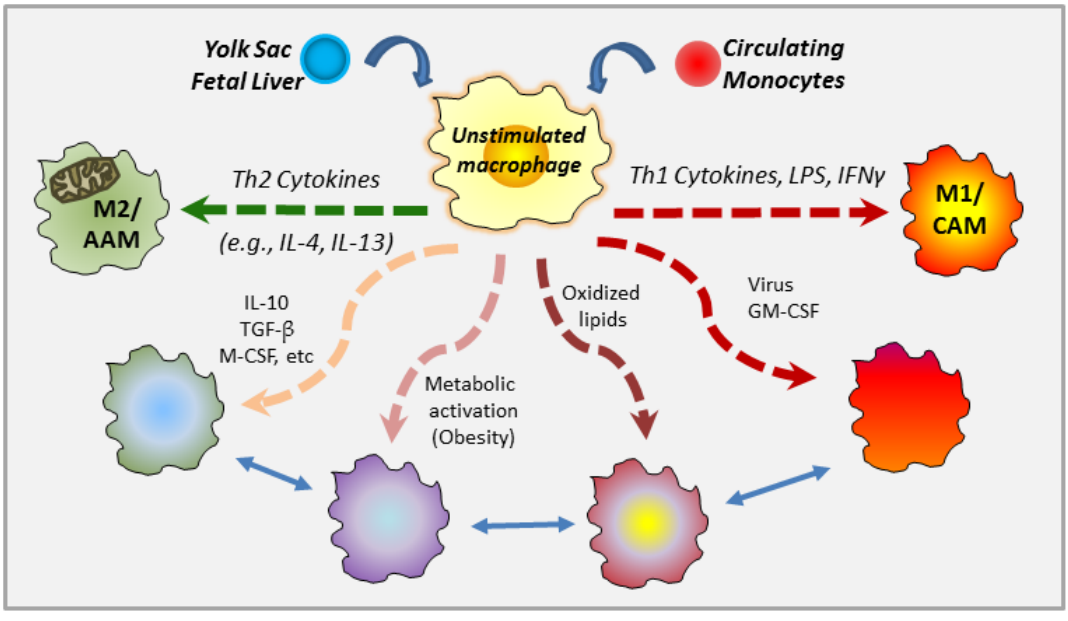

Figure 18. Macrophage activation as a spectrum. Unstimulated macrophages can be polarized *in vitro* to generate M1 macrophages (right) or M2 macrophages (left) using single cytokines or cytokine and other stimuli cocktails. However, tissue macrophages are exquisitely plastic, often expressing one or more markers of both M1 and M2 subtypes. Thus, tissue macrophage activation lies along a spectrum, resulting in mixed phenotype with specific expression and function varying by tissue type and timing of residence.

Importantly, a lack of standardized nomenclature and macrophage polarization strategy [343], coupled with the multifarious nature of tissue macrophages and their exquisite ability to respond to context-dependent cues [344], has resulted in a tremendous influx of literature about the respective roles of M1 vs M2 macrophage subsets in disease that is often contradictory and difficult to reconcile [345]. Furthermore, while much of our understanding of the M1 and M2 phenotypes have come from animal and *in vitro* studies, genomic profiling of human and mouse macrophages treated with M1 or M2 stimuli revealed that only approximately 50% of macrophage polarization markers are shared across both species [346]. With these caveats acknowledged, despite their utility to *in vitro* research, truly polarized macrophages are rare *in vivo.* Instead, tissue macrophages display a diverse array of functional phenotypes and often express one or more markers of both M1 and M2 subtypes, resulting in a mixed phenotype with

specific expression and function varying by tissue type and timing of residence, as discussed below (**Figure 18**) [347-350].

Over the past few decades, macrophage ontogeny studies have revealed multiple origins for what are now referred to as “tissue resident” macrophage populations (for two excellent reviews on macrophage ontogeny the reader is referred to [348, 351]). During primitive hematopoiesis in early embryonic development, macrophages arise in the blood islands of the yolk sac from an erythromyeloid precursor, differentiating to macrophages without passing through a monocyte stage [352, 353]. These early embryonic macrophages are followed by a second wave derived from fetal monocytes and originating in the fetal liver [352, 353]. Collectively, macrophages within these waves of early hematopoiesis populate tissues throughout the body and develop specialized functions based on their tissue of residence (e.g., microglia in the brain, Kupffer cells of the liver, etc.) [348, 351]. Tissue-resident macrophages persist through adulthood and, in most tissues, self-maintain through local proliferation without significant contribution from circulating monocytes (exceptions include the intestine and the dermis) [354, 355]. Only in later stages of embryonic development and postnatally do macrophages develop from bone marrow-derived circulating monocytes, which are recruited to tissues as needed when insults arise.

Although the embryonic origin of many specialized tissue macrophage populations has been identified, the precise origin of adipose tissue macrophages (ATMs), and the degree to which resident ATM populations are replaced by circulating monocytes, remains unclear (**Figure 19**). In one recent study, Franklin et al. demonstrated that ablation of the CCL2 receptor, CCR2, significantly reduced mammary fat pad macrophage content in lean mice [356]; CCL2 mediates egress of monocytes from bone marrow and thereby augments the abundance of circulating monocytes [357]. This study by Franklin and colleagues therefore suggests that mammary-specific ATMs in lean mice are replenished throughout adulthood by circulating monocytes. Whether this replenishment also occurs in other lean adipose depots under physiologic conditions has not been reported.

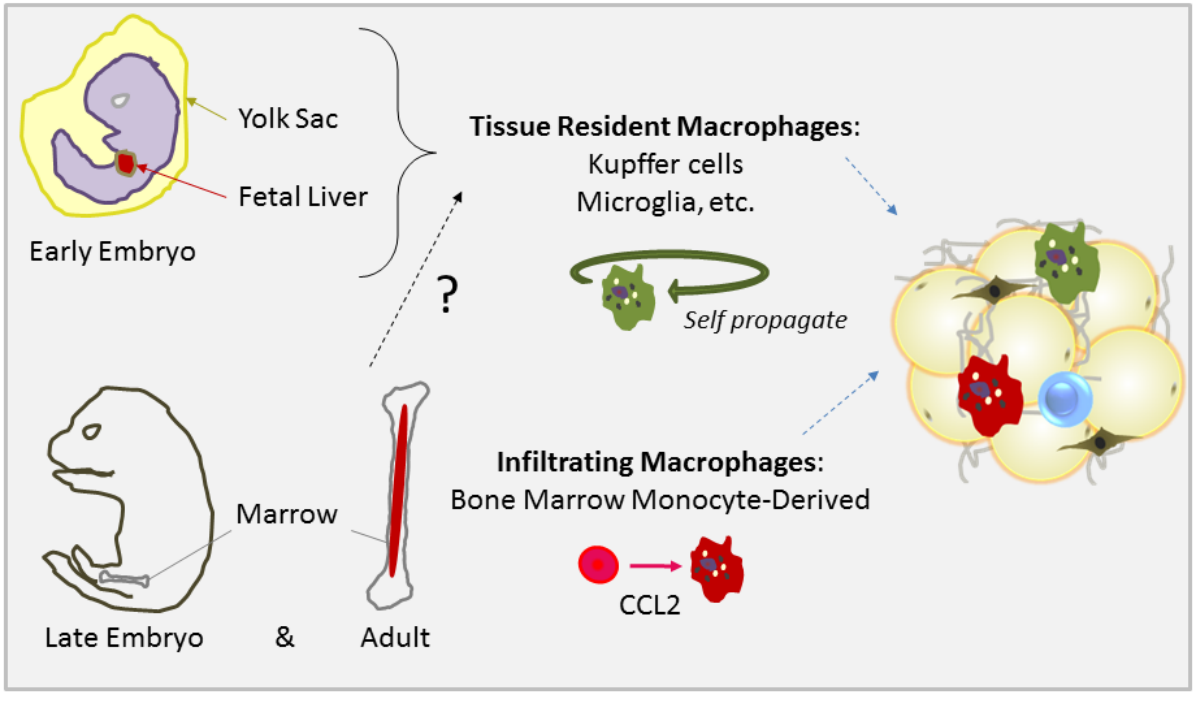

Figure 19. Adipose tissue macrophage ontogeny. Lineage tracing studies have revealed multiple embryonic sources for tissue-resident macrophages (e.g., Kupffer cells, microglia) including the yolk sac and fetal liver. However, the contribution of bone marrow monocyte-derived macrophages to tissue-resident populations remains ambiguous. Moreover, the relative contribution of yolk sac, fetal liver, and bone marrow-derived macrophages within adipose tissue depots has not been established, although the overall proportion of inflammatory, bone-marrow derived macrophages increases in obese adipose.

Macrophage content and phenotypes in obesity

Macrophages are the most highly represented immune cells in adipose tissue, and their numbers increase considerably in both visceral and subcutaneous adipose in obesity. However, the increased presence of ATMs in obesity appears to arise from multiple tissue sources. For example, using bone marrow transplant studies employing *CD45.2*-expressing recipient mice and syngeneic *CD45.1*-expressing donor mice, Weisberg et al. reported that adipose-infiltrating macrophages in obesity had differentiated from bone marrow-derived, circulating monocytes [275]. However, Amano et al. demonstrated that elevated CCL2 in visceral adipose drove local proliferation of macrophages in obesity, which contributed to ATM accumulation [358]. Local ATM proliferation was also observed by Hasse et al., with live imaging of adipose explants

showing that macrophages expressing M2-identifying markers underwent mitosis within CLS, followed by migration to interstitial spaces between adipocytes [359]. Moreover, *in vivo* proliferation in a subset of bone marrow-derived macrophages has also been described, a surprising finding as bone marrow-derived macrophages were long believed to be terminally differentiated and thus non-proliferative [360]. Importantly, however, recruitment of bone marrow-derived macrophages and local ATM proliferation need not be mutually exclusive, and future studies should examine obese ATM ontogeny in a longitudinal fashion.

Regardless of their tissue of origin, the increased presence of macrophages in obese adipose tissue can be best observed histologically as an increase in CLS formation. Indeed, Weisberg et al. demonstrated that macrophage influx and CLS formation in both mice and humans were significantly correlated with both adipocyte diameter and BMI [275]. Time course studies probing the changing immune profile in obesity report that this macrophage accumulation occurs subsequent to neutrophil and T cell infiltration [318, 361]. However, there is variability in both the reported timing of macrophage influx and the degree of infiltration across adipose depots. For example, Elgazar-Carmen et al. observed an increase in CLS formation in murine visceral adipose tissue as early as 3 weeks into high fat feeding, which increased in density over time until the study endpoint at 16 weeks of diet exposure [361]. On the other hand, Nishimura et al. reported that the presence of macrophages in the stromal-vascular fraction of visceral adipose tissue did not increase until 10-12 weeks of high-fat feeding [318]. These temporal differences may be due to variation in the age at which obesity was induced and the dietary composition used to generate adiposity (i.e., both the percent kilocalories obtained from lipids as well as the lipid profile), as each are important considerations in diet-induced obesity studies. Nevertheless, although the initial timing of macrophage infiltration varies across studies, macrophage accumulation continues with prolonged obesity, with ATMs eventually comprising up to 50% of adipose stromal-vascular cells [275, 362-364]. Due to sexual dimorphism in mice with regard to degree of adiposity in response to high-fat feeding, as well as differential contribution of adipose depots to obesity-associated metabolic dysregulation, many obesity

studies have preferentially quantified changes in macrophage content in abdominal adipose depots of male mice (i.e., inguinal and periepididymal). However, we and others have also demonstrated obesity-associated CLS formation in the mammary fat pad of female mice, as well as human breast adipose tissue [321, 322, 365, 366].

As mentioned in previous sections of this review, obese adipose tissue frequently exhibits elevated levels of pro-inflammatory cytokines such as TNF-α and IL-6. Although obese adipocytes have been shown to contribute to the secretion of these factors [367], macrophages and other stromal-vascular cells are thought to be the primary source of pro-inflammatory mediators in both mice [275] and humans [368, 369]. Following initial reports of adipose macrophage influx in 2003 [275, 364], early characterization of ATMs reported the appearance of a CD11c-expressing population of ATMs in adipose tissue of obese, but not lean, mice [370, 371], as well as a phenotypic switch in the collective ATM population from an anti-inflammatory (M2) polarized state in lean animals to a pro-inflammatory (M1) state in obese animals [370]. Importantly, however, more recent research indicates that the nature of ATM phenotypes in obesity is more dynamic and complex than originally expected. For example, the pro-inflammatory phenotype of CD11c-expressing ATMs appears to be malleable and may be modulated by degree of insulin sensitivity in obese animals [372]. In addition, more extensive profiling of ATMs in obese adipose of mice and humans has revealed that these cells harbor a "mixed" pro- and anti-inflammatory phenotype [373, 374]. For example, in human abdominal subcutaneous adipose, ATMs accumulating in CLS expressed both CD11c and the commonly used M2 marker mannose receptor C type 1 (CD206), as well as both pro- and anti-inflammatory interleukins (IL-1β, IL-6, IL-8, and IL-10) [375]. These results are further supported by Nakajima et al., who reported accumulation of ATMs expressing both CD11c and CD163, the latter of which is commonly associated with M2-like macrophages, in abdominal visceral and subcutaneous adipose of obese subjects [376]. Shaul et al. [373] also described a mixed M1/M2 phenotype in obese murine CD11c+ visceral ATMs, suggesting phenotypic and functional similarities between murine and human ATMs in obesity. Interestingly, in the latter study, these

mixed phenotype ATMs exhibited a shift toward a more M2-like transcriptional profile as obesity progressed.

Due to the phenotypic overlap between ATMs and canonical M1- and M2-polarized macrophages, the precise stimuli that activate ATMs, as well as the specific surface marker profile of this cell population, have only recently been described. Using a membrane proteomics approach, Kratz et al. [377] described a unique, ‘‘metabolically-activated’’ phenotype in visceral ATMs from obese mice, which displayed surface markers distinct from those of classically-activated macrophages generated *in vitro.* When these metabolically-activated ATMs were recapitulated *in vitro* by exposure to conditions characteristic of the metabolic syndrome (high glucose, insulin, and palmitate), they were further found to exhibit increased surface expression of M2-associated lipid metabolizing proteins, but not other M2-defining markers. Metabolically-activated ATMs also exhibited increased PPARγ activation, as well as a strong and selective induction of protein sequestome-1/p62, a scaffold protein with a variety of signaling roles including activation of the transcription factor nuclear factor kappa-light-chain-enhancer of activated B cells (NF-κB) [377, 378]. Importantly, PPARγ is a transcription factor crucial in the generation of the M2-like macrophage phenotype, while the NF-κB transcription factor family mediates several aspects of the M1 inflammatory response. Moreover, ablation of PPARγ or p62 in metabolically activated macrophages increased expression of several pro-inflammatory mediators, indicating that PPARγ and/or p62 attenuate pro-inflammatory responses in ATMs in obesity [377]. Moreover, Ferrante and colleagues [379] observed elevated lysosome biogenesis and lipid metabolism in visceral adipose ATMs from obese mice relative to lean, without concomitant activation of inflammatory pathways. In fact, the authors suggested that the driving force for the chronic low-grade inflammation observed in obesity may simply be due to the increased density of macrophages in obese adipose, rather than a shift in the inflammatory potential of individual macrophages. Thus, questions remain regarding our understanding of ATM phenotype and degree of plasticity within adipose tissue.

Adipose tissue macrophages: connections to cancer

Increased ATM content in obesity suggests a clear inflammatory link between obese adipose and initiation of adipose-adjacent cancers. For example, as mentioned previously, macrophage infiltration into obese breast adipose tissue and resulting inflammation are linked to increased risk of mammary carcinogenesis [321, 322]. Additionally, in various sections of this review we have addressed roles for ATMs in development of adipose tissue fibrosis [88, 97], which may influence early stages of tumor initiation. Macrophages are also highly represented within the body and margins of many solid tumor types, and directly promote progression of both early and established tumors [380, 381]. Indeed, macrophages are implicated in every aspect of tumor progression, including induction of the angiogenic switch [382]; generation of an immunosuppressive environment [342]; ECM degradation to facilitate invasion and migration of tumor cells into surrounding tissue; and physical participation in tumor cell metastasis [380, 383]. Macrophages have also been shown to negatively influence response to anticancer therapies in breast and prostate cancers [384-388]. Accordingly, in human breast tumors, degree of macrophage infiltration is an independent prognostic indicator strongly associated with high vascular grade, reduced relapse-free survival, and decreased overall survival [258, 380, 389].

Differences in phenotype and trophic potential between embryonic-resident, locally-proliferating, and bone marrow-derived ATM populations may influence tumor development and ATM participation in the tumor microenvironment. Collectively, macrophages found both along the solid tumor periphery and within the tumor mass are referred to as tumor-associated macrophages (TAMs). Studies investigating the origins of TAMs in mice have reported that circulating bone marrow-derived monocytes are the primary source of TAMs in syngeneically grafted [390] and spontaneously arising mammary tumors [356], as well as in breast cancer pulmonary metastases [391]. Furthermore, Franklin et al. reported that monocyte-derived TAMs in the MMTV-PyMT mouse model of spontaneous breast cancer proliferate within the tumor site and are phenotypically and functionally distinct from the resident mammary tissue macrophages

present before tumor development [356]. Together these observations argue against recruitment of local tissue-resident macrophage populations. However, studies probing TAM ontogeny have investigated this question *exclusively in lean animals*. The term “tissue-resident macrophages” is often used to refer to embryonic macrophages but may also refer to any macrophages residing in a given tissue before an insult induces recruitment of bone marrow-derived inflammatory monocytes. Both expansion of adipose tissue in obesity and the presence of a developing tumor act as inflammatory insults; thus, the marked increase in ATM content in obesity, as well as their variable tissues of origin and distinct phenotypic differences from macrophages in lean adipose, requires an evaluation of the ATM-TAM relationship in the context of obesity.

Similarities between adipose tissue macrophages and tumor-associated macrophages

In a similar vein to ATMs, discrepancies exist between reports of the defining “TAM phenotype”. Conventionally, TAMs have been described as resembling alternatively-activated M2 macrophages [342, 392, 393]. However, large-scale transcriptome analyses of TAMs in breast cancer suggest that TAMs collectively exhibit a mixed phenotype, expressing both M1-like and M2-like markers [394]. Interestingly, this same study also showed that the gene signature of breast TAMs resembled that of fetal macrophages, with increased abundance of transcripts for genes regulating angiogenesis, tissue remodeling, and immune response [394]. On the other hand, Franklin et al. recently reported that TAMs in the MMTV-PyMT model of metastatic, luminal-B breast cancer did not resemble M2-like macrophages, nor were they dependent upon tumor-elicited Th2 immune response [356]. Together these studies indicate that, at least in breast cancer, TAMs are highly heterogeneous, and their phenotypes depend on tumor type, subtype, and location within the tumor (i.e., margins vs. periphery and extent of hypoxia) [383]. Alterations in TAM phenotypes may also occur over the course of tumor development and progression, as Qian and Pollard have described a shift in TAMs throughout

tumorigenesis from an “inflammatory” type during tumor initiation to an anti-inflammatory, M2-like trophic type in later stages of tumor progression [383]. As mentioned previously and discussed further in the following section on *Myeloid-derived suppressor cells*, a similar shift has been described in ATMs over the course of prolonged obesity [373].

Shared characteristics between the tumor and obese adipose microenvironments, such as fibrosis, elevated ECM stiffness, angiogenesis, and regional hypoxia, may foster similarities between ATMs and TAMs. In particular, transient hypoxia activates the NF-κB transcription factor family [395]. While numerous molecules are involved in generating inflammation, NF-κB has long been considered to lie at the center of the inflammatory response. However, due to the plurality of NF-κB family members, as well as the sheer number of combinatorial interactions within canonical and non-canonical signaling pathways, NF-κB activation can have both pro- and anti-inflammatory effects. Inflammatory mediators controlled by canonical NF-κB signaling include the TNF superfamily, IL-1β, IL-6, several chemokines, COX-2, 5-lipooxygenase, MMPs, VEGF, and cell surface adhesion molecules [396]. Some of these gene products also activate NF-κB, with TNF-α being a particularly potent stimulus [396]. On the other hand, non-canonical NF-κB activities, such as regulation of IL-10 and TGF-β, play a role in inflammation resolution [397, 398]. As discussed throughout this review, many of these signaling mediators also contribute to tumor malignancy through a variety of mechanisms, including growth promotion, matrix degradation, and tumor angiogenesis. In fact, NF-κB signaling is a known mediator of the tumor promoting activities of both early-stage, pro-inflammatory TAMs, and late-stage immunosuppressive TAMs [399-402]. A study by Mayi et al. [403] provided direct evidence underscoring the similarities between ATMs and TAMs. Specifically, ATMs from obese individuals expressed several of the same cancer-promoting genes as TAMs, including angiogenic factors, chemokines, cytokines, proteases, and growth factors. In fact, many of these pro-tumoral genes, including VEGF-C and CXCL12, were expressed to an equal or greater extent in obese ATMs compared with TAMs [403], and are known targets of non-canonical NF-κB signaling [404]. Taken together, these findings indicate that chronically

activated NF-κB signaling and dysregulated immune responses are likely unifying themes between ATMs and TAMs.

Myeloid-derived suppressor cells

For reasons that are not well understood, abnormalities in myelopoiesis under conditions of prolonged inflammation such as chronic infections and cancer generate a poorly differentiated group of myeloid lineage cells collectively termed myeloid-derived suppressor cells (MDSCs) [405]. MDSCs include immature monocytes, neutrophils, dendritic cells, and macrophages, and are defined by their expression of the myeloid lineage markers CD11b and Gr1 and their potently immunosuppressive properties [405-407]. Although they are comprised of multiple myeloid cell types, MDSCs are often described as immature macrophages, as MDSCs in mice are frequently reported to lack markers of mature macrophages such as major histocompatibility complex II (MHCII) and/or F4/80 [407, 408].

Factors implicated in promoting the egress of MDSCs from bone marrow, as well as their arrest in an immature state and their immunosuppressive nature, include PGE_2, IL-6, TNF-α, IL-1β, and VEGF [407]. Of these factors, PGE_2 is a particularly potent inducer of MDSCs that triggers upregulation of arginase metabolism, thereby suppressing T cell function [409-411]. Several of these signaling molecules are in turn produced by MDSCs, resulting in a positive feedback loop of MDSC recruitment. Notably, as discussed in various sections throughout this review, each of these factors is also elevated in obese adipose tissue, and increased MDSC content in adipose tissue of obese mice has recently been reported. Indeed, Xia et al. [408] demonstrated that increased MDSC content in peripheral tissues (e.g., adipose and liver) of obese mice acted as an important safeguard of insulin sensitivity in both genetic and diet-induced models of obesity. Depletion of Gr1-expressing cells exacerbated symptoms of glucose intolerance and increased the presence of CD8+ T cells in adipose tissue. On the other hand, adoptive transfer of MDSCs improved fasting glucose and insulin levels in obese mice and

reduced levels of circulating pro-inflammatory cytokines. Interestingly, the onset of MDSC accumulation coincided with previously reported windows of CD8+ T cell and pro-inflammatory macrophage recruitment, supporting the putative role of MDSCs in suppression of a rampant inflammatory response. Accordingly, the percentage of CD11b+ Gr1+ MDSCs in adipose tissue increased with the duration of obesity [408]. Factors contributing to the accumulation of adipose MDSCs in obesity are poorly understood, but may include development of insulin resistance or increased local concentrations of estrogen and IGF-1, each of which have been found to influence MDSC biology [412]. Importantly, influx of MDSCs into adipose in prolonged obesity may provide a partial explanation for reports of a shift in overall ATM phenotype over the course of obesity from pro-inflammatory M1-like to that of more immunosuppressive M2-like macrophages [373]. For example, isolated MDSCs cultured with media conditioned by explanted obese adipose tissue displayed a greater shift toward an M2-like macrophage profile than MDSCs exposed to lean adipose explant-conditioned media [408]. Future studies should examine the extent to which MDSCs in obese adipose differentiate to M2-like macrophages *in vivo*.

While the presence of MDSCs in obese adipose tissue is a relatively recent finding, a large body of literature supports the immunosuppressive functions of MDSCs within the tumor microenvironment. However, similarities in marker expression and immunosuppressive activation states may complicate a clear distinction between TAMs and MDSCs. Moreover, MDSCs can also differentiate into mature TAMs upon entry into the tumor microenvironment [413]. Functional similarities between MDSCs and certain TAM subsets have also been documented. For example, MDSCS suppress the function of critical antitumor defense cells (e.g., CD8+ cytotoxic T cells and NK cells) through expression of cytokines such as IL-10 and TGF-β and through arginine metabolism via the enzymes arginase-1 or inducible nitric oxide synthase (iNOS) [407]. Interestingly, simultaneous expression of arginase-1 and iNOS is a hallmark of MDSCs that is rarely observed in other immune cells [407].

As described in the *T lymphocytes* section above, activation of the PD-1 pathway in T cells is a critical checkpoint promoting immunosuppression in the tumor microenvironment [414]. Prima et al. reported that co-culture of bone marrow-derived myeloid cells with bladder tumor cells elevated production of PGE_2 by both MDSCs and TAMs, and induced expression of the PD-1 ligand, programmed death-1 ligand (PD-L1), in these populations in a PGE_2-dependent manner [415]. Increased expression of PD-1 and its ligands PD-L1 and PD-L2 were also more highly expressed in prostate tumors of obese mice compared to those from lean animals [416]. Importantly, hypoxia-induced HIF-1α activation in TAMs was also recently shown to control TAM-specific PD-L1 expression [417]. Whether regional hypoxia in obese adipose and resulting HIF-1α activation increases PD-L1 expression by ATMs remains to be seen. However, the presence of MDSCs in prolonged obesity, as well as their influence on ATM activation, further suggests that adipose-adjacent cancers in obese individuals may encounter an environment conducive to suppressed immunosurveillance.

Neutrophils

Neutrophils infiltrate adipose tissue early in progression to obesity

Neutrophils are the most abundant white blood cells in human circulation and are typically the first immune cells recruited in response to infection or sterile tissue injury. Upon arrival, neutrophils secrete a variety of pro-inflammatory cytokines and participate in presentation of antigen to, and activation of, T cells, while helping to recruit additional inflammatory cells such as macrophages [418]. In lean animals, neutrophils represent a small fraction of total adipose tissue immune cells (<1%) [419]. However, Elgazar-Carmon and colleagues [361] demonstrated that transient neutrophil infiltration into visceral adipose depots occurs early during the course of adipose tissue expansion in diet-induced obesity models, suggesting induction of an acute inflammatory response. Indeed, neutrophils accumulated in visceral (periepididymal) adipose of male mice as early as 3 days after initiating high-fat feeding

- well before weight gain - with a corresponding increase in the neutrophil enzyme myeloperoxidase. Maximal myeloperoxidase was detected within 3-7 days, followed by a slow decline and return to baseline levels within 2-3 weeks of high fat feeding, and neutrophils were no longer detectable histologically at 16 weeks on diet. Talukdar et al. [420] also reported a rapid and dramatic increase in adipose tissue neutrophil content by 3 days of high fat feeding. This increase was maintained for up to 90 days by fluorescence-activated cell sorting (FACS) analysis of immune cells within the periepididymal adipose stromal-vascular fraction of obese male mice, with a corresponding increase in neutrophil elastase mRNA. However, the exact adipose tissue-derived chemoattractant(s) that mediate neutrophil recruitment so early during the course of adipose tissue expansion remain unclear, as adipocyte hypertrophy and death do not typically occur until several weeks into diet-induced obesity studies. In either case, once inflammation is established, neutrophils in inflamed adipose engage in bidirectional interactions with macrophages, dendritic cells, natural killer cells, lymphocytes, and mesenchymal stem cells, with important implications for adipose metabolic homeostasis. For example, neutrophil elastase appears to be an important mediator in the development of obesity-associated insulin resistance in response to adipose inflammation, signaling through Toll-like receptor 4 and downstream NF-kB activation to influence both recruitment and inflammatory activation state of infiltrating immune cells in obesity, including neutrophils themselves [420].

Tumor-associated neutrophils

Within the tumor microenvironment neutrophils exhibit varied content and multiple phenotypes and have been found to exert both pro- and anti-tumoral effects. Similar to the M1/M2 dichotomy long used for macrophages (but now transitioning out of favor as described above), tumor-associated neutrophils (TANs) have been described as either “N1” (anti-tumoral) or “N2” (pro-tumoral) (**Figure 20**) [421]. The N1 neutrophil profile is reported to be promoted by increased levels of interferon-β [422] and pro-inflammatory cytokines such as IL-1β and TNF-α

[422, 423], while transforming growth factor β (TGF-β) is an important determinant of the N2 phenotype [421]. Relative to N2 neutrophils, N1 neutrophils display elevated oxygen radical-dependent cytotoxicity and increased expression of the chemokine CCL3 and the cell adhesion molecule ICAM [421], which recruit additional inflammatory cells and act to increase adherence and extravasation, respectively.

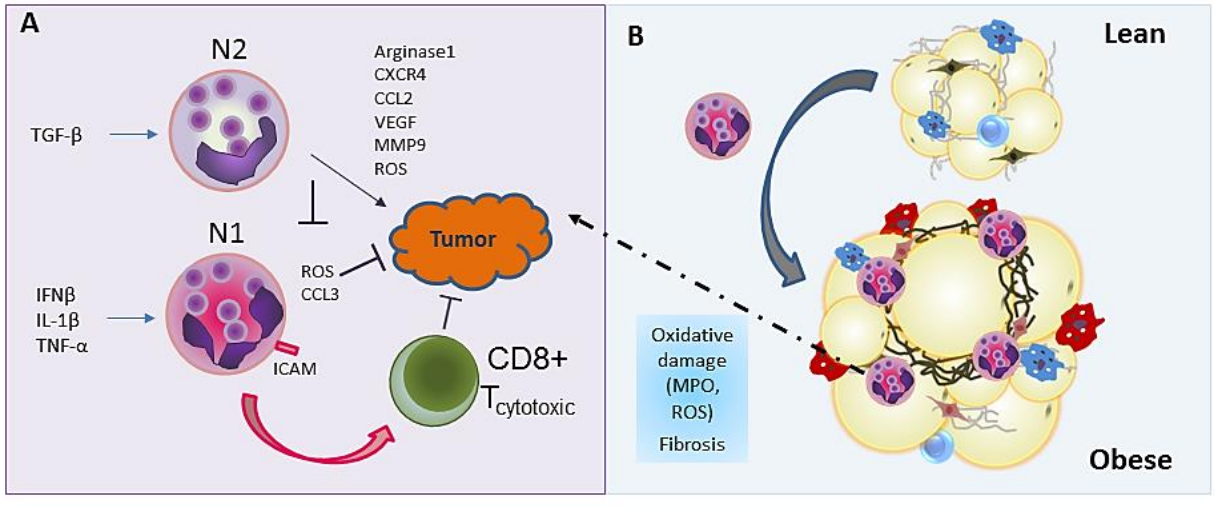

Figure 20. Tumor-associated neutrophils have N1 and N2-like phenotypes. A) Neutrophil content and phenotype is both pro- and anti-tumoral with cytokines such as IFNβ, IL-1β, TNF-α activating the N1 or pro-inflammatory phenotype and TGF-B driving the N2 immunomodulatory phenotype. The N1 neutrophil releases reactive oxygen species (ROS) and proteins that increase cell recruitment and extravasation (ICAM and CCL3 (MIP-1-alpha)). N1 neutrophils support cytotoxic CD8+ T cell activity. N2 neutrophils have a less segmented nucleus than typical and secretes many angiogenic and immunosuppressive mediators, expressing arginase 1 for example. ROS secreted by both N1 and N2 may both promote genotoxicity in tumor initiation, or in contrast, can be cytotoxic to growing tumors. B) Neutrophils infiltrate adipose early during progression to obesity. Neutrophil production of reactive oxygen species, for example, through myeloperoxidase (MPO) expression, contributes to oxidative stress and fibrotic changes.

Pro-inflammatory N1 neutrophils promote CD8+ cytotoxic T cell recruitment and activation by producing T-cell attracting chemokines and pro-inflammatory cytokines [424]. The N2 subpopulation can be distinguished morphologically, with less pronounced segmentation of the nuclei than N1 neutrophils and elevated expression of pro-angiogenic mediators including chemokines (e.g., CXCR4, CCL2), growth factors (e.g., VEGF), and remodeling factors such as MMP9 [423, 425]. For example, neutrophil-derived MMP9 was shown to contribute to the

angiogenic switch in early-stage pancreatic adenocarcinoma [426]. Additionally, tumors formed by highly disseminating variants of prostate carcinoma recruited elevated levels of MMP9-positive TAN, which correlated with tumor cell dissemination and increased levels of angiogenesis and intravasation [425]. N2 neutrophils are also immunosuppressive; elevated expression of the enzyme arginase-1 by N2 neutrophils contributes to depletion of arginase within the tumor microenvironment, inhibiting T-cell receptor expression and antigen-specific T-cell responses [427].

Adipose tissue neutrophils and cancer

Potentially due to the minimal presence of neutrophils in lean adipose, very few studies have addressed the influence of adipose tissue on neutrophils specifically in tumors that are adipose-adjacent or adipose-invading. Wagner et al. reported that melanoma cell lines implanted within white adipose tissue of lean mice showed significantly greater infiltration of CD11b+ cells than tumors implanted at a site distant from adipose [259]. Although these cells were initially described as monocytes and/or macrophages, CD11b is expressed by multiple myeloid lineage cells, including neutrophils [428]. Furthermore, inflamed peritumoral adipose exhibited increased expression of pro-inflammatory cytokines and chemotactic factors implicated in both macrophage and neutrophil recruitment, including CXCL1, macrophage-inflammatory protein-2 (MIP-2), and CCL2 [259]. Moreover, in obese adipose, neutrophils likely contribute to both tumor initiation and tumor progression. In addition to facilitating recruitment of additional inflammatory cells, neutrophils participate in establishment of the mutagenic pro-inflammatory microenvironment associated with cancer initiation. Indeed, neutrophil-derived reactive oxygen species and myeloperoxidase are genotoxic, and are recognized mutagens in certain tumor types, such as lung cancer [429]. Furthermore, the skewed cytokine profile of inflamed obese adipose, such as elevated CCL2, may influence recruitment of neutrophils to developing tumors.

Alternatively, tumor-adjacent adipose may impinge upon the phenotype of TANs. Incio et al. [430] reported that pancreatic tumors from obese animals contained higher concentrations of adipocyte-derived IL-1β than those from lean animals, resulting in increased TAN recruitment, TAN-induced activation of pancreatic stellate cells, and enhanced deposition of fibrillary collagen (i.e., desmoplasia). Obesity was also associated with greater tumor weight, which was reverted to lean levels by TAN depletion. Importantly, tumor formation in this study was induced, via orthotopic cell injection or tumor fragment implant, following 10 weeks on a high fat diet – a period during which, as illustrated above, the presence of neutrophils in visceral adipose depots is elevated [361, 420]. Reversion of tumor growth rate was only observed when TAN depletion was initiated on day 1 following tumor induction, as opposed to day 7 [430]. Thus, it is unclear whether neutrophils recruited from the visceral adipose, as opposed to newly trafficked peripheral blood neutrophils, were the primary contributors to induction of the desmoplastic response.

Taken together, the balance of N1/N2 TAN subtypes is an important factor in tumor progression, and future studies should consider the functions of adipose tissue neutrophils in initiation and/or progression of adipose-adjacent or adipose-invading tumors in obese individuals. Notably, although the presence of neutrophils in visceral adipose is clearly enhanced in early stage obesity, it is important to acknowledge that the time course studies described above regarding neutrophil adipose infiltration used exclusively male mice, and therefore it is unknown to what extent, or when, neutrophils also infiltrate the obese mammary fat pad.

Mast cells

Mast cell content and activation states in adipose tissue

An understudied immune cell in both adipose and tumor biology is the mast cell. Historically described as mediators of allergic hypersensitivity reactions [431], mast cells are found in virtually all tissues and are frequently classified into one of two subtypes: those residing in connective tissues, which express both tryptase and chymase, and those residing in mucosal tissues, which express only tryptase [432]. However, similar to other immune cells, mast cells exhibit plasticity based on microenvironmental conditions, and thus several phenotypic subtypes may exist [433].

Accumulation of mast cells in visceral white adipose in obesity has been reported in both mice [434, 435] and humans [435, 436], with documented heterogeneity across specific adipose depots. Altintas et al. found that mast cell density in the epididymal fat pad of male mice increased up to 230-fold under conditions of prolonged obesity, with mast cells intermingled with macrophages in the interstitial spaces between adipocytes [434]. A similar study published the same year by the same group also found dramatically increased mast cell infiltration in mesenteric and perirenal adipose, but no significant obesity-induced changes in mast cell density in inguinal subcutaneous adipose [437]. However, Liu et al. reported increased numbers of mast cells in abdominal subcutaneous adipose tissue from obese human subjects, as well as significantly elevated serum tryptase levels, relative to lean individuals [435]. Many of these mast cells were found in association with microvessels [435], implicating mast cells in the regulation of endothelial cell biology and angiogenesis in adipose tissue. Interestingly, increased serum tryptase levels were not found in obese children and adolescents, suggesting an adult-specific window of susceptibility to adipose-mast cell interactions [438].

Degree of mast cell activation is also affected by obesity. Divoux et al. [436] reported that mast cells isolated from omental and subcutaneous adipose depots of obese subjects exhibited a more activated state than mast cells isolated from lean subjects, secreting increased

levels of pro-inflammatory cytokines, chemokines, and growth factors. Histological sections also revealed that mast cells in obese subjects preferentially localized to fibrotic bundles or proximate to endothelial vessels and showed increased degranulation relative to those in lean tissue (**Figure 21A**). Collectively, these results suggested that mast cells in obesity harbor a pro-inflammatory profile, a phenotype which was recapitulated by culture of mast cells in a 3D matrix designed to mimic fibrotic conditions. Furthermore, a positive correlation was observed between mast cell density and both fasting glucose and glycated hemoglobin, suggesting a role for mast cells in altered glycemic status in obese subjects. Finally, Zhou et al. recently showed that mast cells in both white adipose and bone marrow of obese mice express elevated levels of leptin, potentially in response to increased regional concentrations of IL-6 or TNF-α in obesity [439].

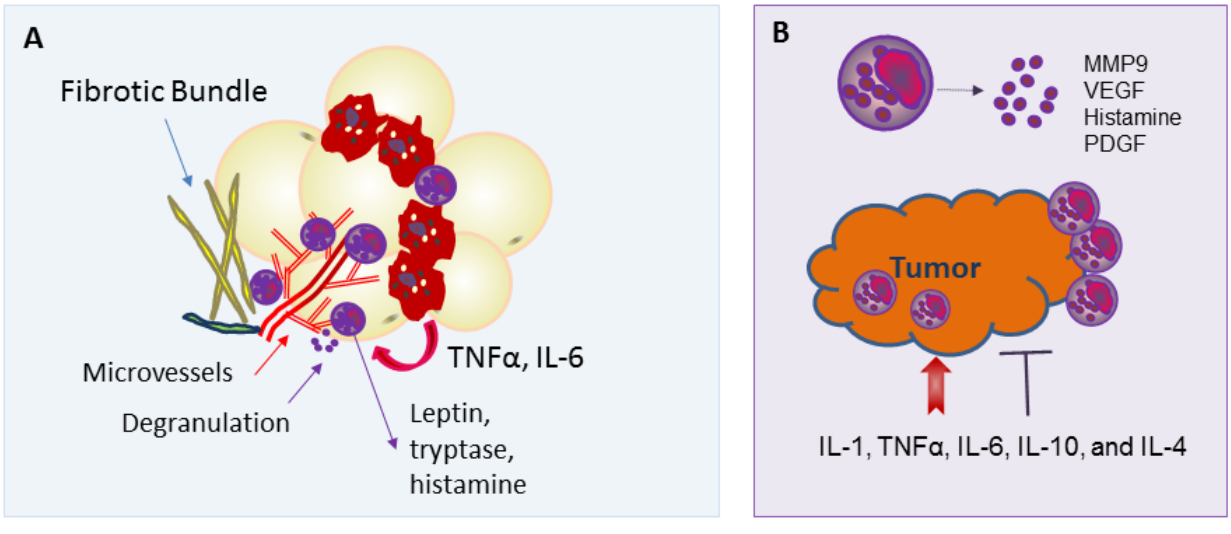

Figure 21. Mast cells: Unappreciated players in adipose and tumor biology. A) Mast cell content in adipose tissue increases with obesity, with mast cells localized to blood vessels and/or within fibrotic bundles. Obesity is also associated with increased mast cell degranulation, an indicator of a mast cell activation. B) In cancer, mast cells contribute to tumor progression through release of pro-angiogenic factors (MMP9, VEGF), immunosuppressive mediators (histamine), or growth factors such as PDGF. Mast cells also secrete cytokines that may promote (arrow) or inhibit (line) tumor progression. Mast cell influence on tumor progression appears to be dependent upon mast cell localization as peri- versus intratumoral.

Similar to the other immune cell populations described above, mast cells have been ascribed both pro- and anti-tumoral roles. Tumor promotion by mast cells has been attributed to

secretion of proangiogenic factors such as MMP9 and VEGF, immunosuppression through release of histamine, or growth promotion by mitogenic factors including PDGF [440]. Mast cells also secrete IL-1, TNF-α, IL-6, IL-10, and IL-4 [440], each of which plays complex – and sometimes controversial – roles in solid tumor biology [441-446]. Thus, below we consider the potential relevance of adipose mast cells to cancer progression with regard to potential changes induced with increased adiposity and prolonged obesity.

Mast cells in breast cancer

In breast cancer, mast cell tryptase levels are linked to angiogenesis and lymphangiogenesis [447, 448], lymph node metastasis [449], and myofibroblast differentiation [450]. Samoszuk et al. [451] reported elevated serum tryptase in the blood of breast cancer patients as compared to healthy controls, as well as mast cell infiltration and mast cell tryptase expression adjacent to or within the stroma of *every* breast cancer patient sample examined, including DCIS specimens. Interestingly, in patients with invasive breast cancers, tryptase was found more frequently as extracellular deposits, suggesting mast cell degranulation, whereas in patients with early stage breast cancer, tryptase was located intracellularly, within intact mast cells [451].

Remarkably, mast cell activation state and influence on the course of tumor development appear to also depend upon their localization within the tumor microenvironment (**Figure 21B**). For example, correlation between mast cell density and lymphatic microvessel density varied based on breast cancer subtype and peritumoral *versus* intratumoral mast cell location [447]. As discussed in an earlier section of this review, peritumoral lymphatic vessel is a prognostic indicator in several cancer types, including cervical, colorectal, breast, and prostate cancers [243-247]. Indeed, *peri*tumoral mast cell density was significantly positively correlated with lymphatic density in luminal A and basal-like breast carcinomas; on the other hand, *intra*tumoral mast cell density showed a low inverse correlation with lymphatic density in both

luminal A and HER2+ breast cancer subtypes, yet a positive correlation with basal-like carcinomas [447]. In addition, Rajput et al. investigated over 4,000 clinically annotated tissue microarrays from invasive breast cancer patients with long-term follow-up, and reported that intratumoral mast cell infiltration was a strong marker of favorable prognosis independent of age, tumor grade, tumor size, lymph node status, and ER or HER2 status [452]. Future work should address the molecular significance of the differential prognostic implications based on mast cell localization observed across breast cancer subtypes.

Mast cells in prostate cancer

Mast cell location also appears to influence prognosis in prostate cancers. Indeed, Nonomura et al. reported that increased peritumoral mast cell count was associated with reduced recurrence-free survival and higher Gleason scores in prostate cancer patients treated with radical prostatectomy, irradiation therapy, or androgen deprivation therapy [453]. Androgen deprivation therapy, also called castration therapy, is the gold standard for treatment of patients with metastatic prostate cancer. However, despite high initial response rates, nearly all men eventually develop progressive disease, referred to as “castration-resistant” prostate cancer. Johansson et al. [454] found that androgen deprivation therapy increased mast cell recruitment to the peritumoral tissue compartment of locally relapsing human prostate tumors, but not to the tumor itself. Peritumoral mast cells also promoted tumor growth and tumor angiogenesis, which were further exacerbated by mast cell degranulation. Moreover, patients with higher peritumoral mast cell density had higher Gleason scores and significantly shorter cancer-specific survival, while patients with low numbers of *intra*tumoral mast cells exhibited the same patterns. Low intratumoral mast cell count was also associated with high tumor stage, higher tumor cell proliferation index, and metastatic spread [454]. Similar results have been reported by others, with poorest outcomes in prostate cancer patients lacking intratumoral mast cells [455]. These studies raise several important questions: how different are peritumoral vs intratumoral mast

cells, and what are the factors determining which phenotype develops? Are these factors tumor-intrinsic or determined by the surrounding tissue, particularly adipose tissue?

Impact of obesity on peritumoral mast cells

Given consistent reports regarding the increased mast cell content and altered mast cell activation state in obese adipose, we were surprised to find not a single publication addressing the impact of obesity or adipose tissue on the density or phenotype of peritumoral mast cells. In fact, the only study found even peripherally linking mast cells in adipose tissue to cancer outcomes addressed the frequency of metastatic ovarian cancer colonization within “milky spots”, vascularized accumulations of mononuclear cells in human omental adipose that include mast cells [456]. It must also be noted that BMI was not included as a variable in any of the aforementioned studies addressing mast cell function in breast and prostate tumors.

Increased adipose tissue mast cell density in obesity suggests the potential for elevated peritumoral mast cell concentrations in adipose-infiltrating tumors of obese individuals. However, although increases in adipose mast cell density have been reported in visceral adipose tissue of obese mice [434] and abdominal subcutaneous adipose of obese patients [435], whether obesity influences mast cell density in breast subcutaneous or periprostatic adipose tissue has not been reported. Ishijima et al. demonstrated that mast cells influence preadipocyte-adipocyte transition under both physiological and pathological conditions [457], suggesting a possible role for mast cells in adipose expansion. Furthermore, adipose tissue hematopoietic progenitor cells contain a population committed to the mast cell lineage, allowing white adipose tissue to act as a reservoir for mast cells that traffic to other tissues such as skin and, potentially, developing tumors [458]. Thus, considering the differential associations between peritumoral vs. intratumoral mast cells and cancer outcomes, future studies should

investigate the positioning and granulation status of peritumoral mast cells in relation to adipose tissue in lean and obese patients.

Eosinophils

Eosinophils are granulocytes typically associated with allergy and asthma that play key immunoregulatory roles in antigen presentation, suppression of inflammation, and maintenance of metabolic homeostasis [459, 460]. Under physiologic conditions, circulating eosinophils are rare however, eosinophils comprise ~4-5% of cells in the stromal-vascular fraction of lean adipose [461]. Indeed, Wu et al. [461] demonstrated that eosinophils are the primary source of IL-4 in adipose tissue, as ~ 90% of IL-4-expressing cells recovered from visceral adipose of lean mice were eosinophils [461]. Interestingly, they also noted an inverse relationship between adiposity and adipose eosinophil content in both genetic and diet-induced models of obesity. Furthermore, mice engineered to be eosinophil-deficient developed significantly greater adiposity and impaired glucose tolerance in response to high-fat diet feeding. These results were attributed to impaired eosinophil-mediated maintenance of alternatively activated, anti-inflammatory macrophages, which are generated upon exposure to IL-4 and/or IL-13 and are generally considered to be protective against diet-induced obesity and associated metabolic dysregulation. Subsequent studies have revealed that visceral adipose eosinophil populations, and thus alternatively activated macrophages, are in turn dependent upon innate lymphoid type 2 cells (ILC2s) through their production of IL-13 and IL-5, an eosinophil colony-stimulating factor [462]. In light of their direct or indirect anti-inflammatory effects, it is tempting to speculate that the presence of eosinophils and ILC2s in lean adipose, and their relative absence in inflamed obese adipose, may be a contributing factor to the differential cancer risk profile in lean *vs.* obese individuals.

In light of the role of eosinophils in the maintenance of alternatively activated macrophages in normal, uninflamed adipose, it may seem surprising that these cells appear to promote pro-inflammatory macrophage polarization in tumors. Accordingly, an E1/E2 classification scheme analogous to the macrophage M1/M2 and T helper cell Th1/Th2 subsets has been proposed [463]. Eosinophil peroxidase enhances TNF-α and hydrogen peroxide release by human monocyte-derived macrophages, suggesting that paracrine signaling between eosinophils and macrophages within the tumor microenvironment may be relevant in promoting activity of certain tumoricidal TAM populations [464]. In agreement with this proposition, injection of exogenous eosinophils in a mouse melanoma model reportedly reprogrammed TAMs toward a pro-inflammatory, tumoricidal phenotype, a result attributed to increased production of eosinophil-derived IFN-γ [465]. However, it should be noted that while eosinophils facilitate tumor rejection in numerous cancer models, increased levels of circulating eosinophils are associated with poor prognosis in some hematologic malignancies, such as non-Hodgkin's and T cell lymphomas [463]. Therefore, future research should systematically address relationships between local and circulating eosinophil content, site-specific tumor promotion vs. rejection, and eosinophil-mediated modulation of macrophage polarization.

Although little research has addressed these functions in the context of obesity, it is clear that eosinophils also facilitate anti-tumor immune reactions independent of their effects on macrophage polarization. For example, Carretero et al. [465] recently reported that eosinophil-mediated production of the chemoattractants CCL5, CXCL9, and CXCL10 promoted cytotoxic T cell recruitment in developing melanomas. Antibody-mediated depletion of eosinophils reduced CD8+ T cell infiltration, impaired tumor rejection, and severely reduced animal survival. Moreover, injection of melanoma cells together with exogenous eosinophils resulted in tumor vessel normalization, as evidenced by reduced permeability, enhanced perfusion, and reduced tumor hypoxia, alterations sometimes associated with reduced tumor aggression and more efficient vascular delivery of chemotherapies. In addition to their effects on other immune cells within the tumor microenvironment, eosinophils may also exhibit direct cytotoxicity. Tepper et al.

[466] reported that mouse melanoma and plasmacytoma cells engineered to express IL-4 exhibited reduced or absent tumorigenicity in transplant studies due to elicitation of an inflammatory infiltrate comprised predominantly of macrophages and cytotoxic eosinophils. Accordingly, administration of a monoclonal antibody with granulocyte-specific cytotoxicity depleted eosinophils and restored tumorigenicity of IL-4-producing cells. However, these results were called into question by a subsequent study in which eosinophil-deficient IL-5-knockout mice showed similar degrees of IL-4-expressing melanoma rejection as wild-type animals, a phenotype attributed to a neutrophil-mediated response [467]. Ultimately, the conflicting results of these two studies indicate that the putative cytotoxic functions of eosinophils in anti-tumor immunity warrant further study. Moreover, additional investigation into eosinophil content in lean vs. obese adipose and their potential influence on adipose-tumor interactions should yield interesting findings.

Conclusion

Although adipocytes comprise the bulk of adipose tissue volume, adipose also contains a rich variety of stromal and vascular cells, as well as matrix and signaling components, which together constitute the adipose tissue microenvironment. A growing body of literature indicates that reciprocal, heterotypic interactions between developing tumors and the local adipose milieu influence the course of solid tumor progression. Herein, we have provided an overview of interactions between select adipose tissue components and developing adipose-adjacent cancers, emphasizing breast and prostate cancers and the known or potential impact of changes that occur in the adipose tissue microenvironment during progression to obesity. As described throughout this review, obesity-associated adipose modifications often resemble aberrations observed within the tumor microenvironment. For example, similar to tumors, dysregulated, obese adipose tissue is characterized by chronic low-grade inflammation, macrophage infiltration, hypoxia, and aberrant wound healing responses, including an increase

in myofibroblast and activated fibroblast content. Obese adipose tissue is also a harbor for soluble mediators of cancer development, including metabolites, exosomes, cytokines, growth factors, and extracellular matrix scaffolding proteins, which collectively provide a critical link between adiposity and tumorigenesis. Thus, we posit that adipose-adjacent epithelium in obese individuals encounters an environment particularly conducive to tumor initiation and progression.

Despite a recent increase in research regarding the contributions of adipose tissue in cancer development, many questions still remain. For example, the identities of many adipose-derived microenvironmental signaling mediators that modify tumor biology are largely unknown. Furthermore, while immune cells in both adipose tissue and cancer biology have been characterized individually, few studies have attempted to quantify recruitment of immune cells originating in adipose tissue adjacent to tumors. This potential for recruitment becomes especially important in the context of obesity, wherein adipose tissue immune cell content is greatly increased, yet the relative immune composition and phenotype shifts dramatically. Thus, the extent to which specific adipose-derived cell lineages contribute to tumor development and/or progression remains inconclusive. Ultimately, given the rising global prevalence of obesity, a better understanding of the molecular interactions between adipose tissue components and tumor cells is critical for the identification of novel targets for prevention and/or treatment of obesity-associated cancers.

CHAPTER 2: CMET INHIBITOR CRIZOTINIB IMPAIRS ANGIOGENESIS AND REDUCES TUMOR BURDEN IN THE C3(1)-TAG MODEL OF BASAL-LIKE BREAST CANCER[2]

Background

Basal-like breast cancer (BBC) accounts for 15-20% of total breast cancers, with a higher prevalence in young and minority women such as African Americans and Hispanics [468, 469]. BBC is typically estrogen receptor (ER), progesterone receptor (PR) and human epidermal growth factor receptor-2 (HER2) negative (so called “triple-negative”) and is highly aggressive, exhibiting an early pattern of metastasis and poor overall prognosis. Thus, BBC presents a formidable challenge, as it lacks the molecular targets for current targeted drug treatments. High body mass index (BMI) is associated with poorer prognosis in breast cancer patients, including increased risk of lymph node metastasis, vascular invasion, disease recurrence, and mortality [24, 52, 53]. Epidemiologic studies indicate that obesity is strongly associated with the BBC subtype in both pre- and post-menopausal women [52, 469]. Obesity mediates, and can exacerbate, both normal and tumor microenvironment dysfunction [296, 470]. In obesity, rapid expansion in mammary adipose tissue leads to alterations in the stroma that mediate normal and tumor microenvironment dysfunction yet are poorly understood in breast cancer risk and progression [296, 470-472]. Given that obesity has increasing prevalence and is one of few modifiable risk factors for breast cancer, it is important to better elucidate the mechanisms for this obesity-associated cancer.

[2]This chapter previously appeared as an article in the journal SpringerPlus, in a special Breast Cancer Edition. The original citation is as follows: Cozzo AJ, Sundaram S, Zattra O, et al. cMET inhibitor crizotinib impairs angiogenesis and reduces tumor burden in the C3(1)-TAg model of basal-like breast cancer. *SpringerPlus.* 2016; 5:348. doi:10.1186/s40064-016-1920-3.

We have shown that BBC is characterized by unique epithelial-stromal interactions, which likely play a role in BBC etiology [142, 473-475]. An elevated level of hepatocyte growth factor (HGF), a pleiotropic growth factor that signals through the receptor tyrosine kinase cMET, is characteristic of BBC [476]. Elevation of circulating HGF is also seen in obese patients [147]. HGF/cMET signaling initiates an invasive growth program that promotes cell migration, invasion, proliferation, and angiogenesis [141]. Endothelial cell upregulation of cMET has also been attributed to inherent or acquired resistance to antiangiogenic therapies targeting vascular endothelial growth factor (VEGF) in patients [265, 266]. Marking the first work in preclinical models paralleling human epidemiologic BBC findings, we used C3(1)-TAg mice, a unique GEMM of spontaneous BBC, to demonstrate that high fat diet (HFD)-induced obesity accelerated onset of tumor development and increased tumor aggressiveness as compared to low fat diet (LFD)-fed lean controls [43]. HFD also increased mammary gland HGF concentration and enhanced expression and activation of cMET. Using primary murine fibroblasts isolated from mammary glands or tumors, we further reported that obesity increased HGF production by mammary gland normal- and cancer-associated fibroblasts (NAF and CAF) [43]. Through signaling inhibition *via* an HGF blocking antibody, we showed that obese CAF-induced epithelial cell migration occurred through an HGF-dependent mechanism. Furthermore, using the intervention strategy of weight loss prior to tumor latency, we reported that weight loss blunted effects of HFD-induced obesity on multiple tumor parameters compared to mice maintained on HFD. Importantly, HFD-induced elevation of HGF/cMET signaling in normal mammary gland and cMET in tumors was significantly reversed with weight loss in C3(1)-TAg mice, with a concomitant and complete reversal of HFD-driven tumor progression [264].

Given the precedent for the role of HGF signaling in invasive breast cancer [477], a better understanding of HGF's role in BBC tumorigenesis was necessary. We hypothesized that inhibition of cMET signaling through crizotinib therapy (PF-02341066) would reduce HFD-induced BBC. We first sought to inhibit tumor progression in existing tumors and began

crizotinib treatment upon identification of the first palpable tumor. Crizotinib significantly reduced total tumor burden in both LFD- and HFD-fed C3(1)-TAg mice, with a corresponding reduction in microvascular density. We next investigated whether we could inhibit or delay tumorigenesis by treating C3(1)-TAg mice with crizotinib prior to tumor development. Crizotinib treatment paradoxically increased progression of the initially detected tumor in both diet groups. However, at sacrifice there were no differences between diet or treatment groups in total preneoplastic lesions, total tumor progression or tumor burden. In summary, cMET inhibition disrupted tumor vascularization and limited subsequent BBC tumor development in tumor-bearing mice. Our results suggest that reduction of microvascular density through cMET inhibition may be a viable therapeutic target in the treatment of BBC.

Methods

Antibodies and drugs

Crizotinib (PF-2341066 [(R)-3-[1-(2,6-dichloro-3-fluoro-phenyl)-ethoxy]-5-(1-piperidin-4-yl-1H-pyrazol-4-yl)-pyridin-2-ylamine) was purchased from Selleck Chemical (Catalog No. S1068). Primary antibodies include: Rabbit anti-mouse CD31 (Abcam #ab28364, Lot GR212364-5; 1:400); Rabbit anti-mouse phospho-cMET (Abcam #ab5662, Lot GR159296-1; 1:4000); Goat anti-mouse cMET (R&D Systems #AF527, Lot CTB0310091; 1:1000)) diluted in Renoir Red Diluent (BM #PD904H). Additional reagents included biotin-conjugated Goat anti-rabbit IgG (Jackson #111-065-144, Lot 110335; 1:500); Donkey anti-goat IgG (Jackson #705-065-147, Lot 110544; 1:1000). ABC Elite (Vector #PK-6100, 1:50) and 3,3' Diaminobenzidine (DAB) (Thermo Scientific #TA-125-QHDX).

Animals and diet

Animal studies were performed with approval and in accordance with the guidelines of the Institutional Animal Care and Use Committee at the University of North Carolina at Chapel Hill. Animals were cared for according to the recommendations of the Panel on Euthanasia of the American Veterinary Medical Association. The veterinary care provided at UNC is in compliance with the Public Health Service Policy on Humane Care and Use of Laboratory Animals and meets the National Institutes of Health standards as set forth in the Guide for the Care and Use of Laboratory Animals (DHHS Publication No. (NIH) 85-23 Revised 1985). The animal facility is Association for Assessment and Accreditation of Laboratory Animal Care (AAALAC) approved and is responsible for the health and husbandry of animals. UNC also accepts as mandatory the PHS Policy on Humane Care and Use of Laboratory Animals be Awardee Institutions and NIH Principles for the Utilization and Care of Vertebrate Animals Used in Testing, Research, and Training. Animal studies comply with the ARRIVE guidelines. Mice were housed in a climate controlled Department of Laboratory Animal Medicine facility with a 12 hour light:dark cycle and *ad libitium* access to food and water or special diets as defined below. Female C3(1)-TAg mice were obtained in collaboration with the UNC Lineberger Comprehensive Cancer Center (LCCC) Mouse Phase I Unit (MP1U). C3(1)-TAg mice [150], a model of BBC, were generated by crossing heterozygous male mice with FVB/N non-transgenic female mice.

For the tumor treatment study, N= 46 female C3(1)-TAg mice were bred and maintained on chow diet (Harlan 2918) until nulliparous female were randomly assigned to LFD (N=24) and HFD (N=22) at 10 weeks of age. Diets obtained from Research Diets Inc. (New Brunswick, NJ, USA) were matched for protein, vitamins, and minerals, and provided 10% kcal (“LFD”; # D11012202); and 60% kcal (“HFD” ; # D11012204) derived from fat. Diets were sucrose-free, and soy-free. Additional details of diet components are provided in Sundaram et al. [43]. For the prevention study, during breeding and after weaning mice were put on Prolab Isopro RMH 3000

chow from LabDiet (St. Louis, MO, USA). At 8 weeks of age, nulliparous female C3(1)-TAg mice were randomly assigned to LFD (N=43) and HFD (N=45) diet.

Tumor latency, number, and progression

Mice were monitored for tumor development by palpating twice weekly. Tumor latency was defined as age in weeks at detection of first tumor. Tumor volumes were measured twice weekly over 3 weeks using calipers to measure the width (short diameter) and length (long diameter) in millimeters for each tumor. Tumor volumes were calculated using the formula: length × width^2 × 0.5. Tumor progression is reported as percent change in volume from latency to sacrifice 3 weeks later. Primary tumor progression refers to the first tumor identified; total tumor progression includes all tumors palpated. The total number of visible tumors per mouse was counted at sacrifice for total tumor burden (multiplicity).

Crizotinib treatment

Crizotinib dosage was 50 mg crizotinib/kg of body weight [478]. In the treatment study, crizotinib administration by oral gavage began at identification of the first palpable tumor and persisted for 3 weeks until sacrifice (5 days on drug, 2 days rest). Briefly, drug was prepared by dissolving 20 mg of crizotinib powder in 200 µL 1 N hydrochloric acid (HCl), then brought to a total volume of 1 mL with vehicle (0.5% glucose in phosphate-buffered saline) to yield a 2x crizotinib solution. Immediately prior to gavage administration, the 2x solution was diluted with an equal volume of vehicle to yield a 1x solution. In the prevention study, drug was prepared as a 1x solution by dissolving 10 mg of crizotinib powder in 200 µL 1 N HCl, then brought to a total volume of 1 mL with vehicle; crizotinib treatment began for all mice at 9 weeks of age and continued for 3 weeks (5 days on drug, 2 days rest).

Body weight & composition

Body weight was measured at start of diet and weekly until sacrifice. Body composition including lean mass, fat mass, free water content and total water content of non-anesthetized mice was measured using EchoMRI-100 quantitative magnetic resonance whole body composition analyzer (Echo Medical Systems, Houston, TX). Fat mass is presented as (fat mass/total body weight)×100% [43, 264]. There were no significant changes in absolute lean mass in grams (data not shown).

Tissue and blood collection

Three weeks after detection of the first palpable tumor, mice were fasted for six hours and anesthetized by an intraperitoneal (i.p.) injection of avertin (tribromoethanol/amylene hydrate, 1.25%) (Sigma Aldrich, St. Louis, MO). Blood was collected via cardiac puncture using an EDTA-coated syringe into 5µL of 250mM EDTA. Plasma was separated from other blood components by centrifugation at 10,000xg for 2 minutes at 4°C. Mammary tumors, unaffected inguinal mammary gland, liver, spleen, and lungs were flash frozen in liquid nitrogen or were placed into a cassette and formalin-fixed for immunohistochemistry (IHC) and H&E analysis. All frozen samples were stored at -80°C until analyzed.

Immunohistochemistry

Briefly, formalin-fixed and paraffin-embedded tissues were sectioned at 5 microns and mounted for histological staining [43]. Tissues were baked, deparaffinized, and hydrated. Following heat-induced epitope retrieval (Rodent Decloaker BM#RD913L)), slides were treated with 3% hydrogen peroxide in de-ionized water. Tissues were treated with Avidin/Biotin Block (Vector #SP-2001) and exposed to primary antibodies (anti-CC3, anti-Ki67 anti-CD31; anti-phospho-cMET; anti-cMET) diluted in Renoir Red Diluent at 4°C overnight. Following incubation with biotin-conjugated secondary antibodies [Goat anti-rabbit IgG; Donkey anti-goat IgG] tissue sections were treated with ABC Elite and DAB. Digital immunohistochemistry quantification was

performed following the protocol previously described in Sundaram et al.[43]. Stained slides were scanned into the Aperio Scanscope CS system (Aperio Technologies, Vista, CA, USA) at a magnification of 40× and were quantified using the Aperio Imagescope software. Scanned slides were analyzed using algorithms as described previously [42]. N=5-6 random areas from sections (n=2 sections per mouse) were quantified and averaged per tumor per animal (n=9-10 mice per diet or exposure group). Images shown are representative.

Statistical Analysis

Data are expressed as mean ± standard error of the mean (SEM). All means were compared by 2-way analysis of variance (ANOVA) with Tukey's post-hoc test for statistical differences using GraphPad Prism 5 software (GraphPad Software, Inc. La Jolla, CA). Kaplan-Meier analyses were conducted using GraphPad Prism 5 software to estimate tumor latency. Log rank and chi-square tests were used to investigate differences among groups. P values < 0.05 were considered statistically significant.

Results

Diet-induced adiposity accelerated tumor latency in C3(1)-TAg mice

In the treatment arm of our study, adult female C3(1)-TAg mice were randomly assigned to diet groups at 10 weeks of age (*N*=11-15; see **Figure 22**, Model of Treatment study design). Body weight and body composition were monitored, as were tumor latency and progression (by palpation and calipers).

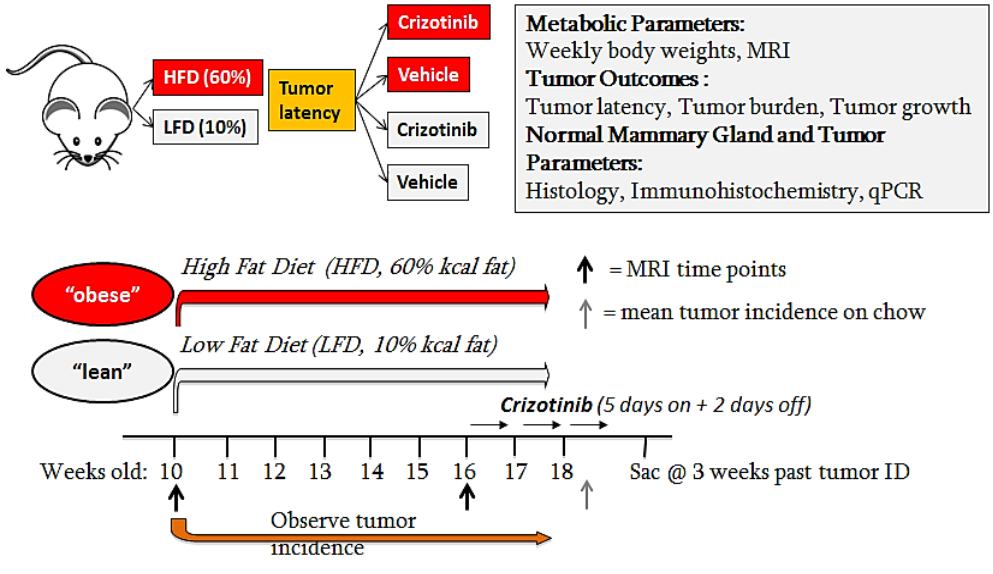

Figure 22. Model of Treatment Study design. At 10 weeks of age female mice were randomized to LFD or HFD and palpation began for identification of tumor onset. Vehicle or crizotinib treatment by daily oral gavage began at detection of first palpable tumor and lasted for 3 weeks, 5 days on and 2 days off. Mice were sacrificed at 3 weeks past tumor onset. Metabolic and other parameters were measured as indicated.

Body weight was not significantly altered by diet or drug treatment group for the study duration (**Figure 23A**). Adiposity as measured by MRI was increased with HFD exposure but did not reach significance (**Figure 23B**). This result may in part have been due to daily oral gavage of vehicle or drug, as adiposity initially declined in all groups following onset of the treatment protocol, irrespective of diet or treatment (i.e., vehicle vs. control) (**Figure 23B**). However, gonadal fat pad mass was significantly greater in mice fed HFD compared to mice fed LFD ($P = 0.0173$, **Figure 23C**). Consistent with our previously reported results [43], C3(1)-TAg mice fed HFD exhibited significantly accelerated tumor latency compared with mice fed LFD (LFD median 17.3 weeks; HFD median 15.5 weeks; $P < 0.0001$, **Figure 23D**). Using a log-rank (Mantel-Cox) chi-square test with a degree of freedom of 1, LFD vs HFD equaled 15.72.

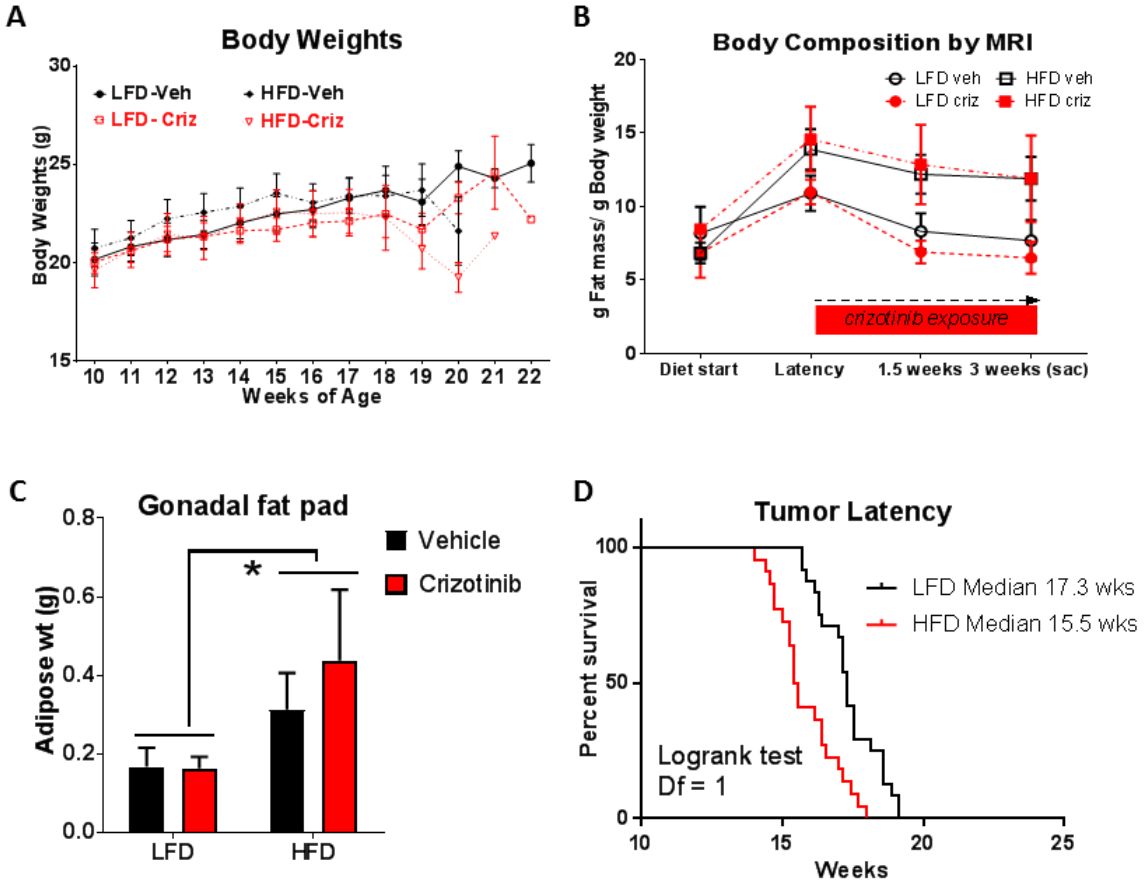

Figure 23. High-fat diet exposure accelerated basal-like tumor latency in C3(1)-TAg mice. A) Body weights did not differ by diet or treatment group. B) Body composition was measured at diet start, tumor latency (week 0 of crizotinib), 1.5 weeks on crizotinib treatment, and 3 weeks on crizotinib treatment (at sacrifice). C) Gonadal fat pad mass was weighed at sacrifice (LFD vs. HFD N = 11–13 per group *P = 0.017). D) Tumor latency was reported as age at detection of the first palpable tumor (LFD median 17.3 weeks, N = 24; HFD median 15.5 weeks, N = 22; P < 0.0001.

Crizotinib treatment inhibited secondary tumor development, reduced overall tumor burden

Tumor progression of the primary (first detected) tumor and all subsequent palpable tumors was monitored via electronic calipers throughout the 3-week measurement period between latency and sacrifice. No differences by diet or treatment group were detected in either primary tumor progression (**Figure 24A**) or total tumor progression (total percentage volume change in all palpable tumors throughout 3-week monitoring period) (**Figure 24B**). However, Crizotinib treatment significantly reduced total tumor burden (multiplicity) by 27.96% and

37.29% in LFD- and HFD-fed C3(1)-TAg mice, respectively, compared to mice treated with vehicle (P = 0.0085, **Figure 24C**). A minor diet effect on tumor burden was also detected: HFD-fed animals in both vehicle- and crizotinib-treated groups exhibited lower overall tumor burden at sacrifice compared to LFD-fed mice (P = 0.0491, **Figure 24C**).

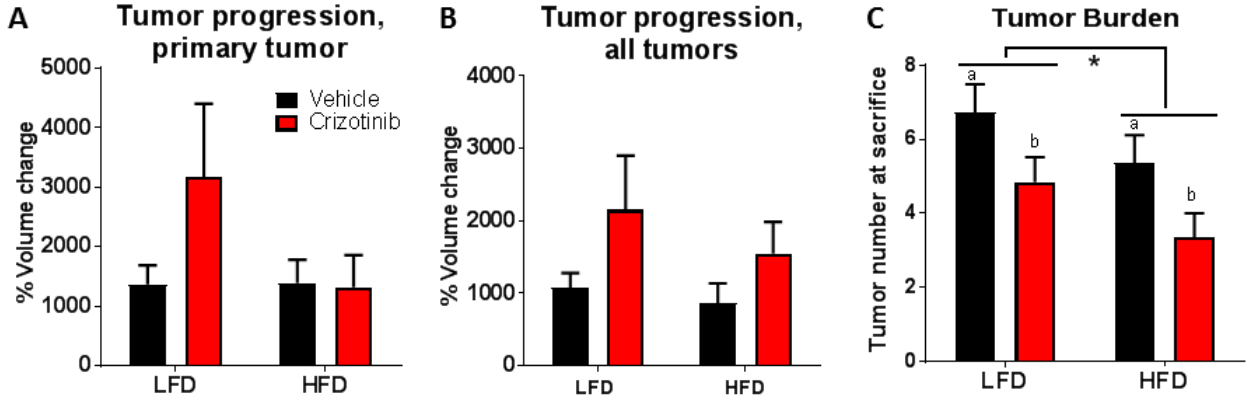

Figure 24. Crizotinib treatment inhibited subsequent tumor development. No significant differences were observed in A) primary or B) total tumor progression, measured as percentage volume change during monitoring period C) Total number of visible tumors was assessed at sacrifice (LFD vs HFD *P = 0.0491; Vehicle (a) versus crizotinib (b) P = 0.0085).

Crizotinib treatment disrupted tumor vascularization

We next measured expression of CD31, a marker of endothelial and lymphendothelial cells [479], in tumors using immunohistochemistry (IHC) (**Figure 25A-E**). CD31 expression was reported as percent CD31-positive area out of total tissue area analyzed. Crizotinib administration significantly reduced mean intratumoral CD31 expression by 35.04% and 33.52% in LFD and HFD groups, respectively (P = 0.014, **Figure 25F**). There were no detected diet effects on CD31 positivity. Also quantified was total tumor cMET and phosphorylated (active) cMET protein expression, also by IHC. Although total intratumoral cMET positivity did not differ by diet or treatment group (**Figure 26A**), phosphorylated cMET was significantly higher in mice fed HFD (P = 0.014, **Figure 26B**).

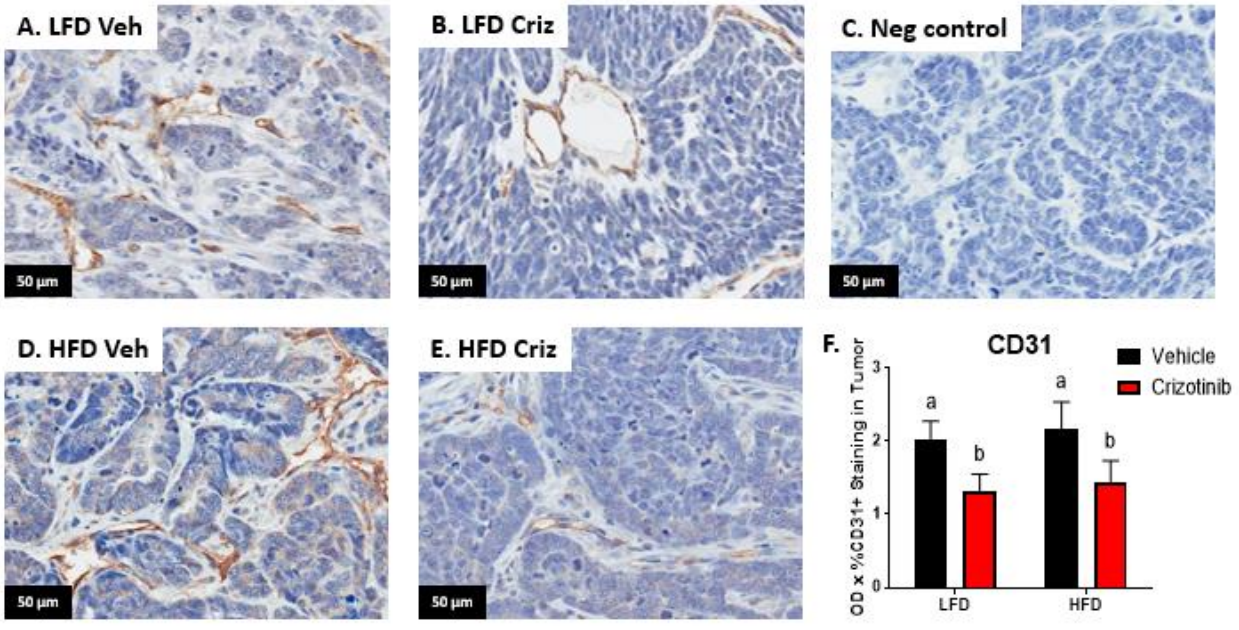

Figure 25. Crizotinib impaired tumor vascularization. A-E) Representative photomicrographs (40×) of CD31 staining in negative control and indicated LFD, HFD, vehicle (veh) and crizotinib (criz) treated groups. F) CD31 was quantified on 5–6 randomly selected 20x regions of *n* = 2 sections each from each mouse. N = 9–10 mice (a vs b, Veh vs Criz, P = 0.014).

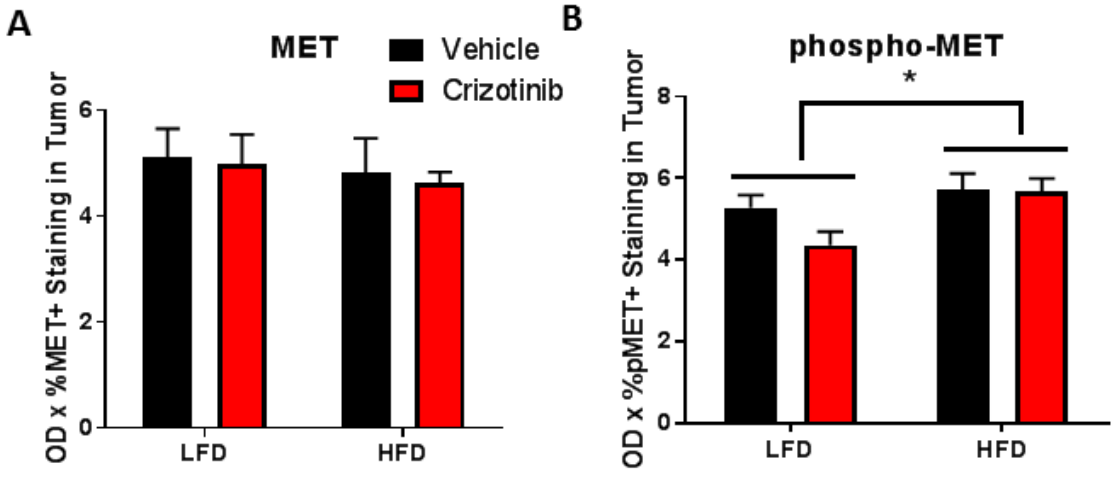

Figure 26. High fat diet exposure increased active cMET in tumors. A) Total MET staining did not differ by diet or treatment group. B) Phosphorylated (active) MET was significantly higher in mice fed HFD (2-way ANOVA *P = 0.0141).

Prophylactic crizotinib administration did not affect body weight or adiposity

As crizotinib treatment reduced tumor multiplicity in tumor-bearing mice, we next investigated whether we could inhibit or delay tumorigenesis by treating with crizotinib *prior to* tumor development. C3(1)-TAg tumors progress along the following approximate timeline: atypical hyperplasia (AH) of the mammary ductal epithelium at 8 weeks of age, mammary intraepithelial neoplasia (resembling human carcinoma in situ [CIS]) at 12 weeks of age, and invasive carcinomas at 16 weeks of age with 100% penetrance [150]. Thus, in the prevention arm of the study, mice were started on diet 2 weeks earlier than in the treatment study above to ensure crizotinib administration occurred within the primary window of AH/CIS precursor lesions. Starting at 8 weeks of age, mice were randomly assigned to LFD or HFD, with crizotinib treatment beginning at 9 weeks of age and continuing until 12 weeks of age (see **Figure 27, Model of Prevention Study design**).

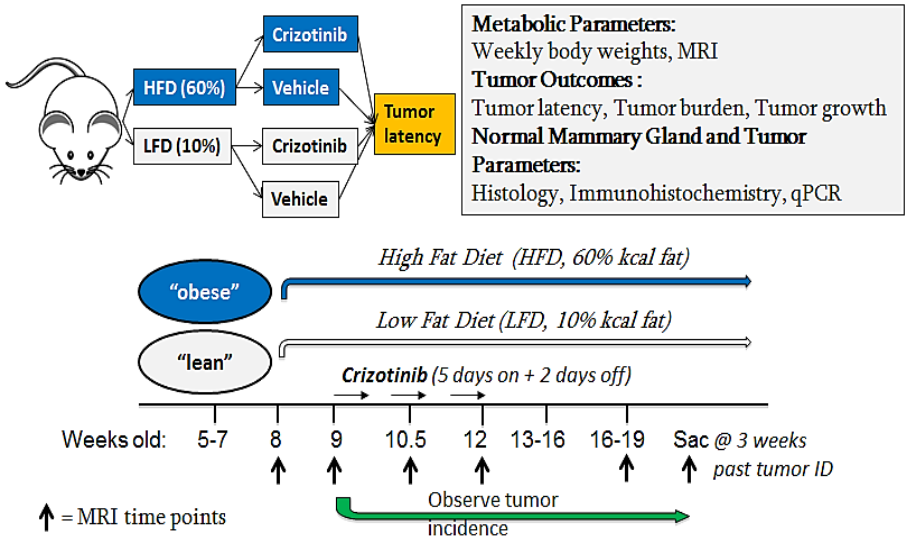

Figure 27. Model of Prevention Study design. At 8 weeks of age female mice were randomized to LFD or HFD. At 9 weeks of age vehicle or crizotinib treatment by oral gavage began and lasted for 3 weeks, 5 days on and 2 days off. Palpation began for identification o of tumor onset also began at 9 weeks of age. Mice were sacrificed at 3 weeks past tumor onset. Metabolic and other parameters were measured as indicated.

Mice fed HFD diet gained significantly more weight than the LFD mice, with greater body weights from 9-16 weeks of age ($P < 0.05$, **Figure 28A**). Body composition differed significantly between LFD- and HFD-fed mice beginning at 1 week on diet (9 weeks of age) and remained significant until sacrifice ($P < 0.0001$ for all data points, **Figure 28B**). Crizotinib- and vehicle-

treated mice fed HFD had significantly greater gonadal fat pad mass when compared to LFD-fed mice (P < 0.0001, **Figure 28C**). No difference was detected in body weight or adiposity between the crizotinib and vehicle treated mice.

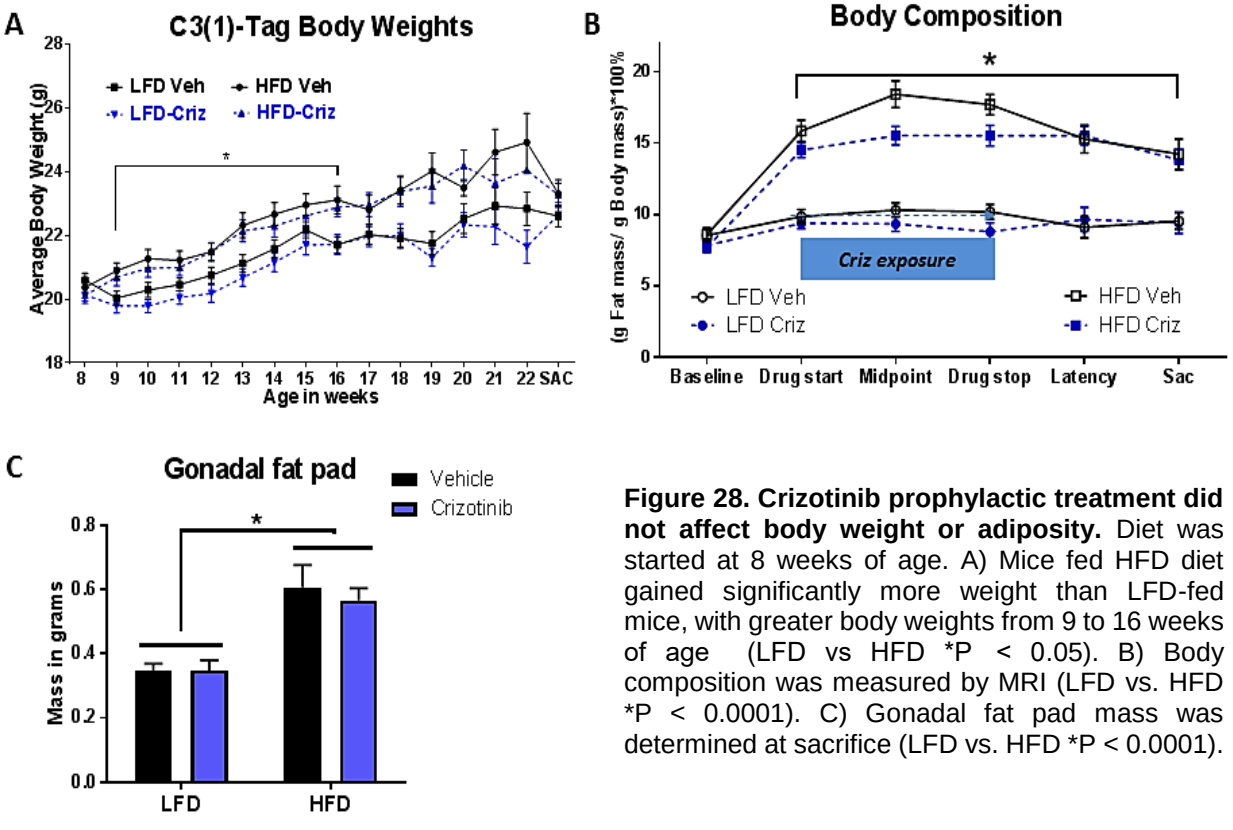

Figure 28. Crizotinib prophylactic treatment did not affect body weight or adiposity. Diet was started at 8 weeks of age. A) Mice fed HFD diet gained significantly more weight than LFD-fed mice, with greater body weights from 9 to 16 weeks of age (LFD vs HFD *P < 0.05). B) Body composition was measured by MRI (LFD vs. HFD *P < 0.0001). C) Gonadal fat pad mass was determined at sacrifice (LFD vs. HFD *P < 0.0001).

Prophylactic crizotinib administration increased primary tumor progression without significantly altering tumor burden or precursor lesion development

Upon initiation of crizotinib or vehicle administration (9 weeks of age), mice were palpated twice weekly for detection of tumor onset. Median tumor latency did not vary significantly between diet or treatment groups (LFD vehicle-treated median 15.0 weeks; LFD crizotinib-treated median 16.1 weeks; HFD vehicle median 16.0 weeks; HFD crizotinib median 16.2 weeks, **Figure 29A**). Progression of the primary, initially detected tumor was significantly increased with crizotinib treatment in both diet groups (P = 0.04, **Figure 29B**). However, when all tumors were considered there were no differences between diet or treatment groups in total

tumor progression (**Figure 29B**) or tumor burden (**Figure 29D**) at sacrifice. Non-tumor mammary tissue was analyzed for AH and CIS premalignant lesions in of HFD-fed vehicle- or crizotinib-treated mice. There were no significant diet- or crizotinib-mediated effects on precursor lesion formation detected (**Figure 29E**).

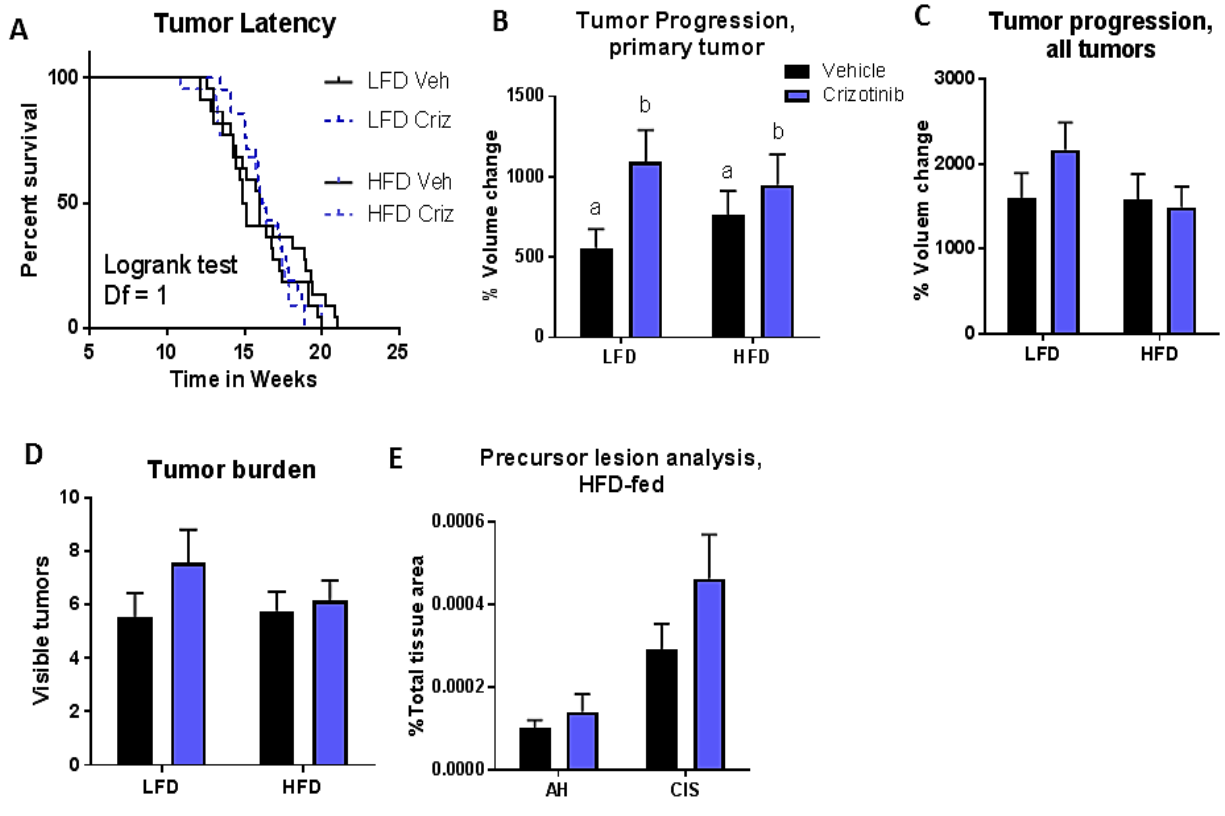

Figure 29. Preventive administration of crizotinib prior to tumor onset did not alter tumor latency or overall tumor burden. A) Median tumor latency did not differ across diet or treatment groups. B) Progression of the primary (first detected) tumor was significantly increased with crizotinib treatment (a vs b, P = 0.036 by 2-way ANOVA). C) Crizotinib treatment did not significantly influence total tumor progression or D) total tumor burden, assessed at sacrifice. (*N* = 21-22). E) There were no significant diet- or crizotinib-mediated effects on precursor lesion formation within the mammary fat pad (AH: atypical hyperplasia, CIS: carcinoma in situ) *n* = 7/diet + treatment group.

Discussion

We have previously demonstrated that HFD exposure during adulthood increased cMET expression and activation in normal mammary and tumors [43]. Diet-induced upregulation of cMET in tumors was also evident in mice fed HFD from weaning and could be reversed by weight loss [264]. Our previous work further revealed that HFD-induced weight gain resulted in increased mammary adipose HGF that was reversed with weight loss [264]. Reduction in HGF due to weight loss correlated with diminished tumor progression or deceleration of tumor latency, depending on whether the diet was initiated at weaning or adult onset, respectively. Altogether, our previously published studies implicated HGF/cMET signaling as a mediator of obesity-driven BBC tumor aggression. Therefore, the studies herein aimed to specifically inhibit cMET signaling as a potential BBC treatment or prevention strategy, hypothesizing that disruption of HGF/cMET signaling would mimic the effects of weight loss on BBC tumorigenesis.

C3(1)-TAg mice are a GEMM that develop BBC in 100% of female mice [150]. Initial characterization of the C3(1)-TAg model reported grossly palpable tumors at ~16 weeks of age; in our hands, median tumor latency occurs between 15-19 weeks, dependent on diet composition and age at diet start [42, 264, 470]. As shown here, in the crizotinib treatment arm of our study, initiating diets at 10 weeks of age resulted in detection of tumor latency two weeks earlier in mice that were fed HFD compared to mice fed LFD, consistent with our previous C(3)1-TAg studies in which identical diets were initiated at the same age [43]. However, in the crizotinib prevention arm of our study, in which HFD was initiated at 8 weeks of age, we did not see this diet effect of accelerated latency – these results parallel our second previously published study, in which female C3(1)-TAg mice were weaned onto LFD or HFD and no difference in latency was observed [264]. Several groups have reported “windows of susceptibility” during which HFD and/or obesity may play a disproportionately greater role in promoting breast cancer onset [470, 480]. Interestingly, pubertal exposure to HFD has been linked to stunted mammary duct elongation and reduced mammary epithelial cell proliferation in

murine models [481], a finding that was not seen in mice started on diet at 10 weeks of age or older. Collectively, our results here and in our previous studies support the concept that exposures extrinsic to the cancer cell (i.e., diet-induced alterations in the mammary microenvironment) can impact tumorigenesis, while age at diet start is an important variable contributing to diet effects on tumor latency.

Herein, we showed that crizotinib treatment after BBC latency inhibited subsequent tumor formation such that total tumor burden was reduced at sacrifice, regardless of diet. The degree of tumor inhibition was paralleled by a similar degree of suppression of MVD, also irrespective of diet. Reduction in MVD in our crizotinib-treated tumor-bearing C3(1)-TAg mice could explain the significant reduction of tumor burden compared to vehicle-treated controls. In tumors, an “angiogenic switch” occurs, in which an increase in MVD in and near the tumor allows for exponential growth of cancer cells, tumor survival, and metastasis [482]. Increases in HGF in the tumor microenvironment contribute to this angiogenic switch [483, 484], while cMET signaling in cancer cells facilitates invasion and migration away from the hypoxic interior of the tumor, entry into the new and leaky vessels, and metastasis to distant locations [477]. Indeed, obesity-promoted HGF production by fibroblasts, adipocytes, macrophages, and endothelial cells [43, 141, 142, 264, 485] may be a unique mechanism to increase blood vessel density and alleviate the hypoxia of obese adipose tissue. The fact that no changes were detected in MVD in the prevention arm of our study suggests that the HGF/cMET axis may play a greater role in invasive BBC carcinoma than in earlier stages of BBC progression.

The HGF/cMET signaling pathway has long been studied in ductal morphogenesis during mammary gland development [486] as well as invasive breast cancer [140, 487-491] and invasive biology of several other cancers due to its angiogenic, mitogenic, and morphogenic effects [492, 493]. Notably, single nucleotide polymorphisms in the *MET* gene may be associated with metastatic breast cancer [494]. HGF/cMET signaling is also relevant in BBCs, specifically. In patients, we demonstrated through gene expression analyses that 86% of BBCs

expressed an HGF/cMET activation signature [142]. Furthermore, a comprehensive meta-analysis including over 6,000 cases showed a significant association between cMET over-expression and poor survival in breast cancer patients, particularly among patients with triple-negative breast cancers [495]. HGF is also an excellent candidate mediator of obesity-induced effects on cancer, as serum HGF is elevated in obese individuals and reduced with weight loss [146-148]. Moreover, adipose-derived HGF has been detected in normal and malignant breast tissue [140].

Inhibition of cMET as an effective anti-angiogenic agent has been shown in initial mechanism-of-action studies for crizotinib, in which dose-dependent inhibition of cMET in gastric carcinoma, glioblastoma, and prostate carcinoma resulted in reduction of microvessel density (CD31) [478]. Angiogenic suppression by cMET inhibition has also been shown in xenograft models of aggressive cancers such as lung [496] and pancreatic cancers [497]. Moreover, the use of other cMET inhibitors in triple-negative breast cancer models such as ours has yielded promising results in preclinical studies [498]. However, to date clinical trials using the cMET inhibitors tivantinib or onartuzamab in isolation or in combination with chemotherapy have demonstrated little therapeutic benefit in metastatic breast cancer [499-501]. At the time of publication, clinical trials investigating crizotinib alone (ClinicalTrials.gov:NCT 02101385 [268]) or in combination with anti-VEGF therapy (ClinicalTrials.gov:NCT 02074878 [269]) for the treatment of advanced triple negative breast cancer are currently underway. Breast cancer ranks as the fifth cause of death from cancer overall and is now the second cause of cancer death among women following lung cancer [502, 503]. With the growing global prevalence of obesity and the notable racial and ethnic disparities in BBC outcomes [502], it is imperative that approaches are identified to effectively address the increased risk of breast cancer onset and progression to malignancy for an increasingly overweight and obese US population.

CHAPTER 3: WEIGHT LOSS NORMALIZES OVERWEIGHT-ASSOCIATED CLAUDIN-LOW BREAST CANCER PROGRESSION: ROLE OF MAMMARY FAT PAD INFLAMMATION AND MYELOID CELL INFILTRATES[3]

Background

Over the past four decades the worldwide prevalence of obesity has more than doubled among women [17]. Within the United States, 77.3% of adult women are overweight or obese [504], defined as having a body mass index (BMI) of 25.0-29.9 and $\geq$30 kg/m^2, respectively. Importantly, among breast cancer patients overweight and obesity are associated with increased risk of invasive cancer, development of distant metastases, tumor recurrence, and mortality [505].

Interactions with the local adipose milieu are important mediators of malignancy in triple-negative breast cancers (TNBCs), a heterogeneous collection of highly proliferative and invasive breast cancers primarily comprised of the basal-like (BBC) and claudin-low (CLBCs) molecular subtypes. TNBCs represent approximately 15-20% of breast cancer cases [506], are typically poorly differentiated and highly enriched for vascular and immune response genes [507, 508], and exhibit elevated recurrence and metastasis rates relative to other breast cancer subtypes [509]. Importantly, in the context of TNBC overweight and obesity are negatively associated with both breast cancer-specific and overall survival in premenopausal women [510]. Animal studies also indicate that excess weight and dietary energy intake promote progression of both BBC and CLBC. For example, we have previously demonstrated that high fat diet-induced weight gain accelerated pre-neoplastic lesion formation [263], tumor onset (latency) [43, 263] and tumor progression [264] in the transgenic C3(1)-TAg model of spontaneous BBC.

[3] A modified version of this manuscript has been submitted for review, and the final published version is likely to differ from that which is included here.

On the other hand, weight loss before tumor onset in this transgenic model reversed the effects of mammary adiposity on both pre-neoplastic lesion formation [263] and tumor progression [264]. Similarly, obesity enhanced CLBC tumor progression, as evidenced by upregulation of migration and invasion markers associated with the epithelial-mesenchymal transition [511, 512]; however these studies were conducted in the postmenopausal setting. Accordingly, the impacts of premenopausal weight gain, overweight without frank obesity, and weight loss on mammary inflammation and CLBC progression remain underexplored.

The mechanisms whereby overweight and obesity exacerbate TNBC progression are likely multifactorial, yet inflammation plays a pivotal role. In visceral (intra-abdominal) adipose tissue depots, obesity is associated with a dynamic infiltration of innate and adaptive immune cells that produce inflammatory cytokines, chemokines, growth factors, and matrix-degrading enzymes, triggering chronic low-grade adipose inflammation and development of metabolic dysfunction (reviewed in detail in [505]). We and others have demonstrated that obesity-associated inflammatory changes, including formation of crown-like structures (CLS), foci of macrophages and other inflammatory cells surrounding dead and dying adipocytes, also occurs in mouse mammary fat pad and human breast adipose tissue [321, 322, 366]. Importantly, increased breast CLS density has been observed in both overweight and obese patients with early-stage breast cancers, demonstrating that macrophage influx into breast adipose occurs in response to even minor changes in adiposity [366, 513].

In addition to altering macrophage-associated inflammation, adipose accumulation also appears to increase both content and activation of mast cells in multiple adipose tissue depots [435, 436]. In the normal breast, mast cells play a significant role in pubertal mammary gland branching morphogenesis, promoting proliferation in ducts and terminal end buds through secretion of growth factors and tissue-remodeling proteases [514]. However, an increase in mast cell content and/or activation within the overweight or obese breast also has potential to influence the course of a developing breast cancer, as multiple mast cell-derived products are known mediators of tumorigenesis [505]. Remarkably, mast cell influence on the course of

tumor development appears to differ considerably depending upon their localization relative to the tumor. For example, tryptase-positive mast cells are found at high density along the tumor invasive front and are associated with tumor progression and angiogenesis [515]. Increased *peri*tumoral mast cell density also significantly correlated with lymphatic density – a prognostic indicator in several cancer types – in luminal A breast cancers and BBC [452]. Conversely, increased *intra*tumoral mast cell infiltration in invasive breast cancer was a strong marker of favorable prognosis independent of age, tumor grade, tumor size, lymph node status, or hormone receptor status [452]. As invasive breast cancers frequently interact with breast adipose tissue [505], these studies collectively raise important questions regarding the impact of overweight and obesity on the relative abundance and activation states of peritumoral and intratumoral mast cells in invasive breast cancers. However, despite consistent reports regarding increased mast cell content and altered mast cell activation state in obese adipose tissue [435, 436], the impact of excess adiposity on the density or activation phenotype of mast cells in breast adipose tissue has not been explored.

To elucidate associations among changes in weight status, inflammatory changes within the mammary fat pad and CLBC tumor progression, we conducted syngeneic orthotopic transplant studies in female FVB/NJ mice, a model of overweight as opposed to frank obesity [516]. A C3(1)-TAg-derived CLBC cell line (C3-Tag-luc) was orthotopically injected into mice that remained lean, mice fed a high-fat diet to induce weight gain (Overweight), and mice in which a period of overweight was followed by weight loss (Weight Loss, WeLo) induced by a diet switch. Collectively, our results demonstrate that overweight induces inflammatory changes within mammary adipose that are akin to frank obesity and reversible with weight loss. Importantly, weight loss also normalized CLBC growth and reduced intratumoral expression of pathways associated with CLBC progression. Thus, premenopausal weight loss may be an important interventional strategy with regard to prevention of overweight- and obesity-associated CLBC progression.

Methods

Animals and Diets

All animal studies were approved by the Institutional Animal Care and Use Committee of the University of North Carolina at Chapel Hill and were performed in accordance with the recommendations of the Panel on Euthanasia of the American Veterinary Medical Association. Animal facilities at UNC are accredited by the Association for Assessment and Accreditation of Laboratory Animal Care (AAALAC), and veterinary care meets National Institutes of Health standards set forth in the Guide for the Care and Use of Laboratory Animals (DHHS Publication No. (NIH) 85-23 Revised 1985). UNC also accepts as mandatory the Public Health Service Policy on Humane Care and Use of Laboratory Animals by Awardee Institutions, as well as NIH Principles for the Utilization and Care of Vertebrate Animals Used in Testing, Research, and Training. Animal studies comply with the ARRIVE guidelines. In accordance with humane euthanasia regulations, mice were anesthetized by intraperitoneal injection of avertin (tribromoethanol/amylene hydrate, 1.25%) (Sigma Aldrich) and cervical dislocation was performed before tissue collection. Mice were housed in a climate-controlled Department of Laboratory Animal Medicine facility with a 12-hour light:dark cycle, with ad libitum access to water and diets as described below. Female wild-type FVB/NJ mice (strain 001800) were obtained from Jackson Laboratories (Bar Harbor, ME) at 3 weeks of age and allowed to acclimate for 5 weeks before randomization to diets at 8 weeks of age. Diets obtained from Research Diets Inc. (New Brunswick, NJ, USA) were matched for sucrose, protein, vitamins, and minerals, and provided 10% kcal (“LFD”, D12450J) or 60% kcal (“HFD”, D12492) derived from fat. Nulliparous female C3(1)-TAg mice were bred and maintained on chow diet (Harlan 2918) until random assignment to diet groups at 10 weeks of age. Diets obtained from Research Diets Inc. (New Brunswick, NJ, USA) were matched for protein, vitamins, and minerals, and

provided 10% kcal (“LFD”; # D11012202); and 60% kcal (“HFD”; # D11012204) derived from fat (additional information on dietary composition can be found in [43]).

Body Weight and Composition

Body weight was measured at diet start and once weekly until sacrifice. Body composition of non-anesthetized mice, including lean mass, fat mass, free water content, and total water content, was measured at diet start, diet switch, orthotopic injection, and sacrifice using an EchoMRI-100 quantitative magnetic resonance whole body composition analyzer (Echo Medical Systems, Houston, TX).

C3-Tag-luc Cell Line Characterization

C3-Tag-luc cells were established by dissociation of mammary tumors from C3(1)-TAg mice as described [517]. Expression profiling of the C3-Tag-luc cell line was conducted as follows: RNA was isolated from the cell line using the Qiagen RNeasy mini kit (QIAGEN, Valencia, CA) and RNA quality was determined using an Agilent Bioanalyzer. Total RNA was labeled with Cy5 dye using the Agilent Low RNA Input Fluorescent Linear Amplification Kit. Likewise, whole mouse reference [149] RNA was labeled with Cy3 dye. For mouse reference and tumor cell line RNA, labeled RNA (2ug) was co-hybridized overnight to Agilent microarrays (GEO Platform GPL11383 / Agilent Design 25503 144K mouse Agilent Array). Intensity values were then uploaded to the UNC Microarray Database (UMD). In order to examine the features of this cell line, we combined the C3-Tag cell line data with array data associated with the published dataset [518]. For all arrays, expression values were calculated as the $\log_2$ Cy5/Cy3 ratios with Lowess normalization applied. Genes with intensity values greater than 10 in both Cy5 and Cy3 channels were determined as present in each sample. To examine genes in the entire dataset we applied a filtering criteria requiring expression in at least 70% of all samples.

Next, duplicate genes (corresponding to multiple probes) were collapsed to their median expression, and missing values were imputed by K-means nearest neighbor imputation. Prior to clustering, genes were median-centered and arrays were standardized. For intrinsic analysis, the normalized dataset was filtered to the published intrinsic gene list [518]. Genes and arrays were clustered using Cluster 3.0 with selection of the correlation similarity metric and centroid linkage. Finally, results were visualized in Java Tree View[519]. Sample subtype annotations from Pfefferle et al. [518] were used for all previously published array data.

The original C3(1)-TAg model has been characterized as basal-like breast cancer [149]. However, while C3-Tag-luc cells clustered in proximity to tumors from the original C3(1)-TAg basal-like tumors, they were more closely related to the Claudin-low molecular subtype (**Figure 30A**). For example, while both had high expression of proliferation-associated genes, relative to the original C3(1)-TAg model C3-Tag-luc cells exhibited much lower expression of claudins 3 and 7, a defining feature of claudin-low breast cancers [520] (**Figure 30B&C**). On the other hand, keratins 14 and 17, associated with the basal-like gene cluster, showed high expression in C3(1)-TAg tumors and low expression in the C3-Tag-luc cell line (**Figure 30B&C**).

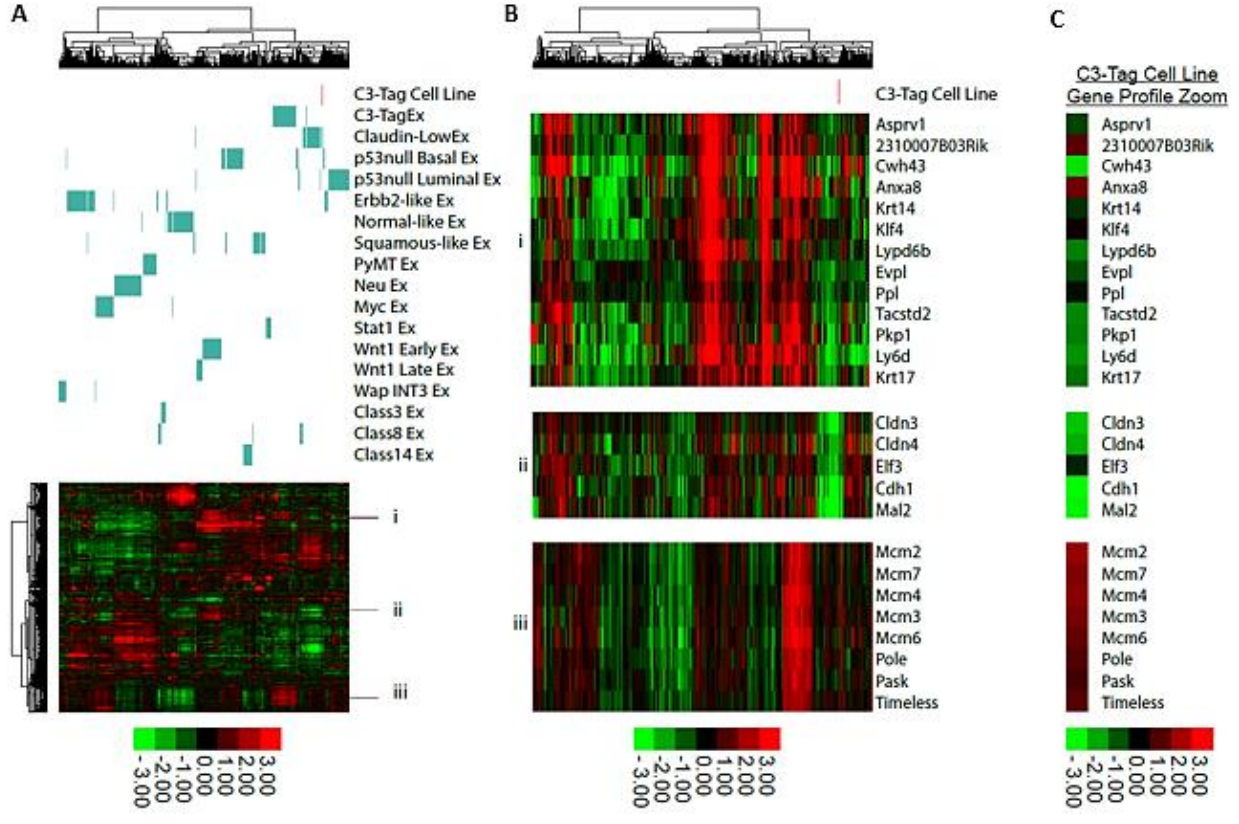

Figure 30. Phenotyping of C3-Tag-luc cell line. A) Hierarchical clustering of our previously published microarray dataset [518] and the C3-Tag-luc cell line. The dataset was filtered to include only intrinsic genes and the dendrogram assembled by centroid linkage, illustrating the relationship of individual samples in the dataset. The red bar beneath the dendrogram indicates the position of the C3-Tag-luc cell line while the blue/turqouise bars depict the position of other tumor subtypes according to row annotations. Note, the C3-Tag-luc cell line clusters with other claudin-low tumor samples. The heatmap below shows the relative expression profile of genes across samples and corresponding to the color bar along the bottom. (B). Using the assembly from panel A, we identified clusters highlighting important features of tumors segregating closely, including (i) the basal-like cluster, (ii) the claudin-cluster, and (iii) the proliferation cluster. (C) Selecting these clusters for just the C3-Tag-luc cell line shows low expression of the basal-like genes, a claudin-low gene expression profile, and high expression of the proliferation cluster.

Orthotopic Injections and Tissue Harvest

C3-Tag-luc cells were generously donated by William Y. Kim, MD, of the UNC Lineberger Comprehensive Cancer Center. Cells were passaged once before orthotopic injection and were grown in DMEM (Cellgro) with 10% FBS and 1% penicillin/streptomycin at 37°C and 5% CO_2. Eighteen-week-old female FVB/NJ mice (*N*=19-20/group) were orthotopically injected in the left fourth (abdominal) mammary fat pad with 2×10^5 viable C3-Tag-luc cells in a

1:1 mixture of high concentration Matrigel® (Cat # 354262, BD Biosciences, Bedford, MA) and Hank's Saline Solution (Sigma Aldrich, St. Louis, MO). Tumor progression was monitored with electronic calipers three times weekly until sacrifice, and volumes were calculated using the modified ellipsoid formula (length × width^2 × 0.5) as in previous studies [43]. Tissues collected included tumor, un-injected abdominal mammary fat pad, tumor-adjacent adipose, and liver. A portion of each tissue sample was frozen in liquid nitrogen and stored at $^{-}$80˚C for gene expression analysis. The remaining tissue was formalin-fixed and paraffin embedded (FFPE) for histological analysis.

At an average age of 18.20 weeks, mammary fat pads of C3(1)-TAg mice without palpable or visible tumors were collected as "normal" unaffected gland, although atypia of ductal epithelium could be present in C3(1)-TAg mice after 8 weeks of age [150].

Flow Cytometric Analysis

Female mice were euthanized via CO_2 asphyxiation and cervical dislocation at 21 weeks of age (*n* = 5 per diet). The left and right abdominal (4th and 7th) mammary adipose pads were removed and the intramammary lymph nodes excised. Fat pads were transferred to ice cold Dulbecco's Modified Eagle's Medium, high glucose (4.5 g/L) (DMEM, Corning, Corning, NY) containing 20 mM HEPES buffer (Cellgro, Manassas, VA), and supplemented with 10% bovine calf serum (HycloneTM, GE Healthcare Life Sciences, South Logan, Utah), 5mM glutamine, and 10mM penicillin-streptomycin. Fat pads were minced with surgical scissors before enzymatic digestion in 2 mg/mL Type I collagenase (Worthington, Lakewood, NJ). A single-cell suspension was generated via mechanical dissociation with a Stomacher® 80 Biomaster small tissue lab paddle blender (Seward, Worthing, West Sussex, United Kingdom). Suspensions were diluted with an equal volume of HEPES-buffered DMEM and filtered through a 100-µm cell strainer, followed by centrifugation at 200 *x* g for 10 min at 4°C and removal of the mature adipocyte layer and red blood cell lysis (ACK lysis buffer; Gibco, Gaithersburg, MD) to generate an

immune cell-enriched stromal-vascular fraction (SVF). The resulting SVF from each mouse was blocked with Fc Block (CD16/32) (Biolegend, San Diego, CA), and stained with pre-titrated antibodies (see **Table 1** for antibody information and dilutions). SVF cells were analyzed on a BD™ LSR II flow cytometer. Data were analyzed with FlowJo (FlowJo, LLC, Ashland, OR).

Tumors were collected and immediately dissociated through enzymatic (collagenase type I; Worthington Biochemical Corporation, Lakewood, NJ) and mechanical dissociation with a Stomacher® 80 Biomaster small tissue lab paddle blender (Seward, Worthing, West Sussex, United Kingdom). Dissociation media was supplement DMEM, high glucose (4.5 g/L) (Sigma Aldrich, St. Louis, MO) containing 20 mM HEPES buffer (Corning, Manassus, VA) as described above. The resulting solution was filtered through a 100 µm filter and subjected to DNA digestion using DNAse I (Sigma Aldrich, St. Louis, MO) at 0.1 mg/mL in HEPES-buffered supplemented DMEM as described above. Cells were pelleted and underwent red blood cell lysis via ACK lysing buffer (Gibco, Grand Island, NY), after which cells were washed in a FACS Wash solution (1x Dulbecco's phosphate-buffered saline [DPBS, Corning, Manassus, VA] containing 1% fetal calf serum, 0.5% endotoxin-tested bovine serum albumin BSA, and 2 mM EDTA). Single cell suspensions were counted using a Scepter™ 2.0 Handheld Automated Cell Counter and blocked with Fc block (CD16/32; Biolegend, San Diego, CA) before staining. Antibody cocktails for staining were prepared in Brilliant Stain Buffer (BD Biosciences, Billerica, MA). Compensation was set using single-stained cellular controls and gating was determined based on fluorescence-minus-one (FMO) controls. Sample analysis was conducted using a FACSAriaII flow cytometer (BD Biosciences, Billerica, MA).

Table 1. Antibodies and dilutions used in analysis.

Antibody	Conjugate	Dilutions	Company	Catalog #	Lot #
CD45	BV605	1:200	BioLegend	103140	B211813
F4/80	PE-Cy7	1:200	eBioscience	25-4801-82	4281123
CD11b	BUV395	1:100	BD Biosciences	563553	7033600
Ly6C	BV421	1:100	BD Biosciences	562727	5357529
MHCII (IA/IE)	BV711	1:200	eBioscience	17-5321-81	6167935
CD206	APC	1:100	R&D Systems	FAB25351A	ADYJ0115081
Tie2	PE	1:50	eBioscience	12-5987-83	E01993-1636
Fc Block (CD16/CD32)	N/A	1:50	BioLegend	101320	B200134
Zombie Green Viability Dye	N/A	1:400	BioLegend	423111	N/A

Histological Analysis

Formalin-fixed, paraffin-embedded (FFPE) tumor and corresponding uninjected mammary fat pad were sectioned at 5 μm in a serial interrupted fashion and mounted onto glass slides.

Immunohistochemistry: Briefly, 5 μm FFPE tumor and normal mammary fat pad sections were baked, deparaffinized, and rehydrated. Following heat-induced epitope retrieval (Rodent Decloaker BM#RD913L), slides were treated with 3% hydrogen peroxide in de-ionized water. Tissues were treated with Avidin/Biotin Block (Vector #SP-2001) and exposed to primary antibodies (anti-CD31, anti-F4/80) diluted in Renoir Red Diluent at 4 °C overnight. Following incubation with biotin-conjugated secondary antibodies [Goat anti-rabbit IgG; Goat anti-rat IgG] tissue sections were treated with ABC Elite and DAB. Digital immunohistochemistry quantification was performed following the protocol previously described in Sundaram et al.[43].

Stained slides were scanned into the Aperio Scanscope CS system (Aperio Technologies, Vista, CA, USA) at a magnification of 20× (F4/80) or 40× (CD31) and were quantified using the Aperio Imagescope software (Leica Biosystem, Buffalo Grove, IL). For CD31 percent positivity, scanned slides were analyzed using algorithms as described previously [42]. Microvessel density was quantified as total number of CD31/PECAM1+ vessels per tissue area (in mm^2) in n=7-8 tumor histological sections per diet group. Crown-like structure density was determined in n = 3 sections per mouse in n = 6-9 mice per diet group by counting the number of visible CLS and normalizing to tissue area analyzed (number/mm^2). Images shown are representative.

Adipocyte diameter: in hematoxylin-eosin (H&E) stained sections of uninjected mammary fat pad, a 20x field of view was randomly selected and the diameter of 100 white (unilocular) adipocytes was determined using the ruler function in ImageScope. (*N* = 7-8 mice/group; 7-800 adipocytes total).

Mast cell analysis: Slides were dewaxed and rehydrated with 60% ethyl alcohol, then exposed to Toluidine Blue O (C.I. 52040) for 1-2 minutes. Slides were then rinsed under water and dehydrated twice through acetone exposure for 1-2 minutes. Stained slides were scanned at a magnification of 40x into the Aperio Scanscope CS System. Total mast cell number in each section was manually counted and total tissue area analyzed was quantified in mm^2 using Aperio Imagescope software. Mast cell density was reported as number of mast cells counted per section normalized to tissue section area.

Quantitative PCR

Snap-frozen un-injected mammary fat pads were pulverized under liquid nitrogen. Total RNA was extracted (RNeasy Mini Plus kit, QIAGEN) and reverse-transcribed (1000 ng per sample; iScript Reverse Transcription Supermix, Bio-Rad) according to the manufacturers' instructions. Gene expression was quantitated via quantitative reverse transcriptase PCR (qRT-PCR) with the eukaryotic ribosomal 18S RNA as an endogenous control. TaqMan Assay-on-

Demand (AOD) Gene Expression Assays (Applied Biosystems, Foster City, CA) were used for all probes, with the exception of *Il10*, *Ccl2*, and *Nos2*, which were measured using Roche Universal Probe Library Assays (Roche Diagnostics US, Indianapolis, IN) with the following oligonucleotide pairs: *Il10*: F: 5'-CAGAGCCACATGCTCCTAGA-3'; R: 5'-GTCCAGCTGGTCCTTTGTTT-3'; *Ccl2*: F: 5'-AGCACCAGCCAACTCTCACT-3'; R: 5'-GTGGGGCGTTAACTGCAT-3'; and *Nos2*: F: 5'-TGACACACAGCGCTACAACA-3'; R: 5'-GCCAGTGTGTGGGTCTCC-3'. Data were analyzed using QuantStudio Real-Time PCR System software (Thermo Fisher Scientific, Waltham, MA) and the comparative $\Delta\Delta C_T$ method.

Microarray sample preparation

FVB/NJ tumors: Total RNA was extracted (RNeasy Mini Plus kit, QIAGEN) and RNA purity and concentrations were determined using a NanoDrop™ spectrophotometer (Thermo Fisher Scientific). All samples were diluted to a final concentration of 200 ng/uL for library preparation. RNA quality was determined using an Agilent TapeStation. One-color (Cy3) cDNA library preparation and microarray hybridization were conducted by the Lineberger Comprehensive Cancer Center Genomics Core using SurePrint G3 Mouse Gene Expression v2 8x60K Microarray Kits (Agilent, Santa Clara, CA) and the Agilent Low RNA Input Fluorescent Linear Amplification Kit. Arrays were scanned using an Agilent Technologies G2505C Scanner with Feature Extraction software.

C3(1)-TAg mammary fat pads: Unaffected mammary fat pads were flash frozen in liquid nitrogen and prepared for microarray analysis as described above. Samples and universal mouse reference RNA were Cy5- and Cy3-labelled, respectively, using Agilent Low RNA Input Fluorescent Linear Amplification Kit, and hybridized to Mouse Gene Expression v2 4x44K microarrays (Agilent) according to the manufacturer's protocol.

Cancer-adjacent normal human breast: The Normal Breast Study (NBS) is an epidemiologic study of normal breast and breast cancer microenvironments conducted at UNC Hospitals in Chapel Hill, NC [521]. Women were eligible for inclusion if they were English-

speaking, at least 18 years of age, undergoing breast surgery (mastectomy, lumpectomy, excisional biopsy, or cosmetic procedure) at UNC Hospitals between October 2009 and April 2013, and consented to donate breast tissue. For microarray analysis, total RNA was extracted from snap-frozen tissue (Qiagen RNeasy) and quality was measured using an Agilent Bioanalyzer. Samples and universal human reference were Cy5- and Cy3-labelled, respectively, using Agilent Low RNA Input Fluorescent Linear Amplification Kit, and hybridized to Human Gene Expression v1 or v2 4x44K microarrays (Agilent). Only genes common to both array platforms were used in further analyses (see below).

Microarray and gene signature analyses

FVB/NJ tumors: Gene expression estimates were calculating using the Agilent Feature Extractor software which performs background adjustment and total signal normalization. The normalized log2 Cy3 intensity was utilized for analysis, and histograms of t-test p-values between groups were used to assess global effects. Tests of gene level differential expression used the 'Two class unpaired' procedure in the Significance Analysis for Microarrays (SAM) algorithm [522]. Significantly up- or down-regulated pathways were identified using the Molecular Signatures Database (MSigDB) for Gene Set Enrichment Analysis. Genes and pathways were visualized using hierarchical cluster analysis ordering of heatmaps. Clustering utilized average linkage with Pearson's correlation as the distance metric.

C3(1)-TAg mammary fat pads, Normal Breast Study cancer-adjacent, and TCGA breast tumor samples: Expression values were calculated as the $\log_2$ Cy5/Cy3 ratios with Lowess normalization applied. Genes with intensity values greater than 10 in both Cy5 and Cy3 channels were determined as present in each sample. Duplicate genes (corresponding to multiple probes) were collapsed by averaging. For C3(1)-TAg samples: Cy3-labeled reference was produced from Stratagene Universal Mouse Reference RNA following amplification with Agilent low RNA input amplification kit. Mouse mammary samples were labeled with Cy5. Data

were Lowess normalized, and probes with a signal <10 dpi in either channel were excluded as missing. In data preprocessing, we (1) eliminated probes without corresponding ENTREZ ID, (2) collapsed duplicate probes by averaging, (3) imputed missing data using k-nearest neighbors (KNN) method with k=10, and (4) median-centered genes. For NBS samples, women for whom microarray and BMI data (BMI $\geq$18.5 kg/m^2) were available were included in this analysis. Patients undergoing cosmetic or prophylactic surgery were excluded, as were those for whom biopsy results indicated "no evidence of active disease" or "normal" tissue status. Specimens obtained from a second breast procedure were also excluded to avoid capturing gene expression patterns related to inflammation induced by a previous surgery (i.e., pre-existing granulation tissue). The final study population consisted of 131 unique patients and 193 tissue specimens. The clinicopathologic characteristics of these patients are included in **Table 2**. NBS microarray data were analyzed as previously described [523]. For TCGA samples, only data from invasive tumors were included (*n* = 1094). TCGA data and methods are available at the TCGA Data Portal (https://cga-data.nci.nih.gov). To calculate mast cell scores, the median centered gene expression profile for each sample was evaluated using published gene signatures. Mouse mammary tissue was analyzed using a previously validated, murine-specific 128-gene signature for connective tissue mast cells [524], the type most commonly found in mammary tissue [514]. Human normal breast tissue was analyzed using a mast cell signature identified by Motakis et al. [525] through a comprehensive study of the mast cell transcriptome of *ex vivo* skin mast cells integrated with data from the FANTOM (Functional Annotation of the Mammalian Genome) consortium. Intratumoral mast cell gene expression was analyzed using the tumor mast cell gene signature described by Bindea et al. [526]. Since all genes in the original signatures were up-regulated in mast cells compared to the other cell types studied, the mast cell scores were derived from the average expression of mast cell signature genes in each sample.

Statistical Analysis

All statistical analyses were conducted using GraphPad Prism 7 software (GraphPad Software, Inc. La Jolla, CA). Data are expressed as mean ± standard error of the mean (SEM) unless stated otherwise. Means were compared as indicated via one- or two-way Analysis of Variance (ANOVA) followed by Tukey's Post Hoc Multiple Comparisons. Statistical outliers were identified using the robust non-linear regression with outlier removal (ROUT) method with Q=1%. P-values ≤0.05 are considered statistically significant.

Results

High-fat feeding and diet switch-induced weight loss modulated mammary adiposity and CLBC tumor growth

Eight-week-old female FVB/NJ mice were randomized to one of three diet groups: "Lean" mice were fed LFD until sacrifice, "Overweight" mice were fed HFD until sacrifice, and "Weight Loss (WeLo)" mice received 5 weeks of HFD to increase adiposity, followed by a 5-week diet switch to LFD to induce weight loss prior to tumor cell injection (*N*=19-20 mice/diet group, see study design diagram in **Figure 31**). Following 10 weeks on assigned diets, C3-Tag-luc CLBC cells were orthotopically transplanted into the left fourth (abdominal) mammary fad pad of each mouse. Tumors were allowed to develop for 21 days, at which point all mice were sacrificed. Body composition and 6-hour fasted glucose were monitored at the indicated time points. Overweight mice displayed significantly greater body weights than Lean beginning two weeks after diet start and continuing until sacrifice (**Figure 32A**; P<0.01-P<0.0001 vs. Lean). Body weights of WeLo mice paralleled Overweight until diet switch (**Figure 32A**; P<0.01-P<0.0001 vs. Lean). Diet switch restored body weights to Lean levels until sacrifice (**Figure 32A**; P<0.01-P<0.0001 vs. Overweight). Similarly, body composition analysis demonstrated an approximately 2-fold increase in overall adiposity in Overweight and WeLo mice after 5 weeks

on HFD (P<0.0001 Overweight vs. Lean; P<0.0001 WeLo vs. Lean) (**Figure 32B**). Following diet switch, adiposity in WeLo mice was restored to Lean levels (P<0.0001 Overweight vs. Lean and vs. WeLo, **Figure 32B**).

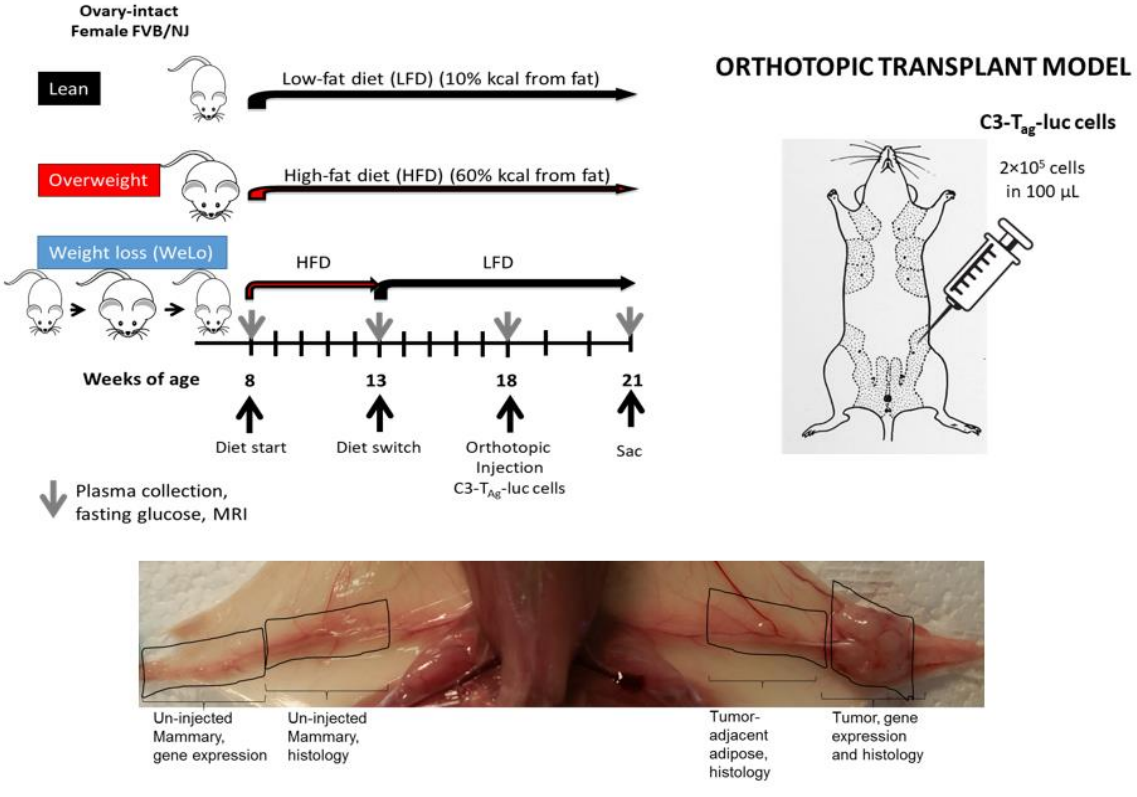

Figure 31. Study design with orthotopic transplant model and tissue collection diagram. N=19/diet.

Following normalization to body weight, liver weight was significantly greater in Overweight compared to Lean and WeLo mice (**Figure 32C**; P<0.0001). A modest but significant elevation in fasting glucose was also observed in Overweight compared to Lean and WeLo mice at the time of orthotopic injection; however, at sacrifice this difference only remained significant between Overweight and Lean (**Figure 32D**). Gonadal (~2.5-fold) (**Figure 32E**) and mammary (~2-fold) (**Figure 33A**) adipose fat pad masses were significantly increased in Overweight mice (P<0.0001 Overweight vs. Lean, WeLo), with no differences observed

between WeLo and Lean mice. Importantly, increased adiposity in Overweight mice corresponded with significantly greater final tumor volume compared to Lean and WeLo (**Figure 33B**; P<0.05 Overweight vs. Lean, P<0.05 Overweight vs. WeLo).

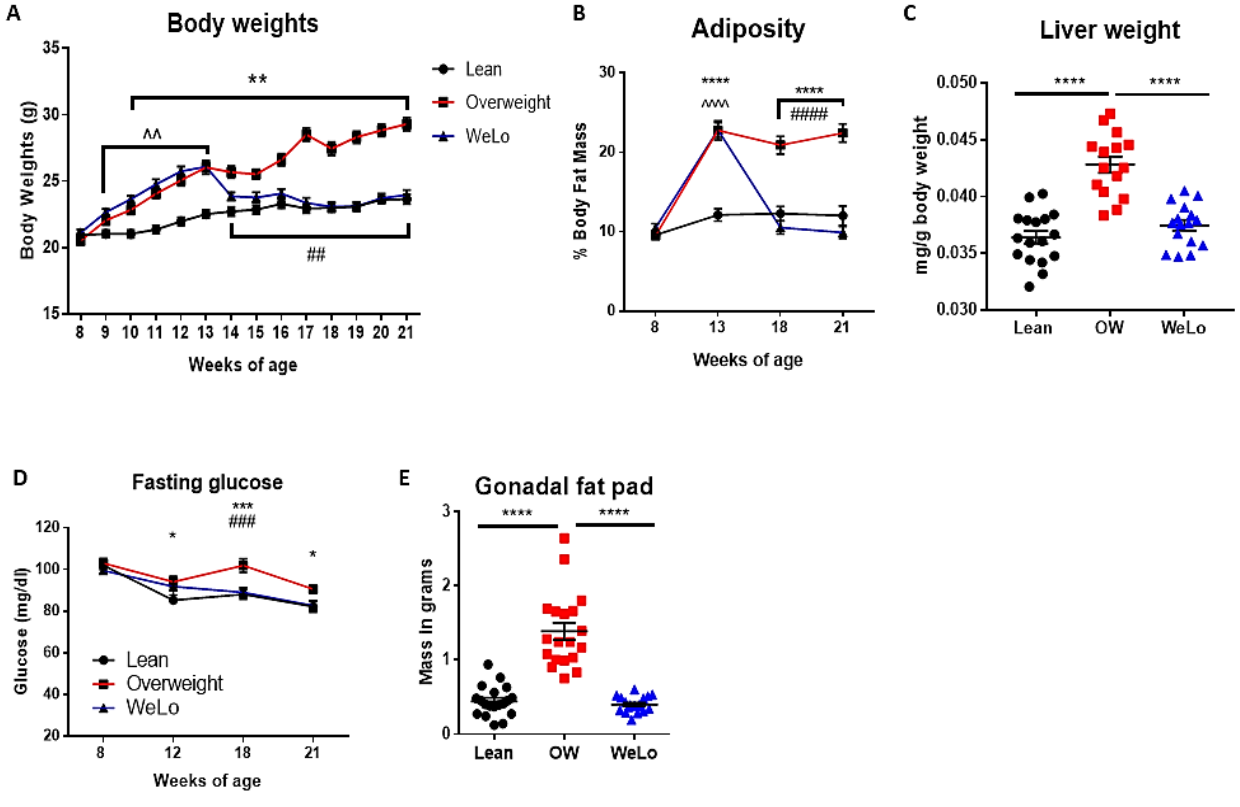

Figure 32. High fat diet induced adiposity in female FVB/NJ mice was normalized by weight loss. A) Body weight was measured at baseline and weekly until sacrifice at 21 weeks of age. ^^P<0.01 Lean vs WeLo, **P<0.01 vs Overweight (OW), ##P<0.01 OW vs WeLo, by two-way ANOVA with post-hoc Tukey's analysis). B) Body composition, including fat mass, was measured at diet start and specified time points until sacrifice using an EchoMRI-100 (****P<0.0001 Lean vs OW, ^^^^Lean vs WeLo, ####OW vs WeLo by two-way ANOVA with post-hoc Tukey's analysis). C) Average liver weight at sacrifice, normalized to body weight (****P <0.0001 by one-way ANOVA with post-hoc Tukey's multiple comparisons). D) Fasting glucose was measured in 6h fasted mice at indicated time points (*P<0.05, ***P<0.001 Lean vs OW, ###P<0.001 OW vs WeLo by two-way ANOVA with post-hoc Tukey's analysis). E) Gonadal fat pad masses at sacrifice (****P < 0.0001 OW vs Lean, WeLo mice by one-way ANOVA with post-hoc Tukey's analysis). All values reported as mean ± SEM. N=19/diet group.

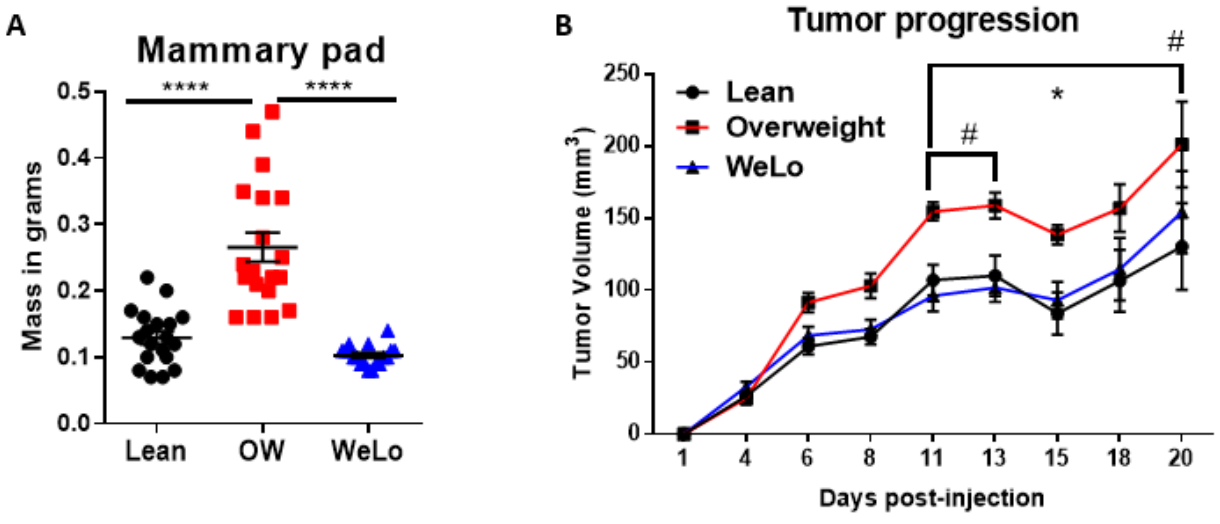

Figure 33. Increased mammary fat pad mass in Overweight mice was associated with increased tumor growth rate. A) mammary fat pad masses at sacrifice (****P < 0.0001 OW vs Lean, WeLo mice by one-way ANOVA with post-hoc Tukey's analysis). B) Tumor growth was measured thrice weekly by electronic calipers (*P<0.05 OW vs Lean; #P<0.05 OW vs WeLo by two-way ANOVA with post-hoc Tukey's multiple comparisons). Mean ± SEM. N=19/diet group.

Accelerated tumor growth rate in Overweight mice was associated with macrophage and neutrophil influx into mammary adipose

Given the known role of mammary inflammation in breast cancer progression [505], we next determined whether the observed increases in mammary adiposity and tumor volume occurred in conjunction with features of adipose inflammation typically observed in visceral adipose pads in obesity. We first compared mammary fat pad adipocyte diameter of Lean, Overweight, and WeLo mice. Average mammary adipocyte diameter was approximately 35% greater in Overweight mice relative to Lean (**Figure 34A&B**; P<0.01) and was not significantly different between WeLo and Lean animals.

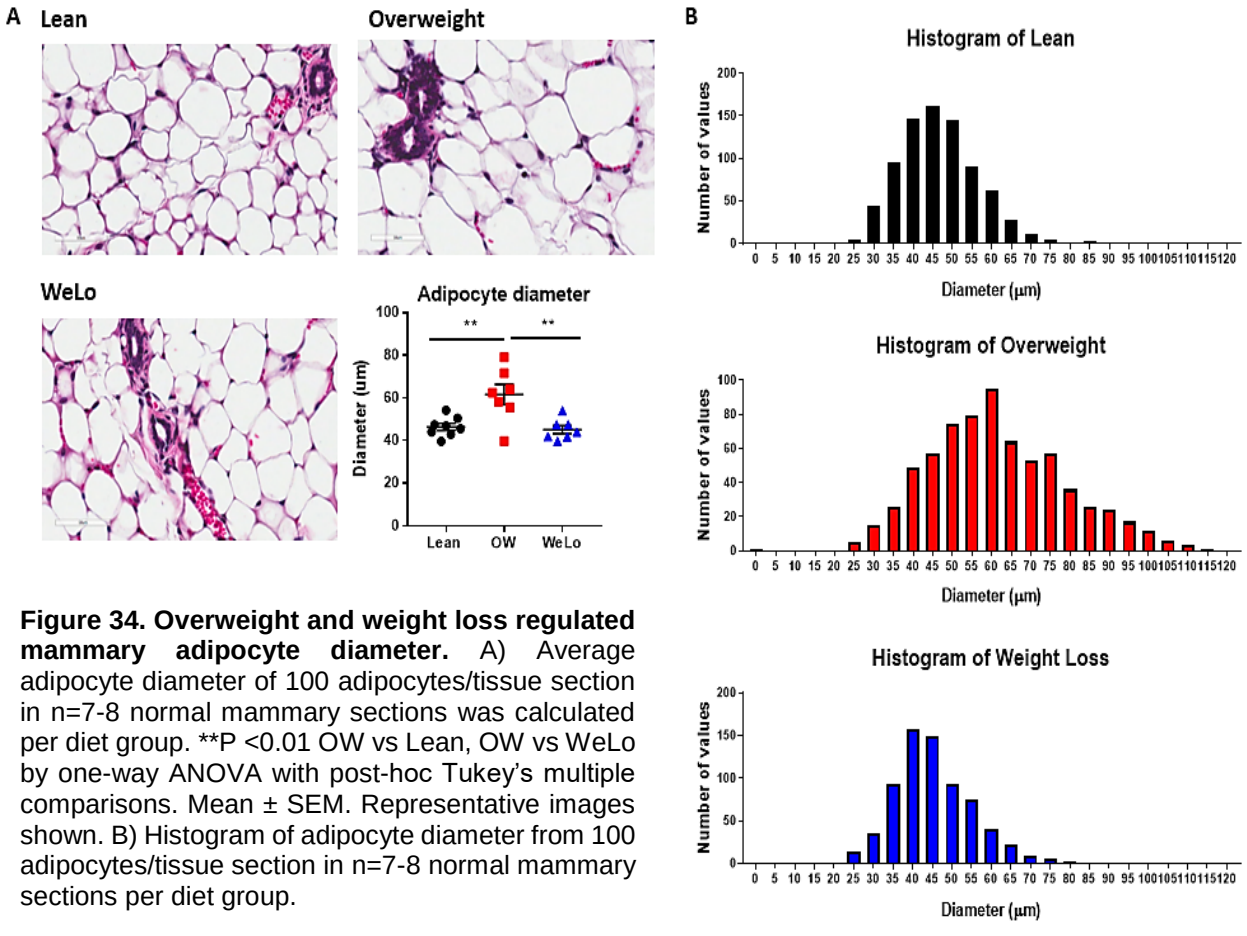

Figure 34. Overweight and weight loss regulated mammary adipocyte diameter. A) Average adipocyte diameter of 100 adipocytes/tissue section in n=7-8 normal mammary sections was calculated per diet group. **P <0.01 OW vs Lean, OW vs WeLo by one-way ANOVA with post-hoc Tukey's multiple comparisons. Mean ± SEM. Representative images shown. B) Histogram of adipocyte diameter from 100 adipocytes/tissue section in n=7-8 normal mammary sections per diet group.

As adipocyte hypertrophy in obesity is associated with increased myeloid cell content in visceral adipose depots, flow cytometric analysis was performed on lean and overweight mice to determine if myeloid content in mammary adipose tissue was also increased by overweight. CD11b-positive myeloid cell content was increased within the stromal-vascular fraction of Overweight mammary adipose by 52% relative to Lean animals (**Figure 35A;** P=0.0035) (complete gating scheme in **Appendix, Supp. Figure 43**). We next quantified markers of neutrophil and macrophage influx in whole mammary fat pad to identify which myeloid populations were regulated by adiposity. Expression of the neutrophil-specific enzyme neutrophil elastase (*Elane*) was significantly >2-fold greater (**Figure 35B**; P<0.01) in Overweight relative to Lean mammary fat pad and was reduced to Lean levels in WeLo mice.

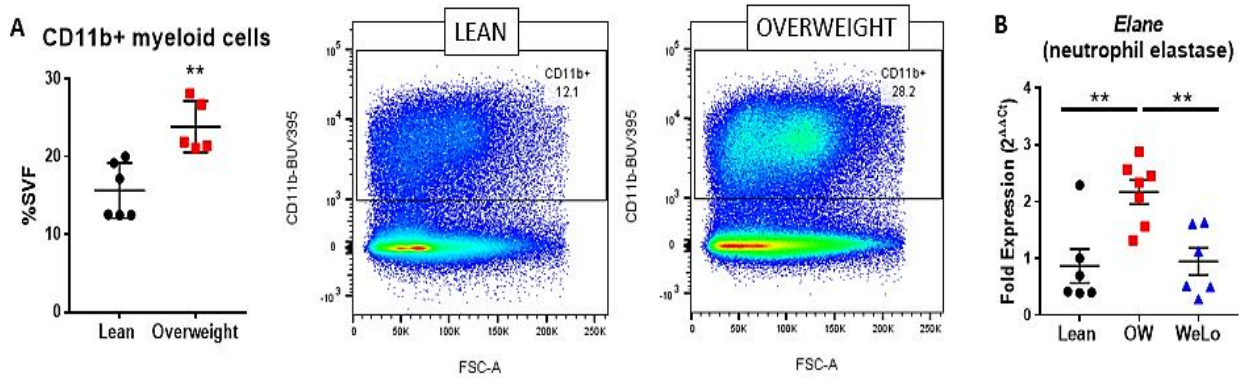

Figure 35. Accelerated tumor growth in Overweight mice occurred in association with increased mammary adipose myeloid cell content. A) CD11b+ myeloid cell composition shown as a percentage of total stromal-vascular cells in abdominal mammary fat pads. n=5-6 per diet group. **P= 0.0043 by Mann-Whitney. Representative dot plots shown along with representative images of mammary fat pads used for flow cytometric analysis. B) mRNA expression of the enzyme neutrophil elastase (*Elane*) was elevated in mammary fat pad of OW mice.

With respect to macrophages, mammary adipose CLS density was 2.20-fold (P=0.040) and 3.76-fold (P=0.0021) greater in Overweight compared to Lean and WeLo animals, respectively (**Figure 36A**). Notably, CLS were present in 90.3% of histologic mammary sections from Overweight mice yet were observed in only 50% of Lean and 31.8% of WeLo tissue sections. Accordingly, Overweight mammary glands exhibited a >4-fold increase in expression of F4/80 (*Emr1*) relative to both Lean and WeLo (**Figure 36B**, P<0.05).

Adipose tissue macrophages express a mixture of canonical pro- and anti-inflammatory markers (e.g., both CD11c [*Itgax*] and Arginase 1 [*Arg1*]) [370, 372, 527]. Consistent with this "mixed" macrophage phenotype, significant increases were observed in both *Itgax* and *Arg1* expression in Overweight mammary adipose (**Figure 36C**, *P<0.05, Overweight vs. Lean, WeLo; **Figure 36D,** **P<0.01 vs. Lean, ***P<0.001 vs. WeLo), while expression of monocyte-chemoattractant protein (MCP1; *Ccl2*) (**Figure 36E**) and tumor necrosis factor alpha (TNF-α, not shown) were increased but not significantly. Collectively, these findings suggest that adiposity-induced changes within the mammary microenvironment regulate myeloid cell content and/or activation, with potential to influence tumor growth in Overweight mice.

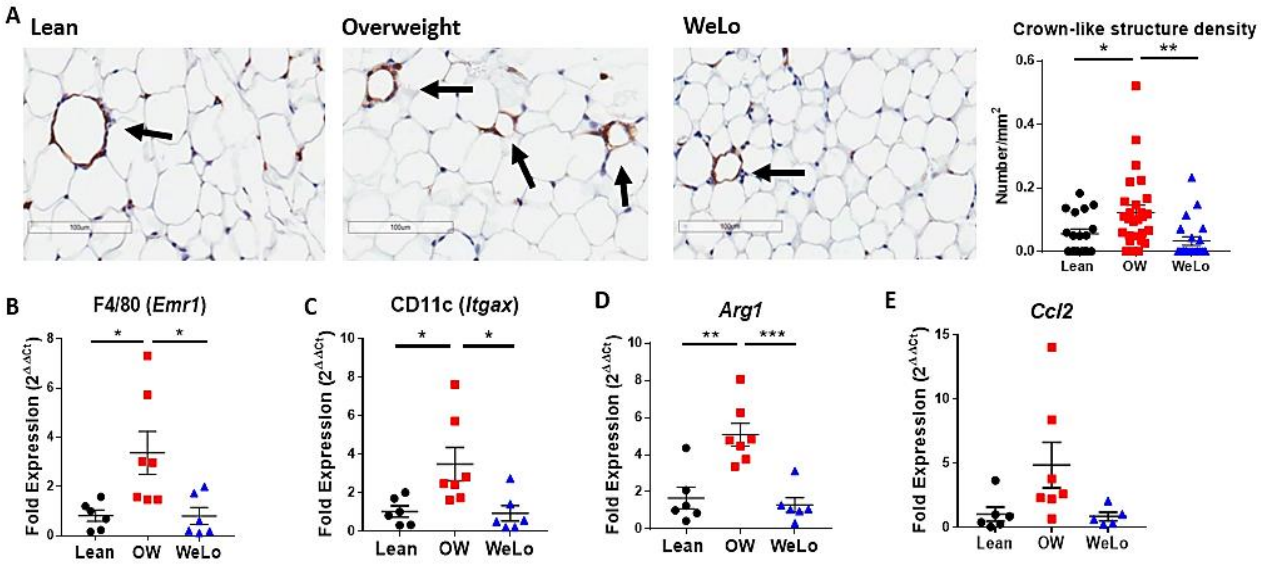

Figure 36. Overweight increased mammary adipose CLS density and expression of macrophage markers. A). Crown-like structure (CLS) density in the mammary fat pad was calculated in n=3 non-sequential sections per mouse from n = 6-9 mice/diet group. Scale bar = 100 µm. *P<0.05 OW vs Lean, **P <0.0001 OW vs WeLo by one-way ANOVA with post-hoc Tukey's multiple comparisons. Representative images shown, CLS indicated with arrows. B-E) mRNA expression of *Emr1*, the enzyme *Arg1*, the integrin *Itgax*, and *Ccl2* (also known as *Mcp1*) were measured in the mammary fat pad by RT-qPCR analysis. All gene expression analyses were normalized by the delta delta Ct method to 18S and the same randomly selected Lean sample. *P<0.05, **P<0.01, ***P<0.001 by one-way ANOVA with post-hoc Tukey's analysis (n=5-7/diet). Mean ± SEM.

Weight loss reversed overweight-associated increases in growth factor and inflammatory cytokine production

To further probe the effect of adiposity and weight loss on mammary inflammation, we next examined expression of select interleukins (ILs) implicated in adipose tissue inflammation and breast tumor growth promotion. Compared to Lean mice, overweight increased expression of IL-6 (*Il6*), while weight loss significantly reduced *Il6* expression by >8-fold relative to Overweight mice (**Figure 37A**; P=0.025 Overweight vs. Lean, P=0.014 Overweight vs. WeLo). Similarly, IL-1β (*Il1b*) expression was upregulated in Overweight mice relative to WeLo animals (P = 0.03) (**Figure 37B**). On the other hand, expression of immunosuppressive IL-10 (*Il10*) [441] was elevated by >4-fold in Overweight compared to Lean mammary fat pad (**Figure 37C**, P = 0.041). *Il10* expression in mammary pad of WeLo mice resembled that of Lean mice but did not

reach significance relative to Overweight (P = 0.054). Consistent with our flow cytometry data, these results support the existence of a mixed pro- and anti-inflammatory milieu within Overweight mammary adipose, with restoration of a lean-like microenvironment upon weight loss.

Weight gain can also increase expression of growth factors that are relevant to breast cancer progression, including hepatocyte growth factor (HGF, *Hgf*) [42, 43, 264, 528] and vascular endothelial growth factor (VEGF; *Vegfa*) [147, 225]. Notably, *Hgf* expression in the mammary fat pad was increased by approximately 2.7-fold in Overweight relative to Lean animals; this upregulation was abrogated in WeLo mice (**Figure 37D**; P=0.038 and P=0.030, respectively). WeLo mice also exhibited a significant reduction in *Vegfa* expression relative to Overweight mice (**Figure 37E**; P=0.025).

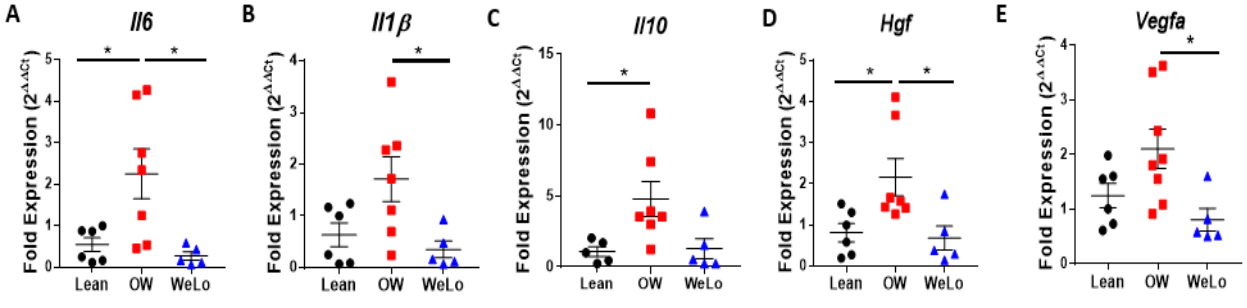

Figure 37. Weight loss restored mammary fat pad expression of mixed inflammatory cytokines, growth factors, and markers of neutrophil infiltration to lean levels. A-E) mRNA expression of the interleukins *Il1β, Il6,* and *Il10*, and the growth factors hepatocyte growth factor (*Hgf*) and vascular endothelial growth factor (*Vegfa*) were measured in the mammary fat pad by RT-qPCR analysis. All gene expression analyses were normalized by the delta delta Ct method to 18S and the same randomly selected Lean sample. *P<0.05, **P<0.01, by one-way ANOVA with post-hoc Tukey's analysis (n=5-7/diet). All graphs shown as mean ± SEM.

Local, obesity-induced changes in the mammary adipose microenvironment may augment angiogenesis and infiltration of immune cells, such as macrophages, into developing mammary tumors [45, 529]. Based on our findings that overweight increased mammary CLS density and expression of the pro-angiogenic growth factors *Hgf* and *Vegfa*, we determined

whether these changes translated into greater tumor microvessel density or tumor-associated macrophage content. However, no significant differences were observed in either CD31+ tumor area or microvessel density (**Figure 38A-B**). Similarly, flow cytometric analyses revealed no diet-induced differences in total leukocytes ($CD45^{+}$) (**Figure 38C**), tumor-associated macrophages (TAMs, defined as $CD45^{+}F4/80^{hi}FSC^{mid}SSC^{mid}$; **Figure 38D**), or other myeloid cells (defined as $CD45^{+}F4/80^{lo/mid}FSC^{hi}SSC^{hi}$; **Figure 38E**) (gating scheme in **Suppl Figure 2**).

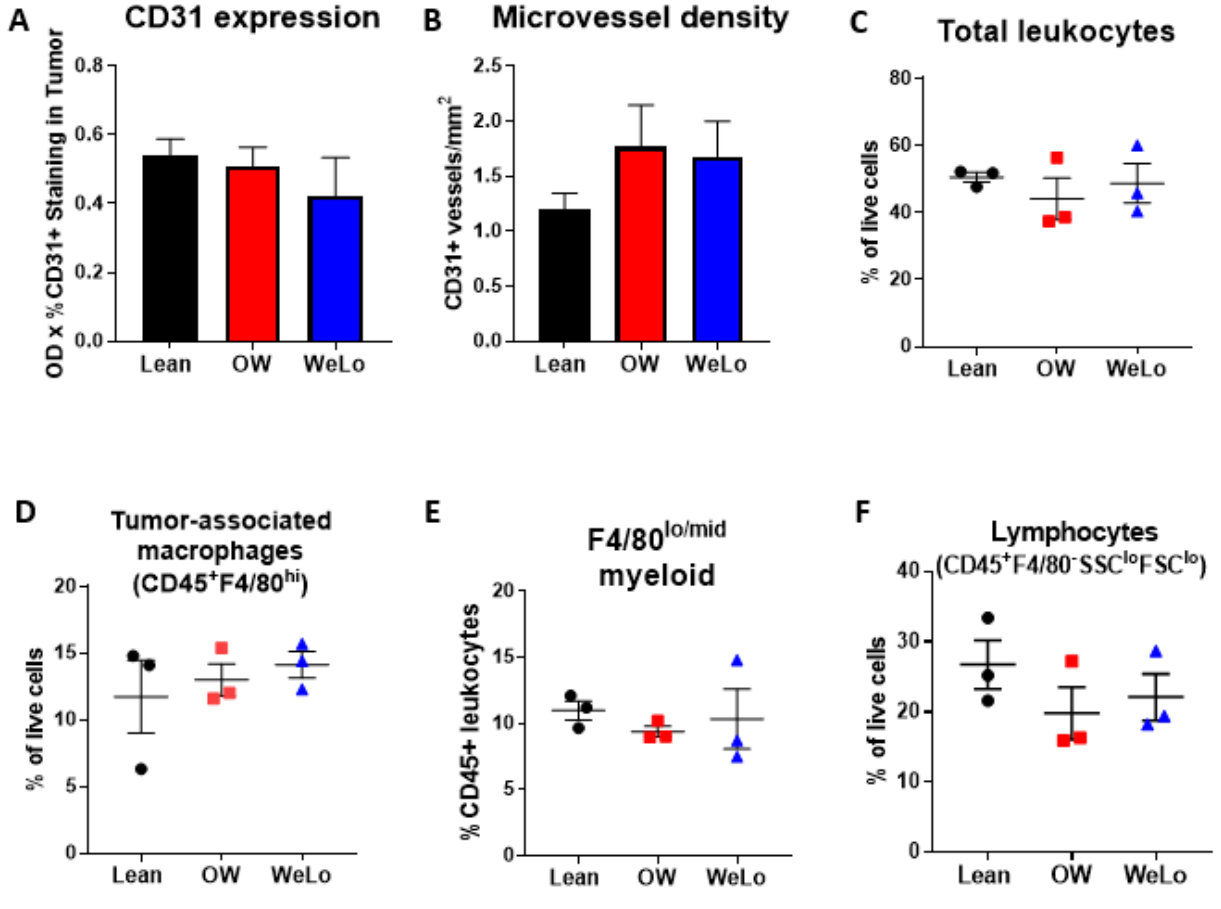

Figure 38. Accelerated early tumor growth in Overweight was not explained by differences in vascular density or leukocyte infiltration. A) Vascular density was measured using immunohistochemistry against the endothelial marker CD31/PECAM1 (n=7-8/diet group) Mean ± SD. B) Microvessel density was quantified as total number of CD31+ vessels per tissue area (mm^2). C-G) Intratumoral leukocyte analysis was conducted via flow cytometry on n=3 tumors/diet group. *P = 0.04, WeLo vs Lean. All values reported as mean ± SEM.

Weight loss reduced expression of mitogenic and metastasis-associated gene pathways

To further probe potential mechanisms whereby changes in weight status influenced tumor progression, we next conducted microarray analysis on total tumor lysates. Tumors were selected based on proximity to the median tumor volume within each respective diet group. Initial analysis comparing all three diet groups revealed minimal differences in gene expression in tumors from Lean and Overweight mice (data not shown), suggesting that increased tumor volume in Overweight mice was not driven by differences within the intratumoral microenvironment. However, WeLo mice exhibited a distinct transcriptional profile, prompting additional analyses using a two class Significance Analysis for Microarray (FDR <5%) to emphasize unique intratumoral changes in response to weight loss (**Figure 39A**). Relative to Lean and Overweight, WeLo mice exhibited downregulation of CXCR4/CXCL12 (**Figure 39B**) and erythropoietin (EPO) signaling (**Figure 39C**), as well as reduced expression of multiple genes within the IGF-1, ERK5, IL-4, and extracellular matrix (ECM) pathways (**Figures 39D-G**).

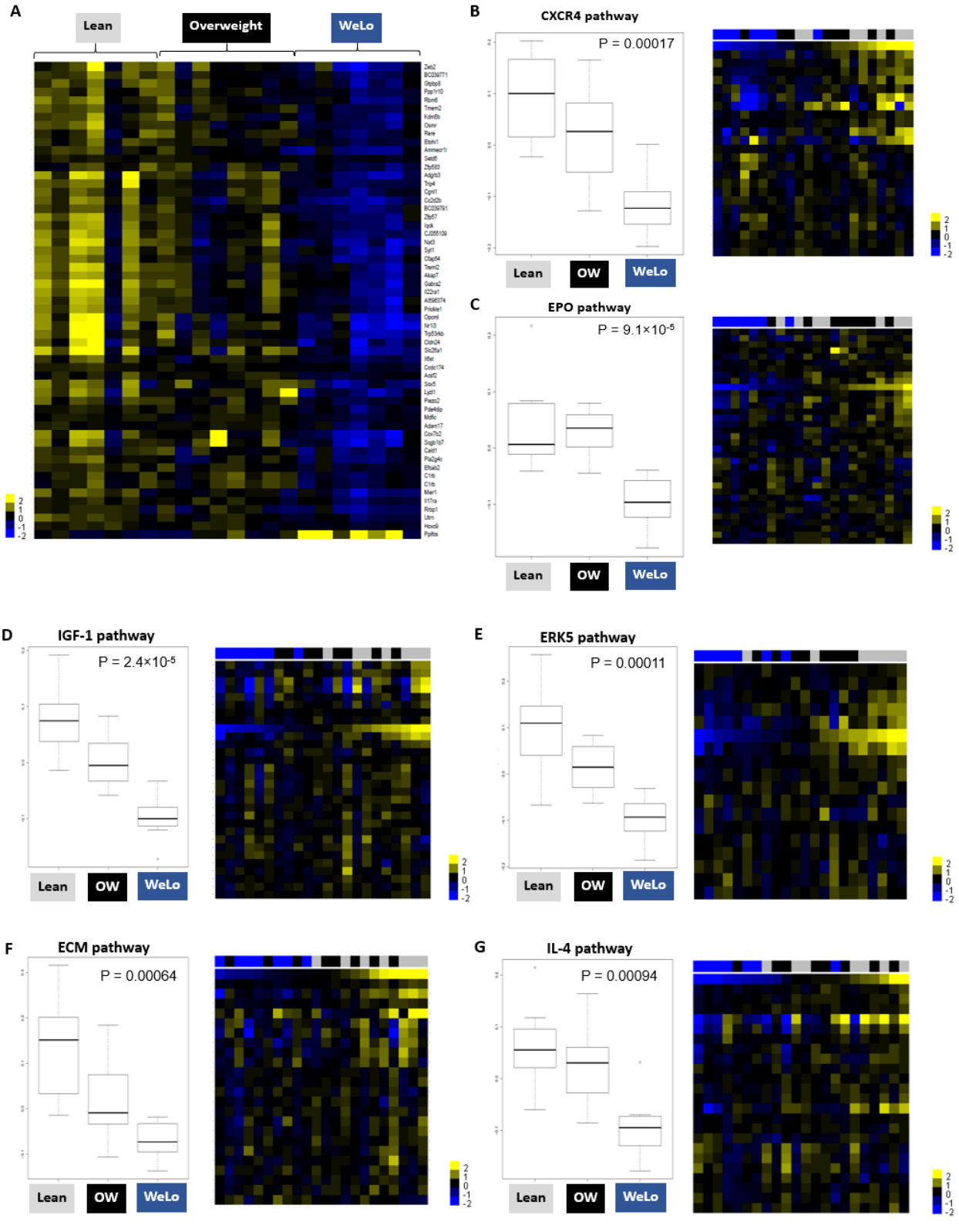

Figure 39. Weight loss altered intratumoral expression of pathways associated with growth, ECM remodeling, immune response, and metastasis. A) Heat map of genes with FDR <5% from a 2-class ANOVA using SAM. B-G) Tumor gene expression pathways significantly altered by diet exposure. Pathway analysis conducted using the Molecular Signatures Database (MSigDB). Y-axis of boxplots shows normalized log gene expression. Indicated P-values correspond to Weight loss vs Other.

Adiposity status regulated mast cell density and activation in mouse mammary fat pad

Similar to other myeloid-lineage immune cells, mast cell-derived factors are also implicated in breast cancer progression. To determine the effect of diet-induced weight gain and weight loss on mammary tissue mast cell content we next quantified mast cell density in un-injected mammary gland. Toluidine blue-positive mast cells were observed most frequently within the collagenous stroma of mammary ducts, in close proximity to ductal epithelial cells (**Figure 40A**), and in the adventitia of mammary blood vessels (not shown). While no significant difference in mast cell density was observed between Lean and Overweight mice, weight loss resulted in an approximately 51% increase in average mast cell density compared to Overweight animals (**Figure 40A**; $P<0.05$ vs. WeLo). On the other hand, the mast cell-specific marker tryptase beta-2 (*Tpsb2*) was non-significantly increased in Overweight mice ($P=0.063$ Overweight vs. Lean), and significantly (>3-fold) reduced by weight loss (**Figure 40B**; $P=0.017$ WeLo vs. Overweight).

To further investigate mast cell activation in response to mammary adiposity, we analyzed pre-existing, unpublished microarray data from lean and overweight nulliparous transgenic C3(1)-TAg mice mammary fat pads. These mice were randomly assigned to LFD and HFD at 10 weeks of age, and mammary fat pads without palpable or visible tumors were collected as unaffected mammary glands at an average of 18.2 weeks of age. We calculated a mast cell score for each sample using a previously validated, murine-specific 128-gene signature for connective tissue mast cells [524], the type most commonly found in mammary tissue [514]. Similar to our histologic findings in FVB/NJ mice, mast cell score was significantly greater in overweight as compared to lean C3(1)-TAg mammary fat pad (**Fig. 40C**).

To determine whether the presence of CLBC influenced mammary mast cell content we next compared mast cell density within un-injected mammary pad to mast cell density within the corresponding tumor-adjacent tissue of the same animal. Interestingly, a significant increase in mast cell density in tumor-adjacent mammary gland relative to the corresponding un-injected

mammary tissue was observed in Overweight mice (**Figure 40E**; P=0.016 vs. un-injected mammary) but not in Lean or WeLo mice (**Figure 40D&F**). However, neither overweight nor weight loss affected intratumoral mast cell density in CLBC tumors (not shown). Likewise, microarray analyses revealed no significant difference in expression of mast cell-associated genes across diet groups in our murine model of CLBC. Restated, mammary adipose conditions in the context of overweight prompted an increase in tumor-adjacent mast cell content in response to CLBC tumor development without affecting intratumoral mast cells.

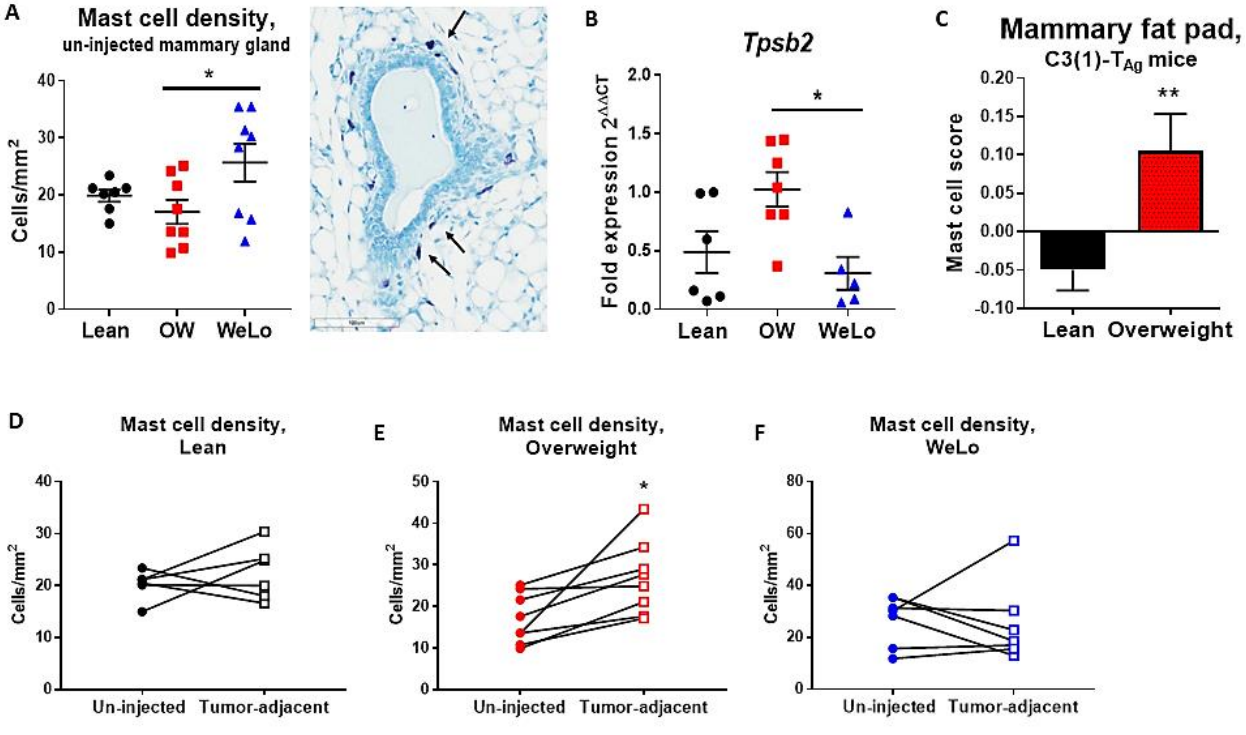

Figure 40. Overweight and weight loss regulated mast cell density and activation in normal and tumor-adjacent mammary adipose. A) Mammary mast cell density was calculated as number of toluidine blue-positive mast cells in a given mammary fat pad tissue section normalized to total tissue area analyzed (cells/mm2) n = 7-8 mammary sections/diet group. *P<0.05 WeLo vs OW. Representative image of toluidine blue staining shown with mast cells indicated by black arrows. B) mRNA expression of tryptase beta-2 (Tpsb2), a mast cell-specific enzyme, was quantified in mammary fat pad from n=5-7 mice/diet group by RT-qPCR analysis. All gene expression analyses were normalized by the delta delta Ct method to 18S and the same randomly selected Lean sample. Reported as mean ± SEM. C) Mast cell score was determined use microarray gene expression analyses of n=4-6 unaffected mammary fat pads from Lean and Overweight female C3(1)-TAg mice. P= 0.0095 by Mann-Whitney analysis. D-F) Mast cell density in un-injected mammary fat pad and corresponding tumor-adjacent adipose (cells/mm2) n =7-8 sections. Overweight *P=0.016 by paired t-test.

Mast cell score is increased in breast tissue of overweight and obese women

Our findings in murine mammary gland indicated the potential for increased mast cell activation in overweight and obese human breast tissue. Thus, we next investigated expression of mast cell-associated genes in existing microarray data from cancer-adjacent normal human breast tissue samples obtained through the UNC Normal Breast Study, a hospital-based study of normal breast tissue and breast cancer microenvironments [521] (see **Table 2** for patient characteristics).

Table 2. Demographic and clinicopathologic features of Normal Breast Study participants.

	Mean ± SD	**n**	**%**
Demographic factors			
Age	54.2 ± 11.8		
<50		44	33.6
≥50		87	66.4
Race			
Caucasian		82	62.6
African American		43	32.8
Other/Not reported		6	4.6
Anthropometric data			
[1]BMI (kg/m^2)	29.8 ± 7.1		
Normal-weight		38	29.0
Overweight		37	28.2
Obese		56	42.7
IHC-based subtype of corresponding tumor			
Luminal A ($ER^+PR^{\pm}HER2^-$)		52	39.7
Luminal B ($ER^+PR^{\pm}HER2^+$)		14	10.7
HER2-enriched ($ER^-PR^-HER2^+$)		15	11.5
Triple-negative ($ER^-PR^-HER2^-$)		24	18.3
[2]Other/Not reported		26	19.8

[1]May not equal 100% due to rounding.

[2]Includes borderline, benign, and *in situ* cases.

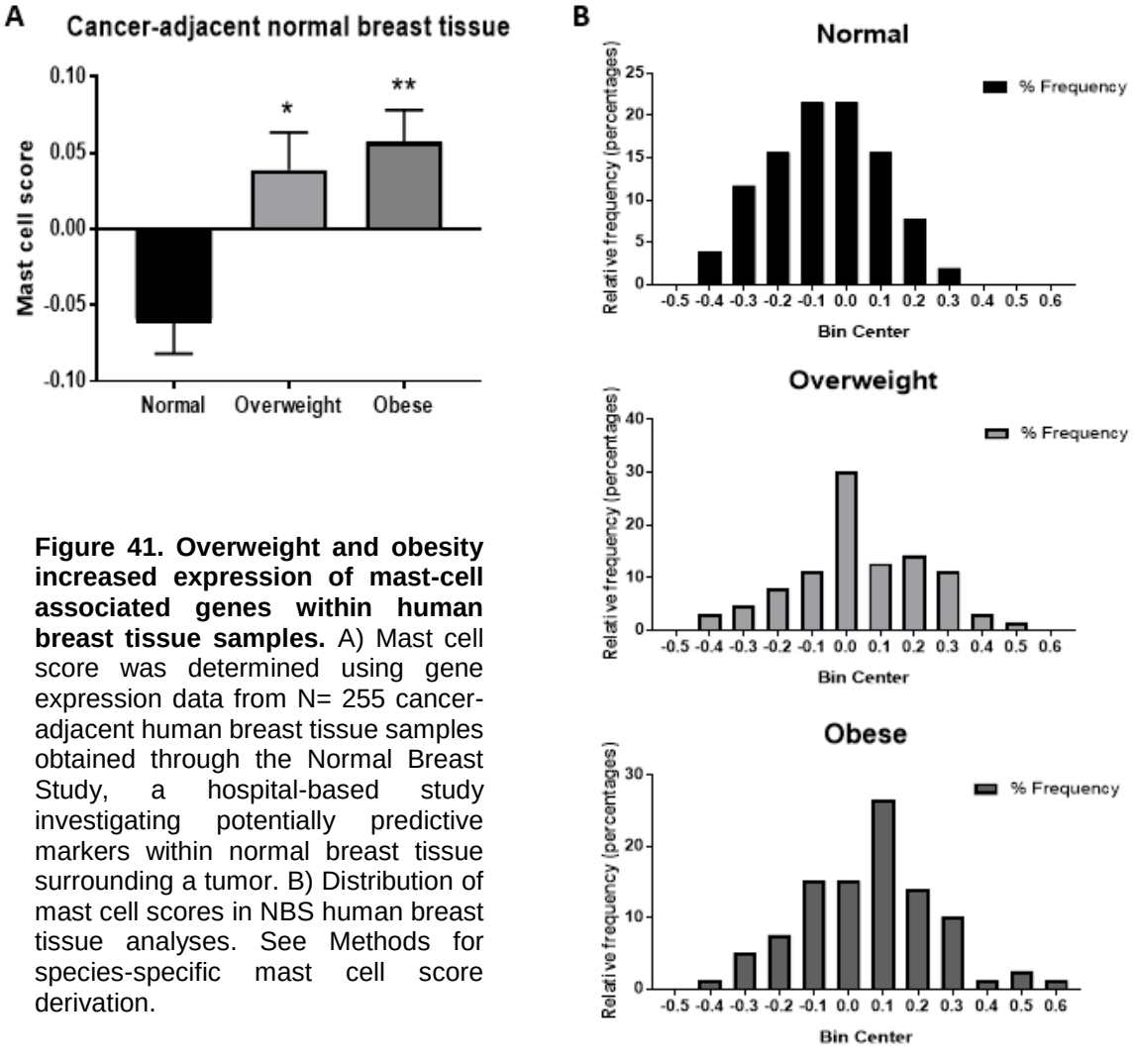

Figure 41. Overweight and obesity increased expression of mast-cell associated genes within human breast tissue samples. A) Mast cell score was determined using gene expression data from N= 255 cancer-adjacent human breast tissue samples obtained through the Normal Breast Study, a hospital-based study investigating potentially predictive markers within normal breast tissue surrounding a tumor. B) Distribution of mast cell scores in NBS human breast tissue analyses. See Methods for species-specific mast cell score derivation.

A mast cell score for each patient was calculated using a previously validated panel of human mast cell-specific genes [525]. Consistent with our murine model data, mast cell score in human breast tissue was elevated with increased adiposity (**Fig**. **41A-B**; P<0.05 Normal weight vs. Overweight, P<0.01 Normal weight vs. Obese). Thus, collectively our results demonstrated adiposity-mediated modulation of mast cell dynamics within both the mammary fat pad of mice and human breast tissue.

Lower intratumoral mast cell score is associated with triple-negative breast cancer and elevated risk of recurrence

Linked anthropometric data such as BMI are often not available for large, publicly-available human breast cancer gene expression datasets. However, as intratumoral mast cell density is correlated with more favorable outcomes in breast cancer [452], and because breast cancer outcomes vary across subtypes [530], we next utilized TCGA breast cancer datasets to inquire whether mast cell score varied in accordance with tumor subtype. Indeed, mast cell scores calculated in basal-like tumors were dramatically lower than those in luminal A cancers, a subtype with relatively high long-term survival rates [530] (**Figure 42A**, BBC vs. Luminal A; $P<0.0001$). A modest, yet significant, difference in mast cell scores was also seen between luminal B and HER2+ breast cancers (**Figure 42A,** $P<0.05$). These data indicate that breast cancer subtype is a strong determinant of intratumoral mast cell content.

The striking underrepresentation of mast cell-associated genes in BBCs, which display elevated 5-year distant recurrence rates relative to other breast cancer subtypes [509], led us to investigate whether mast cell score was also associated with predicted risk of tumor recurrence. For these analyses we used the previously assigned ROR-P score, which is a risk-of-recurrence score weighted to the PAM50 11-gene proliferation index available through TCGA [531]. Consistent with subtype findings, mast cell score was inversely associated with ROR-P score, with the greatest expression of mast cell-associated genes measured in tumors assigned a low ROR-P range, intermediate expression in the medium ROR-P group, and lowest expression in tumors assigned a high ROR-P score (**Figure 42B**, $P<0.0001$ for all comparisons).

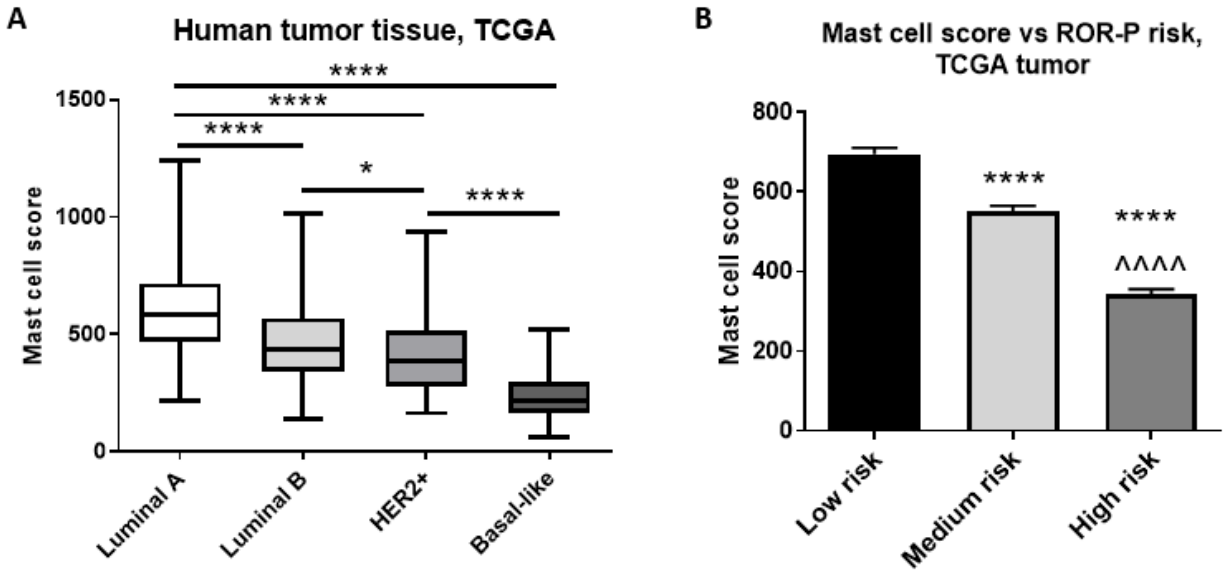

Figure 42. Intratumoral mast cell score was subtype-specific and associated with risk-of-recurrence score. A) Mast cell score by tumor subtype using gene expression data from N=1010 human tumors, generated by The Cancer Genome Atlas (TCGA) Research Network. *P<0.05, ****P<0.0001 B) Mast cell score differed significantly across ROR-P risk groups. Reported as mean ± SEM. See Methods for mast cell score derivation. ****P<0.0001 vs Low risk, ^^^^ VS Medium risk.

Discussion

Obesity at the time of breast cancer diagnosis is associated with an estimated 34% increase in breast cancer-specific mortality in postmenopausal women and a 75% increase in premenopausal women [55]. Importantly, the inflammatory changes seen in obese breast adipose and implicated in promotion of breast cancer progression are also present in overweight women [366, 513]. As overweight and obesity in women are now more than three times as prevalent as normal weight [504], an understanding of the mechanisms whereby excess adiposity and weight loss influence breast cancer aggression is critical to inform public health recommendations and therapeutic approaches.

Our previous findings in the transgenic C3(1)-TAg model of BBC demonstrated accelerated tumor progression in response to weight gain that was reversed in animals wherein weight loss occurred before tumor onset [264]. An unknown was how the mammary gland

microenvironment contributed to tumor growth as opposed to effects of weight gain or loss that were tumor-intrinsic. Herein, we show that overweight mice exhibited significantly greater tumor volume at sacrifice, whereas tumor growth in mice induced to lose weight paralleled that of lean animals. As inflammation is a well-established risk factor for breast cancer onset and progression, our studies herein employed mouse models of overweight and weight loss to identify the influences of changes in adiposity status on inflammation within mammary adipose tissue and the CLBC tumor microenvironment. Prolonged high-fat feeding in Overweight mice resulted in a doubling of overall adiposity, hepatomegaly, elevated fasting glucose, and a nearly 2-fold increase in mammary fat pad weight relative to Lean and WeLo mice, consistent with reports of both regional and systemic effects of high-fat feeding in FVB/NJ mice despite a lower degree of overall adipose gain relative to the C57BL/6 strain [516]. Increased CLBC growth rate in Overweight mice occurred in the context of inflammatory changes within the surrounding mammary fat pad that are characteristic of visceral adipose depots in obesity, including increased adipocyte diameter and greater CLS density [275, 364, 532]. We also observed increased expression of markers (*Itgax* and *Arg1*) supporting infiltration of the overweight mammary fat pad by a population of mixed-phenotype macrophages, as has been reported in obese abdominal adipose depots of both mice and humans [372, 375-377]. Also in accord with previous studies [532], decreased mammary adipocyte diameter in WeLo mice corresponded with a decline in expression of macrophage-associated markers.

In addition to increased macrophage content, our results indicated enhanced neutrophil content in mammary adipose tissue of Overweight mice. Notably, studies to date regarding adipose neutrophil infiltration in response to weight gain have investigated this question exclusively in male mice [361, 420], leaving unclear as to what extent, or when, neutrophils infiltrate the overweight or obese mammary fat pad. Our findings support both the increased presence of neutrophils in mammary fat of overweight mice and a reduction in neutrophil content with weight loss. Weight loss also reversed elevated expression of cytokines (*Il6*, *Il10*,

Il1b) and growth factors (*Hgf* and *Vegfa*) implicated in both inflammation and breast cancer progression [505]. Among these factors, *Hgf* is particularly noteworthy, as HGF/MET signaling appears to be a defining feature of CLBCs [533]. Together with the macrophage findings above, these results describe establishment of an inflammatory microenvironment in overweight mammary fat pad, with restoration of a lean-like cytokine milieu following weight loss.

Despite these changes in the surrounding mammary fat pad, our analyses revealed no diet-mediated differences in either tumor microvessel density or total tumor leukocyte content. However, leukocytes comprised 40-50% of total CLBC tumor cellularity, a dramatic immune infiltrate which is consistent with previous reports of a strong immune signature in CLBCs [507, 508]. Similarly, tumor microarray analysis demonstrated minimal differences in tumors resected from Lean and Overweight mice, results which were paralleled in additional microarray analyses of tumors from lean and overweight transgenic C3(1)-TAg mice (data not shown). However, weight loss before tumor development reduced expression of signaling pathways implicated in ECM remodeling, cancer cell survival and proliferation (IGF-1, ERK5, IL-4) [534-536], and metastasis (CXCR4/CXCL12 and EPO) [536-538]. Of particular interest are the reductions observed in CXCR4 and EPO pathways. CXCR4 is a G-protein coupled receptor with demonstrated roles in promotion of breast cancer metastasis. In mice, overexpression of CXCR4 alone significantly increased bone metastases of a CLBC cell line [537], while blockade of CXCR4 signaling in the same cell line reduced lung metastases [539]. In humans, CXCR4 expression in breast cancer is associated with both lymph node status and distant metastases, as well as reduced 5-year disease-free survival and overall survival [540]. Weight loss also reduced expression of the EPO signaling pathway, which is implicated in tumor-initiating cell self-renewal [517], reduced response to chemotherapy [541], and lymph node metastasis [538]. Additional analyses are ongoing to identify the prognostic potential of these weight loss-associated transcriptional changes with regard to breast cancer outcomes in other molecular subtypes.

In addition to increased macrophage and neutrophil content in mammary adipose, our findings herein also support a novel role for weight gain and loss in regulation of breast tissue mast cell dynamics. Accumulation and proinflammatory activation of mast cells in obese visceral adipose has been reported in both mice [437] and humans [435, 436]. However, to our knowledge ours is the first study to investigate mast cell content and activation with regard to mammary adiposity in both mice and humans and to incorporate a weight loss intervention. Interestingly, our results demonstrated increased mast cell content in un-injected mammary not in overweight mice, but instead in a subset of the mice assigned to undergo weight loss. On the other hand – and more relevant to breast cancer progression – mast cell content in tumor-adjacent adipose was increased relative to un-injected mammary exclusively in overweight animals. Indicators of mast cell activation were also elevated in overweight mammary gland across two different mouse models, an increase which was significantly attenuated by weight loss.

Importantly, increased expression of mast cell-associated genes was also observed in overweight and obese human breast tissue collected through the UNC Normal Breast Study [521]. Others have reported that mast cells isolated from omental (visceral) and subcutaneous adipose depots of obese subjects secreted increased levels of pro-inflammatory cytokines, chemokines, and growth factors relative to those isolated from lean subjects, indicating a more activated state [436]. An increase in mast cell content and/or activation within the obese breast may influence breast cancer progression in obese individuals. For example, tryptase-containing mast cells are typically found in greater number within peritumoral tissue, and are associated with myofibroblast differentiation, higher lymphangiogenic and angiogenic microvessel density, and lymph node metastasis [505]. Notably, our data indicated lower expression of tryptase in mammary mast cells of mice following weight loss. Taken together, our findings of increased mast cell markers in overweight and obese normal breast warrants additional investigation into mast cell-mediated mechanism of obesity-associated tumor progression. The close proximity of

mast cells in normal breast tissue to the ductal epithelium also suggests potential roles for mast cells in progression of pre-neoplastic lesions such as ductal carcinoma *in situ* or neoplastic transformation of mammary ductal epithelium.

Finally, using TCGA data we reported that mast cell gene expression varied based on breast cancer subtype, with low mast cell-associated gene expression observed in BBCs and higher expression in luminal subtypes. Our studies herein also revealed an inverse relationship between intratumoral mast cell markers and risk-of-recurrence category (ROR-P), which provided the most significant prognostic information, compared with other prognostic gene signatures, regarding post-relapse survival when added to a clinical model [531]. Our finding of low mast cell-associated gene expression in BBCs is consistent with reports of a high density of tryptase-positive mast cells in luminal A breast cancers yet low mast cell content in TNBCs [542]. Tryptase-positive mast cell density was also associated with expression of the proliferation marker Ki67 as well as tumor size and Nottingham Histologic Grade [542]. Collectively, these analyses suggest a potential role for mast cells in regulation of tumor characteristics associated with breast cancer recurrence, and complement previous reports of intratumoral mast cells as exerting a protective effect in breast cancer [452]. Additionally, the paradoxical relationship between mast cell localization and tumor prognosis suggests that peritumoral and intratumoral mast cells may in fact exhibit distinct phenotypes. Future analyses should address intratumoral mast cell score in CLBCs, which are not currently well represented in TCGA, and by anthropometric data such as BMI, which is not at this time linked TCGA to breast cancer data sets.

Collectively, our results indicate that local inflammatory changes within the surrounding mammary fat pad, including increased myeloid cell content and growth factor expression, accelerated tumor progression in overweight mice, and suggest the potential for cross-talk between mammary adipose immune populations and developing CLBCs. Moreover, these findings elucidate the impact of overweight and subsequent weight loss on the mammary

microenvironment and progression of CLBC. The distinct patterns of gene expression observed in tumors from mice who experienced weight loss before tumor growth are encouraging for public health and emphasize the importance of clarifying physiological changes within the breast adipose or intratumoral microenvironment in response to body weight fluctuations. Furthermore, our findings of a relationship between weight status and mast cell dynamics in mammary adipose of both mice and humans argues for further investigation into peritumoral mast cells as key players in obesity-associated BBC and CLBC progression.

CHAPTER 4: SYNTHESIS, SIGNIFICANCE, AND FUTURE DIRECTIONS

Triple-negative breast cancers: a heterogeneous disease

The classification of breast cancers and subsequent clinical decisions for treatment remain reliant upon IHC4, a histopathologic scoring system which combines expression of known “molecular drivers” of breast cancer progression – estrogen receptor (ER), progesterone receptor (PR), human epidermal growth factor receptor 2 (HER2), and the proliferation marker Ki67 – with clinicopathological parameters such as Nottingham Histologic Grade. IHC4 provides an estimation of the risk of distant disease recurrence in breast cancer patients and guides treatment selection from within the currently limited arsenal of targeted adjuvant and neoadjuvant therapies. The focus of this dissertation, TNBCs, are called as such because they lack expression of ER, PR, and HER2 when assessed using IHC4. For this reason, TNBCs currently lack FDA-approved targeted therapies, leaving systemic chemotherapy as the standard-of-care treatment for patients with both early- and advanced-stage disease. Importantly, the category of TNBC applies to all tumors that lack ER, PR, and HER2 expression, resulting in profound heterogeneity within this subgroup [543] and complicating identification of actionable molecular targets. While TNBCs, particularly BBCs, are often more sensitive to chemotherapy than other phenotypes (e.g., ER and/or HER2 positive) [544], they paradoxically also exhibit elevated recurrence and metastasis rates relative to other breast cancer subtypes [509]. Critically, fewer than 30% of women with metastatic breast cancer survive five years [545], and virtually all women with metastatic TNBC will ultimately die of their disease.

However, the additional complexity in breast cancer classification exposed by ongoing analyses under The Cancer Genome Atlas (TCGA), in conjunction with high-throughput gene sequencing and transcriptomic profiling, has allowed for molecular subtyping of breast cancers

and increased emphasis on personalized approaches to treatment. The studies presented herein have investigated the effects of weight status on tumor progression using multiple molecular subtypes of TNBC (BBC and CLBC) and employing both orthotopic transplant models and models of spontaneous tumor development. Consideration of molecular subtypes when investigating the impact of overweight and obesity on breast cancer outcomes is paramount. Elucidation of unique mechanisms of overweight- and obesity-related cancer pathogenesis in a subtype-specific manner may reveal therapeutic targets to improve outcomes and further inform personalized treatment options for these patient populations.

In the studies conducted in Chapter 2 of this dissertation we sought to reverse the acceleration of basal-like TNBC latency previously observed in HFD-fed mice and inhibit tumor progression in LFD- and HFD-fed C3(1)-TAg mice using the small molecule cMET inhibitor crizotinib. A strength of our study is that we tested this question in models of both prevention and treatment, providing a better understanding of cMET dependence in both preneoplastic lesions and invasive basal-like mammary carcinoma. In the prevention arm we investigated whether administering crizotinib in a window prior to frank tumor development would inhibit or delay tumorigenesis. Thus, mice were started on diet at 8 weeks of age to ensure crizotinib administration occurred within the primary window of AH/CIS precursor lesions (9-12 weeks of age), based on previous findings of increased precursor lesion formation in C3(1)-TAg mice following HFD-induced weight gain [546]. Although preventive crizotinib administration significantly accelerated tumor progression in the primary (first detected) tumor in both diet groups, no differences were measured when total tumor progression (all tumors considered collectively) was assessed. Similarly, no effect was seen on total tumor multiplicity with prophylactic administration of crizotinib. Interestingly, we also did not observe accelerated tumor latency in HFD-fed mice, as has been seen in our previous studies of adult weight gain [43, 263]. Instead these results paralleled those of female C3(1)-TAg mice weaned onto LFD or HFD – generating a model of lifelong obesity – wherein no difference in latency was observed but tumors progressed an at an accelerated rate [264]. The differences in adiposity-associated

phenotype observed across these studies (shortened tumor latency vs increased rate of tumor progression) emphasize the importance of clarifying “windows of susceptibility” [470, 480] during which overweight and obesity play disproportionately greater, and varied, roles in breast cancer.

In the treatment arm of our study crizotinib administration was initiated upon detection of the first palpable tumor; i.e., in mice with established invasive mammary carcinoma. In mice with established basal-like mammary cancer, crizotinib treatment inhibited subsequent tumor formation in our study such that total tumor multiplicity was significantly reduced at sacrifice, irrespective of diet or weight status. The degree of tumor inhibition was paralleled by a similar degree of suppression of tumor vascularity, which is consistent with HGF/cMET signaling as a potent driver of tumor angiogenesis [265, 497].

Diet, overweight, obesity, and weight loss in breast cancer outcomes

Herein we have also reported that overweight and weight loss reciprocally regulated CLBC tumor volume, along with numerous pro-inflammatory changes in surrounding mammary adipose. Increased CLS density and mammary inflammation in Overweight mice were associated with increased rate of CLBC tumor growth, as well as an increase in mast cell density in tumor-adjacent adipose. Increased expression of a mast cell gene signature was also observed in cancer-adjacent normal breast tissue from both overweight and obese human subjects compared to normal weight. Interestingly, while weight status did not influence intratumoral mast cells, weight loss resulted in reduced expression of mast cell activation markers within the mouse mammary adipose pad and a unique transcriptional signature in tumors of WeLo mice, including reduced expression of mitogenic and metastasis-associated gene pathways.

While the studies in Chapter 3 are primarily descriptive in nature, our selection of a model of overweight, rather than outright obesity, allows insight into potential risk factors for CLBC progression in this understudied population. Additionally, we emphasized tissue- and

species-specificity in selection of the mast cell signatures for microarray analysis, based on reports of nontrivial differences in mast cells across species and in a given tissue context [547]. Importantly, our results indicate that weight loss following overweight significantly attenuated inflammation-induced CLBC progression. As overweight and obesity in women are now more than three times as prevalent as normal weight [504], an understanding of the mechanisms whereby excess adiposity facilitates TNBC aggression is critical, while information regarding efficacy of preventive measures such as weight loss could have tremendous potential for public health.

However, a limitation of diet-induced obesity studies in rodents that must be acknowledged is the high fat content of the diet used to induce adiposity, which raises questions regarding whether dietary composition or adiposity *per se* is the primary driver of the observed acceleration in tumor progression in overweight or obese animals. Our observation of extensive differences in expression of tumor growth-promoting pathways between lean mice and mice induced to lose weight – groups which consumed the same diet both before and during the tumor growth period – supports that adiposity as well as associated local and systemic changes that occur in response to weight loss are nontrivial in tumor biology. Moreover, recent studies evaluating the impact of low-fat diets in breast cancer patient populations argue against the reduction of dietary fat as an effective strategy for mitigating breast cancer risk or improving outcomes. For example, a randomized controlled trial in Canada reported that a low-fat dietary intervention in 4,690 women with high breast density did not significantly influence breast cancer incidence across 10 years of follow-up [548]. Similarly, the Women's Healthy Eating and Living (WHEL) trial randomly assigned 3,088 breast cancer patients to a low-fat diet high in vegetables, fruit, and fiber and observed no differences in disease-free survival or overall survival between intervention and control groups [549]. Moreover, the Women's Health Initiative Dietary Modification trial, a randomized controlled trial in post-menopausal patients within the larger Women's Intervention Nutrition Study (WINS), reported no significant effects on either

breast cancer incidence rate or breast cancer-specific mortality relative to the control group following prolonged consumption of a low-fat diet (16.1 years average follow-up) [550]. However, deaths after breast cancer (all-cause mortality) were significantly reduced in the dietary intervention group [550]. Thus, currently available data does not support an influence of dietary fat composition on breast cancer risk. Additionally, the difference in overall survival findings between the WHEL and WINS studies may be less directly linked to dietary composition and instead due to a modest decrease in weight (average loss of approximately 6 lbs maintained over 5 years) in WINS participants but not those in WHEL.

Nonetheless, the relationship between weight loss and breast cancer incidence and outcomes in overweight and/or obese individuals also remains ambiguous. Despite reports of improvement in levels of metabolic markers associated with cancer progression following weight loss [551], a secondary analysis of the Women's Health Initiative randomized clinical trials found no association between breast cancer risk and weight loss (prior to cancer) among already overweight or obese postmenopausal women over a median of 13 years of follow-up [47]. On the other hand, Chlebowski et al. also evaluated associations between weight change and invasive breast cancer risk in postmenopausal women within the Women's Health Initiative over 11.4 years (mean) of follow-up, and reported a significant 12% reduction in breast cancer risk in women with weight loss ≥ 5%, intentional or otherwise, compared with women of stable weight [552]. Importantly, weight *gain* ≥ 5% significantly increased risk of TNBC by 54%, without affecting overall breast cancer risk [552].

With regard to weight loss and breast cancer outcomes, a meta-analysis of observational studies did not support an association between weight loss and improved survival; in fact, several studies have reported dramatically *increased* mortality associated with weight loss in overweight and obese breast cancer survivors [553]. Critically, several of the included studies did not differentiate between purposeful weight loss and disease-specific weight loss after breast cancer diagnosis. Intentional weight loss through diet and/or exercise is inarguably

different from weight loss due to, for example, cancer-associated cachexia, a fatal energy-wasting syndrome that is estimated to be the immediate cause of death in approximately 20-40% of end-stage cancer patients [195].

Collectively, the limited evidence supporting improved prognosis in response to weight loss after diagnosis, and the lack of studies separating intentional weight loss from disease-associated weight loss, complicates recommendations regarding weight loss for breast cancer survivors. However, the studies reviewed above regarding breast cancer risk, as well as our results herein, argue for further investigation into the potential impact of weight loss before cancer diagnosis on breast cancer risk and outcomes. Finally, our use of murine pre-clinical models, human tissue samples collected through the Normal Breast Study, and secondary analysis of existing, publicly available data sets (TCGA) informs future translational studies with potential for clinical impact.

Directions for future research

Our crizotinib treatment arm results presented in Chapter 2 are consistent with initial mechanism-of-action studies for crizotinib, which showed a dose-dependent reduction of microvessel density (CD31+ area) in response to cMET inhibition in gastric carcinoma, glioblastoma, and prostate carcinoma [478]. cMET inhibition has also shown promising results in xenograft models of aggressive cancers such as lung [496] and pancreatic cancers [497] as well as pre-clinical models of TNBC models such as ours [498]. However, clinical trials investigating cMET inhibitors in metastatic TNBCs have so far not been in accord with preclinical findings, and at the time of submission of this dissertation no receptor tyrosine kinase inhibitors primarily targeting cMET have been approved for the treatment of breast cancer. Bearing this caveat in mind, inhibition of the cMET signaling pathway through chemical or antibody-mediated inhibition in a patient population may not be as effective as preclinical studies, including ours, have suggested. Of note, a potential contributor to the high rate of

attrition when translating preclinical to clinical contexts may be that essentially all preclinical drug studies are conducted in lean mice fed chow diets. In America, and increasingly worldwide, individuals of normal body weight are the minority. Perhaps inclusion of overweight and obese animal models in preclinical drug studies would more adequately predict therapeutic success in human trials.

Nonetheless, clinical pursuit of the HGF/cMET pathway as a potential TNBC target continues, though the plan of attack has changed. Two currently active clinical trials are exploring efficacy of chimeric antigen receptor T cells (CAR-T cells) programmed to target cMET. One employs autologous cMET-redirected T cells administered intravenously in patients with melanoma or TNBC (ClinicalTrials.gov Identifier: NCT03060356), while the other administers autologous cMET-redirected T cells intratumorally in patients with metastatic breast cancer or newly diagnosed TNBC (ClinicalTrials.gov Identifier: NCT01837602). CAR-T cells have shown incredible promise in hematologic malignancies such as lymphoma [554]; unfortunately, they have been largely ineffective in patients with metastatic solid cancers, in part due to tumor heterogeneity and the paucity of suitable cell-surface targetable molecules expressed by solid cancers. In both of the highlighted trials, inclusion criteria specify ≥30% cMET positivity by IHC, and I eagerly await the results of these two trials.

Data presented in Chapter 3 suggested that weight status influences breast mast cell dynamics in both mice and humans. However, the analyses conducted did not allow for differentiation between an increase in mast cell content as opposed to an increase in activation status of existing mast cells. Flow cytometric analyses of mammary mast cells from normal and tumor-adjacent mammary tissue of lean and overweight or obese mice would address this question, allowing for both quantification of mast cell content in mammary tissue as well as quantification of mediators of interest, such as select serine proteases or histamine. *In vitro* culture of isolated mast cells with media conditioned by lean and obese mammary adipose tissue would further clarify whether the obese mammary microenvironment alters activation

status of mast cells. The close proximity of mast cells in normal breast tissue to the ductal epithelium also suggests potential roles for mast cells in progression of pre-neoplastic lesions such as ductal carcinoma *in situ* or neoplastic transformation of mammary ductal epithelium*. In vitro* cell culture studies utilizing bone marrow-derived mast cells or mast cell-derived mediators could be used to determine the impact of an increased concentration of mast-cell derived factors, such as tryptase-β2, on various stages within the progression of breast cancer available through the MCF10 breast cancer cell series - MCF10A, MCF10AT1, MCF10DCIS.com and MCF10CA1a [555].

The biological significance of the difference in mast cell content by breast cancer subtype seen in our study and that of Glajcar et al. [542] is intriguing, particularly in light of our finding that higher mast cell gene expression was significantly associated with a lower risk of recurrence score. To investigate whether mast cells directly influence tumor characteristics associated with breast cancer recurrence, co-culture studies with breast cancer cell lines could be conducted to determine whether mast cells increase migration, invasion of the basement membrane, or colony formation. Incorporation of cell lines of various molecular subtypes would also probe whether they do so in a subtype-specific manner and could be further used to determine the directionality of any observed effects. For example, perhaps production of mast cell-eliciting chemokines differs by breast cancer molecular subtype. Orthotopic transplant studies in mast-cell deficient and wild-type mice would also confirm molecular subtype-specific mast cell interactions *in vivo*. Studies reporting a differential association between peritumoral and intratumoral mast cell density and breast cancer prognosis suggest that analysis at a single-cell level of phenotypic differences between peritumoral and intratumoral mast cell phenotypes may also yield interesting findings.

Finally, our analysis of tumor gene expression revealed a unique gene expression profile in tumors resected from mice that lost weight before orthotopic transplant. However, additional questions are raised by these findings, including: can the weight loss gene expression signature

– particularly the reduced signaling observed through the CXCR4 and EPO signaling pathways - be recapitulated by interventions such as caloric restriction or exercise? Does weight loss result in consistent transcriptional changes in other breast cancer subtypes? To the latter point, additional analyses are ongoing to identify an intratumoral weight loss “signature” and establish its prognostic potential with regard to breast cancer outcomes in human breast cancers and across molecular subtypes.

Cancer research has traditionally focused on identifying altered gene expression and cell signaling within tumor cells. However, the tumor microenvironment, including immune cells and the signaling extracellular milieu, also strongly influences tumor onset and progression. This is the “seed and soil” hypothesis originally posed by Dr. Stephen Paget [556], and furthered developed by pioneers such as Mina Bissell, Ph.D. [557], wherein the seed (cancer cell) must be nurtured by the metabolites, growth factors, or angiogenic factors provided by the surrounding soil (stroma). The body of work presented herein speaks to the importance in overweight- and obesity-associated breast cancers of considering not only tumor-intrinsic factors, but also changes to the normal mammary and tumor-adjacent microenvironments.

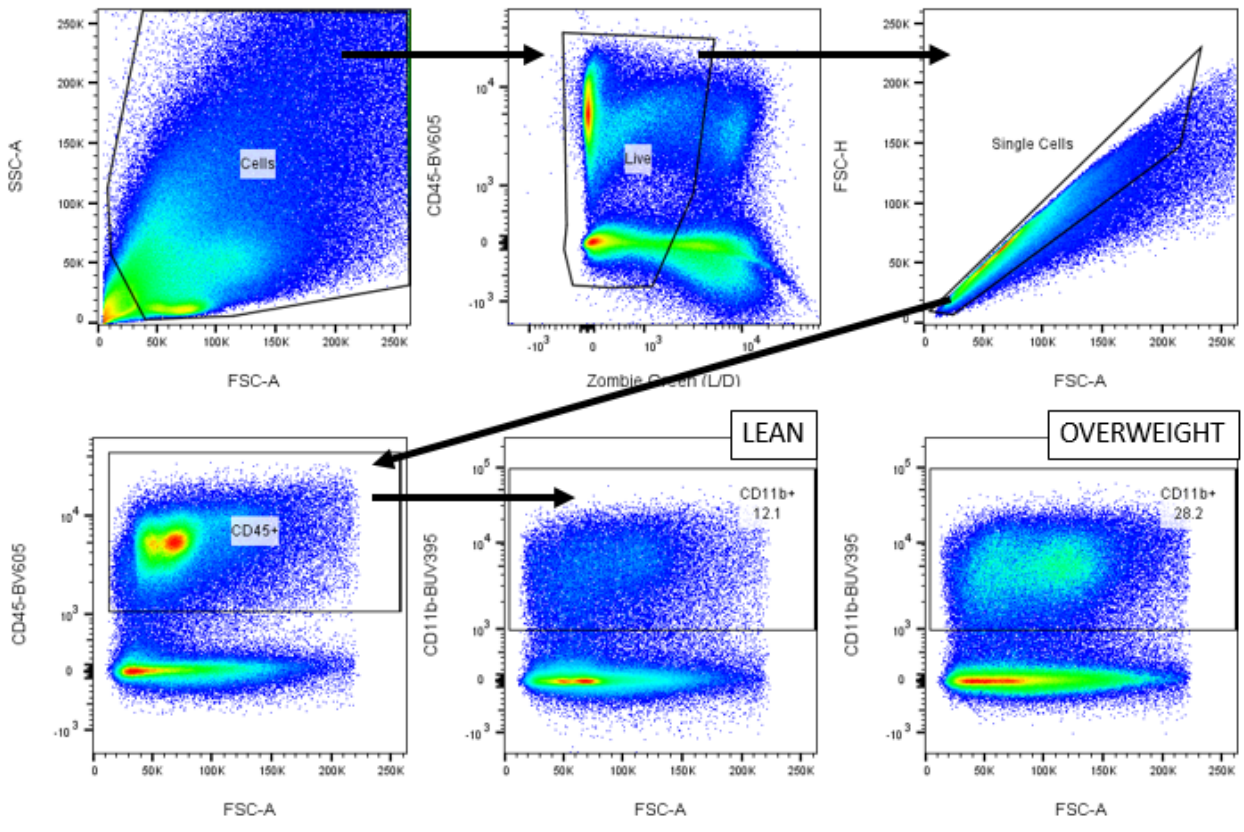

Supplemental Figure 43. Complete gating scheme for analysis of total leukocyte and CD11b+ myeloid cell content of Lean and Overweight mammary fat pads.

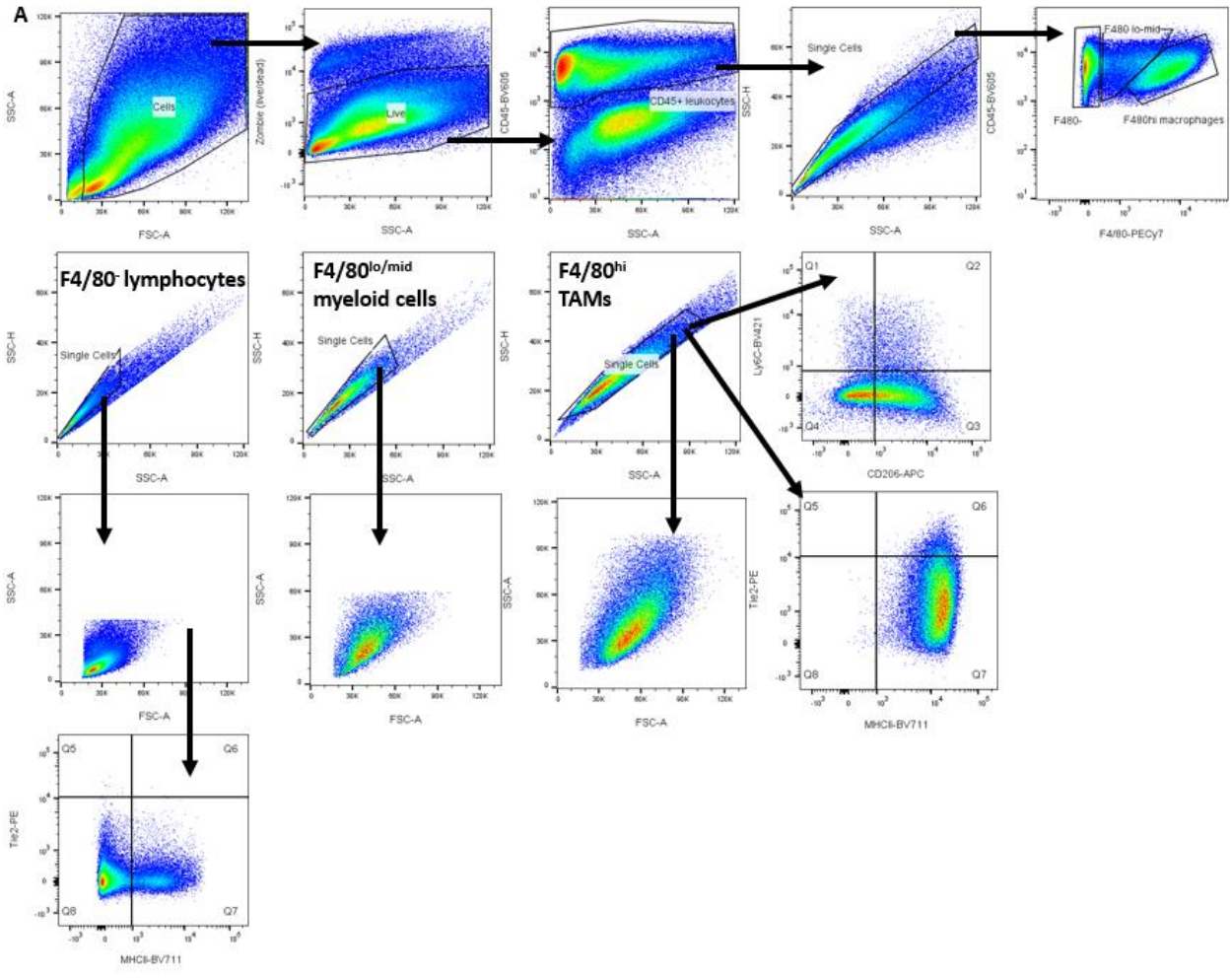

Supplemental Figure 44. Complete gating scheme for analysis of leukocyte infiltration into claudin-low tumors of Lean, Overweight, and WeLo mice

REFERENCES

1. Hanahan, D. and R.A. Weinberg, *Hallmarks of cancer: the next generation.* Cell, 2011. **144**(5): p. 646-74.

2. Valastyan, S. and R.A. Weinberg, *Tumor metastasis: molecular insights and evolving paradigms.* Cell, 2011. **147**(2): p. 275-92.

3. Albini, A. and M.B. Sporn, *The tumour microenvironment as a target for chemoprevention.* Nat Rev Cancer, 2007. **7**(2): p. 139-47.

4. Bissell, M.J. and D. Radisky, *Putting tumours in context.* Nat Rev Cancer, 2001. **1**(1): p. 46-54.

5. Tabassum, D.P. and K. Polyak, *Tumorigenesis: it takes a village.* Nat Rev Cancer, 2015. **15**(8): p. 473-83.

6. Trujillo, M.E. and P.E. Scherer, *Adipose tissue-derived factors: impact on health and disease.* Endocr Rev, 2006. **27**(7): p. 762-78.

7. Trottier, M.D., et al., *Enhancement of hematopoiesis and lymphopoiesis in diet-induced obese mice.* Proc Natl Acad Sci U S A, 2012. **109**(20): p. 7622-9.

8. Lee, M.J., Y. Wu, and S.K. Fried, *Adipose tissue heterogeneity: Implication of depot differences in adipose tissue for obesity complications.* Mol Aspects Med, 2013. **34**(1): p. 1-11.

9. Giralt, M. and F. Villarroya, *White, brown, beige/brite: different adipose cells for different functions?* Endocrinology, 2013. **154**(9): p. 2992-3000.

10. Harms, M. and P. Seale, *Brown and beige fat: development, function and therapeutic potential.* Nat Med, 2013. **19**(10): p. 1252-63.

11. de Jong, J.M., et al., *A stringent validation of mouse adipose tissue identity markers.* Am J Physiol Endocrinol Metab, 2015. **308**(12): p. E1085-105.

12. Bourin, P., et al., *Stromal cells from the adipose tissue-derived stromal vascular fraction and culture expanded adipose tissue-derived stromal/stem cells: a joint statement of the International Federation for Adipose Therapeutics (IFATS) and Science and the International Society for Cellular Therapy (ISCT).* Cytotherapy, 2013. **15**(6): p. 641-8.

13. Pasco, J.A., et al., *Body mass index and measures of body fat for defining obesity and underweight: a cross-sectional, population-based study.* BMC Obes, 2014. **1**: p. 9.

14. Shah, N.R. and E.R. Braverman, *Measuring adiposity in patients: The utility of body mass index (BMI), percent body fat, and leptin.* PLoS One, 2012. **7**(4).

15. Bergman, R.N., et al., *A better index of body adiposity.* Obesity (Silver Spring), 2011. **19**(5): p. 1083-9.

16. Caballero, B., *The global epidemic of obesity: an overview.* Epidemiol Rev, 2007. **29**: p. 1-5.

17. NCD Risk Factor Collaboration (NCD-RisC), a., *Trends in adult body-mass index in 200 countries from 1975 to 2014: a pooled analysis of 1698 population-based measurement studies with 19.2 million participants.* Lancet, 2016. **387**(10026): p. 1377-96.

18. Flegal, K.M., et al., *Trends in obesity among adults in the United States, 2005 to 2014.* JAMA, 2016. **315**(21): p. 2284-2291.

19. Ogden, C.L., et al., *Trends in obesity prevalence among children and adolescents in the United States, 1988-1994 through 2013-2014.* JAMA, 2016. **315**(21): p. 2292-9.

20. Siegel, R.L., K.D. Miller, and A. Jemal, *Cancer statistics, 2015.* CA Cancer J Clin, 2015. **65**(1): p. 5-29.

21. Ramos Chaves, M., et al., *The diversity of nutritional status in cancer: new insights.* Oncologist, 2010. **15**(5): p. 523-30.

22. Gioulbasanis, I., et al., *Nutritional assessment in overweight and obese patients with metastatic cancer: does it make sense?* Ann Oncol, 2015. **26**(1): p. 217-21.

23. Calle, E.E. and M.J. Thun, *Obesity and cancer.* Oncogene, 2004. **23**(38): p. 6365-78.

24. Calle, E.E., et al., *Overweight, obesity, and mortality from cancer in a prospectively studied cohort of U.S. adults.* N Engl J Med, 2003. **348**(17): p. 1625-38.

25. Vainio, H., R. Kaaks, and F. Bianchini, *Weight control and physical activity in cancer prevention: international evaluation of the evidence.* Eur J Cancer Prev, 2002. **11 Suppl 2**: p. S94-100.

26. Basen-Engquist, K. and M. Chang, *Obesity and cancer risk: Recent review and evidence.* Curr Oncol Rep, 2011. **13**(1): p. 71-6.

27. Kyrgiou, M., et al., *Adiposity and cancer at major anatomical sites: umbrella review of the literature.* BMJ, 2017. **356**: p. j477.

28. Lauby-Secretan, B., et al., *Body Fatness and Cancer--Viewpoint of the IARC Working Group.* N Engl J Med, 2016. **375**(8): p. 794-8.

29. Ligibel, J.A., et al., *American Society of Clinical Oncology position statement on obesity and cancer.* J Clin Oncol, 2014. **32**(31): p. 3568-74.

30. Strulov Shachar, S. and G.R. Williams, *The obesity paradox in cancer-moving beyond BMI.* Cancer Epidemiol Biomarkers Prev, 2017. **26**(1): p. 13-16.

31. Lennon, H., et al., *The obesity paradox in cancer: a review.* Curr Oncol Rep, 2016. **18**(9).

32. Gonzalez, M.C., et al., *Obesity paradox in cancer: new insights provided by body composition.* Am J Clin Nutr, 2014. **99**(5): p. 999-1005.

33. Martin, L., et al., *Cancer cachexia in the age of obesity: skeletal muscle depletion is a powerful prognostic factor, independent of body mass index.* J Clin Oncol, 2013. **31**(12): p. 1539-47.

34. Deng, T., et al., *Obesity, inflammation, and cancer.* Annu Rev Pathol, 2016. **11**: p. 421-49.

35. Park, J., et al., *Obesity and cancer--mechanisms underlying tumour progression and recurrence.* Nat Rev Endocrinol, 2014. **10**(8): p. 455-65.

36. Yamaguchi, J., et al., *Prognostic impact of marginal adipose tissue invasion in ductal carcinoma of the breast.* Am J Clin Pathol, 2008. **130**(3): p. 382-8.

37. Anderson, G.L. and M.L. Neuhouser, *Obesity and the risk for premenopausal and postmenopausal breast cancer.* Cancer Prev Res (Phila), 2012. **5**(4): p. 515-21.

38. Amadou, A., et al., *Overweight, obesity and risk of premenopausal breast cancer according to ethnicity: a systematic review and dose-response meta-analysis.* Obes Rev, 2013. **14**(8): p. 665-78.

39. Chen, L., et al., *Body mass index and risk of luminal, HER2-overexpressing, and triple negative breast cancer.* Breast Cancer Res Treat, 2016. **157**(3): p. 545-54.

40. Pierobon, M. and C.L. Frankenfeld, *Obesity as a risk factor for triple-negative breast cancers: a systematic review and meta-analysis.* Breast Cancer Res Treat, 2013. **137**(1): p. 307-14.

41. Turkoz, F.P., et al., *The prognostic impact of obesity on molecular subtypes of breast cancer in premenopausal women.* J BUON, 2013. **18**(2): p. 335-41.

42. Sundaram, S., et al., *Obesity-mediated regulation of HGF/c-Met is associated with reduced basal-like breast cancer latency in parous mice.* PLoS One, 2014. **9**(10): p. e111394.

43. Sundaram, S., et al., *Role of HGF in obesity-associated tumorigenesis: C3(1)-TAg mice as a model for human basal-like breast cancer.* Breast Cancer Res Treat, 2013. **142**(3): p. 489-503.

44. Cowen, S., et al., *High-fat, high-calorie diet enhances mammary carcinogenesis and local inflammation in MMTV-PyMT mouse model of breast cancer.* Cancers (Basel), 2015. **7**(3): p. 1125-42.

45. Arendt, L.M., et al., *Obesity promotes breast cancer by CCL2-mediated macrophage recruitment and angiogenesis.* Cancer Res, 2013. **73**(19): p. 6080-93.

46. Gillespie, E.F., et al., *Obesity and angiolymphatic invasion in primary breast cancer.* Ann Surg Oncol, 2010. **17**(3): p. 752-9.

47. Neuhouser, M.L., et al., *Overweight, obesity, and postmenopausal invasive breast cancer risk: A secondary analysis of the Women's Health Initiative Randomized Clinical Trials.* JAMA Oncol, 2015. **1**(5): p. 611-21.

48. Ewertz, M., et al., *Effect of obesity on prognosis after early-stage breast cancer.* J Clin Oncol, 2011. **29**(1): p. 25-31.

49. Osman, M.A. and B.T. Hennessy, *Obesity correlation with metastases development and response to first-line metastatic chemotherapy in breast cancer.* Clin Med Insights Oncol, 2015. **9**: p. 105-12.

50. Mazzarella, L., et al., *Obesity increases the incidence of distant metastases in oestrogen receptor-negative human epidermal growth factor receptor 2-positive breast cancer patients.* Eur J Cancer, 2013. **49**(17): p. 3588-97.

51. Sestak, I., et al., *Effect of body mass index on recurrences in tamoxifen and anastrozole treated women: an exploratory analysis from the ATAC trial.* J Clin Oncol, 2010. **28**(21): p. 3411-5.

52. Biglia, N., et al., *Body mass index (BMI) and breast cancer: impact on tumor histopathologic features, cancer subtypes and recurrence rate in pre and postmenopausal women.* Gynecol Endocrinol, 2013. **29**(3): p. 263-7.

53. Dawood, S., et al., *Prognostic value of body mass index in locally advanced breast cancer.* Clin Cancer Res, 2008. **14**(6): p. 1718-25.

54. Azrad, M. and W. Demark-Wahnefried, *The association between adiposity and breast cancer recurrence and survival: A review of the recent literature.* Curr Nutr Rep, 2014. **3**(1): p. 9-15.

55. Chan, D.S., et al., *Body mass index and survival in women with breast cancer-systematic literature review and meta-analysis of 82 follow-up studies.* Ann Oncol, 2014. **25**(10): p. 1901-14.

56. Widschwendter, P., et al., *The influence of obesity on survival in early, high-risk breast cancer: results from the randomized SUCCESS A trial.* Breast Cancer Res, 2015. **17**: p. 129.

57. von Drygalski, A., et al., *Obesity is an independent predictor of poor survival in metastatic breast cancer: retrospective analysis of a patient cohort whose treatment included high-dose chemotherapy and autologous stem cell support.* Int J Breast Cancer, 2011. **2011**: p. 523276.

58. Loi, S., et al., *Obesity and outcomes in premenopausal and postmenopausal breast cancer.* Cancer Epidemiol Biomarkers Prev, 2005. **14**(7): p. 1686-91.

59. Abrahamson, P.E., et al., *General and abdominal obesity and survival among young women with breast cancer.* Cancer Epidemiol Biomarkers Prev, 2006. **15**(10): p. 1871-7.

60. Barrington, W.E., et al., *Difference in association of obesity with prostate cancer risk between US African American and non-Hispanic white men in the Selenium and Vitamin E Cancer Prevention Trial (SELECT).* JAMA Oncol, 2015. **1**(3): p. 342-9.

61. Augustin, H., *Obesity and prostate cancer: an ambiguous relationship.* Eur J Cancer, 2007. **43**(7): p. 1114-6.

62. O'Malley, R.L. and S.S. Taneja, *Obesity and prostate cancer.* Can J Urol, 2006. **13 Suppl 2**: p. 11-7.

63. Boehm, K., et al., *Waist circumference, waist-hip ratio, body mass index, and prostate cancer risk: results from the North-American case-control study Prostate Cancer & Environment Study.* Urol Oncol, 2015. **33**(11): p. 494.e1-7.

64. Freedland, S.J. and W.J. Aronson, *Examining the relationship between obesity and prostate cancer.* Rev Urol, 2004. **6**(2): p. 73-81.

65. Zhang, X., et al., *Impact of obesity upon prostate cancer-associated mortality: A meta-analysis of 17 cohort studies.* Oncol Lett, 2015. **9**(3): p. 1307-12.

66. Kristal, A.R. and Z. Gong, *Obesity and prostate cancer mortality.* Future Oncol, 2007. **3**(5): p. 557-67.

67. Inman, J.L., et al., *Mammary gland development: cell fate specification, stem cells and the microenvironment.* Development, 2015. **142**(6): p. 1028-42.

68. Hennighausen, L. and G.W. Robinson, *Signaling pathways in mammary gland development.* Dev Cell, 2001. **1**(4): p. 467-75.

69. Moumen, M., et al., *The mammary myoepithelial cell.* Int J Dev Biol, 2011. **55**(7-9): p. 763-71.

70. Smalley, M. and A. Ashworth, *Stem cells and breast cancer: A field in transit.* Nat Rev Cancer, 2003. **3**(11): p. 832-44.

71. Dontu, G. and T.A. Ince, *Of mice and women: A comparative tissue biology perspective of breast stem cells and differentiation.* J Mammary Gland Biol Neoplasia, 2015. **20**(1-2): p. 51-62.

72. Atherton, A.J., et al., *Differential expression of type XIV collagen/undulin by human mammary gland intralobular and interlobular fibroblasts.* Cell Tissue Res, 1998. **291**(3): p. 507-11.

73. Atherton, A.J., et al., *Ectoenzyme regulation by phenotypically distinct fibroblast sub-populations isolated from the human mammary gland.* J Cell Sci, 1994. **107 (Pt 10)**: p. 2931-9.

74. Vandeweyer, E. and D. Hertens, *Quantification of glands and fat in breast tissue: an experimental determination.* Ann Anat, 2002. **184**(2): p. 181-4.

75. *The Human Protein Atlas, www.proteinatlas.org. Human breast cancer - Female, 50 years, lobular carcinoma, grade 1, Elston-Ellis score 5.* Available from: v16.proteinatlas.org/learn/dictionary/cancer/breast+cancer+4.

76. Uhlen, M., et al., *Proteomics. Tissue-based map of the human proteome.* Science, 2015. **347**(6220): p. 1260419.

77. Ittmann, M., et al., *Animal models of human prostate cancer: The Consensus Report of the New York Meeting of the Mouse Models of Human Cancers Consortium Prostate Pathology Committee.* Cancer Res, 2013. **73**(9): p. 2718-36.

78. Grabowska, M.M., et al., *Mouse models of prostate cancer: Picking the best model for the question.* Cancer Metastasis Rev, 2014. **33**(0): p. 377-97.

79. Oliveira, D.S.M., et al., *The mouse prostate: a basic anatomical and histological guideline.* Bosn J Basic Med Sci, 2016. **16**(1): p. 8-13.

80. Walz, J., et al., *A critical analysis of the current knowledge of surgical anatomy related to optimization of cancer control and preservation of continence and erection in candidates for radical prostatectomy.* Eur Urol, 2010. **57**(2): p. 179-92.

81. Bostwick, D.G. and L. Cheng, *Urologic Surgical Pathology*. 2008: Elsevier Health Sciences.

82. Sung, M.T., J.N. Eble, and L. Cheng, *Invasion of fat justifies assignment of stage pT3a in prostatic adenocarcinoma.* Pathology, 2006. **38**(4): p. 309-11.

83. Tang, K.D., et al., *Adipocytes promote prostate cancer stem cell self-renewal through amplification of the cholecystokinin autocrine loop.* Oncotarget, 2016. **7**(4): p. 4939-48.

84. Ribeiro, R., et al., *Human periprostatic adipose tissue promotes prostate cancer aggressiveness in vitro.* J Exp Clin Cancer Res, 2012. **31**(1): p. 32.

85. Toren, P. and V. Venkateswaran, *Periprostatic adipose tissue and prostate cancer progression: new insights into the tumor microenvironment.* Clin Genitourin Cancer, 2014. **12**(1): p. 21-6.

86. Kapoor, J., et al., *Extraprostatic extension into periprostatic fat is a more important determinant of prostate cancer recurrence than an invasive phenotype.* J Urol, 2013. **190**(6): p. 2061-6.

87. Barlow, J., et al., *Palmitate-induced impairment of glucose-stimulated insulin secretion precedes mitochondrial dysfunction in mouse pancreatic islets.* Biochem J, 2015.

88. Sun, K., et al., *Fibrosis and Adipose Tissue Dysfunction.* Cell Metab, 2013. **18**(4): p. 470-7.

89. Mariman, E.C. and P. Wang, *Adipocyte extracellular matrix composition, dynamics and role in obesity.* Cell Mol Life Sci, 2010. **67**(8): p. 1277-92.

90. Trayhurn, P., *Hypoxia and adipose tissue function and dysfunction in obesity.* Physiol Rev, 2013. **93**(1): p. 1-21.

91. Spencer, M., et al., *Adipose tissue macrophages in insulin-resistant subjects are associated with collagen VI and fibrosis and demonstrate alternative activation.* Am J Physiol Endocrinol Metab, 2010. **299**(6): p. E1016-27.

92. Divoux, A., et al., *Fibrosis in human adipose tissue: Composition, distribution, and link with lipid metabolism and fat mass loss.* Diabetes, 2010. **59**(11): p. 2817-2825.

93. Khan, T., et al., *Metabolic dysregulation and adipose tissue fibrosis: role of collagen VI.* Mol Cell Biol, 2009. **29**(6): p. 1575-91.

94. Halberg, N., et al., *Hypoxia-inducible factor 1alpha induces fibrosis and insulin resistance in white adipose tissue.* Mol Cell Biol, 2009. **29**(16): p. 4467-83.

95. Nishimura, S., et al., *In vivo imaging in mice reveals local cell dynamics and inflammation in obese adipose tissue.* J Clin Invest, 2008. **118**(2): p. 710-721.

96. Murano, I., et al., *Dead adipocytes, detected as crown-like structures, are prevalent in visceral fat depots of genetically obese mice.* J Lipid Res, 2008. **49**(7): p. 1562-8.

97. Wynn, T.A. and L. Barron, *Macrophages: master regulators of inflammation and fibrosis.* Semin Liver Dis, 2010. **30**(3): p. 245-57.

98. Batista, M.L., Jr., et al., *Cachexia-associated adipose tissue morphological rearrangement in gastrointestinal cancer patients.* J Cachexia Sarcopenia Muscle, 2016. **7**(1): p. 37-47.

99. Alves, M.J., et al., *Adipose tissue fibrosis in human cancer cachexia: the role of TGFβ pathway.* BMC Cancer, 2017. **17**(1): p. 190.

100. Bissell, M.J., P.A. Kenny, and D.C. Radisky, *Microenvironmental regulators of tissue structure and function also regulate tumor induction and progression: the role of extracellular matrix and its degrading enzymes.* Cold Spring Harb Symp Quant Biol, 2005. **70**: p. 343-56.

101. Ghajar, C.M. and M.J. Bissell, *Extracellular matrix control of mammary gland morphogenesis and tumorigenesis: insights from imaging.* Histochem Cell Biol, 2008. **130**(6): p. 1105-18.

102. Lu, P., V.M. Weaver, and Z. Werb, *The extracellular matrix: a dynamic niche in cancer progression.* J Cell Biol, 2012. **196**(4): p. 395-406.

103. Schedin, P. and P.J. Keely, *Mammary gland ECM remodeling, stiffness, and mechanosignaling in normal development and tumor progression.* Cold Spring Harb Perspect Biol, 2011. **3**(1).

104. Wozniak, M.A., et al., *ROCK-generated contractility regulates breast epithelial cell differentiation in response to the physical properties of a three-dimensional collagen matrix.* J Cell Biol, 2003. **163**(3): p. 583-95.

105. Provenzano, P.P., et al., *Matrix density-induced mechanoregulation of breast cell phenotype, signaling and gene expression through a FAK-ERK linkage.* Oncogene, 2009. **28**(49): p. 4326-43.

106. Nelson, C.M. and M.J. Bissell, *Of extracellular matrix, scaffolds, and signaling: Tissue architecture regulates development, homeostasis, and cancer.* Annu Rev Cell Dev Biol, 2006. **22**: p. 287-309.

107. Dvorak, H.F., *Tumors: wounds that do not heal. Similarities between tumor stroma generation and wound healing.* N Engl J Med, 1986. **315**(26): p. 1650-9.

108. Moorman, A.M., et al., *The prognostic value of tumour-stroma ratio in triple-negative breast cancer.* Eur J Surg Oncol, 2012. **38**(4): p. 307-13.

109. Ayala, G., et al., *Reactive stroma as a predictor of biochemical-free recurrence in prostate cancer.* Clinical Cancer Research, 2003. **9**(13): p. 4792-4801.

110. Levental, K.R., et al., *Matrix crosslinking forces tumor progression by enhancing integrin signaling.* Cell, 2009. **139**(5): p. 891-906.

111. Razzaghi, H., et al., *Mammographic density and breast cancer risk in White and African American Women.* Breast Cancer Res Treat, 2012. **135**(2): p. 571-80.

112. Yaffe, M.J., *Mammographic density. Measurement of mammographic density.* Breast Cancer Res, 2008. **10**(3): p. 209.

113. Ursin, G., et al., *Greatly increased occurrence of breast cancers in areas of mammographically dense tissue.* Breast Cancer Res, 2005. **7**(5): p. R605-8.

114. Boyd, N.F., et al., *Breast tissue composition and susceptibility to breast cancer.* J Natl Cancer Inst, 2010. **102**(16): p. 1224-37.

115. Yaghjyan, L., et al., *Mammographic breast density and subsequent risk of breast cancer in postmenopausal women according to tumor characteristics.* J Natl Cancer Inst, 2011. **103**(15): p. 1179-89.

116. Huo, C.W., et al., *High mammographic density is associated with an increase in stromal collagen and immune cells within the mammary epithelium.* Breast Cancer Res, 2015. **17**: p. 79.

117. Frantz, C., K.M. Stewart, and V.M. Weaver, *The extracellular matrix at a glance.* J Cell Sci, 2010. **123**(Pt 24): p. 4195-200.

118. DeFilippis, R.A., et al., *CD36 repression activates a multicellular stromal program shared by high mammographic density and tumor tissues.* Cancer Discov, 2012. **2**(9): p. 826-39.

119. Shao, Z.M., M. Nguyen, and S.H. Barsky, *Human breast carcinoma desmoplasia is PDGF initiated.* Oncogene, 2000. **19**(38): p. 4337-45.

120. Shimoda, M., K.T. Mellody, and A. Orimo, *Carcinoma-associated fibroblasts are a rate-limiting determinant for tumour progression.* Semin Cell Dev Biol, 2010. **21**(1): p. 19-25.

121. De Wever, O., et al., *Stromal myofibroblasts are drivers of invasive cancer growth.* Int J Cancer, 2008. **123**(10): p. 2229-38.

122. Karagiannis, G.S., et al., *Cancer-associated fibroblasts drive the progression of metastasis through both paracrine and mechanical pressure on cancer tissue.* Mol Cancer Res, 2012. **10**(11): p. 1403-18.

123. Seo, B.R., et al., *Obesity-dependent changes in interstitial ECM mechanics promote breast tumorigenesis.* Sci Transl Med, 2015. **7**(301): p. 301ra130.

124. Hinz, B., et al., *The myofibroblast: One function, multiple origins.* Am J Pathol, 2007. **170**(6): p. 1807-16.

125. Khamis, Z.I., Z.J. Sahab, and Q.X. Sang, *Active roles of tumor stroma in breast cancer metastasis.* Int J Breast Cancer, 2012. **2012**: p. 574025.

126. Direkze, N.C., et al., *Bone marrow contribution to tumor-associated myofibroblasts and fibroblasts.* Cancer Res, 2004. **64**(23): p. 8492-5.

127. Phan, S.H., *Biology of fibroblasts and myofibroblasts.* Proc Am Thorac Soc, 2008. **5**(3): p. 334-7.

128. Micallef, L., et al., *The myofibroblast, multiple origins for major roles in normal and pathological tissue repair.* Fibrogenesis Tissue Repair, 2012. **5**(Suppl 1): p. S5.

129. Bochet, L., et al., *Adipocyte-derived fibroblasts promote tumor progression and contribute to the desmoplastic reaction in breast cancer.* Cancer Res, 2013. **73**(18): p. 5657-68.

130. Pasarica, M., et al., *Adipose tissue collagen VI in obesity.* J Clin Endocrinol Metab, 2009. **94**(12): p. 5155-62.

131. Sun, K., et al., *Endotrophin triggers adipose tissue fibrosis and metabolic dysfunction.* Nat Commun, 2014. **5**: p. 3485.

132. Trujillo, K.A., et al., *Markers of fibrosis and epithelial to mesenchymal transition demonstrate field cancerization in histologically normal tissue adjacent to breast tumors.* Int J Cancer, 2011. **129**(6): p. 1310-21.

133. Chandler, E.M., et al., *Adipose progenitor cells increase fibronectin matrix strain and unfolding in breast tumors.* Phys Biol, 2011. **8**(1): p. 015008.

134. Vogel, W.F., *Collagen-receptor signaling in health and disease.* Eur J Dermatol, 2001. **11**(6): p. 506-14.

135. Park, J. and P.E. Scherer, *Adipocyte-derived endotrophin promotes malignant tumor progression.* J Clin Invest, 2012. **122**(11): p. 4243-56.

136. Iyengar, P., et al., *Adipocyte-derived collagen VI affects early mammary tumor progression in vivo, demonstrating a critical interaction in the tumor/stroma microenvironment.* J Clin Invest, 2005. **115**(5): p. 1163-76.

137. Iyengar, P., et al., *Adipocyte-secreted factors synergistically promote mammary tumorigenesis through induction of anti-apoptotic transcriptional programs and proto-oncogene stabilization.* Oncogene, 2003. **22**(41): p. 6408-23.

138. Park, J., T.S. Morley, and P.E. Scherer, *Inhibition of endotrophin, a cleavage product of collagen VI, confers cisplatin sensitivity to tumours.* EMBO Mol Med, 2013. **5**(6): p. 935-48.

139. Vona-Davis, L. and D.P. Rose, *Adipokines as endocrine, paracrine, and autocrine factors in breast cancer risk and progression.* Endocr Relat Cancer, 2007. **14**(2): p. 189-206.

140. Tuck, A.B., et al., *Coexpression of hepatocyte growth factor and receptor (Met) in human breast carcinoma.* Am J Pathol, 1996. **148**(1): p. 225-32.

141. Mizuno, S. and T. Nakamura, *HGF-MET Cascade, a Key Target for Inhibiting Cancer Metastasis: The Impact of NK4 Discovery on Cancer Biology and Therapeutics.* Int J Mol Sci, 2013. **14**(1): p. 888-919.

142. Casbas-Hernandez, P., et al., *Role of HGF in epithelial–stromal cell interactions during progression from benign breast disease to ductal carcinoma in situ.* Breast Cancer Res, 2013. **15**(5): p. R82.

143. Sheen-Chen, S.M., et al., *Serum levels of hepatocyte growth factor in patients with breast cancer.* Cancer Epidemiol Biomarkers Prev, 2005. **14**(3): p. 715-7.

144. Ho-Yen, C.M., J.L. Jones, and S. Kermorgant, *The clinical and functional significance of c-Met in breast cancer: a review.* Breast Cancer Res, 2015. **17**(1): p. 1-11.

145. Ho-Yen, C.M., et al., *C-Met in invasive breast cancer: is there a relationship with the basal-like subtype?* Cancer, 2014. **120**.

146. Hiratsuka, A., et al., *Strong association between serum hepatocyte growth factor and metabolic syndrome.* J Clin Endocrinol Metab, 2005. **90**(5): p. 2927-2931.

147. Bell, L.N., et al., *Adipose tissue production of hepatocyte growth factor contributes to elevated serum HGF in obesity.* Am J Physiol Endocrinol Metab, 2006. **291**(4): p. E843-8.

148. Swierczynski, J., et al., *Serum hepatocyte growth factor concentration in obese women decreases after vertical banded gastroplasty.* Obesity Surgery, 2005. **15**(6): p. 803-808.

149. Herschkowitz, J.I., et al., *Identification of conserved gene expression features between murine mammary carcinoma models and human breast tumors.* Genome Biol, 2007. **8**(5): p. R76.

150. Green, J.E., et al., *The C3 (1)/SV40 T-antigen transgenic mouse model of mammary cancer: ductal epithelial cell targeting with multistage progression to carcinoma.* Oncogene, 2000. **19**(8): p. 1020-1027.

151. Tuxhorn, J.A., et al., *Reactive stroma in human prostate cancer: induction of myofibroblast phenotype and extracellular matrix remodeling.* Clin Cancer Res, 2002. **8**(9): p. 2912-23.

152. Stewart, D.A., C.R. Cooper, and R.A. Sikes, *Changes in extracellular matrix (ECM) and ECM-associated proteins in the metastatic progression of prostate cancer.* Reprod Biol Endocrinol, 2004. **2**: p. 2.

153. van Roermund, J.G.H., et al., *Periprostatic fat measured on computed tomography as a marker for prostate cancer aggressiveness.* World J Urol, 2010. **28**(6): p. 699-704.

154. van Roermund, J.G., et al., *Periprostatic fat correlates with tumour aggressiveness in prostate cancer patients.* BJU Int, 2011. **107**(11): p. 1775-9.

155. Woo, S., et al., *Periprostatic fat thickness on MRI: correlation with Gleason score in prostate cancer.* AJR Am J Roentgenol, 2015. **204**(1): p. W43-7.

156. Wu, J., et al., *Beige adipocytes are a distinct type of thermogenic fat cell in mouse and human.* Cell, 2012. **150**(2): p. 366-76.

157. Tilg, H. and A.R. Moschen, *Adipocytokines: mediators linking adipose tissue, inflammation and immunity.* Nat Rev Immunol, 2006. **6**(10): p. 772-83.

158. Cao, Y., *Angiogenesis modulates adipogenesis and obesity.* J Clin Invest 2007. **117**(117 (9)): p. 2362-2368.

159. Garofalo, C. and E. Surmacz, *Leptin and cancer.* J Cell Physiol, 2006. **207**(1): p. 12-22.

160. Park, J. and P.E. Scherer, *Leptin and cancer: from cancer stem cells to metastasis.* Endocr Relat Cancer, 2011. **18**(4): p. C25-9.

161. Obeid, S. and L. Hebbard, *Role of adiponectin and its receptors in cancer.* Cancer Biol Med, 2012. **9**(4): p. 213-20.

162. Kelesidis, I., T. Kelesidis, and C.S. Mantzoros, *Adiponectin and cancer: a systematic review.* Br J Cancer, 2006. **94**(9): p. 1221-5.

163. Nieman, K.M., et al., *Adipose tissue and adipocytes supports tumorigenesis and metastasis.* Biochim Biophys Acta, 2013. **1831**(10): p. 1533-41.

164. Wagner, M. and A.C. Dudley, *A three-party alliance in solid tumors: Adipocytes, macrophages and vascular endothelial cells.* Adipocyte, 2013. **2**(2): p. 67-73.

165. Wang, Y.Y., et al., *Adipose tissue and breast epithelial cells: a dangerous dynamic duo in breast cancer.* Cancer Lett, 2012. **324**(2): p. 142-51.

166. Allen, E., et al., *Metabolic symbiosis enables adaptive resistance to anti-angiogenic therapy that is dependent on mTOR signaling.* Cell Rep, 2016. **15**(6): p. 1144-60.

167. Nakajima, E.C. and B. Van Houten, *Metabolic symbiosis in cancer: refocusing the Warburg lens.* Mol Carcinog, 2013. **52**(5): p. 329-37.

168. Martinez-Outschoorn, U.E., F. Sotgia, and M.P. Lisanti, *Power surge: supporting cells "fuel" cancer cell mitochondria.* Cell Metab, 2012. **15**(1): p. 4-5.

169. Meyer, K.A., et al., *Adipocytes promote pancreatic cancer cell proliferation via glutamine transfer.* Biochem Biophys Rep, 2016. **7**: p. 144-149.

170. Nieman, K.M., et al., *Adipocytes promote ovarian cancer metastasis and provide energy for rapid tumor growth.* Nat Med, 2011. **17**(11): p. 1498-503.

171. Gazi, E., et al., *Direct evidence of lipid translocation between adipocytes and prostate cancer cells with imaging FTIR microspectroscopy.* J Lipid Res, 2007. **48**(8): p. 1846-56.

172. Wang, Y.Y., et al., *Mammary adipocytes stimulate breast cancer invasion through metabolic remodeling of tumor cells.* JCI Insight, 2017. **2**(4): p. e87489.

173. Lazar, I., et al., *Adipocyte exosomes promote melanoma aggressiveness through fatty acid oxidation: A novel mechanism linking obesity and cancer.* Cancer Res, 2016.

174. Hovey, R.C. and L. Aimo, *Diverse and Active Roles for Adipocytes During Mammary Gland Growth and Function.* J Mammary Gland Biol Neoplasia, 2010. **15**(3): p. 279-90.

175. Couldrey, C., et al., *Adipose tissue: a vital in vivo role in mammary gland development but not differentiation.* Dev Dyn, 2002. **223**(4): p. 459-68.

176. Landskroner-Eiger, S., et al., *Morphogenesis of the developing mammary gland: stage-dependent impact of adipocytes.* Dev Biol, 2010. **344**(2): p. 968-78.

177. Carter, J.C. and F.C. Church, *Mature breast adipocytes promote breast cancer cell motility.* Exp Mol Pathol, 2012. **92**(3): p. 312-7.

178. Dirat, B., et al., *Cancer-associated adipocytes exhibit an activated phenotype and contribute to breast cancer invasion.* Cancer Res, 2011. **71**(7): p. 2455-65.

179. Tisdale, M.J., *Molecular pathways leading to cancer cachexia.* Physiology (Bethesda), 2005. **20**: p. 340-8.

180. Picon-Ruiz, M., et al., *Interactions between adipocytes and breast cancer cells stimulate cytokine production and drive Src/Sox2/miR-302b-mediated malignant progression.* Cancer Res, 2016. **76**(2): p. 491-504.

181. Massa, M., et al., *Interaction between breast cancer cells and adipose tissue cells derived from fat grafting.* Aesthet Surg J, 2016. **36**(3): p. 358-63.

182. Mestak, O., et al., *Evaluation of oncological safety of fat grafting after breast-conserving therapy: A prospective study.* Ann Surg Oncol, 2016. **23**(3): p. 776-81.

183. Balkwill, F., *Cancer and the chemokine network.* Nat Rev Cancer, 2004. **4**(7): p. 540-50.

184. Huber, J., et al., *CC chemokine and CC chemokine receptor profiles in visceral and subcutaneous adipose tissue are altered in human obesity.* J Clin Endocrinol Metab, 2008. **93**(8): p. 3215-21.

185. Laurent, V., et al., *Periprostatic adipocytes act as a driving force for prostate cancer progression in obesity.* Nat Commun, 2016. **7**.

186. Ito, Y., et al., *Adipocyte-derived monocyte chemotactic protein-1 (MCP-1) promotes prostate cancer progression through the induction of MMP-2 activity.* Prostate, 2015. **75**(10): p. 1009-19.

187. Hardaway, A.L., et al., *Bone marrow fat: linking adipocyte-induced inflammation with skeletal metastases.* Cancer Metastasis Rev, 2014. **33**(0): p. 527-43.

188. Li, X., et al., *A destructive cascade mediated by CCL2 facilitates prostate cancer growth in bone.* Cancer Res, 2009. **69**(4): p. 1685-92.

189. Keto, C.J., et al., *Obesity is associated with castration-resistant disease and metastasis in men treated with androgen deprivation therapy after radical prostatectomy: results from the SEARCH database.* BJU Int, 2012. **110**(4): p. 492-8.

190. Herroon, M.K., et al., *Bone marrow adipocytes promote tumor growth in bone via FABP4-dependent mechanisms.* Oncotarget, 2013. **4**(11): p. 2108-23.

191. Ribeiro, R.J., et al., *Tumor cell-educated periprostatic adipose tissue acquires an aggressive cancer-promoting secretory profile.* Cell Physiol Biochem, 2012. **29**(1-2): p. 233-40.

192. Finley, D.S., et al., *Periprostatic adipose tissue as a modulator of prostate cancer aggressiveness.* J Urol, 2009. **182**(4): p. 1621-7.

193. Miyake, H., I. Hara, and H. Eto, *Serum level of cathepsin B and its density in men with prostate cancer as novel markers of disease progression.* Anticancer Res, 2004. **24**(4): p. 2573-7.

194. Beckham, T.H., et al., *Acid ceramidase-mediated production of sphingosine 1-phosphate promotes prostate cancer invasion through upregulation of cathepsin B.* Int J Cancer, 2012. **131**(9): p. 2034-43.

195. Tisdale, M.J., *Cachexia in cancer patients.* Nat Rev Cancer, 2002. **2**(11): p. 862-71.

196. Kir, S., et al., *Tumour-derived PTH-related protein triggers adipose tissue browning and cancer cachexia.* Nature, 2014. **513**(7516): p. 100-4.

197. Petruzzelli, M., et al., *A switch from white to brown fat increases energy expenditure in cancer-associated cachexia.* Cell Metab, 2014. **20**(3): p. 433-47.

198. Agustsson, T., et al., *Mechanism of increased lipolysis in cancer cachexia.* Cancer Res, 2007. **67**(11): p. 5531-7.

199. Das, S.K., et al., *Adipose triglyceride lipase contributes to cancer-associated cachexia.* Science, 2011. **333**(6039): p. 233-8.

200. Rohm, M., et al., *An AMP-activated protein kinase-stabilizing peptide ameliorates adipose tissue wasting in cancer cachexia in mice.* Nat Med, 2016. **22**(10): p. 1120-1130.

201. Tisdale, M.J., *Cancer cachexia.* Curr Opin Gastroenterol, 2010. **26**.

202. Zuk, P.A., et al., *Human adipose tissue is a source of multipotent stem cells.* Mol Biol Cell, 2002. **13**(12): p. 4279-95.

203. Kolle, S.F., et al., *Enrichment of autologous fat grafts with ex-vivo expanded adipose tissue-derived stem cells for graft survival: a randomised placebo-controlled trial.* Lancet, 2013. **382**(9898): p. 1113-20.

204. Tsekouras, A., et al., *Adipose-derived stem cells for breast reconstruction after breast surgery–preliminary results.* Case Reports in Plastic Surgery and Hand Surgery, 2017. **4**(1): p. 35-41.

205. Bodle, J.C., et al., *Age-related effects on the potency of human adipose-derived stem cells: Creation and evaluation of superlots and implications for musculoskeletal tissue engineering applications.* Tissue Eng Part C Methods, 2014. **20**(12): p. 972-83.

206. Kidd, S., et al., *Origins of the tumor microenvironment: quantitative assessment of adipose-derived and bone marrow-derived stroma.* PLoS One, 2012. **7**(2): p. e30563.

207. Gehmert, S., et al., *Breast cancer cells attract the migration of adipose tissue-derived stem cells via the PDGF-BB/PDGFR-beta signaling pathway.* Biochem Biophys Res Commun, 2010. **398**(3): p. 601-5.

208. Ribeiro, R., et al., *Human periprostatic white adipose tissue is rich in stromal progenitor cells and a potential source of prostate tumor stroma.* Exp Biol Med (Maywood), 2012. **237**(10): p. 1155-62.

209. Strong, A.L., et al., *Obesity associated alterations in the biology of adipose stem cells mediate enhanced tumorigenesis by estrogen dependent pathways.* Breast Cancer Res, 2013. **15**(5): p. R102.

210. Zhang, T., et al., *CXCL1 mediates obesity-associated adipose stromal cell trafficking and function in the tumour microenvironment.* Nat Commun, 2016. **7**.

211. Ghosh, S., et al., *Association of obesity and circulating adipose stromal cells among breast cancer survivors.* Mol Biol Rep, 2014. **41**(5): p. 2907-16.

212. Strong, A.L., et al., *Obesity-associated dysregulation of calpastatin and MMP-15 in adipose-derived stromal cells results in their enhanced invasion.* Stem Cells, 2012. **30**(12): p. 2774-83.

213. Zhang, Y., et al., *Stromal progenitor cells from endogenous adipose tissue contribute to pericytes and adipocytes that populate the tumor microenvironment.* Cancer Res, 2012. **72**(20): p. 5198-208.

214. Tam, J., et al., *Blockade of VEGFR2 and not VEGFR1 can limit diet-induced fat tissue expansion: role of local versus bone marrow-derived endothelial cells.* PLoS One, 2009. **4**(3): p. e4974.

215. Rupnick, M.A., et al., *Adipose tissue mass can be regulated through the vasculature.* Proc Natl Acad Sci U S A, 2002. **99**(16): p. 10730-10735.

216. Brakenhielm, E., et al., *Angiogenesis inhibitor, TNP-470, prevents diet-induced and genetic obesity in mice.* Circ Res, 2004. **94**(12): p. 1579-88.

217. Werno, C., et al., *Knockout of HIF-1alpha in tumor-associated macrophages enhances M2 polarization and attenuates their pro-angiogenic responses.* Carcinogenesis, 2010. **31**(10): p. 1863-72.

218. Tahergorabi, Z. and M. Khazaei, *The relationship between inflammatory markers, angiogenesis, and obesity.* ARYA Atheroscler, 2013. **9**(4): p. 247.

219. Lijnen, H.R., *Angiogenesis and obesity.* Cardiovasc Res, 2008. **78**(2): p. 286-93.

220. Murdoch, C., et al., *The role of myeloid cells in the promotion of tumour angiogenesis.* Nat Rev Cancer, 2008. **8**(8): p. 618-31.

221. Hausman, G.J. and R.L. Richardson, *Adipose tissue angiogenesis.* J Anim Sci, 2004. **82**(3): p. 925-34.

222. Ferrara, N., H.P. Gerber, and J. LeCouter, *The biology of VEGF and its receptors.* Nat Med, 2003. **9**(6): p. 669-76.

223. Kobayashi, H., L.M. DeBusk, and P.C. Lin, *Angiopoietin/Tie2 signaling regulates tumor angiogenesis*, in *Antiangiogenic Agents in Cancer Therapy*, B.A. Teicher and L.M. Ellis, Editors. 2008, Humana Press: Totowa, NJ. p. 171-187.

224. Hakanpaa, L., et al., *Endothelial destabilization by angiopoietin-2 via integrin beta1 activation.* Nat Commun, 2015. **6**: p. 5962.

225. Miyazawa-Hoshimoto, S., et al., *Elevated serum vascular endothelial growth factor is associated with visceral fat accumulation in human obese subjects.* Diabetologia, 2003. **46**(11): p. 1483-1488.

226. Silha, J.V., et al., *Angiogenic factors are elevated in overweight and obese individuals.* Int J Obes (Lond), 2005. **29**(11): p. 1308-14.

227. Bergers, G. and L.E. Benjamin, *Tumorigenesis and the angiogenic switch.* Nat Rev Cancer, 2003. **3**(6): p. 401-10.

228. Hanahan, D. and J. Folkman, *Patterns and emerging mechanisms of the angiogenic switch during tumorigenesis.* Cell, 1996. **86**(3): p. 353-364.

229. Ribatti, D. and A. Vacca, *Overview of angiogenesis during tumor growth*, in *Angiogenesis*. 2008, Springer. p. 161-168.

230. Eberhard, A., et al., *Heterogeneity of angiogenesis and blood vessel maturation in human tumors: implications for antiangiogenic tumor therapies.* Cancer Res, 2000. **60**(5): p. 1388-93.

231. Maniotis, A.J., et al., *Vascular channel formation by human melanoma cells in vivo and in vitro: vasculogenic mimicry.* Am J Pathol, 1999. **155**(3): p. 739-52.

232. Dunleavey, J.M., et al., *Vascular channels formed by subpopulations of PECAM1+ melanoma cells.* Nat Commun, 2014. **5**: p. 5200.

233. Lim, S., et al., *Co-option of pre-existing vascular beds in adipose tissue controls tumor growth rates and angiogenesis.* Oncotarget, 2016.

234. Dudley, A.C., *Tumor endothelial cells.* Cold Spring Harb Perspect Med, 2012. **2**(3).

235. Azzi, S., J.K. Hebda, and J. Gavard, *Vascular permeability and drug delivery in cancers.* Front Oncol, 2013. **3**.

236. Dvorak, H.F., *Vascular permeability factor/vascular endothelial growth factor: a critical cytokine in tumor angiogenesis and a potential target for diagnosis and therapy.* J Clin Oncol, 2002. **20**(21): p. 4368-80.

237. Cao, R., Brakenhielm, E, Wahlestedt, C, Thyberg, J, Cao, Y., *Leptin induces vascular permeability and synergistically.* Proc Natl Acad Sci U S A, 2001. **98**(11): p. 6390-5.

238. Albrecht, I. and G. Christofori, *Molecular mechanisms of lymphangiogenesis in development and cancer.* Int J Dev Biol, 2011. **55**(4-5): p. 483-94.

239. Zumsteg, A., et al., *Myeloid cells contribute to tumor lymphangiogenesis.* PLoS One, 2009. **4**(9): p. e7067.

240. Schledzewski, K., et al., *Lymphatic endothelium-specific hyaluronan receptor LYVE-1 is expressed by stabilin-1+, F4/80+, CD11b+ macrophages in malignant tumours and wound healing tissue in vivo and in bone marrow cultures in vitro: implications for the assessment of lymphangiogenesis.* J Pathol, 2006. **209**(1): p. 67-77.

241. Religa, P., et al., *Presence of bone marrow-derived circulating progenitor endothelial cells in the newly formed lymphatic vessels.* Blood, 2005. **106**(13): p. 4184-90.

242. He, Y., et al., *Preexisting lymphatic endothelium but not endothelial progenitor cells are essential for tumor lymphangiogenesis and lymphatic metastasis.* Cancer Res, 2004. **64**(11): p. 3737-40.

243. Gao, P., et al., *Lymphatic vessel density as a prognostic indicator for patients with stage I cervical carcinoma.* Hum Pathol, 2006. **37**(6): p. 719-25.

244. Saad, R.S., et al., *Lymphatic microvessel density as prognostic marker in colorectal cancer.* Mod Pathol, 2006. **19**(10): p. 1317-23.

245. Mohammed, R.A., et al., *Lymphatic and blood vessels in basal and triple-negative breast cancers: characteristics and prognostic significance.* Mod Pathol, 2011. **24**(6): p. 774-85.

246. El-Gohary, Y.M., et al., *Prognostic significance of intratumoral and peritumoral lymphatic density and blood vessel density in invasive breast carcinomas.* Am J Clin Pathol, 2008. **129**(4): p. 578-86.

247. Datta, K., et al., *Mechanism of lymph node metastasis in prostate cancer.* Future Oncol, 2010. **6**(5): p. 823-36.

248. Padera, T.P., et al., *Lymphatic metastasis in the absence of functional intratumor lymphatics.* Science, 2002. **296**(5574): p. 1883-6.

249. Vleugel, M.M., et al., *Lack of lymphangiogenesis during breast carcinogenesis.* J Clin Pathol, 2004. **57**(7): p. 746-51.

250. Williams, C.S., et al., *Absence of lymphangiogenesis and intratumoural lymph vessels in human metastatic breast cancer.* J Pathol, 2003. **200**(2): p. 195-206.

251. Trojan, L., et al., *Lymph and blood vessel architecture in benign and malignant prostatic tissue: lack of lymphangiogenesis in prostate carcinoma assessed with novel lymphatic marker lymphatic vessel endothelial hyaluronan receptor (LYVE-1).* J Urol, 2004. **172**(1): p. 103-7.

252. Wong, S.Y., et al., *Tumor-secreted vascular endothelial growth factor-C is necessary for prostate cancer lymphangiogenesis, but lymphangiogenesis is unnecessary for lymph node metastasis.* Cancer Res, 2005. **65**(21): p. 9789-98.

253. Skobe, M., et al., *Induction of tumor lymphangiogenesis by VEGF-C promotes breast cancer metastasis.* Nat Med, 2001. **7**(2): p. 192-8.

254. Schneider, B.P. and K.D. Miller, *Angiogenesis of breast cancer.* J Clin Oncol, 2005. **23**(8): p. 1782-90.

255. Fox, S.B., D.G. Generali, and A.L. Harris, *Breast tumour angiogenesis.* Breast Cancer Res, 2007. **9**(6): p. 1-11.

256. Fox, S.B., et al., *Relationship of endothelial cell proliferation to tumor vascularity in human breast cancer.* Cancer Res, 1993. **53**(18): p. 4161-3.

257. Djonov, V., A.-C. Andres, and A. Ziemiecki, *Vascular remodelling during the normal and malignant life cycle of the mammary gland.* Microscopy Research and Technique, 2001. **52**(2): p. 182-189.

258. Leek, R.D., et al., *Association of macrophage infiltration with angiogenesis and prognosis in invasive breast carcinoma.* Cancer Res, 1996. **56**(20): p. 4625-9.

259. Wagner, M., et al., *Inflamed tumor-associated adipose tissue is a depot for macrophages that stimulate tumor growth and angiogenesis.* Angiogenesis, 2012. **15**(3): p. 481-95.

260. Gu, J.-W., et al., *Postmenopausal obesity promotes tumor angiogenesis and breast cancer progression in mice.* Cancer Biol Ther, 2011. **11**(10): p. 910-917.

261. Lee, T.J., et al., *Enhancement of long-term angiogenic efficacy of adipose stem cells by delivery of FGF2.* Microvasc Res, 2012. **84**(1): p. 1-8.

262. Cozzo, A.J., et al., *cMET inhibitor crizotinib impairs angiogenesis and reduces tumor burden in the C3(1)-Tag model of basal-like breast cancer.* Springerplus, 2016. **5**.

263. Qin, Y., et al., *Weight loss reduces basal-like breast cancer through kinome reprogramming.* Cancer Cell Int, 2016. **16**: p. 26.

264. Sundaram, S., et al., *Weight Loss Reversed Obesity-Induced HGF/c-Met Pathway and Basal-Like Breast Cancer Progression.* Front Oncol, 2014. **4**: p. 175.

265. Shojaei, F., et al., *HGF/c-Met acts as an alternative angiogenic pathway in sunitinib-resistant tumors.* Cancer Res, 2010. **70**(24): p. 10090-100.

266. Ding, S., et al., *HGF receptor up-regulation contributes to the angiogenic phenotype of human endothelial cells and promotes angiogenesis in vitro.* Blood, 2003. **101**(12): p. 4816-22.

267. Sulpice, E., et al., *Cross-talk between the VEGF-A and HGF signalling pathways in endothelial cells.* Biol Cell, 2009. **101**(9): p. 525-39.

268. Schneider, B., *Randomized Controlled Trial of Genomically Directed Therapy in Patients With Triple Negative Breast Cancer.* In: ClinicalTrials.gov [Internet]. 2016.

269. Baylor Breast Care Center, B.C.o.M., *CRIZENT: Crizotinib and Sunitinib in Metastatic Breast Cancer.* In: ClinicalTrials.gov [Internet]. 2015.

270. Welford, A.F., et al., *TIE2-expressing macrophages limit the therapeutic efficacy of the vascular-disrupting agent combretastatin A4 phosphate in mice.* J Clin Invest, 2011. **121**(5): p. 1969.

271. Rivera, L.B. and G. Bergers, *Intertwined regulation of angiogenesis and immunity by myeloid cells.* Trends Immunol, 2015. **36**(4): p. 240-9.

272. Rapisarda, A. and G. Melillo, *Role of the hypoxic tumor microenvironment in the resistance to anti-angiogenic therapies.* Drug Resist Updat, 2009. **12**(3): p. 74-80.

273. McIntyre, A. and A.L. Harris, *Metabolic and hypoxic adaptation to anti-angiogenic therapy: a target for induced essentiality.* EMBO Mol Med, 2015. **7**(4): p. 368-79.

274. Amor, S., et al., *Peritumoral adipose tissue as a source of inflammatory and angiogenic factors in colorectal cancer.* Int J Colorectal Dis, 2016. **31**(2): p. 365-75.

275. Weisberg, S.P., et al., *Obesity is associated with macrophage accumulation in adipose tissue.* J Clin Invest, 2003. **112**(12): p. 1796-808.

276. Karaman, S., et al., *Blockade of VEGF-C and VEGF-D modulates adipose tissue inflammation and improves metabolic parameters under high-fat diet.* Mol Metab, 2015. **4**(2): p. 93-105.

277. Cao, R., et al., *Hepatocyte growth factor is a lymphangiogenic factor with an indirect mechanism of action.* Blood, 2006. **107**(9): p. 3531-6.

278. Weitman, E.S., et al., *Obesity impairs lymphatic fluid transport and dendritic cell migration to lymph nodes.* PLoS One, 2013. **8**(8): p. e70703.

279. Arngrim, N., et al., *Reduced adipose tissue lymphatic drainage of macromolecules in obese subjects: a possible link between obesity and local tissue inflammation[quest].* Int J Obes, 2013. **37**(5): p. 748-750.

280. Nores, G.D., et al., *Obesity but not high-fat diet impairs lymphatic function.* Int J Obes (Lond), 2016.

281. Garcia Nores, G.D., et al., *Obesity but not high-fat diet impairs lymphatic function.* Int J Obes (Lond), 2016.

282. Harvey, N.L., et al., *Lymphatic vascular defects promoted by Prox1 haploinsufficiency cause adult-onset obesity.* Nat Genet, 2005. **37**(10): p. 1072-81.

283. Escobedo, N., et al., *Restoration of lymphatic function rescues obesity in Prox1-haploinsufficient mice.* JCI Insight. **1**(2).

284. Takeda, K., et al., *Adipose-derived stem cells promote proliferation, migration, and tube formation of lymphatic endothelial cells in vitro by secreting lymphangiogenic factors.* Ann Plast Surg, 2015. **74**(6): p. 728-36.

285. Shimizu, Y., et al., *Therapeutic lymphangiogenesis with implantation of adipose-derived regenerative cells.* J Am Heart Assoc, 2012. **1**(4).

286. Yoshida, S., et al., *Adipose-derived stem cell transplantation for therapeutic lymphangiogenesis in a mouse secondary lymphedema model.* Regen Med, 2015. **10**(5): p. 549-62.

287. Venkatasubramanian, P.N., et al., *Periprostatic adipose tissue from obese prostate cancer patients promotes tumor and endothelial cell proliferation: a functional and MR imaging pilot study.* Prostate, 2014. **74**(3): p. 326-35.

288. Ribeiro, A.M., et al., *Prostate cancer cell proliferation and angiogenesis in different obese mice models.* Int J Exp Pathol, 2010. **91**(4): p. 374-86.

289. Moreira, Â., et al., *Obesity inhibits lymphangiogenesis in prostate tumors.* Int J Clin Exp Pathol, 2014. **7**(1): p. 348-52.

290. Briganti, A., et al., *Obesity does not increase the risk of lymph node metastases in patients with clinically localized prostate cancer undergoing radical prostatectomy and extended pelvic lymph node dissection.* Int J Urol, 2009. **16**(8): p. 676-681.

291. Coussens, L.M. and Z. Werb, *Inflammation and cancer.* Nature, 2002. **420**(6917): p. 860-7.

292. Balkwill, F. and A. Mantovani, *Inflammation and cancer: back to Virchow?* Lancet, 2001. **357**(9255): p. 539-45.

293. Engblom, C., C. Pfirschke, and M.J. Pittet, *The role of myeloid cells in cancer therapies.* Nat Rev Cancer, 2016. **16**(7): p. 447-62.

294. Pollard, J.W., *Macrophages define the invasive microenvironment in breast cancer.* J Leukoc Biol, 2008. **84**(3): p. 623-630.

295. Whiteside, T.L., *The role of immune cells in the tumor microenvironment.* Cancer Treat Res, 2006. **130**: p. 103-24.

296. Johnson, A.R., J. Justin Milner, and L. Makowski, *The inflammation highway: metabolism accelerates inflammatory traffic in obesity.* Immunol Rev, 2012. **249**(1): p. 218-238.

297. Sonnenberg, G.F. and D. Artis, *Innate lymphoid cells in the initiation, regulation and resolution of inflammation.* Nat Med, 2015. **21**(7): p. 698-708.

298. Yeh, H.C., et al., *A prospective study of the associations between treated diabetes and cancer outcomes.* Diabetes Care, 2012. **35**(1): p. 113-8.

299. Giovannucci, E., et al., *Diabetes and cancer: A consensus report.* Diabetes Care, 2010. **33**(7): p. 1674-85.

300. Freemerman, A.J., et al., *Metabolic reprogramming of macrophages: glucose transporter 1 (GLUT1)-mediated glucose metabolism drives a proinflammatory phenotype.* J Biol Chem, 2014. **289**(11): p. 7884-96.

301. Johnson, A.R., et al., *Metabolic reprogramming through fatty acid transport protein 1 (FATP1) regulates macrophage inflammatory potential and adipose inflammation.* Mol Metab, 2016. **5**(7): p. 506-26.

302. Chang, C.H. and E.L. Pearce, *Emerging concepts of T cell metabolism as a target of immunotherapy.* Nat Immunol, 2016. **17**(4): p. 364-8.

303. Hattori, Y., K. Hattori, and T. Hayashi, *Pleiotropic benefits of metformin: macrophage targeting its anti-inflammatory mechanisms.* Diabetes, 2015. **64**(6): p. 1907-9.

304. Eikawa, S., et al., *Immune-mediated antitumor effect by type 2 diabetes drug, metformin.* Proc Natl Acad Sci U S A, 2015. **112**(6): p. 1809-14.

305. Nishikawa, H. and S. Sakaguchi, *Regulatory T cells in tumor immunity.* Int J Cancer, 2010. **127**(4): p. 759-67.

306. Zou, W., *Regulatory T cells, tumour immunity and immunotherapy.* Nat Rev Immunol, 2006. **6**(4): p. 295-307.

307. Hori, S., T. Nomura, and S. Sakaguchi, *Control of regulatory T cell development by the transcription factor Foxp3.* Science, 2003. **299**(5609): p. 1057-61.

308. Fontenot, J.D., M.A. Gavin, and A.Y. Rudensky, *Foxp3 programs the development and function of CD4+CD25+ regulatory T cells.* Nat Immunol, 2003. **4**(4): p. 330-6.

309. Takahashi, T., et al., *Immunologic self-tolerance maintained by CD25(+)CD4(+) regulatory T cells constitutively expressing cytotoxic T lymphocyte-associated antigen 4.* J Exp Med, 2000. **192**(2): p. 303-10.

310. Wang, L., et al., *Programmed death 1 ligand signaling regulates the generation of adaptive Foxp3+CD4+ regulatory T cells.* Proc Natl Acad Sci U S A, 2008. **105**(27): p. 9331-6.

311. Amarnath, S., et al., *The PDL1-PD1 axis converts human Th1 cells into regulatory T cells.* Sci Transl Med, 2011. **3**(111): p. 111ra120.

312. Josefowicz, S.Z., L.F. Lu, and A.Y. Rudensky, *Regulatory T cells: mechanisms of differentiation and function.* Annu Rev Immunol, 2012. **30**: p. 531-64.

313. Bates, G.J., et al., *Quantification of regulatory T cells enables the identification of high-risk breast cancer patients and those at risk of late relapse.* J Clin Oncol, 2006. **24**(34): p. 5373-80.

314. Wilke, C.M., et al., *Prognostic significance of regulatory T cells in tumor.* Int J Cancer, 2010. **127**(4): p. 748-58.

315. Flammiger, A., et al., *High tissue density of FOXP3+ T cells is associated with clinical outcome in prostate cancer.* Eur J Cancer, 2013. **49**(6): p. 1273-9.

316. Feuerer, M., et al., *Lean, but not obese, fat is enriched for a unique population of regulatory T cells that affect metabolic parameters.* Nat Med, 2009. **15**(8): p. 930-9.

317. Yang, H., et al., *Obesity increases the production of proinflammatory mediators from adipose tissue T cells and compromises TCR repertoire diversity: implications for systemic inflammation and insulin resistance.* J Immunol, 2010. **185**(3): p. 1836-45.

318. Nishimura, S., et al., *CD8+ effector T cells contribute to macrophage recruitment and adipose tissue inflammation in obesity.* Nat Med, 2009. **15**(8): p. 914-20.

319. Travers, R.L., et al., *The impact of adiposity on adipose tissue-resident lymphocyte activation in humans.* Int J Obes (Lond), 2015. **39**(5): p. 762-9.

320. Zeyda, M., et al., *Inflammation correlates with markers of T-cell subsets including regulatory T cells in adipose tissue from obese patients.* Obesity (Silver Spring), 2011. **19**(4): p. 743-8.

321. Subbaramaiah, K., et al., *Increased levels of COX-2 and prostaglandin E2 contribute to elevated aromatase expression in inflamed breast tissue of obese women.* Cancer Discov, 2012. **2**(4): p. 356-65.

322. Morris, P.G., et al., *Inflammation and increased aromatase expression occur in the breast tissue of obese women with breast cancer.* Cancer Prev Res (Phila), 2011. **4**(7): p. 1021-9.

323. van Kruijsdijk, R.C., E. van der Wall, and F.L. Visseren, *Obesity and cancer: the role of dysfunctional adipose tissue.* Cancer Epidemiol Biomarkers Prev, 2009. **18**(10): p. 2569-78.

324. Cleary, M.P. and M.E. Grossmann, *Minireview: Obesity and breast cancer: the estrogen connection.* Endocrinology, 2009. **150**(6): p. 2537-42.

325. Polanczyk, M.J., et al., *Enhanced FoxP3 expression and Treg cell function in pregnant and estrogen-treated mice.* J Neuroimmunol, 2005. **170**(1-2): p. 85-92.

326. Valor, L., et al., *Estradiol-dependent perforin expression by human regulatory T-cells.* Eur J Clin Invest, 2011. **41**(4): p. 357-64.

327. Baratelli, F., et al., *Prostaglandin E2 induces FOXP3 gene expression and T regulatory cell function in human CD4+ T cells.* J Immunol, 2005. **175**(3): p. 1483-90.

328. Sharma, S., et al., *Tumor cyclooxygenase-2/prostaglandin E2-dependent promotion of FOXP3 expression and CD4+ CD25+ T regulatory cell activities in lung cancer.* Cancer Res, 2005. **65**(12): p. 5211-20.

329. Baratelli, F., et al., *PGE(2) contributes to TGF-β induced T regulatory cell function in human non-small cell lung cancer.* Am J Transl Res, 2010. **2**(4): p. 356-67.

330. Dixit, V.D., *Thymic fatness and approaches to enhance thymopoietic fitness in aging.* Curr Opin Immunol, 2010. **22**(4): p. 521-8.

331. Taub, D.D. and D.L. Longo, *Insights into thymic aging and regeneration.* Immunol Rev, 2005. **205**: p. 72-93.

332. Weng, N., *Aging of the immune system: How much can the adaptive immune system adapt?* Immunity, 2006. **24**(5): p. 495-9.

333. Yang, H., et al., *Obesity accelerates thymic aging.* Blood, 2009. **114**(18): p. 3803-12.

334. Karlsson, E.A. and M.A. Beck, *The burden of obesity on infectious disease.* Exp Biol Med (Maywood), 2010. **235**(12): p. 1412-24.

335. Paich, H.A., Sheridan, P. A., Handy, J., Karlsson, E. A., Schultz-Cherry, S., Hudgens, M. G., Noah, T. L., Weir, S. S., Beck, M. A., *Overweight and obese adult humans have a defective cellular immune response to pandemic H1N1 influenza A virus.* Obesity (Silver Spring), 2013. **21**(11): p. 2377-86.

336. Chen, L. and X. Han, *Anti-PD-1/PD-L1 therapy of human cancer: past, present, and future.* J Clin Invest, 2015. **125**(9): p. 3384-91.

337. Shirakawa, K., et al., *Obesity accelerates T cell senescence in murine visceral adipose tissue.* J Clin Invest, 2016. **126**(12): p. 4626-4639.

338. Kadl, A., et al., *Identification of a novel macrophage phenotype that develops in response to atherogenic phospholipids via Nrf2.* Circ Res, 2010. **107**(6): p. 737-46.

339. Sampey, B.P., et al., *Metabolomic profiling reveals mitochondrial-derived lipid biomarkers that drive obesity-associated inflammation.* PloS One, 2012. **7**(6): p. e38812.

340. Sampey, B.P., et al., *Cafeteria diet is a robust model of human metabolic syndrome with liver and adipose inflammation: comparison to high-fat diet.* Obesity (Silver Spring), 2011. **19**(6): p. 1109-17.

341. Gordon, S., *The macrophage: past, present and future.* Eur J Immunol, 2007. **37 Suppl 1**: p. S9-17.

342. Mantovani, A., et al., *Tumor-associated macrophages and the related myeloid-derived suppressor cells as a paradigm of the diversity of macrophage activation.* Hum Immunol, 2009. **70**(5): p. 325-30.

343. Murray, P.J., et al., *Macrophage activation and polarization: nomenclature and experimental guidelines.* Immunity, 2014. **41**(1): p. 14-20.

344. Gautier, E.L., et al., *Gene expression profiles and transcriptional regulatory pathways underlying mouse tissue macrophage identity and diversity.* Nat Immunol, 2012. **13**(11): p. 1118-28.

345. Martinez, F.O. and S. Gordon, *The M1 and M2 paradigm of macrophage activation: time for reassessment.* F1000Prime Rep, 2014. **6**.

346. Martinez, F.O., et al., *Transcriptional profiling of the human monocyte-to-macrophage differentiation and polarization: new molecules and patterns of gene expression.* J Immunol, 2006. **177**(10): p. 7303-11.

347. Mosser, D.M. and J.P. Edwards, *Exploring the full spectrum of macrophage activation.* Nat Rev Immunol, 2008. **8**(12): p. 958-969.

348. Lavin, Y., et al., *Regulation of macrophage development and function in peripheral tissues.* Nat Rev Immunol, 2015. **15**(12): p. 731-44.

349. Xue, J., et al., *Transcriptome-based network analysis reveals a spectrum model of human macrophage activation.* Immunity, 2014. **40**(2): p. 274-88.

350. Davies, L.C. and P.R. Taylor, *Tissue-resident macrophages: then and now.* Immunology, 2015. **144**(4): p. 541-8.

351. Ginhoux, F. and M. Guilliams, *Tissue-resident macrophage ontogeny and homeostasis.* Immunity, 2016. **44**(3): p. 439-49.

352. Mass, E., et al., *Specification of tissue-resident macrophages during organogenesis.* Science, 2016. **353**(6304).

353. Gomez Perdiguero, E., et al., *Tissue-resident macrophages originate from yolk-sac-derived erythro-myeloid progenitors.* Nature, 2015. **518**(7540): p. 547-51.

354. Hashimoto, D., et al., *Tissue-resident macrophages self-maintain locally throughout adult life with minimal contribution from circulating monocytes.* Immunity, 2013. **38**(4): p. 792-804.

355. Davies, L.C., et al., *A quantifiable proliferative burst of tissue macrophages restores homeostatic macrophage populations after acute inflammation.* Eur J Immunol, 2011. **41**(8): p. 2155-64.

356. Franklin, R.A., et al., *The cellular and molecular origin of tumor-associated macrophages.* Science, 2014. **344**(6186): p. 921-5.

357. Serbina, N.V. and E.G. Pamer, *Monocyte emigration from bone marrow during bacterial infection requires signals mediated by chemokine receptor CCR2.* Nat Immunol, 2006. **7**(3): p. 311-7.

358. Amano, S.U., et al., *Local proliferation of macrophages contributes to obesity-associated adipose tissue inflammation.* Cell Metab, 2014. **19**(1): p. 162-71.

359. Haase, J., et al., *Local proliferation of macrophages in adipose tissue during obesity-induced inflammation.* Diabetologia, 2014. **57**(3): p. 562-71.

360. Davies, L.C., Rosas, M., Jenkins, S. J., Liao, C., Scurr, M. J., Brombacher, F., Fraser, D. J., Allen, J. E., Jones, S. A., Taylor, P. R., *Distinct bone marrow-derived and tissue resident macrophage-lineages proliferate at key stages during inflammation.* Nat. Commun., 2013. **4**.

361. Elgazar-Carmon, V., et al., *Neutrophils transiently infiltrate intra-abdominal fat early in the course of high-fat feeding.* J Lipid Res, 2008. **49**(9): p. 1894-903.

362. Curat, C.A., et al., *From blood monocytes to adipose tissue-resident macrophages: induction of diapedesis by human mature adipocytes.* Diabetes, 2004. **53**(5): p. 1285-1292.

363. Ortega Martinez de Victoria, E., et al., *Macrophage content in subcutaneous adipose tissue: Associations with adiposity, age, inflammatory markers, and whole-body insulin action in healthy Pima Indians.* Diabetes, 2009. **58**(2): p. 385-93.

364. Xu, H., et al., *Chronic inflammation in fat plays a crucial role in the development of obesity-related insulin resistance.* J Clin Invest, 2003. **112**(12): p. 1821-30.

365. Subbaramaiah, K., et al., *Obesity is associated with inflammation and elevated aromatase expression in the mouse mammary gland.* Cancer Prev Res (Phila), 2011. **4**(3): p. 329-46.

366. Sun, X., et al., *Normal breast tissue of obese women is enriched for macrophage markers and macrophage-associated gene expression.* Breast Cancer Res Treat, 2012. **131**(3): p. 1003-12.

367. Fried, S.K., D.A. Bunkin, and A.S. Greenberg, *Omental and subcutaneous adipose tissues of obese subjects release interleukin-6: depot difference and regulation by glucocorticoid.* J Clin Endocrinol Metab, 1998. **83**(3): p. 847-50.

368. Curat, C.A., et al., *Macrophages in human visceral adipose tissue: increased accumulation in obesity and a source of resistin and visfatin.* Diabetologia, 2006. **49**(4): p. 744-7.

369. Fain, J.N., S.W. Bahouth, and A.K. Madan, *TNFalpha release by the nonfat cells of human adipose tissue.* Int J Obes Relat Metab Disord, 2004. **28**(4): p. 616-22.

370. Lumeng, C.N., J.L. Bodzin, and A.R. Saltiel, *Obesity induces a phenotypic switch in adipose tissue macrophage polarization.* J Clin Invest, 2007. **117**(1): p. 175-84.

371. Fujisaka, S., et al., *Regulatory mechanisms for adipose tissue M1 and M2 macrophages in diet-induced obese mice.* Diabetes, 2009. **58**(11): p. 2574-82.

372. Li, P., et al., *Functional heterogeneity of CD11c-positive adipose tissue macrophages in diet-induced obese mice.* J Biol Chem, 2010. **285**(20): p. 15333-45.

373. Shaul, M.E., et al., *Dynamic, M2-like remodeling phenotypes of CD11c+ adipose tissue macrophages during high-fat diet--induced obesity in mice.* Diabetes, 2010. **59**(5): p. 1171-81.

374. Zeyda, M., et al., *Human adipose tissue macrophages are of an anti-inflammatory phenotype but capable of excessive pro-inflammatory mediator production.* Int J Obes (Lond), 2007. **31**(9): p. 1420-8.

375. Wentworth, J.M., et al., *Pro-inflammatory CD11c+CD206+ adipose tissue macrophages are associated with insulin resistance in human obesity.* Diabetes, 2010. **59**(7): p. 1648-56.

376. Nakajima, S., et al., *Accumulation of CD11c+CD163+ adipose tissue macrophages through upregulation of intracellular 11beta-HSD1 in human obesity.* J Immunol, 2016. **197**(9): p. 3735-3745.

377. Kratz, M., et al., *Metabolic dysfunction drives a mechanistically distinct proinflammatory phenotype in adipose tissue macrophages.* Cell Metab, 2014. **20**(4): p. 614-25.

378. Moscat, J. and M.T. Diaz-Meco, *p62 at the crossroads of autophagy, apoptosis, and cancer.* Cell, 2009. **137**(6): p. 1001-4.

379. Xu, X., et al., *Obesity activates a program of lysosomal-dependent lipid metabolism in adipose tissue macrophages independently of classic activation.* Cell Metab, 2013. **18**(6): p. 816-30.

380. Williams, C.B., E.S. Yeh, and A.C. Soloff, *Tumor-associated macrophages: unwitting accomplices in breast cancer malignancy.* npj Breast Cancer, 2016. **2**.

381. Quail, D. and J. Joyce, *Microenvironmental regulation of tumor progression and metastasis.* Nat Med, 2013. **19**(11): p. 1423-37.

382. Lin, E.Y., et al., *Macrophages regulate the angiogenic switch in a mouse model of breast cancer.* Cancer Res, 2006. **66**(23): p. 11238-46.

383. Qian, B.Z. and J.W. Pollard, *Macrophage diversity enhances tumor progression and metastasis.* Cell, 2010. **141**(1): p. 39-51.

384. DeNardo, D.G., et al., *Leukocyte complexity predicts breast cancer survival and functionally regulates response to chemotherapy.* Cancer Discov, 2011. **1**(1): p. 54-67.

385. De Palma, M. and C.E. Lewis, *Macrophage regulation of tumor responses to anticancer therapies.* Cancer Cell, 2013. **23**(3): p. 277-86.

386. Mantovani, A. and P. Allavena, *The interaction of anticancer therapies with tumor-associated macrophages.* J Exp Med, 2015. **212**(4): p. 435-45.

387. Shree, T., et al., *Macrophages and cathepsin proteases blunt chemotherapeutic response in breast cancer.* Genes Dev, 2011. **25**(23): p. 2465-79.

388. Escamilla, J., et al., *CSF1 receptor targeting in prostate cancer reverses macrophage-mediated resistance to androgen blockade therapy.* Cancer Res, 2015. **75**(6): p. 950-62.

389. Campbell, M.J., et al., *Proliferating macrophages associated with high grade, hormone receptor negative breast cancer and poor clinical outcome.* Breast Cancer Res Treat, 2011. **128**(3): p. 703-711.

390. Movahedi, K., et al., *Different tumor microenvironments contain functionally distinct subsets of macrophages derived from Ly6C(high) monocytes.* Cancer Res, 2010. **70**(14): p. 5728-39.

391. Qian, B.Z., Li, J., Zhang, H., Kitamura, T., Zhang, J., Campion, L. R., Kaiser, E. A., Snyder, L. A., Pollard, J. W., *CCL2 recruits inflammatory monocytes to facilitate breast tumor metastasis.* Nature Australia, 2011. **475**(7355): p. 222-5.

392. Mantovani, A., et al., *Macrophage polarization: tumor-associated macrophages as a paradigm for polarized M2 mononuclear phagocytes.* Trends Immunol, 2002. **23**(11): p. 549-55.

393. Eruslanov, E., et al., *Pivotal Advance: Tumor-mediated induction of myeloid-derived suppressor cells and M2-polarized macrophages by altering intracellular PGE(2) catabolism in myeloid cells.* J Leukoc Biol, 2010. **88**(5): p. 839-48.

394. Ojalvo, L.S., et al., *High-density gene expression analysis of tumor-associated macrophages from mouse mammary tumors.* Am J Pathol, 2009. **174**(3): p. 1048-64.

395. Taylor, C.T., *Interdependent roles for hypoxia inducible factor and nuclear factor-κB in hypoxic inflammation.* J Physiol, 2008. **586**(Pt 17): p. 4055-9.

396. Aggarwal, B.B. and P. Gehlot, *Inflammation and cancer: how friendly is the relationship for cancer patients?* Curr Opin Pharmacol, 2009. **9**(4): p. 351-69.

397. Lawrence, T., et al., *Possible new role for NF-kappaB in the resolution of inflammation.* Nat Med, 2001. **7**(12): p. 1291-7.

398. Lawrence, T. and C. Fong, *The resolution of inflammation: anti-inflammatory roles for NF-kappaB.* Int J Biochem Cell Biol, 2010. **42**(4): p. 519-23.

399. Biswas, S.K. and C.E. Lewis, *NF-kappaB as a central regulator of macrophage function in tumors.* J Leukoc Biol, 2010. **88**(5): p. 877-84.

400. Hagemann, T., et al., *Regulation of macrophage function in tumors: the multifaceted role of NF-kappaB.* Blood, 2009. **113**(14): p. 3139-46.

401. Hagemann, T., et al., *"Re-educating" tumor-associated macrophages by targeting NF-kappaB.* J Exp Med, 2008. **205**(6): p. 1261-8.

402. Ortega, R.A., et al., *Manipulating the NF-κB pathway in macrophages using mannosylated, siRNA-delivering nanoparticles can induce immunostimulatory and tumor cytotoxic functions.* Int J Nanomedicine, 2016. **11**: p. 2163-77.

403. Mayi, T.H., et al., *Human adipose tissue macrophages display activation of cancer-related pathways.* J Biol Chem, 2012. **287**(26): p. 21904-13.

404. Madge, L.A. and M.J. May, *Classical NF-kappaB activation negatively regulates noncanonical NF-kappaB-dependent CXCL12 expression.* J Biol Chem, 2010. **285**(49): p. 38069-77.

405. Gabrilovich, D.I., et al., *The terminology issue for myeloid-derived suppressor cells.* Cancer Res, 2007. **67**(1): p. 425-6.

406. Gabrilovich, D.I. and S. Nagaraj, *Myeloid-derived suppressor cells as regulators of the immune system.* Nat Rev Immunol, 2009. **9**(3): p. 162-74.

407. Poschke, I. and R. Kiessling, *On the armament and appearances of human myeloid-derived suppressor cells.* Clin Immunol, 2012. **144**(3): p. 250-68.

408. Xia, S., et al., *Gr-1+ CD11b+ myeloid-derived suppressor cells suppress inflammation and promote insulin sensitivity in obesity.* J Biol Chem, 2011. **286**(26): p. 23591-9.

409. Rodriguez, P.C., et al., *Arginase I in myeloid suppressor cells is induced by COX-2 in lung carcinoma.* J Exp Med, 2005. **202**(7): p. 931-9.

410. Sinha, P., et al., *Prostaglandin E2 promotes tumor progression by inducing myeloid-derived suppressor cells.* Cancer Res, 2007. **67**(9): p. 4507-13.

411. Ochoa, A.C., et al., *Arginase, prostaglandins, and myeloid-derived suppressor cells in renal cell carcinoma.* Clin Cancer Res, 2007. **13**(2 Pt 2): p. 721s-726s.

412. Okwan-Duodu, D., et al., *Obesity-driven inflammation and cancer risk: role of myeloid derived suppressor cells and alternately activated macrophages.* Am J Cancer Res, 2013. **3**(1): p. 21-33.

413. Kusmartsev, S. and D.I. Gabrilovich, *STAT1 signaling regulates tumor-associated macrophage-mediated T cell deletion.* J Immunol, 2005. **174**(8): p. 4880-91.

414. Topalian, S.L., C.G. Drake, and D.M. Pardoll, *Targeting the PD-1/B7-H1(PD-L1) pathway to activate anti-tumor immunity.* Curr Opin Immunol, 2012. **24**(2): p. 207-12.

415. Prima, V., et al., *COX2/mPGES1/PGE2 pathway regulates PD-L1 expression in tumor-associated macrophages and myeloid-derived suppressor cells.* Proc Natl Acad Sci U S A, 2017. **114**(5): p. 1117-1122.

416. Yang, S., et al., *PD-1, PD-L1 and PD-L2 expression in mouse prostate cancer.* Am J Clin Exp Urol, 2016. **4**(1): p. 1-8.

417. Noman, M.Z., et al., *PD-L1 is a novel direct target of HIF-1alpha, and its blockade under hypoxia enhanced MDSC-mediated T cell activation.* J Exp Med, 2014. **211**(5): p. 781-90.

418. Wright, H.L., et al., *Neutrophil function in inflammation and inflammatory diseases.* Rheumatology (Oxford), 2010. **49**(9): p. 1618-31.

419. Ferrante, A.W., *The immune cells in adipose tissue.* Diabetes Obes Metab, 2013. **15**(0 3): p. 34-8.

420. Talukdar, S., et al., *Neutrophils mediate insulin resistance in high fat diet fed mice via secreted elastase.* Nat Med, 2012. **18**(9): p. 1407-12.

421. Fridlender, Z.G., et al., *Polarization of tumor-associated neutrophil phenotype by TGF-beta: "N1" versus "N2" TAN.* Cancer Cell, 2009. **16**(3): p. 183-94.

422. Piccard, H., R.J. Muschel, and G. Opdenakker, *On the dual roles and polarized phenotypes of neutrophils in tumor development and progression.* Crit Rev Oncol Hematol, 2012. **82**(3): p. 296-309.

423. Oliveira, A.G., et al., *Tumor-associated neutrophils*, in *Trends in Stem Cell Proliferation and Cancer Research*. 2013, Springer. p. 479-501.

424. Scapini, P., et al., *The neutrophil as a cellular source of chemokines.* Immunol Rev, 2000. **177**: p. 195-203.

425. Bekes, E.M., et al., *Tumor-recruited neutrophils and neutrophil TIMP-free MMP-9 regulate coordinately the levels of tumor angiogenesis and efficiency of malignant cell intravasation.* Am J Pathol, 2011. **179**(3): p. 1455-70.

426. Nozawa, H., C. Chiu, and D. Hanahan, *Infiltrating neutrophils mediate the initial angiogenic switch in a mouse model of multistage carcinogenesis.* Proc Natl Acad Sci U S A, 2006. **103**(33): p. 12493-8.

427. Rodriguez, P.C., et al., *Arginase I production in the tumor microenvironment by mature myeloid cells inhibits T-cell receptor expression and antigen-specific T-cell responses.* Cancer Res, 2004. **64**(16): p. 5839-49.

428. van Spriel, A.B., et al., *Mac-1 (CD11b/CD18) is essential for Fc receptor–mediated neutrophil cytotoxicity and immunologic synapse formation.* Blood, 2001. **97**(8): p. 2478-2486.

429. Knaapen, A.M., et al., *Neutrophils and respiratory tract DNA damage and mutagenesis: a review.* Mutagenesis, 2006. **21**(4): p. 225-36.

430. Incio, J., et al., *Obesity-induced inflammation and desmoplasia promote pancreatic cancer progression and resistance to chemotherapy.* Cancer Discov, 2016. **6**(8): p. 852-69.

431. da Silva, E.Z., M.C. Jamur, and C. Oliver, *Mast cell function: a new vision of an old cell.* J Histochem Cytochem, 2014. **62**(10): p. 698-738.

432. Irani, A.A., et al., *Two types of human mast cells that have distinct neutral protease compositions.* Proc Natl Acad Sci U S A, 1986. **83**(12): p. 4464-8.

433. Galli, S.J., et al., *Mast cells as "tunable" effector and immunoregulatory cells: recent advances.* Annu Rev Immunol, 2005. **23**: p. 749-86.

434. Altintas, M.M., et al., *Apoptosis, mastocytosis, and diminished adipocytokine gene expression accompany reduced epididymal fat mass in long-standing diet-induced obese mice.* Lipids Health Dis, 2011. **10**: p. 198.

435. Liu, J., et al., *Deficiency and pharmacological stabilization of mast cells reduce diet-induced obesity and diabetes in mice.* Nature Medicine, 2009. **15**(8): p. 940-5.

436. Divoux, A., et al., *Mast cells in human adipose tissue: link with morbid obesity, inflammatory status, and diabetes.* J Clin Endocrinol Metab, 2012. **97**(9): p. E1677-85.

437. Altintas, M.M., et al., *Mast cells, macrophages, and crown-like structures distinguish subcutaneous from visceral fat in mice.* J Lipid Res, 2011. **52**(3): p. 480-8.

438. Ward, B.R., et al., *Obesity is not linked with increased whole-body mast cell burden in children.* J Allergy Clin Immunol, 2012. **129**(4): p. 1164-1166.e4.

439. Zhou, Y., et al., *Leptin deficiency shifts mast cells toward anti-inflammatory actions and protects mice from obesity and diabetes by polarizing M2 macrophages.* Cell Metab, 2015. **22**(6): p. 1045-58.

440. Theoharides, T.C. and P. Conti, *Mast cells: the Jekyll and Hyde of tumor growth.* Trends Immunol, 2004. **25**(5): p. 235-41.

441. Oft, M., *IL-10: master switch from tumor-promoting inflammation to antitumor immunity.* Cancer Immunol Res, 2014. **2**(3): p. 194-9.

442. Li, Z., L. Chen, and Z. Qin, *Paradoxical roles of IL-4 in tumor immunity.* Cell Mol Immunol, 2009. **6**(6): p. 415-22.

443. Fisher, D.T., M.M. Appenheimer, and S.S. Evans, *The two faces of IL-6 in the tumor microenvironment.* Semin Immunol, 2014. **26**(1): p. 38-47.

444. Balkwill, F., *Tumour necrosis factor and cancer.* Nat Rev Cancer, 2009. **9**(5): p. 361-371.

445. Apte, R.N., et al., *The involvement of IL-1 in tumorigenesis, tumor invasiveness, metastasis and tumor-host interactions.* Cancer Metastasis Rev, 2006. **25**(3): p. 387-408.

446. Fernandez-Garcia, B., et al., *Prognostic significance of inflammatory factors expression by stroma from breast carcinomas.* Carcinogenesis, 2016. **37**(8): p. 768-76.

447. Raica, M., et al., *Interplay between mast cells and lymphatic vessels in different molecular types of breast cancer.* Anticancer Res, 2013. **33**(3): p. 957-63.

448. Marech, I., et al., *Serum tryptase, mast cells positive to tryptase and microvascular density evaluation in early breast cancer patients: possible translational significance.* BMC Cancer, 2014. **14**: p. 534.

449. Xiang, M., et al., *Mast cell tryptase promotes breast cancer migration and invasion.* Oncol Rep, 2010. **23**(3): p. 615-9.

450. Mangia, A., et al., *Tissue remodelling in breast cancer: human mast cell tryptase as an initiator of myofibroblast differentiation.* Histopathology, 2011. **58**(7): p. 1096-106.

451. Samoszuk, M. and M.A. Corwin, *Mast cell inhibitor cromolyn increases blood clotting and hypoxia in murine breast cancer.* Int J Cancer, 2003. **107**(1): p. 159-63.

452. Rajput, A.B., et al., *Stromal mast cells in invasive breast cancer are a marker of favourable prognosis: a study of 4,444 cases.* Breast Cancer Res Treat 2008. **107**(2): p. 249-257.

453. Nonomura, N., et al., *Decreased number of mast cells infiltrating into needle biopsy specimens leads to a better prognosis of prostate cancer.* Br J Cancer, 2007. **97**(7): p. 952-6.

454. Johansson, A., et al., *Mast cells are novel independent prognostic markers in prostate cancer and represent a target for therapy.* Am J Pathol, 2010. **177**(2): p. 1031-41.

455. Fleischmann, A., et al., *Immunological microenvironment in prostate cancer: high mast cell densities are associated with favorable tumor characteristics and good prognosis.* Prostate, 2009. **69**(9): p. 976-81.

456. Clark, R., et al., *Milky spots promote ovarian cancer metastatic colonization of peritoneal adipose in experimental models.* Am J Pathol, 2013. **183**(2): p. 576-91.

457. Ishijima, Y., S. Ohmori, and K. Ohneda, *Mast cell deficiency results in the accumulation of preadipocytes in adipose tissue in both obese and non-obese mice.* FEBS Open Bio, 2013. **4**: p. 18-24.

458. Poglio, S., et al., *Adipose tissue as a dedicated reservoir of functional mast cell progenitors.* Stem Cells, 2010. **28**(11): p. 2065-72.

459. Davis, B.P. and M.E. Rothenberg, *Eosinophils and cancer.* Cancer Immunol Res, 2014. **2**(1): p. 1-8.

460. Akuthota, P., et al., *Immunoregulatory roles of eosinophils: a new look at a familiar cell.* Clin Exp Allergy, 2008. **38**(8): p. 1254-63.

461. Wu, D., et al., *Eosinophils sustain adipose alternatively activated macrophages associated with glucose homeostasis.* Science, 2011. **332**(6026): p. 243-7.

462. Molofsky, A.B., et al., *Innate lymphoid type 2 cells sustain visceral adipose tissue eosinophils and alternatively activated macrophages.* J Exp Med, 2013. **210**(3): p. 535-49.

463. Sakkal, S., et al., *Eosinophils in cancer: Favourable or unfavourable?* Curr Med Chem, 2016. **23**(7): p. 650-66.

464. Spessotto, P., et al., *Human eosinophil peroxidase enhances tumor necrosis factor and hydrogen peroxide release by human monocyte-derived macrophages.* Eur J Immunol, 1995. **25**(5): p. 1366-73.

465. Carretero, R., et al., *Eosinophils orchestrate cancer rejection by normalizing tumor vessels and enhancing infiltration of CD8(+) T cells.* Nat Immunol, 2015. **16**(6): p. 609-17.

466. Tepper, R.I., R.L. Coffman, and P. Leder, *An eosinophil-dependent mechanism for the antitumor effect of interleukin-4.* Science, 1992. **257**(5069): p. 548-51.

467. Noffz, G., et al., *Neutrophils but not eosinophils are involved in growth suppression of IL-4-secreting tumors.* J Immunol, 1998. **160**(1): p. 345-50.

468. Carey, L.A., et al., *Race, breast cancer subtypes, and survival in the Carolina Breast Cancer Study.* JAMA, 2006. **295**(21): p. 2492-502.

469. Boyle, P., *Triple-negative breast cancer: epidemiological considerations and recommendations.* Ann Oncol, 2012. **23**(suppl 6): p. vi7-vi12.

470. Sundaram, S., A.R. Johnson, and L. Makowski, *Obesity, metabolism and the microenvironment: Links to cancer.* J Carcinog, 2013. **12**.

471. Iyengar, N.M., C.A. Hudis, and A.J. Dannenberg, *Obesity and cancer: local and systemic mechanisms.* Annu Rev Med, 2015. **66**: p. 297-309.

472. Ford, N.A., et al., *Deconvoluting the obesity and breast cancer link: secretome, soil and seed interactions.* J Mammary Gland Biol Neoplasia, 2013. **18**(3-4): p. 267-75.

473. Camp, J.T., et al., *Interactions with Fibroblasts are Distinct in Basal-like and Luminal Breast Cancers.* Mol Cancer Res, 2011. **9**(1): p. 3-13.

474. Brauer, H.A., et al., *Impact of tumor microenvironment and epithelial phenotypes on metabolism in breast cancer.* Clin Cancer Res, 2013. **19**(3): p. 571-85.

475. Stewart, D.A., et al., *Basal-like Breast Cancer Cells Induce Phenotypic and Genomic Changes in Macrophages.* Mol Cancer Res, 2012. **10**(6): p. 727-738.

476. Ponzo, M.G. and M. Park, *The Met receptor tyrosine kinase and basal breast cancer.* Cell Cycle, 2010. **9**(6): p. 1043-50.

477. Gastaldi, S., P.M. Comoglio, and L. Trusolino, *The Met oncogene and basal-like breast cancer: another culprit to watch out for.* Breast Cancer Res, 2010. **12**(4): p. 208.

478. Zou, H.Y., et al., *An orally available small-molecule inhibitor of c-Met, PF-2341066, exhibits cytoreductive antitumor efficacy through antiproliferative and antiangiogenic mechanisms.* Cancer Res, 2007. **67**(9): p. 4408-17.

479. Choi, W.W., et al., *Angiogenic and lymphangiogenic microvessel density in breast carcinoma: correlation with clinicopathologic parameters and VEGF-family gene expression.* Mod Pathol, 2005. **18**(1): p. 143-52.

480. Biro, F.M. and J. Deardorff, *Identifying opportunities for cancer prevention during preadolescence and adolescence: puberty as a window of susceptibility.* J Adolesc Health, 2013. **52**(5 Suppl): p. S15-20.

481. Olson, L.K., et al., *Pubertal exposure to high fat diet causes mouse strain-dependent alterations in mammary gland development and estrogen responsiveness.* Int J Obes (Lond), 2010. **34**(9): p. 1415-26.

482. Lin, E.Y. and J.W. Pollard, *Tumor-associated macrophages press the angiogenic switch in breast cancer.* Cancer Res, 2007. **67**(11): p. 5064-6.

483. Wagatsuma, S., et al., *Tumor angiogenesis, hepatocyte growth factor, and c-Met expression in endometrial carcinoma.* Cancer, 1998. **82**(3): p. 520-30.

484. Abounader, R. and J. Laterra, *Scatter factor/hepatocyte growth factor in brain tumor growth and angiogenesis.* Neuro Oncol, 2005. **7**(4): p. 436-51.

485. Casbas-Hernandez, P., J.M. Fleming, and M.A. Troester, *Gene expression analysis of in vitro cocultures to study interactions between breast epithelium and stroma.* J Biomed Biotechnol, 2011. **2011**: p. 520987.

486. Garner, O.B., et al., *Stage-dependent regulation of mammary ductal branching by heparan sulfate and HGF-cMet signaling.* Developmental Biology. **355**(2): p. 394-403.

487. Yamashita, J.-i., et al., *Immunoreactive Hepatocyte Growth Factor Is a Strong and Independent Predictor of Recurrence and Survival in Human Breast Cancer.* Cancer Res, 1994. **54**(7): p. 1630-1633.

488. Elliott, B.E., et al., *The role of hepatocyte growth factor (scatter factor) in epithelial–mesenchymal transition and breast cancer.* Can J Physiol Pharmacol, 2002. **80**(2): p. 91-102.

489. Wang, Y., et al., *Hepatocyte growth factor/scatter factor expression in human mammary epithelium.* Am J Pathol, 1994. **144**(4): p. 675-82.

490. Jin, L., et al., *Expression of scatter factor and c-met receptor in benign and malignant breast tissue.* Cancer, 1997. **79**(4): p. 749-760.

491. Beviglia, L., et al., *Expression of the C-Met/HGF receptor in human breast carcinoma: Correlation with tumor progression.* Int J Cancer, 1997. **74**(3): p. 301-309.

492. Stella, M.C., et al., *Negative Feedback Regulation of Met-Dependent Invasive Growth by Notch.* Mol Cell, 2005. **25**(10): p. 3982-3996.

493. Sam, M.R., B.E. Elliott, and C.R. Mueller, *A novel activating role of SRC and STAT3 on HGF transcription in human breast cancer cells.* Mol Cancer, 2007. **6**: p. 69.

494. Liu, S., *HGF-MET as a breast cancer biomarker.* Aging (Albany NY), 2015. **7**(3): p. 150-1.

495. Yan, S., et al., *Prognostic significance of c-Met in breast cancer: a meta-analysis of 6010 cases.* Diagn Pathol, 2015. **10**.

496. Puri, N., et al., *A selective small molecule inhibitor of c-Met, PHA665752, inhibits tumorigenicity and angiogenesis in mouse lung cancer xenografts.* Cancer Res, 2007. **67**(8): p. 3529-34.

497. You, W.K., et al., *VEGF and c-Met blockade amplify angiogenesis inhibition in pancreatic islet cancer.* Cancer Res, 2011. **71**(14): p. 4758-68.

498. Sameni, M., et al., *Cabozantinib (XL184) Inhibits Growth and Invasion of Preclinical TNBC Models.* Clin Cancer Res, 2015.

499. Tolaney, S.M., et al., *Phase II study of tivantinib (ARQ 197) in patients with metastatic triple-negative breast cancer.* Invest New Drugs, 2015. **33**(5): p. 1108-14.

500. Dieras, V., et al., *Randomized, phase II, placebo-controlled trial of onartuzumab and/or bevacizumab in combination with weekly paclitaxel in patients with metastatic triple-negative breast cancer.* Ann Oncol, 2015. **26**(9): p. 1904-10.

501. Sharma, N. and A.A. Adjei, *In the clinic: ongoing clinical trials evaluating c-MET-inhibiting drugs.* Ther Adv Med Oncol, 2011. **3**(1 Suppl): p. S37-50.

502. Brewster, A.M., M. Chavez-MacGregor, and P. Brown, *Epidemiology, biology, and treatment of triple-negative breast cancer in women of African ancestry.* Lancet Oncol, 2014. **15**(13): p. e625-34.

503. Cancer, I.A.f.R.o. and W.H. Organization, *GLOBOCAN: Estimated Cancer Incidence, Mortality, and Prevalence Worldwide in 2012*. 2014: IARC.

504. Fryar, C.D., Carroll, Margaret D., Ogden, Cynthia L. *Prevalence of overweight, obesity, and extreme obesity among adults: United States, trends 1960–1962 through 2013–2014*. National Center for Health Statistics 2016 July 18, 2016 [cited 2018 January 26];

Available from:
https://www.cdc.gov/nchs/data/hestat/obesity_adult_13_14/obesity_adult_13_14.htm.

505. Cozzo, A.J., A.M. Fuller, and L. Makowski, *Contribution of Adipose Tissue to Development of Cancer.* Compr Physiol, 2017. **8**(1): p. 237-282.

506. Kohler, B.A., et al., *Annual Report to the Nation on the Status of Cancer, 1975-2011, Featuring Incidence of Breast Cancer Subtypes by Race/Ethnicity, Poverty, and State.* J Natl Cancer Inst, 2015. **107**(6): p. djv048.

507. Prat, A. and C.M. Perou, *Deconstructing the molecular portraits of breast cancer.* Mol Oncol, 2011. **5**(1): p. 5-23.

508. Perou, C.M., *Molecular stratification of triple-negative breast cancers.* Oncologist, 2011. **16 Suppl 1**: p. 61-70.

509. Dent, R., et al., *Pattern of metastatic spread in triple-negative breast cancer.* Breast Cancer Res Treat, 2009. **115**(2): p. 423-8.

510. Hao, S., et al., *Overweight as a Prognostic Factor for Triple-Negative Breast Cancers in Chinese Women.* PLoS One, 2015. **10**(6): p. e0129741.

511. Dunlap, S.M., et al., *Dietary Energy Balance Modulates Epithelial-To-Mesenchymal Transition and Tumor Progression in Murine Claudin-Low and Basal-Like Mammary Tumor Models.* Cancer Prev Res (Phila), 2012. **5**(7): p. 10.1158/1940-6207.CAPR-12-0034.

512. Ford, N.A., et al., *Omega-3-Acid Ethyl Esters Block the Protumorigenic Effects of Obesity in Mouse Models of Postmenopausal Basal-like and Claudin-Low Breast Cancer.* Cancer Prev Res (Phila), 2015. **8**(9): p. 796-806.

513. Vaysse, C., et al., *Inflammation of mammary adipose tissue occurs in overweight and obese patients exhibiting early-stage breast cancer.* NPJ Breast Cancer, 2017. **3**: p. 19.

514. Lilla, J.N. and Z. Werb, *Mast cells contribute to the stromal microenvironment in mammary gland branching morphogenesis.* Dev Biol, 2010. **337**(1): p. 124-33.

515. Khazaie, K., et al., *The significant role of mast cells in cancer.* Cancer and Metastasis Reviews, 2011. **30**(1): p. 45-60.

516. Montgomery, M.K., et al., *Mouse strain-dependent variation in obesity and glucose homeostasis in response to high-fat feeding.* Diabetologia, 2013. **56**(5): p. 1129-39.

517. Zhou, B., et al., *Erythropoietin promotes breast tumorigenesis through tumor-initiating cell self-renewal.* J Clin Invest, 2014. **124**(2): p. 553-63.

518. Pfefferle, A.D., et al., *Transcriptomic classification of genetically engineered mouse models of breast cancer identifies human subtype counterparts.* Genome Biol, 2013. **14**(11): p. R125.

519. Saldanha, A.J., *Java Treeview—extensible visualization of microarray data.* Bioinformatics, 2004. **20**(17): p. 3246-3248.

520. Prat, A., et al., *Phenotypic and molecular characterization of the claudin-low intrinsic subtype of breast cancer.* Breast Cancer Res, 2010. **12**(5): p. R68.

521. Sandhu, R., et al., *Digital histologic analysis reveals morphometric patterns of age-related involution in breast epithelium and stroma.* Hum Pathol, 2016. **48**: p. 60-8.

522. Tusher, V.G., R. Tibshirani, and G. Chu, *Significance analysis of microarrays applied to the ionizing radiation response.* Proc Natl Acad Sci U S A, 2001. **98**(9): p. 5116-21.

523. Casbas-Hernandez, P., et al., *Tumor intrinsic subtype is reflected in cancer-adjacent tissue.* Cancer Epidemiol Biomarkers Prev, 2015. **24**(2): p. 406-14.

524. Dwyer, D.F., N.A. Barrett, and K.F. Austen, *Expression profiling of constitutive mast cells reveals a unique identity within the immune system.* Nat Immunol, 2016. **17**(7): p. 878-87.

525. Motakis, E., et al., *Redefinition of the human mast cell transcriptome by deep-CAGE sequencing.* Blood, 2014. **123**(17): p. e58-67.

526. Bindea, G., et al., *Spatiotemporal dynamics of intratumoral immune cells reveal the immune landscape in human cancer.* Immunity, 2013. **39**(4): p. 782-95.

527. Novak, M.L. and T.J. Koh, *Macrophage phenotypes during tissue repair.* J Leukoc Biol, 2013. **93**(6): p. 875-81.

528. Boccaccio, C. and P.M. Comoglio, *Invasive growth: a MET-driven genetic programme for cancer and stem cells.* Nat Rev Cancer, 2006. **6**(8): p. 637-45.

529. Incio, J., et al., *PlGF/VEGFR-1 Signaling Promotes Macrophage Polarization and Accelerated Tumor Progression in Obesity.* Clin Cancer Res, 2016. **22**(12): p. 2993-3004.

530. Haque, R., et al., *Impact of breast cancer subtypes and treatment on survival: an analysis spanning two decades.* Cancer Epidemiol Biomarkers Prev, 2012. **21**(10): p. 1848-55.

531. Falato, C., et al., *Intrinsic subtypes and genomic signatures of primary breast cancer and prognosis after systemic relapse.* Mol Oncol, 2016. **10**(4): p. 517-25.

532. Kosteli, A., et al., *Weight loss and lipolysis promote a dynamic immune response in murine adipose tissue.* J Clin Invest, 2010. **120**(10): p. 3466-79.

533. Knight, J.F., et al., *Met synergizes with p53 loss to induce mammary tumors that possess features of claudin-low breast cancer.* Proc Natl Acad Sci U S A, 2013. **110**(14): p. E1301-10.

534. Christopoulos, P.F., P. Msaouel, and M. Koutsilieris, *The role of the insulin-like growth factor-1 system in breast cancer.* Mol Cancer, 2015. **14**: p. 43.

535. Ortiz-Ruiz, M.J., et al., *Therapeutic potential of ERK5 targeting in triple negative breast cancer.* Oncotarget, 2014. **5**(22): p. 11308-18.

536. Venmar, K.T., et al., *IL4 receptor ILR4alpha regulates metastatic colonization by mammary tumors through multiple signaling pathways.* Cancer Res, 2014. **74**(16): p. 4329-40.

537. Kang, Y., et al., *A multigenic program mediating breast cancer metastasis to bone.* Cancer Cell, 2003. **3**(6): p. 537-49.

538. Lee, A.S., et al., *Erythropoietin induces lymph node lymphangiogenesis and lymph node tumor metastasis.* Cancer Res, 2011. **71**(13): p. 4506-17.

539. Liang, Z., et al., *Inhibition of breast cancer metastasis by selective synthetic polypeptide against CXCR4.* Cancer Res, 2004. **64**(12): p. 4302-8.

540. Zhang, Z., et al., *Expression of CXCR4 and breast cancer prognosis: a systematic review and meta-analysis.* BMC Cancer, 2014. **14**: p. 49.

541. Todaro, M., et al., *Erythropoietin activates cell survival pathways in breast cancer stem-like cells to protect them from chemotherapy.* Cancer Res, 2013. **73**(21): p. 6393-400.

542. Glajcar, A., et al., *The relationship between breast cancer molecular subtypes and mast cell populations in tumor microenvironment.* Virchows Arch, 2017. **470**(5): p. 505-515.

543. Bianchini, G., et al., *Triple-negative breast cancer: challenges and opportunities of a heterogeneous disease.* Nat Rev Clin Oncol, 2016. **13**(11): p. 674-690.

544. Carey, L.A., et al., *The triple negative paradox: primary tumor chemosensitivity of breast cancer subtypes.* Clin Cancer Res, 2007. **13**(8): p. 2329-34.

545. Oncology, A.S.o.C. *Breast Cancer: Statistics*. 2017 [cited 2018 March 26]; Available from: https://www.cancer.net/cancer-types/breast-cancer/statistics.

546. Qin, Y., et al., *Weight loss reduces basal-like breast cancer through kinome reprogramming.* Cancer Cell Int, 2016. **16**.

547. Bischoff, S.C., *Role of mast cells in allergic and non-allergic immune responses: comparison of human and murine data.* Nat Rev Immunol, 2007. **7**(2): p. 93-104.

548. Martin, L.J., et al., *A randomized trial of dietary intervention for breast cancer prevention.* Cancer Res, 2011. **71**(1): p. 123-33.

549. Pierce, J.P., et al., *Influence of a diet very high in vegetables, fruit, and fiber and low in fat on prognosis following treatment for breast cancer: the Women's Healthy Eating and Living (WHEL) randomized trial.* JAMA, 2007. **298**(3): p. 289-98.

550. Chlebowski, R.T., et al., *Low-Fat Dietary Pattern and Breast Cancer Mortality in the Women's Health Initiative Randomized Controlled Trial.* J Clin Oncol, 2017. **35**(25): p. 2919-2926.

551. Rock, C.L., et al., *Favorable changes in serum estrogens and other biologic factors after weight loss in breast cancer survivors who are overweight or obese.* Clin Breast Cancer, 2013. **13**(3): p. 188-95.

552. Chlebowski, R., et al., *Abstract GS5-07: Weight change in postmenopausal women and breast cancer risk in the women's health initiative observational study.* Cancer Res, 2018. **78**(4 Supplement): p. GS5-07-GS5-07.

553. Jackson, S.E., et al., *Weight Loss and Mortality in Overweight and Obese Cancer Survivors: A Systematic Review.* PLoS One, 2017. **12**(1): p. e0169173.

554. Yong, C.S.M., et al., *CAR T-cell therapy of solid tumors.* Immunol Cell Biol, 2016. **95**: p. 356.

555. So, J.Y., et al., *Differential Expression of Key Signaling Proteins in MCF10 Cell Lines, a Human Breast Cancer Progression Model.* Mol Cell Pharmacol, 2012. **4**(1): p. 31-40.

556. Paget, S., *The distribution of secondary growths in cancer of the breast. 1889.* Cancer Metastasis Rev, 1989. **8**(2): p. 98-101.

557. Bissell, M.J. and W.C. Hines, *Why don't we get more cancer? A proposed role of the microenvironment in restraining cancer progression.* Nat Med, 2011. **17**(3): p. 320-9.